

20. 166
LBS 1004183

UNIVERSIDAD DE SEVILLA
FACULTAD DE MATEMÁTICAS
BIBLIOTECA

043
121

BCK

Universidad de Sevilla

Dpto. de Ecuaciones Diferenciales y Análisis Numérico

ALGUNAS APLICACIONES DEL METODO DE ELEMENTOS FINITOS A PROBLEMAS EN DERIVADAS PARCIALES NO LINEALES

Vº. Bº. DEL DIRECTOR
DEL TRABAJO



Fdo. Enrique Fernández Cara
Catedrático de Análisis Matemático
de la Universidad de Sevilla

Memoria que presenta
Rosa Echevarría Líbano
para optar al grado de
Doctor en Matemáticas

Sevilla, Julio 1995

Fdo. Rosa Echevarría Líbano

A mis padres,
a Nerea y Alvaro

UNIVERSIDAD DE SEVILLA
SECRETARIA GENERAL

Queda registrada esta Tesis Doctoral
al folio 250 número 37 del libro
correspondiente.

Sevilla, 30 JUN. 1995

El Jefe del Negociado de Tesis,

Alejo Laffito

Deseo expresar mi agradecimiento a las siguientes personas

En primer lugar, evidentemente, a Enrique Fernández Cara, por la dirección de este trabajo, y por tantas cosas que es imposible mencionar aquí.

A Don Antonio Valle, que me admitió en el Departamento y que me prestó en todo momento su apoyo incondicional.

A mis primeros compañeros, Pepe Real, Pepe Martín y Julio Couce, por su acogida, sus enseñanzas y, sobre todo, por su amistad.

Junto con ellos, al resto de los compañeros del proyecto Hermes, Tomás Chacón y Paco Ortegón, por haber hecho posible parte de este trabajo.

Y a Manolo Delgado y Manolo G. Burgos, por su colaboración y sus indicaciones.

Sevilla, Julio de 1995

Introducción

Esta memoria trata sobre la resolución numérica de diversos problemas en derivadas parciales no lineales. Se compone de varios trabajos que se agrupan en dos partes.

En la Parte I, se recoge parcialmente un trabajo llevado a cabo con el soporte económico de la Agencia Espacial Europea y el Consejo de Europa, en el marco de un Proyecto de Investigación puesto en marcha con motivo del Plan Espacial Europeo (Contrato de Investigación HERMES RDANE 23/87 entre la Universidad de Sevilla y Avions Marcel Dassault-Bréguet Aviation: *Modelado Matemático de la Turbulencia: Validación Numérica de la Turbulencia mediante Técnicas Asintóticas. Análisis Bidimensional de la Transferencia de Calor en la Zona de Recirculación del Avión Espacial HERMES*). El Responsable Científico de este contrato fue el Profesor E. Fernández Cara, que también es el Director de esta Tesis. En el desarrollo del trabajo, intervinieron, además del Profesor Fernández Cara y la autora, los Profesores T. Chacón, J. Couce, J.D. Martín y F. Ortegón.

Los objetivos del mencionado trabajo son:

- (a) La deducción de modelos asintóticos de tipo M.P.P. para flujos compresibles isentrópicos y para flujos completamente compresibles en presencia de capas límites turbulentas,
- (b) La validación numérica de estos modelos mediante técnicas de elementos finitos sobre determinados casos test,
- (c) La deducción de modelos del tipo anterior para capas límites turbulentas.

Entre otras cosas, se presentan aquí los resultados obtenidos en relación con los apartados (a) y (b), que son aquéllos en los que la autora de esta memoria ha intervenido directamente.

Los cuatro capítulos de que consta esta primera parte se presentan en su forma original, tal como aparecen en los sucesivos Informes del Proyecto. La numeración de las páginas no es, pues, correlativa. En cada capítulo, las referencias bibliográficas se encuentran al final.

La segunda parte de la memoria, versa sobre la resolución numérica de varios problemas elípticos semilineales con no linealidades discontinuas. Se proponen algoritmos que usan técnicas propias de la dualidad no convexa, en combinación con la regularización exacta.

Los problemas abordados tienen su origen en diversos campos de la Ciencia (física, química, biología,...) y plantean varios tipos de dificultades: restricciones que pueden escribirse como pertenencia la frontera de un convexo, ausencia de formulación variacional, el hecho de que algunos de los problemas planteados sean no escalares, posible no unicidad de solución....

Los resultados presentados en esta segunda parte son de varios tipos. En primer lugar, mencionemos que se recuerdan algunos, de carácter teórico, esencialmente debidos a los Profesores M. Delgado, E. Fernández Cara y C. Moreno. Por otro lado, se describen y se ponen en práctica métodos numéricos (que utilizan técnicas de elementos finitos). El comportamiento de cada uno de los algoritmos propuestos es, además, ilustrado sobre ejemplos significativos.

Los tres capítulos en los que se divide la segunda parte corresponden a otros tantos artículos ya publicados, o de próxima aparición y han sido presentados en su forma original.

A continuación, describimos de forma más detallada los contenidos de esta memoria. Las referencias bibliográficas se encuentran al final de la Introducción.

Introducción a la Parte I

Hoy día, se admite que las ecuaciones de Navier-Stokes gobiernan las variables que describen el comportamiento de un flujo compresible (un gas) prácticamente en cualquier circunstancia. Una vez adimensionalizadas, se escriben en la forma:

$$\begin{cases} \partial_t \rho + \nabla \cdot (\rho \vec{u}) = 0 \\ \partial_t (\rho \vec{u}) + \nabla \cdot (\rho \vec{u} \otimes \vec{u}) + \nabla p = \frac{1}{\text{Re}} \nabla \cdot (\rho D(\vec{u})) \\ \partial_t (\rho \epsilon) + \nabla \cdot ((\epsilon + p) \vec{u}) = \frac{1}{\text{Re}} \nabla \cdot (\vec{u} \cdot D(\vec{u})) + \frac{\gamma}{\text{Pr}} \nabla \theta \\ \epsilon = \rho(\theta + \frac{1}{2} |\vec{u}|^2), \quad p = (\gamma - 1)\rho\theta \end{cases}$$

donde se ha usado la notación

$$D(\vec{u}) = \nabla \vec{u} + \nabla \vec{u}^t - \frac{2}{3} (\nabla \cdot \vec{u}) \text{Id.}$$

Se supone que estas ecuaciones han de verificarse en $\Omega \times (0, T)$, donde $\Omega \subset \mathbb{R}^N$ es el abierto ocupado por el fluido y $(0, T)$ es el intervalo de observación temporal ($N = 2$ ó 3). Las funciones $\vec{u}(x, t)$, $\rho(x, t)$ y $p(x, t)$ son, respectivamente, el campo de velocidades, la densidad y la presión y $\epsilon(x, t)$ y $\theta(x, t)$ son, respectivamente, la energía total y la temperatura. γ es una constante propia del fluido (se trata de la razón de los calores específicos). Pr y Re son constantes adimensionales que caracterizan el tipo de flujo. Más precisamente, Pr es el número de Prandtl y Re es el número de Reynolds del problema, que viene definido por

$$\text{Re} = \frac{LU}{\nu}$$

donde L es una longitud característica de Ω , U es una velocidad característica y ν es la viscosidad cinemática. Naturalmente, es preciso completar estas ecuaciones con condiciones de contorno e iniciales.

El número de Reynolds, Re , determina en cierto modo "clases de equivalencia" para distintos problemas de Navier-Stokes. Por ejemplo, si los flujos de un mismo fluido en dos situaciones geométricas distintas pero "similares" conducen al mismo número de Reynolds, las correspondientes soluciones son "semejantes", i.e. pueden ser obtenidas cada una a partir de la otra mediante cambios de unidades y traslaciones. Esto hace posible la simulación experimental, a escala reducida, de fenómenos de gran tamaño, por ejemplo en túneles de viento. Otra ventaja de este hecho es que permite comparar fácilmente resultados numéricos.

El principal interés en disponer de modelos y códigos informáticos bien adaptados para la resolución efectiva del problema de Navier-Stokes radica en el hecho de que determinadas condiciones reales son imposibles de simular en un túnel de viento. Esto ocurre, por ejemplo, con las que se darían en ciertas fases de la reentrada en la atmósfera de un avión espacial.

Para números de Reynolds por debajo de determinados valores críticos, el flujo se encuentra en régimen laminar, sin grandes fluctuaciones de velocidad, presión, etc. En este caso, tanto la simulación experimental como la numérica pueden efectuarse directamente a partir de las ecuaciones de Navier-Stokes.

Sin embargo, para números de Reynolds más elevados, el flujo se comporta de forma mucho más irregular y se dice que está en régimen turbulento. La principal característica del régimen turbulento es la superposición de escalas, i.e. el hecho de que aparezcan "remolinos" de talla grande (comparable a la longitud característica L) junto con remolinos de talla extremadamente pequeña. En estas circunstancias, la resolución numérica directa de las ecuaciones de Navier-Stokes es inviable, debido al enorme número de incógnitas que deberían tener los problemas discretizados para poder reflejar el comportamiento de los pequeños remolinos¹. De aquí, la necesidad de utilizar modelos matemáticos de turbulencia, distintos de las ecuaciones de Navier-Stokes, que describan el flujo de forma aproximada. Digamos en términos generales que estos modelos renuncian a una descripción exacta del comportamiento del fluido y, en cambio, propor-

¹Y, en la práctica, esto es cierto sea cual sea el método numérico elegido.

cionan una descripción macroscópica basada en el conocimiento de cantidades "promediadas".

Los modelos M.P.P. de turbulencia utilizan técnicas de desarrollos asintóticos propias de la teoría de Homogeneización periódica. La novedad principal de estos modelos frente a los modelos clásicos de turbulencia radica en su deducción absolutamente formal, carente de hipótesis físicas. En la deducción de un modelo M.P.P., se supone que los fenómenos producidos por el movimiento a gran escala (variables promediadas) se encuentran netamente separados de los producidos por las pequeñas estructuras (los pequeños remolinos). En este sentido, se introduce un pequeño parámetro, ϵ , que debe interpretarse como la razón entre las longitudes características de las pequeñas y grandes estructuras. Se descompone el campo de velocidades (y todas las demás incógnitas) en la suma de un campo medio y un campo fluctuante y se imponen desarrollos asintóticos de las incógnitas, en potencias de ϵ . Tras cálculos formales (sustitución e identificación de coeficientes en los desarrollos), truncando éstos en el orden adecuado, la compatibilidad de las igualdades resultantes conduce a un sistema de EDP para las variables promediadas donde también aparecen nuevas variables: la energía cinética turbulenta media k , la helicidad media h y la coordenada Lagrangiana inversa \tilde{a} (cf. el capítulo 2).

En estas EDP aparecen, además, dos tensores y dos funciones escalares (los términos de cierre) que, a su vez, dependen de $\nabla \tilde{a}$, k y h a través de la solución del denominado *problema canónico en microestructura*. Dada la naturaleza de éste, la única estrategia posible consiste en "tabular" los términos de cierre, resolviendo sucesivamente problemas en microestructura para un conjunto adecuado de posibles valores de $\nabla \tilde{a}$, k y h .

Este modelo fue inicialmente desarrollado por D. McLaughlin, G. Papanicolaou y O. Pironneau [21] para fluidos ideales incompresibles, i.e. en el caso más sencillo de la ecuación de Euler. Posteriormente, fue adaptado por C. Bègue, T. Chacón, F. Ortegón y O. Pironneau a situaciones más complicadas: flujos incompresibles débilmente viscosos y flujos incompresibles donde los efectos térmicos no son despreciables (cf. [2], [6], [7], [9], [24], [25]). En [7] y en el marco del proyecto Hermes-Sevilla (cf. [8]), se desarrollaron modelos para flujos compresibles isentrópicos y para flujos completamente compresibles en presencia de capas límites.

La primera parte de esta memoria comprende:

- (a) La deducción de este tipo de modelos, teniendo en cuenta la presencia de capas límites turbulentas.
- (b) Una descripción de las técnicas numéricas utilizadas para resolver los sistemas de EDP resultantes.
- (c) Los resultados obtenidos en dos casos test propuestos por la dirección científica del Proyecto Hermes. Estos tests están diseñados para validar la simulación numérica de la turbulencia por métodos asintóticos.

La primera parte de esta memoria se compone de cuatro capítulos. Presentaremos a continuación una breve descripción de los mismos.

En el capítulo 1 describimos, a modo de preliminares, diversos métodos de discretización en tiempo de las ecuaciones de Navier-Stokes para flujos compresibles isentrópicos, así como ciertos métodos de resolución de los problemas elípticos, lineales y no lineales, a los que dichos esquemas conducen. Estos métodos están basados en los que fueron introducidos por M.O. Bristeau y J. Périaux [4], R. Glowinski [14] y R. Glowinski y O. Pironneau [15]. Se exponen asimismo varias ideas sobre el modelado de capas límites turbulentas.

En el capítulo 2, presentamos la deducción de un modelo asintótico de tipo M.P.P. para flujos compresibles isentrópicos, sin tener en cuenta en principio la presencia de capas límites. Al final del capítulo, se describen ciertas condiciones de contorno alternativas, basadas en el uso de leyes experimentales de pared.

Señalemos que uno de los objetivos del proyecto en el que está enmarcada la primera parte de esta memoria fue, precisamente, la deducción de modelos asintóticos de tipo M.P.P. para capas límites turbulentas. Los resultados obtenidos pueden encontrarse en el Informe 4 del mencionado proyecto (cf. [8]). No han sido incluidos en esta memoria, ya que la autora no participó activamente en esta parte del trabajo.

El capítulo 3 está dedicado a exponer en detalle el método numérico utilizado para resolver el modelo M.P.P. compresible isentrópico bidimensional. Es en este capítulo y en el siguiente donde se encuentran los principales resultados de la primera parte de la memoria. Las ecuaciones son las

siguientes:

$$\left\{ \begin{array}{l} \partial_t \vec{u} + (\vec{u} \cdot \nabla) \vec{u} + \frac{1}{\rho} \nabla \cdot (\rho k R^1(\nabla \vec{a})) - \frac{1}{\rho} A_1 \nabla \cdot (\rho \sqrt{k} D(\vec{u})) + \frac{1}{\rho} \nabla p = 0 \\ \partial_t \rho + \nabla \cdot (\rho \vec{u}) = 0 \\ \partial_t k + \vec{u} \cdot \nabla k + [R^1(\nabla \vec{a}) : \nabla \vec{u} + \mu_0 \psi^1(\nabla \vec{a})] k - A_2 \frac{1}{\rho} \nabla \cdot (\rho \sqrt{k} \nabla k) = 0 \\ \partial_t \vec{a} + (\vec{u} \cdot \nabla) \vec{a} = 0 \\ p = K \rho^\gamma \end{array} \right.$$

Por simplicidad, completamos este sistema con las siguientes condiciones de contorno e iniciales:

$$\left\{ \begin{array}{l} \vec{u} = \vec{u}_\infty \\ \rho = \rho_\infty \\ k = k_\infty \\ \vec{a} = \vec{x} - t \vec{u}_\infty \end{array} \right. \quad \text{sobre } \Gamma_\infty^-$$

$$\left\{ \begin{array}{l} \vec{u} = 0 \\ k = k_B \end{array} \right. \quad \text{sobre } \Gamma_B$$

$$\left\{ \begin{array}{l} [-p \text{ Id.} - \rho k R^1(\nabla \vec{a}) + A_1 \rho \sqrt{k} D(\vec{u})] \cdot \vec{n} = 0 \\ \frac{\partial k}{\partial n} = 0 \end{array} \right. \quad \text{sobre } \Gamma_\infty^+$$

$$\left\{ \begin{array}{l} \vec{u}(x, 0) = \vec{u}_0(x) \\ \rho(x, 0) = \rho_0(x) \\ k(x, 0) = k_0(x) \\ \vec{a}(x, 0) = x \end{array} \right.$$

Aquí, se supone que Γ_∞^- es la parte de la frontera de Ω por donde “entra” el flujo, Γ_∞^+ es la parte de la frontera por donde “sale” y Γ_B es la frontera del ó de los posibles obstáculos (ó paredes sólidas). Observamos que no aparece ecuación para la helicidad h , ya que el problema es bidimensional. $R^1(\nabla \vec{a})$ y $\psi^1(\nabla \vec{a})$ son los términos de cierrre que, admitida la invarianza de las EDP respecto de cambios de sistemas de referencia, pueden depender sólo de los invariantes de $\nabla \vec{a} \cdot \nabla \vec{a}^t$ (cf. [24], [25]).

El problema es en primer lugar reformulado introduciendo una nueva variable, la densidad logarítmica, $\sigma = \log \rho$. La discretización en tiempo del sistema resultante se lleva a cabo utilizando un esquema implícito de dos pasos (Gear) para las ecuaciones en \vec{u} , σ y k y un esquema explícito (Lax-Wendroff) para la ecuación de transporte para \vec{a} . Un esquema completamente implícito conduciría obviamente a sistemas de resolución muy difícil (por no decir imposible). Para la primera etapa en tiempo se utiliza un esquema de Euler retrógrado, con paso $\frac{2\Delta t}{3}$, ya que así el sistema resultante posee la misma matriz que los sistemas posteriores, provenientes de la discretización mediante el esquema de Gear.

De esta manera, en la etapa $(n + 1)$ -ésima, las EDP resultantes son de la forma:

$$\begin{cases} \alpha \vec{u} - \mu \Delta \vec{u} + \beta \nabla \sigma - \Phi(\sigma, \vec{u}, k, \nabla \vec{a}) = \vec{f}_n \\ \alpha \sigma + \nabla \cdot \vec{u} + \vec{u} \cdot \nabla \sigma = h_n \\ \alpha k - \lambda \Delta k - \Pi(\sigma, \vec{u}, k, \nabla \vec{a}) = g_n \end{cases}$$

$$\vec{a} = \Psi_n(\vec{u})$$

donde Φ , Π y Ψ_n son funciones adecuadas.

Para resolver este sistema, se utilizan tres variantes de un algoritmo de relajación por bloques que desacopla las ecuaciones para \vec{a} , k y (σ, \vec{u}) . Así, en cada iteración del algoritmo de relajación, hay que resolver:

- Una ecuación explícita para la coordenada Lagrangiana inversa \vec{a} .
- Un problema de contorno para una EDP no lineal para la energía cinética turbulenta k ,
- Un problema de contorno para un sistema no lineal de EDP para la velocidad y la densidad logarítmica, \vec{u} y σ .

Se recurre a las formulaciones débiles de los problemas no lineales precedentes. Posteriormente, éstos son escritos como problemas de mínimos cuadrados. Estos problemas son resueltos mediante un algoritmo de gradiente conjugado de tipo Buckley-LeNir (cf. [5]). Al aplicar este algoritmo, la mayor dificultad consiste en el cálculo de los gradientes de los funcionales respectivos, que está detallado en este capítulo.

En el caso del sistema acoplado para \vec{u} y σ , el cálculo del gradiente se basa parcialmente en la resolución de un problema adjunto adecuado. Esto

obliga a resolver problemas de Stokes generalizados. Más precisamente, uno se encuentra en repetidas ocasiones con sistemas lineales tales como

$$\left\{ \begin{array}{l} \alpha\sigma + \nabla \vec{u} = h \\ \alpha\vec{u} - \mu\Delta\vec{u} + \beta\nabla\sigma = \vec{f} \\ \vec{u} = \vec{u}_\infty \quad \sigma = \sigma_\infty \quad \text{sobre } \Gamma_\infty^- \\ \vec{u} = 0 \quad \text{sobre } \Gamma_B \\ \mu \frac{\partial \vec{u}}{\partial n} - \beta\sigma \vec{n} = g \quad \text{sobre } \Gamma_\infty^+ \end{array} \right.$$

(donde \vec{f} , h y g son conocidas). En este contexto, hemos recurrido a una generalización de un algoritmo, debido a R. Glowinski y O. Pironneau [15], descrito en el capítulo 1 de la memoria. Desde el punto de vista computacional, el algoritmo utilizado se reduce a una "cascada" de problemas de Poisson, más un problema lineal en la incógnita $\sigma|_{\Gamma_B}$.

La discretización en espacio de los problemas se lleva a cabo mediante elementos finitos P_1 -Lagrange. Los problemas discretos son obtenidos tras aproximaciones estándar de los espacios funcionales involucrados y de las correspondientes formulaciones débiles.

Finalmente, en el capítulo 4 de la memoria, se presenta un modelo asintótico de turbulencia (de nuevo de tipo M.P.P.) para flujos compresibles bidimensionales, donde se incluye una ecuación para la temperatura θ . Se expone brevemente el método de resolución numérica (esencialmente éste recurre a técnicas similares a las que acabamos de recordar). Para terminar, se exponen con detalle las características de algunos ejemplos test así como diversos resultados numéricos, para cuya preparación y visualización se ha recurrido a la biblioteca MODULEF (cf. [3]). Como se ha dicho antes, estas experiencias numéricas pueden usarse para validar diversos modelos de turbulencia.

A modo de resumen, indiquemos cuáles son las aportaciones originales correspondientes a la primera parte de la memoria:

- La deducción y el análisis de modelos asintóticos de turbulencia para fluidos compresibles, incluyendo situaciones en las que la hipótesis de isentropicidad no es adecuada. Los modelos introducidos obedecen a la estructura general diseñada en [21] (modelos de tipo M.P.P.).

- La resolución numérica de estos modelos en el caso de flujos bidimensionales. Como se ha dicho, se usan esquemas de diverso tipo para la discretización en tiempo (explícitos en \vec{a} e implícitos en el resto de las variables), elementos finitos para la discretización en espacio, reformulación mínimos cuadrados y algoritmos de gradiente conjugado de tipo Buckley-LeNir para la resolución de los problemas no lineales y generalizaciones del algoritmo de Glowinski-Pironneau para la resolución de los problemas lineales (de tipo Stokes) resultantes.
- Los resultados numéricos sobre ejemplos test significativos (cf. las experiencias numéricas presentadas en el capítulo 4). Mencionaremos que, cuando fueron obtenidas (1988-89), eran todavía contadas las ocasiones en las que uno podía encontrar resultados numéricos para flujos turbulentos compresibles en la literatura.

Las principales dificultades encontradas en relación con estos logros son las que se detallan a continuación:

- La complejidad de los problemas originales considerados (sistemas de EDP de evolución no lineales donde el número de incógnitas es ≥ 6 , fuertes variaciones de la solución, complicada situación geométrica, etc...). En este sentido, merece la pena destacar la ausencia casi total de resultados teóricos significativos².
- La complejidad de los modelos de turbulencia que se deducen. Aumenta el número de incógnitas con la introducción de la energía cinética turbulenta k y de la coordenada Lagrangiana inversa \vec{a} . Por otra parte, los llamados términos de cierre dependen de $\nabla \vec{a} \cdot \nabla \vec{a}^t$ de manera "difícil de controlar". Hay posibilidad de capas límites, etc...
- El hecho de que sea necesario concatenar un gran número de técnicas distintas para poder resolver numéricamente estos modelos. En la aplicación de cada una de ellas aparecen dificultades específicas, cuyo tratamiento dificulta y encarece la tarea.

²Tan sólo cabe mencionar un resultado de existencia y unicidad de solución (cf. [20]). Con posterioridad a la elaboración del trabajo, ha habido aportaciones interesantes, principalmente de D. Hoff [16], A.V. Kazhikov [17] y P.L. Lions [18], [19].

- A nivel de programación, la resolución numérica es muy compleja y precisa una “cascada” de rutinas. Tanto el orden lógico en que deben ser realizadas las distintas etapas, como el formato de entrada/salida para datos/resultados intermedios, el post-tratamiento ó visualización de las soluciones numéricas, etc... contribuyen a que las dificultades sean aún mayores.

Introducción a la Parte II

En esta segunda parte, se considera la resolución numérica de diversos problemas elípticos semilineales con una característica común: la presencia de no linealidades discontinuas. Los problemas considerados se exponen a continuación. En todos ellos, H es el operador maximal monótono dependiente de un parámetro $a \in \mathbb{R}$, asociado a la función de Heaviside, siguiente:

$$H(s) = \begin{cases} 0 & \text{si } s < 0 \\ [0, a] & \text{si } s = 0 \\ a & \text{si } s > 0 \end{cases}$$

En primer lugar, se considera el siguiente problema, de origen puramente académico:

$$(1) \quad \left\{ \begin{array}{l} \text{Hallar } u \in H^2(\Omega) \text{ tal que} \\ -\Delta u(x) \in H(u(x) + a(x)) \text{ c.p.d. en } \Omega \\ u = 0 \text{ sobre } \partial\Omega \end{array} \right.$$

Aquí, $a : \Omega \rightarrow \mathbb{R}$ es una función dada que posee discontinuidades.

A continuación, se consideran tres problemas del mismo tipo, pero con mayor número de incógnitas y con una condición adicional que, en todos los casos, puede ser escrita como la pertenencia a la frontera de un convexo apropiado:

$$(2) \quad \left\{ \begin{array}{l} \text{Hallar } u \in H^2(\Omega) \text{ y } \beta \in \mathbb{R} \text{ tales que} \\ -\mathcal{L}u \equiv -\frac{\partial}{\partial r}\left(\frac{1}{r}\frac{\partial u}{\partial r}\right) - \frac{\partial}{\partial z}\left(\frac{1}{r}\frac{\partial u}{\partial z}\right) \in rH(u) \quad \text{c.p.d. en } \Omega \\ u = \beta \quad \text{sobre } \partial\Omega \\ -\int_{\partial\Omega} \frac{1}{r} \frac{\partial u}{\partial n} d\sigma = I \end{array} \right.$$

$$(3) \quad \left\{ \begin{array}{l} \text{Hallar } u \in H^2(\Omega) \text{ y } W \in \mathbb{R} \text{ tales que} \\ -\Delta u(x) \in H(u(x) - Wx_1) \quad \text{c.p.d. en } \Omega \\ u = 0 \quad \text{sobre } \partial\Omega \\ \int_{\Omega} |\nabla u|^2 dx = \eta \end{array} \right.$$

$$(4) \quad \left\{ \begin{array}{l} \text{Hallar } u \in H^2(\Omega) \text{ y } Z \in \mathbb{R} \text{ tales que} \\ -\Delta u(x) \in H(u(x) - Wx_1 - Z) \quad \text{c.p.d. en } \Omega \\ u = 0 \quad \text{sobre } \partial\Omega \\ \int_{\Omega} |\nabla u|^2 dx = \eta \end{array} \right.$$

El problema (2) modela el equilibrio de un plasma confinado en una cavidad axisimétrica (máquina Tokamak; cf. [26], [27]). El dominio Ω es la sección transversal del dominio tridimensional ocupado por el plasma (se supone que $\Omega \subset \{(r, z) \in \mathbb{R}^2; r > R_0\}$ para algún $R_0 > 0$). El parámetro I es dado y representa la corriente total que atraviesa el plasma ($I > 0$). La incógnita u es la función de flujo magnético.

Los problemas (3) y (4) tienen su origen en la teoría de vórtices estacionarios. Aparecen cuando se intenta describir el equilibrio de un par de vórtices planos en un fluido ideal (cf. [13], [23]). El parámetro positivo η es dado y representa la energía cinética de movimiento del vórtice. W es la velocidad constante del fluido en el infinito, y Z mide la cantidad de fluido entre el vórtice y el eje de simetría. Para el problema (4) no existe formulación variacional conocida.

Por último, se consideran dos problemas relativos a un sistema elíptico semilineal (de nuevo con no linealidades discontinuas):

$$(5) \quad \begin{cases} -\Delta u(x) \in -\mu^2 H(u(x) + 1) \exp\left(\frac{\gamma v(x)}{v(x) + 1}\right) & \text{c.p.d. en } \Omega \\ -\Delta v(x) \in \nu \mu^2 H(u(x) + 1) \exp\left(\frac{\gamma v(x)}{v(x) + 1}\right) \\ u = v = 0 \quad \text{sobre } \partial\Omega \end{cases}$$

$$(6) \quad \begin{cases} -\Delta u(x) \in -\mu^2 H(u(x) + 1) \exp\left(\frac{\gamma v(x)}{v(x) + 1}\right) & \text{c.p.d. en } \Omega \\ -\Delta v(x) \in \nu \mu^2 H(u(x) + 1) \exp\left(\frac{\gamma v(x)}{v(x) + 1}\right) \\ u = 0 \quad \text{on } \Gamma_1 \cup \Gamma_3, \quad \frac{\partial u}{\partial n} = 0 \quad \text{on } \Gamma_2 \\ v = 0 \quad \text{on } \Gamma_1, \quad \frac{\partial v}{\partial n} = 0 \quad \text{on } \Gamma_2 \cup \Gamma_3 \end{cases}$$

Estas ecuaciones modelan el estado de equilibrio en una reacción química simple, irreversible y no isotérmica de orden cero (cf. [1], [11]). Aquí, u y v son, respectivamente, la concentración y la temperatura del reactante, y γ , ν y μ^2 son parámetros que identifican la reacción. Las condiciones de contorno impuestas en (5) poseen interpretación física, mientras que en el problema (6) han sido elegidas con vistas a ilustrar la adaptación del algoritmo propuesto y su comportamiento (cf. el capítulo 3).

Para resolver estos problemas, se utilizan ciertas técnicas, originalmente introducidas en [12] para problemas escalares y posteriormente extendidas al caso de un sistema de dos ecuaciones en [10]. En esencia, se trata de métodos propios de la dualidad no convexa en combinación con la regularización exacta que serán brevemente recordados a continuación.

En primer lugar, consideremos un problema no convexo del tipo siguiente:

$$(7) \quad \begin{cases} \text{Minimizar } J(v) = f(v) - g(Bv) \\ \text{sujeto a } v \in V \end{cases}$$

Aquí, V y H son espacios de Hilbert, $B : V \rightarrow H$ es un operador lineal acotado y $f : V \rightarrow (-\infty, +\infty]$ y $g : H \rightarrow (-\infty, +\infty]$ son funciones convexas, semicontinuas inferiormente y propias.

La razón principal por la que tiene interés considerar estas cuestiones es que una buena cantidad de problemas con discontinuidades pueden ser escritos en la forma (7) para determinadas elecciones de V , H , f , g y B . Tal es el caso, por ejemplo del sistema (1).

Al problema (7) se le puede asociar el problema dual

$$(8) \quad \begin{cases} \text{Minimizar } J^*(r) = g^*(q) - f^*(B^*q) \\ \text{sujeto a } q \in H \end{cases}$$

donde f^* y g^* son las funciones convexas conjugadas de f y g respectivamente y B^* es el operador adjunto de B . Los puntos críticos, u y p respectivamente de (7) y (8), satisfacen la siguiente condición de optimidad, formulada en términos de las subdiferenciales de f y g :

$$(9) \quad u \in \partial f^*(B^*p), \quad p \in \partial g(Bu).$$

En tales circunstancias, se hace uso de la siguiente propiedad, de carácter fundamental:

$$p \in \partial g(Bu) \iff p = g'_\lambda(Bu + \lambda p)$$

donde λ es *cualquier número real positivo* y g'_λ es la *regularizada Yosida* del operador maximal monótono ∂g , es decir:

$$g'_\lambda = \frac{1}{\lambda}(Id - (Id + \lambda \partial g)^{-1})$$

Es bien conocido que g'_λ es univaluada y Lipschitz-continua. Utilizando la equivalencia que precede para evitar la ambigüedad en la segunda relación de (9), en [12] se propone el siguiente esquema semi-implícito para calcular una solución de (8) y, consecuentemente, de (7):

Algoritmo A

- (a) Fijar $\lambda > 0$ y $p_0 \in H$.
 - (b) Después, dados $k \geq 0$ y $p_k \in H$, calcular $u_{k+1} \in V$ y $p_{k+1} \in H$ tales que
- (10) $\partial f(u_{k+1}) \ni B^* p_k, \quad p_{k+1} = g'_\lambda(B u_{k+1} + \lambda p_k).$

■

En el caso particular del problema (1), el algoritmo A precedente se reduce a lo siguiente:

Algoritmo A'

- (a) Fijar $\lambda > 0$ y $p_0 \in L^2(\Omega)$.
- (b) Después, dados $k \geq 0$ y $p_k \in L^2(\Omega)$,

 - (b.1) Calcular $u_{k+1} \in H_0^1(\Omega)$, solución de $\begin{cases} -\Delta u = p_k \text{ en } \Omega \\ u = 0 \text{ sobre } \partial\Omega \end{cases}$
 - (b.2) Tomar $p_{k+1}(x) = H_\lambda(u_{k+1}(x) + \alpha(x) + \lambda p_k(x))$ c.p.d. en Ω .

■

A continuación, consideremos un segundo problema de carácter general, esta vez un problema con restricciones. Se trata de

$$(11) \quad \left\{ \begin{array}{l} \text{Minimizar } J^*(v) = g^*(q) - f^*(B^* q) \\ \text{sujeto a } q \in \partial K \end{array} \right.$$

donde f , g y B son como antes y K es un subconjunto convexo cerrado de H , de frontera ∂K no vacía. Para elecciones adecuadas de V , H , f , g , B y K , los problemas (2) y (3) pueden escribirse en la forma (11). Por analogía con lo que precede, tiene sentido recurrir al siguiente esquema, propuesto por primera vez en [12]:

Algoritmo B

- (a) Fijar $\lambda > 0$ y $p_0 \in H$.
- (b) Despues, dados $k \geq 0$ y $p_k \in H$, calcular $u_{k+1} \in V$ y $p_{k+1} \in H$ tales que

$$(12) \quad \begin{aligned} u_{k+1} &\in \partial f^*(B^* p_k) + B^{-1} N_{\partial K}(p_k), \\ p_{k+1} &= g'_\lambda(B u_{k+1} + \lambda p_k), \quad p_{k+1} \in \partial K. \end{aligned}$$

Aquí, $N_{\partial K}(p)$ es el subcono normal a ∂K en p , y las iteraciones en (12) deben ser interpretadas en el sentido siguiente: La elección de la "componente" de u_{k+1} en $B^{-1} N_{\partial K}(p_k)$ debe ser tal que se tenga $p_{k+1} \in \partial K$.

Por ejemplo, en el caso del problema (2), ha de tomarse

$$K = \{ q \in L^2(\Omega); \int_\Omega q \, dx \leq I \}$$

de donde $N_{\partial K}(p) = \mathbb{R} \quad \forall p \in \partial K$. En esta situación particular, el algoritmo B se reduce a:

Algoritmo B'

- (a) Fijar $\lambda > 0$ y $p_0 \in L^2(\Omega)$
- (b) Despues, dados $k \geq 0$ y $p_k \in L^2(\Omega)$,
 - (b.1) Calcular $u_{k+1} \in H_0^1(\Omega)$, solución de $\begin{cases} -\mathcal{L}u = p_k & \text{en } \Omega \\ u = 0 & \text{sobre } \partial\Omega \end{cases}$
 - (b.2) Calcular $\beta_{k+1} \in \mathbb{R}$ resolviendo la ecuación escalar

$$F_k(\beta) \equiv \int_\Omega (rH)_\lambda(u_{k+1} + \beta + \lambda p_k) \, dx = I$$
 - (b.3) Tomar $p_{k+1}(x) = (rH)_\lambda(u_{k+1}(x) + \beta_{k+1} + \lambda p_k(x))$ c.p.d. en Ω .

En lo que respecta a los problemas (5) y (6), se utilizan técnicas que reposan sobre las mismas ideas y que han sido adaptadas al caso de sistemas elípticos de dos ecuaciones. Por simplicidad de exposición, admitamos que las EDP de (5) pueden ser re-escritas en la forma

$$(13) \quad \begin{cases} -\Delta u(x) + \alpha(u(x))f(v(x)) \ni 0 \\ -\Delta v(x) + \beta(u(x))g(v(x)) \ni 0 \end{cases} \quad \text{c.p.d. en } \Omega$$

para adecuadas funciones $f, g \in C^1(\mathbb{R})$ y adecuados operadores maximales monótonos α y β .

Los argumentos de [12] no tienen aplicación en este caso, ya que es inútil buscar funciones convexas F y Q tales que cualquier solución de la inclusión

$$\partial F\begin{pmatrix} u \\ v \end{pmatrix} - \partial Q\begin{pmatrix} u \\ v \end{pmatrix} \ni 0$$

resuelva (13). Debido a ello, razonando como en [10], se introduce el siguiente problema, de carácter general:

$$(14) \quad \begin{cases} \text{Hallar } \begin{pmatrix} \bar{u} \\ \bar{v} \end{pmatrix} \in V_1 \times V_2 \text{ tal que} \\ \partial F\begin{pmatrix} \bar{u} \\ \bar{v} \end{pmatrix} - (K_{\bar{v}}^* \circ \partial G)\left(\sigma\begin{pmatrix} \bar{u} \\ \bar{v} \end{pmatrix}\right) \ni 0 \end{cases}$$

Aquí, V_1 , V_2 , X_1 y X_2 son espacios de Hilbert tales que $V_i \hookrightarrow X_i$ con inyección compacta y densa para $i = 1, 2$, y para los que se hacen las identificaciones habituales

$$V_i \hookrightarrow X_i \equiv X'_i \hookrightarrow V'_i$$

Se supone también que $F : V_1 \times V_2 \rightarrow \mathbb{R}$ es una función convexa y C^1 , $G : X_1 \times X_2 \rightarrow \mathbb{R}$ es una función convexa, semicontinua inferiormente y propia, $\sigma \in \mathcal{L}(V_1 \times V_2; X_1 \times X_2)$ y $K_w \in \mathcal{L}(V_1 \times V_2; X_1 \times X_2)$ para cada $w \in V_2$. Los problemas (5) y (6) son casos particulares de (14) para determinadas elecciones de V_i , X_i , F , G , σ y los K_w .

En las aplicaciones a problemas elípticos semilineales con términos discontinuos, F corresponde a la "parte elíptica" de las EDP, mientras que G vendrá determinada por los términos no lineales.

El algoritmo propuesto en [10] para resolver (14) es el siguiente:

Algoritmo C

(a) Fijar $\lambda > 0$, $\begin{pmatrix} p_0 \\ q_0 \end{pmatrix} \in X_1 \times X_2$ y $v_0 \in V_2$.

(b) Después, dados $k \geq 0$, $\begin{pmatrix} p_k \\ q_k \end{pmatrix} \in X_1 \times X_2$ y $v_k \in V_2$, calcular $\begin{pmatrix} u_{k+1} \\ v_{k+1} \end{pmatrix} \in V_1 \times V_2$ y $\begin{pmatrix} p_{k+1} \\ q_{k+1} \end{pmatrix} \in X_1 \times X_2$ tales que

$$(15) \quad \begin{aligned} \partial F \begin{pmatrix} u_{k+1} \\ v_{k+1} \end{pmatrix} &\ni K_{v_k}^* \begin{pmatrix} p_k \\ q_k \end{pmatrix} \\ \begin{pmatrix} p_{k+1} \\ q_{k+1} \end{pmatrix} &= G'_\lambda \left(\sigma \begin{pmatrix} u_{k+1} \\ v_{k+1} \end{pmatrix} + \lambda \begin{pmatrix} p_k \\ q_k \end{pmatrix} \right) \end{aligned}$$

Por ejemplo, en la situación particular que corresponde al problema (5), el algoritmo C es como sigue:

Algoritmo C'

(a) Fijar $\lambda > 0$, $\begin{pmatrix} p_0 \\ q_0 \end{pmatrix} \in L^2(\Omega) \times L^2(\Omega)$ y $v_0 \in H_0^1(\Omega)$.

(b) Después, dados $k \geq 0$, $\begin{pmatrix} p_k \\ q_k \end{pmatrix} \in L^2(\Omega) \times L^2(\Omega)$ y $v_k \in H_0^1(\Omega)$, calcular $u_{k+1} \in H_0^1(\Omega)$, solución de

$$\begin{cases} -\Delta u = -\mu^2 p_k \exp\left(\frac{\gamma v_k}{v_k + 1}\right) & \text{en } \Omega \\ u = 0 & \text{sobre } \partial\Omega \end{cases}$$

y $v_{k+1} \in H_0^1(\Omega)$, solución de

$$\begin{cases} -\Delta v = \nu \mu^2 q_k \exp\left(\frac{\gamma v_k}{v_k + 1}\right) & \text{en } \Omega \\ v = 0 & \text{sobre } \partial\Omega \end{cases}$$

Tomar

$$\begin{aligned} p_{k+1} &= H_\lambda(u_{k+1} + 1 + \lambda p_k) \\ q_{k+1} &= H_\lambda(u_{k+1} + 1 + \lambda q_k) \end{aligned}$$

En la segunda parte de esta memoria, presentamos

- (a) Diversas consideraciones de carácter teórico sobre los problemas elípticos (1) a (6), las formulaciones generales (7), (8), (11) y (14) y los algoritmos **A**, **B** y **C** que preceden. Junto con éstos, se formulan otros que dan lugar a iteraciones mejor condicionadas desde el punto de vista numérico.
- (b) Un análisis detallado de las versiones "discretas" de estos algoritmos (aproximaciones en el sentido de los elementos finitos).
- (c) Resultados numéricos sobre diversos problemas test. En la obtención de estos resultados, se ha usado la biblioteca MODULEF (cf. [3]).

La segunda parte de esta memoria consta de tres capítulos. A continuación, haremos una breve descripción de los mismos.

En el capítulo 1, se describe y se lleva a cabo la resolución numérica de los problemas (1) y (2). En el estudio teórico previo, se usan (con ligeras variantes) los argumentos de [12] para la demostración de un resultado de convergencia. Las experiencias numéricas son diversas. En el caso más interesante del problema (2), han sido comparadas satisfactoriamente con otras previas.

En el capítulo 2, se resuelven desde el punto de vista numérico los problemas (3) y (4). En el caso del problema (3), se usa la versión correspondiente del algoritmo **B** y un nuevo algoritmo, cuyo comportamiento numérico parece ser más adecuado (cf. el algoritmo 2 en este capítulo). En el contexto del problema (4), al no ser posible una reformulación tal como (11), la situación es más complicada. Con todo, se consigue formular un nuevo esquema (cf. el algoritmo 3), basado en ideas análogas. El capítulo también contiene consideraciones de carácter teórico y los resultados de varias experiencias numéricas.

Finalmente, el capítulo 3 está dedicado a la resolución numérica de los problemas (5) y (6). Como hemos dicho, se han usado ideas que tienen su origen en [10]. Se recuerdan algunos resultados de convergencia y, de nuevo, se ilustra el comportamiento de los algoritmos propuestos con algunos resultados numéricos.

Las aportaciones originales correspondientes a la segunda parte de esta memoria son las siguientes:

- La formulación de nuevos algoritmos de regularización exacta (y su validación numérica), en el caso de "problemas no variacionales".
- El análisis numérico de este tipo de algoritmos, que han sido discretizados por el método de los elementos finitos (versión P_1 -Lagrange) y, también, los resultados numéricos obtenidos sobre una gran variedad de ejemplos test significativos.

Las principales dificultades encontradas fueron las siguientes:

- El hecho de que los problemas considerados posean no linealidades discontinuas, que "obliga" a cambiar la formulación de partida.
- En algunos casos, la ausencia de formulación variacional, que dificulta la formulación y el análisis de los algoritmos correspondientes.
- La posible no unicidad de solución y su incidencia en la convergencia de los algoritmos propuestos.

Referencias

- [1] R. ARIS, *The Mathematical Theory of Diffusion and Reaction in Permeable Catalysts*. Clarendon Press, Oxford, 1975.
- [2] C. BEGUE, O. PIRONNEAU, *Hyperbolic Systems with Periodic Boundary Condition: An Example with Euler Equations*. Comp. & Math. with Appl. Vol. 11, pp. 113-128, 1985.
- [3] M. BERNADOU et al., *MODULEF: Une Bibliothèque Modulaire d'Éléments Finis*. INRIA, Rocquencourt, 1985.
- [4] M.O. BRISTEAU, J. PÉRIAUX, *Finite Element Methods for the Calculation of Compressible Viscous Flows using Self-Adaptive Mesh Refinement*. L. N. Comp. Fluid Dynamics, 1986.
- [5] A. BUCKLEY, A. LENIR, *QN-like variable storage conjugate gradients*. Math. Programming 27, 2, pp. 155-175, 1984.
- [6] T. CHACÓN, *Etude d'un Modèle pour la Convection des Microstructures*. Thèse 3ème Cycle, Université P. & M. Curie (Paris VI), 1985.
- [7] T. CHACÓN, *Oscillations Due to the Transport of Microstructures*. SIAM J. Appl. Math 8, No. 5, 1988, pp. 1128-1146.
- [8] T. CHACÓN, J. COUCE, R. ECHEVARRÍA, E. FERNÁNDEZ-CARA, J.D. MARTÍN, F. ORTEGÓN, *Mathematical Modelling of Turbulence: Validation of the Numerical Simulation of Turbulence by Asymptotic Techniques. Two-Dimensional Analysis of the Heat Transfert in the Re-circulating Zone of the HERMES Aircraft*. Reports 1, 2, 3 and 4 of the HERMES Contract RDANE 23/87, (University of Sevilla, Avions Marcel Dassault-Breguet Aviation), 1987-1990.

- [9] T. CHACÓN, O. PIRONNEAU. *On the Mathematical Foundations of $k-\varepsilon$ Turbulent Model.* Vistas in Applied Mathematics, A.V. Balaji Krishnan, A. Dorodnitsyn, J.L. Lions eds., Springer-Verlag, pp. 44-56, New York, 1986.
- [10] M. DELGADO, E. FERNÁNDEZ-CARA, *An Iterative Method for the Solution of Some Semilinear Elliptic Systems with Discontinuities.* Appl. Math. Optim.. No. 31, 1995, pp. 101-116.
- [11] J.I. DÍAZ, J. HERNÁNDEZ, *On the existence of a free boundary for a class of reaction-diffusion systems.* SIAM J. Math. Anal., Vol. 15, No. 4, July 1984, pp. 670-685.
- [12] E. FERNÁNDEZ-CARA, C. MORENO, *Critical Point Approximation Through Exact Regularization.* Math. of Comp. Vol. 50, No. 181, January 1988, pp. 139-153.
- [13] L.E. FRAENKEL, M.S. BERGER, *On the global theory of vortex rings in an ideal fluid.* Acta Math.. Vol. 132, 1974, pp. 13-51.
- [14] R. GLOWINSKI, *Numerical Methods for Nonlinear Variational Problems.* Springer Series in Comp. Phys., Springer-Verlag, New York, 1984.
- [15] R. GLOWINSKI, O. PIRONNEAU, *On a Mixed Finite Element Approximation of the Stokes Problems (I): Convergence of Approximate Solution.* Num. Math. 33, pp. 397-424, 1979.
- [16] D. HOFF, *Global Solutions of the Navier-Stokes Equations for Multi-dimensional Compressible Flow with Discontinuous Initial Data.* En Proceedings of the Fourth International Conference on Navier-Stokes Equations, Toulon-Hyères, Mayo 1995 (aparecerá).
- [17] A.V. KAZHIKHOV, *On the Global Existence Theorem for Two-Dimensional Compressible Viscous Flows.* En Proceedings of the Fourth International Conference on Navier-Stokes Equations, Toulon-Hyères, Mayo 1995 (aparecerá).
- [18] P.L. LIONS. C. R. Acad. Sci. Paris, t. 316, Série I, pp. 1335-1340; t. 317, Série I, pp. 115-120; t. 317, Série I, pp. 1197-1202. 1993.

- [19] P.L. LIONS, *Sur les équations de Navier-Stokes Compressibles.* En Proceedings of the Fourth International Conference on Navier-Stokes Equations, Toulon-Hyères, Mayo 1995 (aparecerá).
- [20] A. MATSUMURA, T. NISHIDA, *Initial-Boundary Value Problems for the Equations of Motion of General Fluids.* En Proceedings of Computing Methods in Applied Sciences and Engineering. V, Versailles. 1981, R. Glowinski & J.L. Lions eds., North-Holland. Amsterdam 1982.
- [21] D. McLAUGHLIN, G. PAPANICOLAOU, O. PIRONNEAU, *Convection of Microstructures and Related Problems.* SIAM J. Appl. Math. 45. pp. 780-797 (1985).
- [22] B. MOHAMMADI, O. PIRONNEAU, *Analysis of the k-epsilon Turbulence Model.* Wiley-Masson, Paris 1994.
- [23] J. NORBURY, *Steady planar vortex pairs in an ideal fluid.* Comm. Pure Appl. Math., Vol. 28, 1975, pp. 679-700.
- [24] F. ORTEGÓN, *Tabulations of the Closure Tensors for the M.P.P. Model of Turbulence.* Rapport de Recherche I.N.R.I.A. No. 757, Rocquencourt, 1987.
- [25] F. ORTEGÓN, *Modélisation des Ecoulements Turbulents à deux Echelles par méthode d'Homogénéisation.* Thèse de Doctorat, Université P. & M. Curie (Paris VI), 1989.
- [26] R. TÉMAM, *A nonlinear eigenvalue problem: The shape at equilibrium of a confined plasma.* Arch. Rational Mech. Anal., Vol. 60, 1975. pp. 51-73.
- [27] R. TÉMAM, *Remarks on a free boundary problem arising in plasma physics.* Comm. Partial Differential Equations. Vol. 2. 1977. pp. 41-61.

PARTE I

A continuación se presentan los capítulos 1 a 4 de la primera parte,
que corresponden, respectivamente a los capítulos 1, 3 y 4 del Informe No. 2
y al capítulo 2 del Informe No. 4 del Contrato de Investigación

HERMES RDANE 23/87

(Universidad de Sevilla—Avions Marcel Dassault-Bréguet Aviation)

Capítulo 1

Estudio preliminar

1. PRELIMINARY STUDY

1.1 The compressible 2D Navier-Stokes problem

The nonconservative and conservative formulations:

$$(1) \quad \frac{\partial p}{\partial t} + \nabla \cdot (\rho \vec{u}) = 0$$

$$(2) \quad \frac{\partial}{\partial t}(\rho \vec{u}) + \nabla \cdot (\rho \vec{u} \otimes \vec{u}) + \nabla p = \frac{1}{Re} \nabla \cdot \left\{ \rho \left(\nabla \vec{u} + \nabla \vec{u}^T - \frac{2}{3} (\nabla \cdot \vec{u}) \text{Id} \right) \right\}$$

$$(3) \quad \frac{\partial p}{\partial t} + \nabla \cdot ((e+p)\vec{u}) = \frac{1}{Re} \left\{ \nabla \cdot \left(\vec{u} \cdot \left(\nabla \vec{u} + \nabla \vec{u}^T - \frac{2}{3} (\nabla \cdot \vec{u}) \text{Id} \right) \right) + \frac{\gamma}{Pr} \Delta \varepsilon \right\}$$

$$(4) \quad e = p \left(\varepsilon + \frac{1}{2} |\vec{u}|^2 \right)$$

in $\Omega \times (0, T)$

$$(5) \quad p = (\gamma - 1) \rho \varepsilon$$

$$(6) \quad \varepsilon = \theta$$

This can be rewritten as follows:

$$(7) \quad \frac{\partial}{\partial t} \vec{U} + \frac{\partial}{\partial x_1} F^1 + \frac{\partial}{\partial x_2} F^2 = \frac{1}{Re} \left(\frac{\partial}{\partial x_1} G^1 + \frac{\partial}{\partial x_2} G^2 \right)$$

$$\vec{U} = \begin{bmatrix} p \\ \rho u_1 \\ \rho u_2 \\ e \end{bmatrix} \quad F^1 = \begin{bmatrix} pu_1 \\ pu_1^2 + p \\ pu_1 u_2 \\ u_1(e+p) \end{bmatrix} \quad F^2 = \begin{bmatrix} pu_2 \\ pu_1 u_2 \\ pu_2^2 + p \\ u_2(e+p) \end{bmatrix}$$

$$G^1 = \begin{bmatrix} 0 \\ \frac{4}{3} \frac{\partial u_1}{\partial x_1} - \frac{2}{3} \frac{\partial u_2}{\partial x_2} \\ \frac{\partial u_1}{\partial x_2} + \frac{\partial u_2}{\partial x_1} \\ u_1 \left(\frac{4}{3} \frac{\partial u_1}{\partial x_1} - \frac{2}{3} \frac{\partial u_2}{\partial x_2} \right) + u_2 \left(\frac{\partial u_1}{\partial x_2} + \frac{\partial u_2}{\partial x_1} \right) + \frac{\gamma}{Pr} \frac{\partial \varepsilon}{\partial x_1} \end{bmatrix}$$

$$G^2 = \begin{bmatrix} 0 \\ \frac{\partial u_1}{\partial x_2} + \frac{\partial u_2}{\partial x_1} \\ \frac{4}{3} \frac{\partial u_2}{\partial x_2} - \frac{2}{3} \frac{\partial u_1}{\partial x_1} \\ u_1 \left(\frac{\partial u_1}{\partial x_2} + \frac{\partial u_2}{\partial x_1} \right) + u_2 \left(\frac{4}{3} \frac{\partial u_2}{\partial x_2} - \frac{2}{3} \frac{\partial u_1}{\partial x_1} \right) + \frac{\gamma}{Pr} \frac{\partial \varepsilon}{\partial x_2} \end{bmatrix}$$

All quantities have been made dimensionless by means of reference density, velocity, length and specific heat parameters, resp.

ρ_r , $|\vec{u}_r|$, l_r and c_v .

In terms of ρ , \vec{u} and θ , (1)-(6) take the following non-conservative form:

$$(8) \quad \frac{\partial \rho}{\partial t} + \rho \nabla \cdot \vec{u} + \vec{u} \cdot \nabla \rho = 0$$

$$(9) \quad \rho \frac{\partial \vec{u}}{\partial t} + \rho (\vec{u} \cdot \nabla) \vec{u} + (\gamma - 1) \nabla (\rho \theta) = \frac{1}{Re} \nabla \cdot \left\{ \rho \left(\frac{\nabla \vec{u}}{\sim} + \frac{\nabla \vec{u}^T}{\sim} - \frac{2}{3} (\nabla \cdot \vec{u}) \text{Id.} \right) \right\}$$

$$(10) \quad \rho \frac{\partial \theta}{\partial t} + \rho \vec{u} \cdot \nabla \theta + (\gamma - 1) \rho \theta \nabla \cdot \vec{u} = \frac{1}{Re} \left(\frac{\gamma}{Pr} \Delta \theta + F(\nabla \vec{u}) \right)$$

with

$$\begin{aligned} F(\nabla \vec{u}) &\equiv \frac{4}{3} \left(\left(\frac{\partial u_1}{\partial x_1} \right)^2 + \left(\frac{\partial u_2}{\partial x_2} \right)^2 + \left(\frac{\partial u_3}{\partial x_3} \right)^2 \right) \\ &+ \left(\frac{\partial u_1}{\partial x_2} + \frac{\partial u_2}{\partial x_1} \right)^2 + \left(\frac{\partial u_1}{\partial x_3} + \frac{\partial u_3}{\partial x_1} \right)^2 + \left(\frac{\partial u_2}{\partial x_3} + \frac{\partial u_3}{\partial x_2} \right)^2 \\ &- \frac{4}{3} \left(\frac{\partial u_1}{\partial x_1} \frac{\partial u_2}{\partial x_2} + \frac{\partial u_1}{\partial x_1} \frac{\partial u_3}{\partial x_3} + \frac{\partial u_2}{\partial x_2} \frac{\partial u_3}{\partial x_3} \right) \end{aligned}$$

We are primarily concerned with isentropic flows, for which

$$(11) \quad \bar{\rho} = K \rho^\gamma$$

The energy equation (10) disappears and (5), (6), (8), (9) give:

$$(12) \quad \frac{\partial \rho}{\partial t} + \rho \nabla \cdot \vec{u} + \vec{u} \cdot \nabla \rho = 0$$

$$(13) \quad \frac{\partial \vec{u}}{\partial t} + (\vec{u} \cdot \nabla) \vec{u} + K \gamma \rho^{\gamma-2} \nabla \rho = \frac{1}{\rho Re} \nabla \cdot \left\{ \rho \left(\frac{\nabla \vec{u}}{\sim} + \frac{\nabla \vec{u}^T}{\sim} - \frac{2}{3} (\nabla \cdot \vec{u}) \text{Id.} \right) \right\}$$

Introducing $\sigma = \log \rho$, one has:

$$(12) \quad \frac{\partial \sigma}{\partial t} + \nabla \cdot \vec{u} + \vec{u} \cdot \nabla \sigma = 0$$

$$(13) \quad \frac{\partial \vec{u}}{\partial t} + (\vec{u} \cdot \nabla) \vec{u} + K \gamma e^{(\gamma-1)\sigma} \nabla \sigma = \frac{\epsilon^{-\sigma}}{Re} \nabla \cdot \left(e^{\sigma} (\nabla \vec{u} + \nabla \vec{u}^T - \frac{2}{3} (\nabla \cdot \vec{u}) \text{Id.}) \right)$$

1.2 Boundary conditions for: - Channel flow

- Flow around and past an obstacle

A) The fluid flows in a channel (Fig. 1)

Variables : σ and \vec{u}

$$(14) \quad \sigma = \sigma_\infty \text{ on } \Gamma_\infty^- \quad (\sigma_\infty \text{ a constant, possibly } 0)$$

$$(15) \quad \vec{u} = \vec{u}_\infty \text{ on } \Gamma_\infty^- \quad (\text{possibly Poiseuille profile})$$

$$(16) \quad \vec{u} = 0 \text{ on } \Gamma_B$$

$$(17) \quad \begin{cases} \left\{ -\frac{K\gamma}{\gamma-1} e^{(\gamma-1)\sigma} \text{Id.} + \frac{1}{Re} \left(\nabla \vec{u} + \nabla \vec{u}^T - \frac{2}{3} (\nabla \cdot \vec{u}) \text{Id.} \right) \right\} \cdot \vec{n} = 0 \\ \text{on } \Gamma_\infty^+ \quad (\text{the natural condition}) \end{cases}$$

B) The fluid flows around and past an obstacle (Fig. 2)

$$(18) \quad \sigma = \sigma_\infty \text{ on } \Gamma_\infty^- \quad (\sigma_\infty \text{ a constant, possibly } 0)$$

$$\Gamma_\infty^- = \{x / x \in \Gamma, \vec{u}_\infty \cdot \vec{n}(x) < 0\}, \quad \Gamma_\infty^+ = \Gamma \setminus \Gamma_\infty^-$$

$$(19) \quad \vec{u} = \vec{u}_\infty \text{ on } \Gamma_\infty^- \quad (\vec{u}_\infty \text{ a constant unit vector})$$

$$(20) \quad \vec{u} = 0 \text{ on } \Gamma_B$$

$$(21) \quad \begin{cases} \left\{ -\frac{K\gamma}{\gamma-1} e^{(\gamma-1)\sigma} \text{Id.} + \frac{1}{Re} \left(\nabla \vec{u} + \nabla \vec{u}^T - \frac{2}{3} (\nabla \cdot \vec{u}) \text{Id.} \right) \right\} \cdot \vec{n} = 0 \\ \text{on } \Gamma_\infty^+ \quad (\text{the natural condition}) \end{cases}$$

Of course, K is given by

$$(22) \quad K = \frac{1}{\gamma M_\infty^2}.$$

1.3 The numerical solution of the problem

A) Time discretization for the nonconservative formulation (14)-(15)

(A.1) Euler's backward scheme ($\alpha = 1/\Delta t$)

$$(23) \quad \alpha \vec{\sigma}^{n+1} + \nabla \cdot \vec{u}^{n+1} + \vec{u}^{n+1} \cdot \nabla \vec{\sigma}^{n+1} = \alpha \vec{\sigma}^n$$

$$(24) \quad \left\{ \begin{array}{l} \alpha \vec{\sigma}^{n+1} + (\vec{u}^{n+1} \cdot \nabla) \vec{u}^{n+1} + K \tau e^{(\gamma-1)\vec{\sigma}^{n+1}} \nabla \vec{\sigma}^{n+1} \\ - \frac{e^{-\vec{\sigma}^{n+1}}}{Re} \nabla \cdot (e^{\vec{\sigma}^{n+1}} \mathcal{D}(\vec{u}^{n+1})) = \alpha \vec{u}^n \end{array} \right.$$

$$(25) \quad \vec{\sigma}^{n+1} = \vec{\sigma}_\infty, \quad \vec{u}^{n+1} = \vec{u}_\infty \quad \text{on } \Gamma^-$$

$$(26) \quad \vec{u}^{n+1} = 0 \quad \text{on } \Gamma_B$$

$$(27) \quad \left\{ - \frac{K \tau}{\gamma-1} e^{(\gamma-1)\vec{\sigma}^{n+1}} \mathcal{D}(\vec{u}^{n+1}) \right\} \cdot \vec{n} = 0 \quad \text{on } \Gamma^+$$

Of course, $\vec{\sigma}^0$, \vec{u}^0 are given by initial conditions:

$$(28) \quad \vec{\sigma}^0 = \vec{\sigma}_0(x) \quad \text{in } \Omega$$

$$(29) \quad \vec{u}^0 = \vec{u}_0(x) \quad \text{in } \Omega$$

(A.2) Gear's scheme ($\alpha = 3/2\Delta t$)

$$(30) \quad \alpha \vec{\sigma}^{n+1} + \nabla \cdot \vec{u}^{n+1} + \vec{u}^{n+1} \cdot \nabla \vec{\sigma}^{n+1} = \alpha (4\vec{\sigma}^n - \vec{\sigma}^{n-1})$$

$$(31) \quad \left\{ \begin{array}{l} \alpha \vec{\sigma}^{n+1} + (\vec{u}^{n+1} \cdot \nabla) \vec{u}^{n+1} + K \tau e^{(\gamma-1)\vec{\sigma}^{n+1}} \nabla \vec{\sigma}^{n+1} \\ - \frac{e^{-\vec{\sigma}^{n+1}}}{Re} \nabla \cdot (e^{\vec{\sigma}^{n+1}} \mathcal{D}(\vec{u}^{n+1})) = \alpha (4\vec{u}^n - \vec{u}^{n-1}) \end{array} \right.$$

The boundary conditions for $\vec{\sigma}^{n+1}$, \vec{u}^{n+1} are (25)-(27). $\vec{\sigma}^0$ and \vec{u}^0 are given as in (28)-(29) by the initial conditions. $\vec{\sigma}^1$ and \vec{u}^1 are computed as follows:

- One solves twice (23)-(27) with $n=0,1$ but with $\alpha = 3/2\Delta t$

One thus obtains

$$\hat{\sigma}^1, \vec{u}^1 \quad \text{and} \quad \hat{\sigma}^2, \vec{u}^2$$

- Then, one sets

$$(32) \quad \sigma^1 = \frac{1}{2} (\hat{\sigma}^1 + \hat{\sigma}^2), \quad \vec{u}^1 = \frac{1}{2} (\vec{u}^1 + \vec{u}^2)$$

Remark: A possibly more accurate formula for σ^1 and \vec{u}^1 :

$$(33) \quad \sigma^1 = \frac{1}{8} (-\sigma^0 + 6\hat{\sigma}^1 + 3\hat{\sigma}^2), \quad \vec{u}^1 = \frac{1}{8} (-\vec{u}^0 + 6\vec{u}^1 + 3\vec{u}^2)$$

(A.3) A Peaceman-Rachford's scheme ($\alpha = 3/2\Delta t$)

We first reformulate (14)-(15):

$$(34) \quad \frac{\partial \vec{u}}{\partial t} + \nabla \cdot \vec{u} = - \vec{u} \cdot \nabla \sigma$$

$$(35) \quad \frac{\partial \vec{u}}{\partial t} - \mu \Delta \vec{u} + \beta \nabla \sigma = \vec{\Phi}(\sigma, \vec{u})$$

with

$$\begin{aligned} \vec{\Phi}(\sigma, \vec{u}) &\equiv -(\vec{u} \cdot \nabla) \vec{u} + (\beta - K \gamma e^{(r-1)\sigma}) \nabla \sigma \\ &+ \frac{e^{-\sigma}}{Re} \nabla \cdot (e^\sigma \vec{D}(\vec{u})) - \mu \Delta \vec{u} \end{aligned}$$

$$\mu = 1/Re$$

β : a typical value for $K \gamma e^{(r-1)\sigma}$

$$(\text{e.g. } \beta = 1/M_\infty^2)$$

We compute σ^{n+1} , \vec{u}^{n+1} from σ^n , \vec{u}^n in two steps:

First step

$$(36) \quad \alpha \sigma^{n+\frac{1}{2}} + \nabla \cdot \vec{u}^{n+\frac{1}{2}} = - \vec{u}^n \cdot \nabla \sigma^n + \alpha \sigma^n$$

$$(37) \quad \alpha \vec{u}^{n+\frac{1}{2}} - \mu \Delta \vec{u}^{n+\frac{1}{2}} + \beta \nabla \sigma^{n+\frac{1}{2}} = \vec{\Phi}(\sigma^n, \vec{u}^n) + \alpha \vec{u}^n$$

$$(38) \quad \sigma^{n+\frac{1}{2}} = \sigma_\infty, \quad \vec{u}^{n+\frac{1}{2}} = \vec{u}_\infty \quad \text{on } \Gamma_\infty^-$$

$$(39) \quad \vec{u}^{n+\frac{1}{2}} = 0 \quad \text{on } \Gamma_B$$

$$(40) \quad \left\{ \begin{array}{l} (-\beta \sigma^{n+\frac{1}{2}} \text{Id.} + \mu \nabla \vec{u}^{n+\frac{1}{2}}) \cdot \vec{n} \\ = \left\{ (-\beta \sigma^n + \frac{KR}{T-1} e^{(T-1)\sigma^n}) \text{Id.} + \mu \nabla \vec{u}^n - \frac{1}{Re} \mathcal{D}(\vec{u}^n) \right\} \cdot \vec{n} \\ \text{on } \Gamma_\infty^+ \end{array} \right.$$

Second step

$$(41) \quad \alpha \sigma^n + \vec{u}^{n+1} \cdot \nabla \sigma^{n+1} = - \nabla \cdot \vec{u}^{n+\frac{1}{2}} + \alpha \sigma^{n+\frac{1}{2}}$$

$$(42) \quad \alpha \vec{u}^n - \vec{\Phi}(\sigma^{n+1}, \vec{u}^{n+1}) = \mu \Delta \vec{u}^{n+\frac{1}{2}} - \beta \nabla \sigma^{n+\frac{1}{2}} + \alpha \vec{u}^{n+\frac{1}{2}}$$

$$(43) \quad \sigma^n = \sigma_\infty, \quad \vec{u}^n = \vec{u}_\infty \quad \text{on } \Gamma_\infty^-$$

$$(44) \quad \vec{u}^n = 0 \quad \text{on } \Gamma_B$$

$$(45) \quad \left\{ \begin{array}{l} \left\{ -\frac{KR}{T-1} e^{(T-1)\sigma^{n+1}} \text{Id.} + \frac{1}{Re} \mathcal{D}(\vec{u}^{n+1}) \right\} \cdot \vec{n} \\ = (-\beta \sigma^{n+\frac{1}{2}} \text{Id.} + \mu \nabla \vec{u}^{n+\frac{1}{2}}) \cdot \vec{n} \quad \text{on } \Gamma_\infty^+ \end{array} \right.$$

Again, σ^0, \vec{u}^0 are given by the initial conditions, as in (28)-(29). An analysis of this scheme shows that it is probably not too good for the computation of stationary or quasi-stationary solutions.

(A.4) A θ - scheme

$$\theta \in (0, 1/2) \quad \theta' = 1 - 2\theta, \quad \alpha = 1/\theta \Delta t, \quad \alpha' = 1/\theta' \Delta t$$

We use again (34)-(35). We compute σ^{n+1} , \vec{u}^{n+1} from σ^n , \vec{u}^n in three steps:

First step ($a, b > 0$, $a+b=1$)

$$(46) \quad \alpha \sigma^{n+\theta} + \nabla \cdot \vec{u}^{n+\theta} = - \vec{u}^n \cdot \nabla \sigma^n + \alpha \sigma^n$$

$$(47) \quad \left\{ \begin{array}{l} \alpha \vec{u}^{n+\theta} - a\mu \Delta \vec{u}^{n+\theta} + \beta \nabla \sigma^{n+\theta} = \bar{\Phi}(\sigma^n, \vec{u}^n) + b\mu \Delta \vec{u}^n \\ \qquad \qquad \qquad + \alpha \vec{u}^n \end{array} \right.$$

$$(48) \quad \sigma^{n+\theta} = \sigma_\infty, \quad \vec{u}^{n+\theta} = \vec{u}_\infty \quad \text{on } \Gamma_\infty^-$$

$$(49) \quad \vec{u}^{n+\theta} = 0 \quad \text{on } \Gamma_B$$

$$(50) \quad \left\{ \begin{array}{l} \sim (-\beta \sigma^{n+\theta} \text{Id.} + a\mu \nabla \vec{u}^{n+\theta}) \cdot \vec{n} \\ \sim = \left\{ \left(-\beta \sigma^n + \frac{K\tau}{\tau-1} e^{(\tau-1)\sigma^n} \right) \text{Id.} + a\mu \nabla \vec{u}^n - \frac{1}{Re} \mathcal{D}(\vec{u}^n) \right\} \cdot \vec{n} \\ \text{on } \Gamma_\infty^+ \end{array} \right.$$

Second step

$$(51) \quad \alpha' \sigma^{(n+1)-\theta} + \vec{u}^{(n+1)-\theta} \cdot \nabla \sigma^{(n+1)-\theta} = - \nabla \cdot \vec{u}^{n+\theta} + \alpha' \sigma^{n+\theta}$$

$$(52) \quad \left\{ \begin{array}{l} \alpha' \vec{u}^{(n+1)-\theta} - b\mu \Delta \vec{u}^{(n+1)-\theta} - \bar{\Phi}(\sigma^{(n+1)-\theta}, \vec{u}^{(n+1)-\theta}) \\ = a\mu \Delta \vec{u}^{n+\theta} - \beta \nabla \sigma^{n+\theta} + \alpha' \vec{u}^{n+\theta} \end{array} \right.$$

$$(53) \quad \sigma^{(n+1)-\theta} = \sigma_\infty, \quad \vec{u}^{(n+1)-\theta} = \vec{u}_\infty \quad \text{on } \Gamma_\infty^-$$

$$(54) \quad \vec{u}^{(n+1)-\theta} = 0 \quad \text{on } \Gamma_B$$

$$(55) \quad \left\{ \begin{array}{l} \left\{ \left(-\beta \sigma^{(n+1)-\theta} + \frac{K\tau}{\tau-1} e^{(\tau-1)\sigma^{(n+1)-\theta}} \right) \text{Id.} + a\mu \nabla \vec{u}^{(n+1)-\theta} - \frac{1}{Re} \mathcal{D}(\vec{u}^{(n+1)-\theta}) \right\} \cdot \vec{n} \\ = \left(-\beta \sigma^{n+\theta} \text{Id.} + a\mu \nabla \vec{u}^{n+\theta} \right) \cdot \vec{n} \quad \text{on } \Gamma_\infty^+ \end{array} \right.$$

Third step

$$(56) \quad \alpha \sigma^{n+1} + \nabla \cdot \vec{u}^{n+1} = -\vec{u}^{(n+1)-\theta} \cdot \nabla \sigma^{(n+1)-\theta} + \alpha \vec{u}^{(n+1)-\theta}$$

$$(57) \quad \left\{ \begin{array}{l} \alpha \vec{u}^{n+1} - \alpha \mu \Delta \vec{u}^{n+1} + \beta \nabla \sigma^{n+1} = \vec{\Phi}(\sigma^{(n+1)-\theta}, \vec{u}^{(n+1)-\theta}) \\ \qquad \qquad \qquad + b \mu \Delta \vec{u}^{(n+1)-\theta} + \alpha \vec{u}^{(n+1)-\theta} \end{array} \right.$$

$$(58) \quad \sigma^{n+1} = \sigma_\infty, \quad \vec{u}^{n+1} = \vec{u}_\infty \quad \text{on } \Gamma_\infty^-$$

$$(59) \quad \vec{u}^{n+1} = 0 \quad \text{on } P_B$$

$$(60) \quad \left\{ \begin{array}{l} ((-\beta \sigma^{n+1} \underset{\sim}{\text{Id.}} + \alpha \mu \underset{\sim}{\nabla \vec{u}^{n+1}}) \cdot \vec{n} \\ = \{ (-\beta \sigma^{(n+1)-\theta} + \frac{K \tau}{\tau-1} e^{(\tau-1)\sigma^{(n+1)-\theta}}) \underset{\sim}{\text{Id.}} + \alpha \mu \underset{\sim}{\nabla \vec{u}^{(n+1)-\theta}} - \frac{1}{R_2} \underset{\sim}{D}(\vec{u}^{(n+1)-\theta}) \} \cdot \vec{n} \\ \text{on } \Gamma_\infty^+ \end{array} \right.$$

Once again, σ^0 , \vec{u}^0 are given by (28)-(29). A detailed analysis yields:

$$(61) \quad a = \frac{1-2\theta}{1-\theta}, \quad b = \frac{\theta}{1-\theta}, \quad \theta = 1 - \frac{\sqrt{2}}{2}$$

as the optimal parameters. One sees indeed that

i) $\theta = 1 - \frac{\sqrt{2}}{2}$ leads to a second order scheme

ii) $a = (1-2\theta)/(1-\theta)$ and $b = \theta/(1-\theta)$ implies

$$\alpha \underset{\theta}{\text{Id.}} - \alpha \mu \Delta = \frac{1-2\theta}{\theta} (\alpha' \underset{\theta}{\text{Id.}} - b \mu \Delta)$$

(consequently, one is always concerned with the same second order elliptic operator in problems (47), (52) and (57)).

All these time discretization schemes lead to the same kind of elliptic (linear or nonlinear) problems:

Linear problems:

(62) $\alpha_0 \sigma + \nabla \cdot \vec{u} = H$

(63) $\alpha_0 \vec{u} - \mu_0 \Delta \vec{u} + \beta_0 \nabla \sigma = \vec{F}$

(64) $\sigma = \sigma_\infty, \vec{u} = \vec{u}_\infty \text{ on } \Gamma_\infty^-$

(65) $\vec{u} = 0 \text{ on } \Gamma_B$

(66) $(-\beta_0 \underset{\sim}{\text{Id.}} + \mu_0 \underset{\sim}{\nabla \vec{u}}) \cdot \vec{n} = \underset{\sim}{\tau} \cdot \vec{n} \text{ on } \Gamma_\infty^+$

where

$\alpha_0 > 0, \mu_0 > 0, \beta_0 > 0, H, \vec{F}, \sigma_\infty, \vec{u}_\infty, \underset{\sim}{\tau}$

are given. This is a quasi-Stokes (or generalized Stokes) problem.

Nonlinear problems:

(67) $\alpha_0 \sigma + \delta_0 \nabla \cdot \vec{u} = -\vec{u} \cdot \nabla \sigma + H$

(68) $\alpha_0 \vec{u} - \mu_0 \Delta \vec{u} + \beta_0 \nabla \sigma = \vec{\Phi}(\sigma, \vec{u}) + \vec{F}$

(69) $\sigma = \sigma_\infty, \vec{u} = \vec{u}_\infty \text{ on } \Gamma_\infty^-$

(70) $\vec{u} = 0 \text{ on } \Gamma_B$

(71) $\left\{ \begin{array}{l} ((-\beta_0 \sigma \underset{\sim}{\text{Id.}} + \mu_0 \underset{\sim}{\nabla \vec{u}}) \cdot \vec{n} = \left\{ (-\beta \sigma + \frac{K\tau}{\gamma-1} e^{(\gamma-1)\sigma}) \underset{\sim}{\text{Id.}} \right. \\ \left. + \mu \underset{\sim}{\nabla \vec{u}} - \frac{1}{Re} \underset{\sim}{D}(\vec{u}) \right\} \cdot \vec{n} + \underset{\sim}{\tau} \cdot \vec{n} \text{ on } \Gamma_\infty^+ \end{array} \right.$

where

$\alpha_0 > 0, \mu_0 > 0, \beta_0 > 0, \delta_0 \geq 0, H, \vec{F}, \sigma_\infty, \vec{u}_\infty, \underset{\sim}{\tau}$

are given. These will be solved by introducing a least squares reformulation and performing conjugate gradient methods.

B) The numerical solution of the nonlinear problems (67)-(71)

For simplicity, consider problem (67)-(71) with

$$\alpha_0 = \alpha, \delta_0 = 1, \kappa_0 = \mu, \beta_0 = \beta :$$

$$(72) \quad \alpha \sigma + \nabla \cdot \vec{u} = - \vec{u} \cdot \nabla \sigma + H$$

$$(73) \quad \alpha \vec{u} - \mu \Delta \vec{u} + \beta \nabla \sigma = \vec{\Phi}(\sigma, \vec{u}) + \vec{F}$$

$$(74) \quad \sigma = \sigma_\infty, \vec{u} = \vec{u}_\infty \text{ on } \Gamma_\infty^-$$

$$(75) \quad \vec{u} = 0 \text{ on } \Gamma_B$$

$$(76) \quad \left\{ \begin{array}{l} (-\beta \sigma \text{Id.} + \mu \nabla \vec{u}) \cdot \vec{n} = \left\{ \begin{array}{l} (-\beta \sigma + \frac{K \tau}{\tau-1} e^{(\tau-1)\sigma}) \text{Id.} \\ + \mu \nabla \vec{u} - \frac{1}{Re} \vec{D}(\vec{u}) \end{array} \right\} \cdot \vec{n} + \tau \cdot \vec{n} \text{ on } \Gamma_\infty^+ \end{array} \right.$$

Least squares reformulation of problem (72)-(76)

$$(77) \quad \left\{ \begin{array}{l} \text{Minimize } J(\eta, \vec{w}) = \frac{\alpha}{2} \int_{\Omega} |\Omega \cdot \eta|^2 dx + \frac{A}{2} \int_{\Omega} \{ \alpha |\vec{u} - \vec{w}|^2 + \mu |\nabla(\vec{u} - \vec{w})|^2 \} dx \\ \text{Subject to : } (\eta, \vec{w}) \in S_\infty \times W_\infty \end{array} \right.$$

Here, A is a given positive constant and

$$(78) \quad S_\infty = \{ \eta \mid \eta \in H^1(\Omega), \eta = \sigma_\infty \text{ on } \Gamma_\infty^- \}$$

$$(79) \quad W_\infty = \{ \vec{w} \mid \vec{w} \in H^1(\Omega)^2, \vec{w} = \vec{u}_\infty \text{ on } \Gamma_\infty^-, \vec{w} = 0 \text{ on } \Gamma_B \}$$

are linear manifolds in $H^1(\Omega)$ and $H^1(\Omega)^2$ resp. In (77), $(\sigma, \vec{u}) = (\sigma(\eta, \vec{w}), \vec{u}(\eta, \vec{w}))$ is given by the solution of the state equation:

$$(80) \quad \alpha \sigma + \nabla \cdot \vec{u} = -\vec{w} \cdot \nabla \eta + H$$

$$(81) \quad \alpha \vec{u} - \mu \Delta \vec{u} + \beta \nabla \sigma = \vec{\Phi}(\eta, \vec{w}) + \vec{F}$$

$$(82) \quad \sigma = \sigma_\infty, \quad \vec{u} = \vec{u}_\infty \quad \text{on } \Gamma_\infty^-$$

$$(83) \quad \vec{u} = 0 \quad \text{on } \Gamma_B$$

$$(84) \quad \left\{ \begin{array}{l} ((-\beta \sigma \text{Id.} + \mu \nabla \vec{u}) \cdot \vec{n}) = \left\{ \left(-\beta \eta + \frac{K\tau}{\tau-1} e^{(\tau-1)\eta} \right) \text{Id.} \right. \\ \left. + \mu \nabla \vec{u} - \frac{1}{Re} D(\vec{w}) \right\} \cdot \vec{n} + \tau \cdot \vec{n} \quad \text{on } \Gamma_\infty^+ \end{array} \right.$$

The solution of (77) can be achieved by performing a conjugate gradient algorithm. It is thus necessary to know how to compute the gradient

$$J'(\eta, \vec{w}) = \left(\frac{\partial J}{\partial \eta}(\eta, \vec{w}), \frac{\partial J}{\partial \vec{w}}(\eta, \vec{w}) \right)$$

$$\left\langle \frac{\partial J}{\partial \eta}(\eta, \vec{w}), \varphi \right\rangle = \alpha \int_{\Omega} (\sigma - \eta) \left(\frac{\partial \sigma}{\partial \eta} \cdot \varphi - \varphi \right) dx$$

$$+ A \int_{\Omega} \left\{ \alpha (\vec{u} - \vec{w}) \cdot \left(\frac{\partial \vec{u}}{\partial \eta} \cdot \varphi \right) + \mu \nabla (\vec{u} - \vec{w}) \cdot \nabla \left(\frac{\partial \vec{u}}{\partial \eta} \cdot \varphi \right) \right\} dx$$

$$= \alpha \int_{\Omega} (\eta - \sigma) \varphi dx + A \int_{\Omega} \left\{ \alpha (\vec{u} - \vec{w}) \cdot \left(\frac{\partial \vec{u}}{\partial \eta} \cdot \varphi \right) \right. \\ \left. + \mu \nabla (\vec{u} - \vec{w}) \cdot \nabla \left(\frac{\partial \vec{u}}{\partial \eta} \cdot \varphi \right) \right\} dx$$

$$+ \alpha \int_{\Omega} (\sigma - \eta) \left(\frac{\partial \sigma}{\partial \eta} \cdot \varphi \right) dx$$

One introduces the adjoint state $(\xi, \bar{\xi}) = (\xi(\eta, \vec{w}), \bar{\xi}(\eta, \vec{w}))$

given by:

$$(85) \quad \alpha \zeta - \beta \nabla \cdot \vec{\xi} = \alpha (\zeta - \eta)$$

$$(86) \quad \alpha \vec{\xi} - \mu \Delta \vec{\xi} - \nabla \zeta = A \{ \alpha (\vec{u} - \vec{w}) - \mu \Delta (\vec{u} - \vec{w}) \}$$

$$(87) \quad \zeta = 0, \quad \vec{\xi} = 0 \quad \text{on } \Gamma_\infty^-$$

$$(88) \quad \vec{\xi} = 0 \quad \text{on } \Gamma_B$$

$$(89) \quad (\zeta \underset{\sim}{\text{Id.}} + \mu \underset{\sim}{\nabla \vec{\xi}}) \cdot \vec{n} = A \mu \nabla (\vec{u} - \vec{w}) \cdot \vec{n} \quad \text{on } \Gamma_\infty^+$$

Then

$$\begin{aligned} \left\langle \frac{\partial J}{\partial \eta}, \varphi \right\rangle &= \alpha \int_{\Omega} (\eta - \sigma) \varphi \, dx - \int_{\Omega} (\vec{w} \cdot \nabla \varphi) \zeta \, dx \\ &\quad + \left\langle \frac{\partial \vec{\Phi}}{\partial \eta} (\eta, \vec{w}), \varphi, \vec{\xi} \right\rangle \end{aligned}$$

Analogously, one obtains

$$\begin{aligned} \left\langle \frac{\partial J}{\partial w}, \vec{v} \right\rangle &= A \int_{\Omega} \{ \alpha (\vec{u} - \vec{w}) \cdot \vec{v} + \mu \underset{\sim}{\nabla} (\vec{u} - \vec{w}) \cdot \underset{\sim}{\nabla} \vec{v} \} \, dx \\ &\quad - \int_{\Omega} (\vec{v} \cdot \nabla \eta) \zeta \, dx + \left\langle \frac{\partial \vec{\Phi}}{\partial w} (\eta, \vec{w}), \vec{v}, \vec{\xi} \right\rangle \end{aligned}$$

Hence, the task is reduced to solve a certain number of quasi-Stokes problems (80)-(84) and (85)-(89).

- C) The numerical solution of the quasi-Stokes problems (62)-(66), (80)-(84) and (85)-(89)

The general form of these problems ($\alpha_0 = \alpha$, $\mu_0 = \mu$, $\beta_0 = \beta$ in (62)-(66)):

$$(90) \quad \alpha\sigma + \nabla \cdot \vec{u} = h$$

$$(91) \quad \alpha\vec{u} - \mu \Delta \vec{u} + \beta \nabla \sigma = \vec{f}$$

$$(92) \quad \sigma = \sigma_\infty, \quad \vec{u} = \vec{u}_\infty \quad \text{on} \quad \Gamma_\infty^-$$

$$(93) \quad \vec{u} = 0 \quad \text{on} \quad \Gamma_B$$

$$(94) \quad (-\beta\sigma \underset{\sim}{\text{Id.}} + \mu \underset{\sim}{\nabla u}) \cdot \vec{n} = \tau \cdot \vec{n} \quad \text{on} \quad \Gamma_\infty^+$$

Remark: (85)-(89) takes the form (90)-(94) with

$$\sigma = -\frac{1}{\beta} \xi, \quad \vec{u} = \vec{\xi}.$$

Assume (generalized Glowinski & Pironneau's method) :

σ , h and \vec{f} are regular

$\lambda = \sigma|_{\Gamma_B}$ is known

$$\frac{\partial \sigma}{\partial n} = 0 \quad \text{on} \quad \Gamma_\infty^+$$

Then:

$$(95) \quad \alpha^2 \sigma - (\beta + \alpha\mu) \Delta \sigma = \alpha h - \mu \Delta h - \nabla \cdot \vec{f}$$

$$(96) \quad \sigma = \sigma_\infty \quad \text{on} \quad \Gamma_\infty^-$$

$$(97) \quad \sigma = \lambda \quad \text{on} \quad \Gamma_B$$

$$(98) \quad \frac{\partial \sigma}{\partial n} = 0 \quad \text{on} \quad \Gamma_\infty^+$$

From σ , we compute \vec{u} by solving:

$$(99) \quad \alpha\vec{u} - \mu \Delta \vec{u} = \vec{f} - \beta \nabla \sigma$$

$$(100) \quad \vec{u} = \vec{u}_\infty \quad \text{on} \quad \Gamma_\infty^-$$

$$(101) \quad \vec{u} = 0 \quad \text{on} \quad \Gamma_B$$

$$(102) \quad \mu \nabla \vec{u} \cdot \vec{n} = (\beta\sigma \underset{\sim}{\text{Id.}} + \tau) \cdot \vec{n} \quad \text{on} \quad \Gamma_\infty^+$$

This suggests the following method:

a) For $\lambda \in H^{\frac{1}{2}}$, set

$\sigma(\lambda)$: the sol. of (95-98)

$\vec{u}(\lambda)$: the sol. of (99-102) with $\sigma = \sigma(\lambda)$

$\psi(\lambda)$: the sol. of

$$(103) \quad \alpha^2 \psi - (\beta + \alpha \mu) \Delta \psi = \alpha \sigma + \nabla \cdot \vec{u} - h$$

$$(104) \quad \psi = 0 \quad \text{on } \Gamma_{\infty}^-$$

$$(105) \quad \psi = 0 \quad \text{on } \Gamma_B$$

$$(106) \quad \frac{\partial \psi}{\partial n} = 0 \quad \text{on } \Gamma_{\infty}^+$$

with $\sigma = \sigma(\lambda)$, $\vec{u} = \vec{u}(\lambda)$.

b) Also, set

$$(107) \quad A_{GP} \lambda = \left(\frac{\partial \psi(\lambda)}{\partial n} \Big|_{\Gamma_B \cup \Gamma_{\infty}^-}, \psi(\lambda) \Big|_{\Gamma_{\infty}^+} \right) \in H(\Gamma_B \cup \Gamma_{\infty}^-)^{-\frac{1}{2}} \times H(\Gamma_{\infty}^+)^{\frac{1}{2}}$$

and solve the equation

$$(108) \quad A_{GP} \lambda = (0, 0).$$

Space discretization: We introduce a triangulation \mathcal{T}_h of Ω and set

$$(109) \quad S_h = \{ \varphi \mid \varphi \in C^0(\bar{\Omega}), \varphi|_T \in P_1(T) \quad \forall T \in \mathcal{T}_h, \varphi|_{\Gamma_{\infty}^- \cup \Gamma_B} = 0 \}$$

$$(110) \quad W_h = S_h \times S_h$$

$$(111) \quad \left\{ \begin{array}{l} \sigma_{\infty,h} \in C^0(\bar{\Omega}), \quad \sigma_{\infty,h}|_T \in P_1(T) \quad \forall T \in \mathcal{T}_h, \quad \sigma_{\infty,h}|_{P_B^-} = \sigma_\infty, \\ \sigma_{\infty,h}|_{P_B} = 0 \end{array} \right.$$

$$(112) \quad \left\{ \begin{array}{l} \vec{u}_{\infty,h} \in C^0(\bar{\Omega})^2, \quad \vec{u}_{\infty,h}|_T \in P_1(T) \quad \forall T \in \mathcal{T}_h, \quad \vec{u}_{\infty,h}|_{P_B^-} = \vec{u}_\infty, \\ \vec{u}_{\infty,h}|_{P_B} = 0 \end{array} \right.$$

$$(113) \quad \left\{ \begin{array}{l} M_h = \{ \lambda \mid \lambda \in C^0(\bar{\Omega}), \lambda|_T \in P_1(T) \quad \forall T \in \mathcal{T}_h, \\ \lambda(a) = 0 \quad \text{for all vertices } a \notin P_B \cup \{a^*\} \} \end{array} \right.$$

Here, a^* is a fixed vertex on \bar{T}_h .

$$M_h^0 = \{ \lambda \mid \lambda \in M_h, \lambda(a^*) = 0 \}$$

For $\lambda \in M_h$ we set σ_λ as the unique solution of

$$(114) \quad \int_{\Omega} \{ \alpha^2 \sigma_j \cdot \nabla \varphi + (\beta + \alpha \mu) \nabla \sigma_j \cdot \nabla \varphi \} dx = 0 \quad \forall \varphi \in S_h, \sigma_j \in \lambda + S_h$$

Then, we set \vec{u}_λ as the unique solution of

$$(115) \quad \int_{\Omega} \{ \alpha \vec{u}_j \cdot \vec{v} + \mu \nabla \vec{u}_j \cdot \nabla \vec{v} \} dx = \beta \int_{\Omega} \sigma_j (\nabla \cdot \vec{v}) dx \quad \forall \vec{v} \in W_h, \vec{u}_j \in W_h$$

Finally, we set ψ_λ as the unique solution of

$$(116) \quad \int_{\Omega} \{ \alpha^2 \psi_j \cdot \varphi + (\beta + \alpha \mu) \nabla \psi_j \cdot \nabla \varphi \} dx = \int_{\Omega} (\alpha \sigma_j + \nabla \cdot \vec{u}_j) \varphi dx \quad \forall \varphi \in S_h, \psi_j \in S_h$$

We also set $\sigma_0, \vec{u}_0, \psi_0$ as the solutions of the following problems:

$$(117) \quad \int_{\Omega} \{ \alpha^2 \sigma_0 \cdot \varphi + (\beta + \alpha \mu) \nabla \sigma_0 \cdot \nabla \varphi \} dx = \langle \alpha h - \mu \Delta h - \vec{f}, \varphi \rangle$$

$\forall \varphi \in S_h, \sigma_0 \in \sigma_{\infty, h} + S_h$

$$(118) \quad \int_{\Omega} \{ \alpha \vec{u}_0 \cdot \vec{v} + \mu \nabla \vec{u}_0 \cdot \nabla \vec{v} \} dx = \langle \vec{f}, \vec{v} \rangle + \beta \int_{\Omega} \sigma_0 (\nabla \cdot \vec{v}) dx$$

$\forall \vec{v} \in \vec{W}_h, \vec{u}_0 \in \vec{u}_{\infty, h} + \vec{W}_h$

$$(119) \quad \int_{\Omega} \{ \alpha^2 \psi_0 \cdot \varphi + (\beta + \alpha \mu) \nabla \psi_0 \cdot \nabla \varphi \} dx = \int_{\Omega} (\alpha \sigma_0 + \nabla \cdot \vec{u}_0 - h) \varphi dx$$

$\forall \varphi \in S_h, \psi_0 \in S_h$

We compute $\lambda_* \in M_h^\circ$ such that:

$$(120) \quad \left\{ \begin{aligned} \langle B_{GP}^h \lambda_*, \mu \rangle &= \frac{1}{\beta + \alpha \mu} \int_{\Omega} \{ \alpha^2 \psi_{\lambda_*} \cdot \mu + (\beta + \alpha \mu) \nabla \psi_{\lambda_*} \cdot \nabla \mu \} dx \\ &\quad - \frac{1}{\beta + \alpha \mu} \int_{\Omega} \{ \alpha \sigma_{\lambda_*} + \nabla \cdot \vec{u}_{\lambda_*} \} \mu dx \\ &= - \frac{1}{\beta + \alpha \mu} \int_{\Omega} \{ \alpha^2 \psi_0 \cdot \mu + (\beta + \alpha \mu) \nabla \psi_0 \cdot \nabla \mu \} dx \\ &\quad + \frac{1}{\beta + \alpha \mu} \int_{\Omega} (\alpha \sigma_0 + \nabla \cdot \vec{u}_0 - h) \mu dx \\ \forall \mu \in M_h^\circ, \lambda_* \in M_h^\circ \end{aligned} \right.$$

Once λ_* is found, one easily obtains approximations for σ and \vec{u}

$$(121) \quad \sigma \approx \sigma_{\lambda_*} + \sigma_0, \quad \vec{u} \approx \vec{u}_{\lambda_*} + \vec{u}_0.$$

Remarks. In practice, one constructs the matrix

$$\mathcal{B}_{GP} = \{b_{GP}^{ij}\}, \text{ with } b_{GP}^{ij} = \langle \mathcal{B}_{GP}^h \lambda_i, \lambda_j \rangle$$

(λ_i is the i th standard basis function in M_h).

It can be checked that \mathcal{B}_{GP} is symmetric and positive definite.

This method gives an approximation to the solution (σ, \vec{u}) of (90)-(94) and also an approximation to $\sigma|_{T_B}$.

Once \mathcal{B}_{GP} is known, to solve (90)-(94) one has to find the solution of 4+3 (=7) discrete Poisson problems ((117)-(119) and (114)-(115) with $\lambda = \lambda_*$) and one has to solve a linear system of smaller size (with matrix \mathcal{B}_{GP}).

D) The final form of the nonlinear problems (72)-(76)

After space discretization, the problem to solve is:

$$(122) \quad \begin{cases} \text{Minimize } J_h(\eta, \vec{w}) = \frac{\alpha}{2} \int_{\Omega} |\vec{v} - \eta|^2 dx + \frac{A}{2} \int_{\Omega} \{ \alpha |\vec{u} - \vec{w}|^2 + \mu |\nabla(\vec{u} - \vec{w})|^2 \} dx \\ \text{Subject to: } \eta \in T_{\infty, h} + S_h, \vec{w} \in \vec{U}_{\infty, h} + \vec{W}_h \end{cases}$$

Now, the state functions σ and \vec{u} are given by (121) where

σ_0 is given by (117) with $h = -\vec{w} \cdot \nabla \eta + H$, $\vec{f} = \vec{\Phi} + \vec{F}$
 \vec{u}_0 (118)

λ_* (120) with Ψ_0 being the sol. of (119)

The behavior of the gradient:

$$(123) \quad \left\langle \frac{\partial J_h}{\partial \eta}, \psi \right\rangle = \alpha \int_{\Omega} (\eta - \sigma) \psi dx - \int_{\Omega} (\vec{w} \cdot \nabla \eta) \psi dx + \left\langle \frac{\partial \vec{H}}{\partial \eta} \cdot \vec{\psi}, \vec{\psi} \right\rangle$$

$$(124) \quad \left\langle \frac{\partial J_h}{\partial \vec{w}}, \vec{v} \right\rangle = A \int_{\Omega} \{ \alpha (\vec{w} - \vec{u}) \cdot \vec{v} + \mu \nabla(\vec{w} - \vec{u}) \cdot \nabla \vec{v} \} dx - \int_{\Omega} (\vec{v} \cdot \nabla \eta) \psi dx + \left\langle \frac{\partial \vec{F}}{\partial \vec{w}} \cdot \vec{v}, \vec{v} \right\rangle$$

Here, the adjoint state functions ζ and $\bar{\zeta}$ are given resp. by $-\frac{1}{\beta} \sigma$ and \bar{u} , with (ζ, \bar{u}) being given by (121), where

ζ_0 is the sol. of (117) with $h = \alpha(\sigma - \eta)$, $\vec{f} = A(\alpha(\vec{u} - \vec{w})) - \mu A(\vec{u} - \vec{w})$

\bar{u}_0 " " " (118)

λ_0 " " " (120) with ψ_0 being the sol. of (119)

Of course, if a second or third order derivative of a piecewise linear function is needed, it must be replaced by a piecewise linear approximation. In practice, it is interesting:

- 1) To introduce mass-lumping for all "mass" integrals
- 2) To work with new (canonical) variables, for which J_h behaves quasi-quadratically.
- 3) To solve (122) using Buckley & LeNir's conjugate gradient methods

1.4 Turbulent compressible flows

Turbulence is a phenomenon whose most relevant features are:

- irregular motion of the fluid
- Random behavior of density, velocity, etc...
- A wide range of wavelengths

The flow of a fluid around and past an obstacle can be:

- Laminar, if these are not respected (for small Re)
- Transitional, if these rise periodically or almost periodically in time and/or space (for moderately high Re)
- Turbulent, if these hold true (for high Re)

For this kind of flow, one finds several distinctions between laminar and turbulent regime:

- Direct observation (Hagen, 1839) of the flow
- Measurement of tangential forces on the body
- Measurement of the boundary layer thickness.

It is not possible to find a numerical approximation of (say) (1)-(6) by directly solving the Navier-Stokes equations if the flow is known to be turbulent. It is necessary (for the moment being) to strict oneself to the computation of mean quantities.

The usual (standard) method for computing isentropic compressible turbulent flows:

1. The starting point is Navier-Stokes equations:

$$(125) \quad \frac{\partial \rho}{\partial t} + \nabla \cdot (\rho \vec{u}) = 0$$

$$(126) \quad \frac{\partial \vec{u}}{\partial t} + (\vec{u} \cdot \nabla) \vec{u} + \frac{1}{\rho} \nabla p = \frac{1}{\rho} \nabla \cdot (\mu \tilde{D}(\vec{u})) , \quad \mu = \rho \beta$$

$$(127) \quad \vec{p} = K \rho^{\gamma}$$

together with appropriate initial and boundary conditions

2. One makes the following assumptions:

$$(128) \quad \rho = \bar{\rho} + \rho'' \quad \vec{u} = \bar{\vec{u}} + \vec{u}'' = \tilde{\vec{u}} + \vec{u}'$$

with $\bar{\rho}, \bar{\vec{u}}$ being averaged quantities (in a sense to be determined by the nature of the flow) and with $\tilde{\vec{u}}$ being the mass-averaged velocity field:

$$\tilde{\vec{u}} = \overline{\vec{u}''} / \bar{\rho}$$

3. One introduces (128) in (125)-(127) and assumes that $(\rho'')^2 \approx 0$. This leads to the Reynolds equations:

$$(129) \quad \frac{\partial \bar{\rho}}{\partial t} + \nabla \cdot (\bar{\rho} \tilde{\vec{u}}) = 0$$

$$(130) \quad \frac{\partial \tilde{\vec{u}}}{\partial t} + \nabla \cdot (\bar{\rho} \tilde{\vec{u}} \otimes \tilde{\vec{u}}) + \nabla \bar{p} = \nabla \cdot (\bar{\mu} \tilde{D}(\tilde{\vec{u}}) - \bar{\rho} \vec{u}' \otimes \vec{u}')$$

$$(131) \quad \tilde{\vec{p}} = K \bar{\rho}^{\gamma}$$

4. To close (129)-(131), one makes a closure assumption which relates $R = -\bar{\rho} \vec{u}' \otimes \vec{u}'$ to $\bar{\rho}$ and $\tilde{\vec{u}}$.

In many models, one first uses Boussinesq's hypothesis:

$$(132) \quad \tilde{R} = \bar{\rho} \tilde{v}_t D(\tilde{u})$$

where $\tilde{v}_t = \tilde{v}_t(\bar{\rho}, \tilde{u})$ is given either analytically or through the solution of other new pde's.

For example, turbulent kinetic energy models work with

$$(132') \quad \tilde{v}_t = \tilde{k} \cdot \ell(\bar{\rho}, \tilde{u})$$

Here, $\ell(\bar{\rho}, \tilde{u})$ is a given algebraic expression of $\bar{\rho}$ and \tilde{u} while

$$\tilde{k} = \frac{1}{2} \overline{\rho |\tilde{u}|^2} / \bar{\rho}$$

is the solution of a certain transport-diffusion pde.

1.5 Turbulent boundary layers for compressible flows

A) The boundary layer concept

For the flow around and past an obstacle, one finds two regions in which the fluid behaves quite differently:

- Near the body and in the wake behind it, viscous effects are important
- Outside this region, the fluid is practically inviscid

There is a thermal analogy in connection with the transport of vorticity for 2D flows. This situation arises when Re is large enough. "Grosso modo", the boundary layer is the region where vorticity is considerably different from zero.

Through the boundary layer, the tangential velocity has a large transverse gradient and viscous terms become important. In laminar flow, there are estimates on the thickness of the boundary layer:

$$(133) \quad \delta/\ell \approx 5/Re_\ell^{1/2}$$

for a streamlined body of length ℓ .

In practice, δ is taken as the distance from the body at which the tangential velocity reaches 99% of the outer (inviscid) tangential

velocity.

Other thickness parameter:

$$(134) \quad \delta_1 = \int_0^{\delta} \left(1 - \frac{u_s}{U_s}\right) dn \approx \int_0^{\infty} \left(1 - \frac{u_s}{U_s}\right) dn$$

(the displacement thickness; u_s and U_s are resp. the "boundary layer" and the "outer inviscid" tangential velocities, s and n are resp. the tangential and normal coordinates).

B) The physical argument leading to the boundary layer equations

For simplicity, we consider the flow around a flat wall. The mean flow direction is $e_1 = (1, 0)$.

Basic hypothesis: Inside a thin layer, with thickness $\delta = \delta(x)$, viscous terms are of the same order of magnitude than convective terms. Outside this region, those are not important.

Supplementary hypothesis: Sudden accelerations do not occur, i.e.

$$\frac{du}{dt} \sim u \frac{du}{dx}$$

Dimensional analysis leads to the following system of pde's for u , v , ρ and p for isentropic compressible flow in the boundary layer:

$$(135) \quad \frac{\partial p}{\partial t} + \frac{\partial}{\partial x} (\rho u) + \frac{\partial}{\partial y} (\rho v) = 0$$

$$(136) \quad \frac{\partial u}{\partial t} + u \frac{\partial u}{\partial x} + v \frac{\partial u}{\partial y} + \frac{1}{\rho} \frac{\partial p}{\partial x} = - \frac{1}{\rho Re} \frac{\partial}{\partial y} (\rho \frac{\partial u}{\partial y})$$

$$(137) \quad p = K \rho^{\gamma}$$

Now, continuity requirements for p lead to the facts that ρ and p are determined by the inviscid solution. Thus,

- The number of unknowns is now two (u and v)
- The solution is "parabolic in x ", i.e. the task is here reduced to study the evolution along the x -axis of u .

These considerations hold as well for the flow around curved walls

provided curvature does not change rapidly.

C) Asymptotic theory (I) : A mathematical Friedrich's illustration

Consider the model problem (where $\epsilon > 0$ is small):

$$(138) \quad \left\{ \begin{array}{l} \epsilon \frac{du}{dy^2} + \frac{du}{dy} = -\frac{3}{2}(1-3\epsilon)e^{-3y}, \quad y \in (0, +\infty) \\ u|_{y=0} = 0 \quad u|_{y \rightarrow \infty} = 1 \end{array} \right.$$

The standard asymptotic argument to find an approximation of the solution of (say) the third order is:

(C.1) To introduce an outer expansion:

$$(139) \quad u = f(y, \epsilon) \sim f^0(y) + \epsilon \cdot f^1(y) + \epsilon^2 \cdot f^2(y)$$

where f^0, f^1, f^2 have to be determined from formal calculus. (139) means that, for some norm $\|\cdot\|_\epsilon$ on a space of functions defined on $[a(\epsilon), \infty)$ ($a(\epsilon) > 0, a(\epsilon) \rightarrow 0$), one must have:

$$(140) \quad \|f(y, \epsilon) - (f^0(y) + \epsilon f^1(y) + \epsilon^2 f^2(y))\|_\epsilon = O(\epsilon^3)$$

Formal calculus (identification of the powers of ϵ) leads to:

$$(141) \quad \frac{df^0}{dy} = -\frac{3}{2} e^{-3y} \quad f^0(+\infty) = 1$$

$$(142) \quad \frac{df^1}{dy} = -\frac{d^2 f^0}{dy^2} + \frac{9}{2} e^{-3y} \quad f^1(+\infty) = 0$$

$$(143) \quad \frac{df^2}{dy} = -\frac{d^2 f^1}{dy^2} \quad f^2(+\infty) = 0$$

Hence, one necessarily has:

$$(144) \quad \left\{ \begin{array}{l} u = f(y, \epsilon) \sim (1 + \frac{1}{2}e^{-3y}) + \epsilon \cdot 0 + \epsilon^2 \cdot 0 \\ \qquad \qquad \qquad \equiv 1 + \frac{1}{2}e^{-3y} \end{array} \right.$$

(C.2) To introduce an inner expansion:

$$(145) \quad u = F(Y, \varepsilon) \sim F^0(Y) + \varepsilon \cdot F^1(Y) + \varepsilon^2 \cdot F^2(Y), \quad Y = y q(\varepsilon)^{-1}$$

where F^0, F^1, F^2 and $q(\varepsilon)$ have to be found. F^0, F^1 and F^2 will be determined again from formal calculus and $q(\varepsilon)$ has to be such that $q(\varepsilon) \rightarrow \infty$. The meaning of (145) is

$$(146) \quad \|F(Y, \varepsilon) - (F^0(Y) + \varepsilon F^1(Y) + \varepsilon^2 F^2(Y))\|^{\varepsilon} = O(\varepsilon^3)$$

where $\|\cdot\|^\varepsilon$ is a norm on a space of functions defined on $[0, b(\varepsilon)]$ ($b(\varepsilon) > 0, b(\varepsilon) \rightarrow 0$). The choice of $q(\varepsilon)$ is crucial: it must lead to a maximum of richness in the ode!

One sees that $q(\varepsilon) = \varepsilon$ is adequate. Then,

$$(147) \quad \frac{d^2 F^0}{dy^2} + \frac{dF^0}{dy} = 0 \quad F^0(0) = 0$$

$$(148) \quad \frac{d^2 F^1}{dy^2} + \frac{dF^1}{dy} = -\frac{3}{2} \quad F^1(0) = 0$$

$$(149) \quad \frac{d^2 F^2}{dy^2} + \frac{dF^2}{dy} = \frac{9}{2}(1+y) \quad F^2(0) = 0$$

This gives (with A_0, A_1 and A_2 three indetermined constants):

$$(150) \quad \begin{cases} u \sim A_0(1-e^{-y}) + \varepsilon \cdot (A_1(1-e^{-y}) - \frac{3}{2}y) \\ \quad + \varepsilon^2 (A_2(1-e^{-y}) + \frac{9}{4}y^2), \quad y = y\varepsilon^{-1} \end{cases}$$

(C.3) To perform "matching" between (144) and (150).

Matching will prescribe the values of A_0, A_1 and A_2 .

We use Van Dyke's rule:

The three-terms inner expansion of $f^0(y) + \varepsilon f^1(y) + \varepsilon^2 f^2(y)$ and the three-terms outer expansion of $F^0(y) + \varepsilon F^1(y) + \varepsilon^2 F^2(y)$ must coincide.

In other words, one must have:

$$\begin{aligned}
 f^0(\varepsilon Y) + \varepsilon f^1(\varepsilon Y) + \varepsilon^2 f^2(\varepsilon Y) &\equiv 1 + \frac{1}{2} e^{-3\varepsilon Y} \\
 &\sim 1 + \frac{1}{2} (1 - 3\varepsilon Y + \frac{9}{2} \varepsilon^2 Y^2) \\
 &\equiv \frac{3}{2} - \varepsilon \cdot \frac{3}{2} Y + \varepsilon^2 \cdot \frac{9}{4} Y^2
 \end{aligned}$$

(from Taylor's formula) and

$$\begin{aligned}
 F^0\left(\frac{Y}{\varepsilon}\right) + \varepsilon F^1\left(\frac{Y}{\varepsilon}\right) + \varepsilon^2 F^2\left(\frac{Y}{\varepsilon}\right) &\equiv A_0(1 - e^{-Y/\varepsilon}) \\
 &+ \varepsilon \cdot (A_1(1 - e^{-Y/\varepsilon}) - \frac{3}{2} \frac{Y}{\varepsilon}) + \varepsilon^2 \cdot (A_2(1 - e^{-Y/\varepsilon}) + \frac{9}{4} \frac{Y^2}{\varepsilon^2}) \\
 &\sim \left(A_0 - \frac{3}{2} \frac{Y}{\varepsilon} + \frac{9}{4} \frac{Y^2}{\varepsilon^2}\right) + \varepsilon \cdot A_1 + \varepsilon^2 \cdot A_2
 \end{aligned}$$

(from the behavior of $e^{-Y/\varepsilon}$ with fixed Y and $\varepsilon \rightarrow 0$).

Rewriting these expansions in the same variable (for example Y), one obtains:

$$\frac{3}{2} - \varepsilon \cdot \frac{3}{2} Y + \varepsilon^2 \cdot \frac{9}{4} Y^2 = A_0 + \varepsilon \cdot (A_1 - \frac{3}{2} Y) + \varepsilon^2 \cdot (A_2 + \frac{9}{4} Y^2)$$

whence

$$A_0 = \frac{3}{2} \quad A_1 = 0 \quad A_2 = 0$$

Consequently, (150) becomes:

$$(150') \quad u = f(Y, \varepsilon) \equiv F(Y, \varepsilon) \sim \frac{3}{2} (1 - e^{-Y}) - \varepsilon \cdot \frac{3}{2} Y + \varepsilon^2 \cdot \frac{9}{4} Y^2, \quad Y = \frac{Y}{\varepsilon}$$

Now, (144) and (150') give a complete picture of the solution up to the second order in the whole of $[0, +\infty)$. For a composite expansion, we put:

$$\left\{
 \begin{aligned}
 u &\sim 1 + \frac{1}{2} e^{-3Y} + \frac{3}{2} (1 - e^{-Y}) - \lim_{Z \rightarrow \infty, \varepsilon Z \rightarrow 0} \frac{3}{2} (1 - e^{-Z}) \\
 &+ \varepsilon \cdot 0 + \varepsilon \cdot \left(-\frac{3}{2} Y\right) - \lim_{Z \rightarrow \infty, \varepsilon Z \rightarrow 0} \varepsilon \cdot \left(-\frac{3}{2} Z\right) \\
 &+ \varepsilon^2 \cdot 0 + \varepsilon^2 \cdot \left(\frac{9}{4} Y^2\right) - \lim_{Z \rightarrow \infty, \varepsilon Z \rightarrow 0} \varepsilon^2 \cdot \left(\frac{9}{4} Z^2\right)
 \end{aligned}
 \right.$$

That is to say:

$$(152) \quad u \sim 1 + \frac{1}{2} e^{-3Y} - \frac{3}{2} e^{-Y} - \varepsilon \cdot \frac{3}{2} Y + \varepsilon^2 \cdot \frac{9}{4} Y^2, \quad Y = \frac{y}{\varepsilon}$$

There is a theoretical basis for matching, developed by Kerkovian, Cole, Eckhaus, etc... It relies upon the introduction of an intermediate variable

$$(153) \quad \hat{Y} = y h(\varepsilon)^{-1} \text{ with } h(\varepsilon) \rightarrow 0, \quad h(\varepsilon) g(\varepsilon)^{-1} \rightarrow +\infty$$

which determines the region of validity of both outer and inner expansions. The theoretical rule for matching is to identify the various terms of the inner and the outer expansions when they are written in the intermediate variable \hat{Y} .

D) Asymptotic theory (II) : The boundary layer equations for isentropic compressible flow

We next apply the standard asymptotic method to the problem of an isentropic compressible flow around an obstacle. For simplicity, we use a one-term approach.

The outer expansion gives the so-called outer inviscid (first order) problem:

$$(154) \quad \frac{\partial \rho_e}{\partial t} + \nabla \cdot (\rho_e \vec{u}_e) = 0$$

$$(155) \quad \frac{\partial \vec{u}_e}{\partial t} + (\vec{u}_e \cdot \nabla) \vec{u}_e + \frac{1}{\rho_e} \nabla p_e = 0$$

$$(156) \quad p_e = K \rho_e^\gamma$$

$$(157) \quad \rho_e = \rho_\infty, \quad \vec{u}_e = \vec{u}_\infty \quad \text{on } \Gamma_\infty^-$$

$$(158) \quad \vec{u}_e \cdot \vec{n} = 0 \quad \text{on } \Gamma_B$$

The inner expansion leads to Prandtl's equations (here S and n are resp. the tangential and normal coordinates; $N = n / \delta(Re)$, $\delta(Re) = Re^{-1/2}$; notice that $Re^{-1/2}$ is the small parameter!)

$$(159) \quad \frac{\partial p_i}{\partial t} + \frac{\partial}{\partial s} (p_i u) + \frac{\partial}{\partial N} (p_i v) = 0$$

$$(160) \quad \frac{\partial u}{\partial t} + u \frac{\partial u}{\partial s} + v \frac{\partial u}{\partial N} + \frac{1}{p_i} \frac{\partial p_i}{\partial s} = \frac{1}{p_i} \frac{\partial}{\partial N} (p_i \frac{\partial u}{\partial N})$$

$$(161) \quad \frac{\partial p_i}{\partial N} = 0$$

$$(162) \quad p_i = K p_i^r$$

$$(163) \quad u = v = 0 \quad \text{at} \quad N=0$$

Finally, matching gives:

$$(164) \quad u|_{N=\infty} = \vec{u}_e \cdot \vec{s} |_{P_B}$$

$$(165) \quad p_i|_{N=\infty} = p_e |_{P_B}$$

$$(166) \quad p_i|_{N=\infty} = p_e |_{P_B}$$

Hence, the final result is:

1. Outer (one-term) expansion:

$$(167) \quad \vec{u} = \vec{u}(x, t; Re) \sim \vec{u}_e(x, t)$$

$$(168) \quad p = p(x, t; Re) \sim p_e(x, t)$$

$$(169) \quad p = p(x, t; Re) \sim p_e(x, t)$$

with \vec{u}_e, p_e, p_e solving (154)-(158) together with appropriate initial conditions for p_e and \vec{u}_e .

2. Inner (one-term) expansion:

In (s, n) variables, the velocity field is

$$(170) \quad \vec{u} = \vec{u}(s, n, t; Re) \equiv \vec{u}(s, N, t; Re) \sim (u, \delta v);$$

$$(171) \quad p = P(s, N, t; Re) \sim p_i(s, t)$$

$$(172) \quad \rho = R(s, N, t; Re) \sim p_i(s, t)$$

with $N = n/8$, $\delta = Re^{1/2}$,

$$(173) \quad p_i(s, t) = p_e(x(s, 0), t) \quad (\text{on } \Gamma_B !)$$

$$(174) \quad p_i(s, t) = p_e(x(s, 0), t) \quad \text{Id.}$$

and with (u, v) satisfying:

$$(175) \quad \frac{\partial u}{\partial t} + \frac{\partial}{\partial s}(p_i u) + p_i \frac{\partial v}{\partial N} = 0$$

$$(176) \quad \frac{\partial v}{\partial t} + u \frac{\partial u}{\partial s} + v \frac{\partial u}{\partial N} + \frac{1}{p_i} \frac{\partial p_i}{\partial s} = \frac{\partial^2 u}{\partial N^2}$$

$$(177) \quad u(s, 0, t) = v(s, 0, t) = 0$$

$$(178) \quad u(s, \infty, t) = (\vec{u}_e \cdot \vec{s})(x(s, 0), t)$$

together with an appropriate initial condition for u .

If it is desired, the expansions can be further continued.

Generally speaking, one solves the i^{th} outer problem, uses the values of the pressure, the density and the tangential velocity on Γ_B to solve the i^{th} inner problem and uses the values of the normal velocity at infinity to solve the $(i+1)^{\text{th}}$ outer problem.

E) Asymptotic theory (III) : The turbulent boundary layer equations for isentropic compressible flow

We argue as before, but starting from Reynolds equations (129)-(131) for isentropic compressible flow. An averaging procedure has been introduced to define the mean quantities

$$\bar{p}, \bar{u}, \bar{v}$$

and the turbulent fluctuation \tilde{u}' .

Standard application of asymptotic methods (C.1)-(C.3) (see above) yields the following:

1. Outer (one-term) expansion :

$$(179) \quad \tilde{u} = \tilde{u}(x, t; Re) \sim \tilde{u}_e(x, t)$$

$$(180) \quad \bar{p} = \bar{p}(x, t; Re) \sim \bar{p}_e(x, t)$$

$$(181) \quad \bar{R} = \bar{R}(x, t; Re) \sim \bar{R}_e(x, t)$$

$$(182) \quad \tilde{R} = \tilde{R}(x, t; Re) \sim \tilde{R}_e(x, t)$$

Here, \tilde{u}_e , \bar{p}_e , \tilde{p}_e and \tilde{R}_e satisfy:

$$(183) \quad \frac{\partial \tilde{p}_e}{\partial t} + \nabla \cdot (\bar{p}_e \tilde{u}_e) = 0$$

$$(184) \quad \frac{\partial \tilde{u}_e}{\partial t} + (\tilde{u}_e \cdot \nabla) \tilde{u}_e + \frac{1}{\bar{p}_e} \nabla \bar{p}_e = \frac{1}{\bar{p}_e} \nabla \cdot \tilde{R}_e$$

$$(185) \quad \bar{p}_e = K(\bar{p}_e)^r \quad (\text{i.e. } \bar{p}_e'' \approx 0)$$

$$(186) \quad \bar{p}_e = p_\infty, \quad \tilde{u}_e = \tilde{u}_\infty \text{ on } \Gamma_B, \quad \tilde{u}_e \cdot \vec{n} = 0 \text{ on } \Gamma_B$$

together with initial conditions for \bar{p}_e and \tilde{u}_e .

2. Inner (one-term) expansion :

We use again the variables (s, n) .

$$(187) \quad \tilde{u} = \tilde{u}(s, n, t; Re) \equiv \tilde{U}(s, N, t; Re) \sim (\tilde{u}, \delta \tilde{v})$$

$$(188) \quad \bar{p} = \bar{p}(s, N, t; Re) \sim \bar{p}_i(s, t)$$

$$(189) \quad \bar{R} = \bar{R}(s, N, t; Re) \sim \bar{R}_i(s, t)$$

$$(190) \quad \tilde{R} = \tilde{R}(s, N, t; Re) \sim \tilde{R}_i(s, N, t)$$

$$(191) \quad \bar{p}_i(s, t) = \bar{p}_e(x(s, 0), t)$$

$$(192) \quad \tilde{p}_i(s, t) = \tilde{p}_e(x(s, 0), t)$$

and (u, v) satisfying:

$$(193) \quad \frac{\partial \bar{p}_i}{\partial t} + \frac{\partial}{\partial s} (\bar{p}_i \tilde{u}) + \bar{p}_i \frac{\partial \tilde{v}}{\partial N} = 0$$

$$(194) \quad \frac{\partial \tilde{v}}{\partial t} + \tilde{u} \frac{\partial \tilde{u}}{\partial s} + \tilde{v} \frac{\partial \tilde{u}}{\partial N} + \frac{1}{\bar{p}_i} \frac{\partial \bar{p}_i}{\partial s} = \frac{\partial^2 \tilde{u}}{\partial N^2} + \frac{1}{\bar{p}_i} \left(\frac{\partial}{\partial s} (R_i)_{11} + \frac{\partial}{\partial N} (R_i)_{12} \right)$$

$$(195) \quad \bar{p}_i = K(\bar{p}_i)^T$$

$$(196) \quad \tilde{u}(s, 0, t) = \tilde{v}(s, 0, t) = 0$$

$$(197) \quad \tilde{u}(s, \infty, t) = (\vec{u}_e \cdot \vec{s})(x(s, 0), t)$$

together with an appropriate initial condition for \tilde{u} .

One usually introduces the term

$$(198) \quad \frac{1}{\bar{p}_i} \frac{\partial}{\partial s} (R_i)_{11}$$

into the pressure derivative (see below for a more detailed analysis).

F) The composite nature of turbulent boundary layers

According to experimental data and further dimensional analysis, a turbulent boundary layer consists of:

1. An outer region ($\approx 80 - 90\%$ of the complete layer)

Here, turbulent Reynolds stresses (τ_t) are much greater than viscous terms (τ_ℓ).

2. An inner region ($\approx 10 - 20\%$)

Here, τ_t and τ_ℓ are of the same order of magnitude.

It is further composed by

a) The viscous sublayer (vs), where $\tau_\ell \gg \tau_t$.

b) The transitional region (trr), where τ_ℓ diminishes and τ_t grows

c) The fully turbulent region (ftr), where $\tau_\ell \ll \tau_t$.

Through the inner region, $\tau_\ell + \tau_t$ is practically constant.

An appropriate form for the Prandtl-Reynolds' equations for isotropic compressible flow (for simplicity, we consider stationary

flow; we use the notation described above):

$$\begin{aligned} \frac{\partial}{\partial s} (\bar{p}_e \tilde{u}) + \frac{\partial}{\partial n} (\bar{p}_e \bar{v}) &= 0 \\ \tilde{u} \frac{\partial \tilde{v}}{\partial s} + \bar{v} \frac{\partial \tilde{u}}{\partial n} + \frac{1}{\bar{p}_e} \frac{\partial \bar{p}_e}{\partial s} &= \frac{1}{\bar{p}_e} \frac{\partial}{\partial n} \left(\bar{\mu} \frac{\partial \tilde{u}}{\partial n} - \bar{p}_e \overline{u' v'} \right) = \frac{1}{\bar{p}_e} (\tau_t + \tau_b) \\ (\bar{\mu} = \bar{p}_e \nu, \quad \nu = Re^{-1}) \end{aligned}$$

With small pressure gradient, basic assumptions (confirmed by experience) lead to:

$$(199) \quad u^+(s, n^+) = n^+ \quad \text{in the vs} \quad (n^+ < 5 \text{ approx.})$$

$$(200) \quad = \frac{1}{x} \log n^+ + C_{int} \quad (x \approx 40, C_{int} \approx 5.) \quad \text{in the ftr} \\ (n^+ > 50 \text{ approx.})$$

$$(201) \quad = \int_0^{n^+} \frac{2 d\eta}{1 + (1 + 4(x\eta)^2 (1 - \exp(-\eta/A^+))^2)^{1/2}} \quad (A^+ \approx 26.) \quad \text{in the trr}$$

These equalities give the so-called law of the wall:

$$(202) \quad u^+(s, n^+) = \Psi_{int}(n^+) \quad \text{in the inner region.}$$

On the other hand, from Cole's work one obtains the defect law

$$(203) \quad (\tilde{u}_e - \tilde{u}) / u_\infty = f_{ext}(n/\delta) \quad \text{in the outer region,}$$

with

$$(204) \quad \begin{cases} f_{ext}\left(\frac{n}{\delta}\right) = -\frac{1}{x} \log\left(\frac{n}{\delta}\right) + \frac{\Pi(s)}{x} (2 - w\left(\frac{n}{\delta}\right)), \\ \Pi(s) : \text{a given function (nearly a const., 0.55)} \\ w(z) = 2 \sin^2\left(\frac{\pi}{2}z\right) \end{cases}$$

Generalized Milikan's argument supports the idea that (199)-(204) are asymptotically correct:

The behavior of the fluid in a turbulent boundary layer is also

governed by:

a) Wall roughness

This usually produces a shift in the velocity profile. The law of the wall (202) is now slightly modified:

$$(202') \quad u^+(s, n^+) = \hat{\varphi}_{int}(n^+, r^+), \quad r^+ = r u_T / v$$

where r is a roughness parameter.

b) The location of transition (from laminar to turbulent) points

This can be modelled by inserting a factor γ_{tr} in the expression for v_t (see (132')).

G) Some classical models for turbulent boundary layers

The basic equations are:

$$(205) \quad \frac{\partial}{\partial s}(\rho_e u) + \frac{\partial}{\partial n}(\rho_e v) = 0$$

$$(206) \quad u \frac{\partial u}{\partial s} + v \frac{\partial u}{\partial n} + \frac{1}{\rho_e} \frac{\partial p_e}{\partial s} = \frac{1}{\rho_e} \frac{\partial}{\partial n} (\mu \frac{\partial u}{\partial n} - \rho_e \overline{u'v'}) = \frac{1}{\rho_e} (\tau_l + \tau_t)$$

together with appropriate initial and boundary conditions (after time discretization, the instationary problem can be modelled analogously). All quantities in (205)-(206) are macroscopic (they are averaged quantities!).

(G.1) Simple (integral) methods

They do not need, generally speaking, the use of a computer.

They provide some formulae which can be used for a better understanding of the phenomena (mainly due to Von Karman, Schoenherr, Spence, Truckenbrodt, Thwaites, etc...)

The integral methods solve the integrated equations

$$(207) \quad \frac{d}{ds} (\rho_e u_e^2 \theta) + \rho_e u_e \delta_1 \frac{du_e}{ds} = \tau_w$$

$$(208) \quad \frac{d\theta}{ds} + \frac{\theta}{u_e} (H+2) \frac{du_e}{ds} + \frac{\theta}{\rho_e} \frac{dp_e}{ds} = \frac{\tau_w}{\rho_e u_e^2} \equiv \frac{C_f}{2}$$

where δ_1 and θ are resp. the displacement and momentum thickness, $H = \delta_1/\theta$ is the shape factor and C_f is the coefficient of skin friction.

Together with (207)-(208), one uses some expressions for C_f , δ and θ (confirmed by experiences by Dhawan, Smith & Walker, Winter & Gaudet, etc...)

(G.2) Differential (zero-equations) methods

Due to the relatively poor results one can obtain with integral methods, it is necessary to solve (205)-(206) and not simply (207)-(208). In zero-equation models, one uses Boussinesq's or Prandtl's hypotheses, i.e.

$$(209) \quad -\overline{u'v'} = V_t \frac{\partial u}{\partial n} \quad \text{or} \quad -\overline{u'v'} = l^2 \left| \frac{\partial u}{\partial n} \right| \frac{\partial u}{\partial n}$$

together with an empirical law for V_t or l to close the problem.

The most important zero-equations methods are due to Cebeci & Smith, Mellor & Herring, Patankar & Spalding and Crawford & Kays.

They all use the facts that:

- In the outer region, V_t behaves practically as a constant, up to a transitional factor δ_{tr}
- In the inner region, V_t and l depend almost linearly on η .

(G.3) Differential (one-equation) methods

Zero-equation methods are robust and do not need too storage. To be more accurate, one introduces one-equation models. Essentially, one uses Boussinesq's hypothesis, (132') an additional pde for \tilde{k} (or l) and an algebraic expression for l (or \tilde{k}).

For instance, one has the following equation for \tilde{k} :

$$\begin{aligned} & \rho_e \left(\frac{\partial \tilde{k}}{\partial t} + u \frac{\partial \tilde{k}}{\partial s} + v \frac{\partial \tilde{k}}{\partial n} \right) \\ &= - \rho_e \left((\overline{u'})^2 \frac{\partial u}{\partial s} + \overline{u'v'} \frac{\partial u}{\partial n} \right) - \rho_e v \left(\frac{\partial u}{\partial n} \right)^2 \\ & - \frac{\partial}{\partial n} \left(\frac{1}{2} \rho_e (\overline{u'})^2 v' + \rho_e \overline{v'} - \rho_e v \frac{\partial u}{\partial n} \right) + \rho_e \left(\frac{\partial u}{\partial s} + \frac{\partial v}{\partial n} \right). \end{aligned}$$

The task is thus reduced to model the various terms in the right hand side and to fix the dependence of λ with respect to ρ_e , u and V .

Some one-equation methods are due to Glushko, Beckwith & Bushnell, Mellor & Herring, Ng & Spalding, Bradshaw et al., Jones & Launder, Norris & Reynolds, etc...

(G.4) Differential methods with two or more equations

They use additional variables (two or more) to close (205)-(206). It seems that the most appropriate choices are \tilde{k} and the rate of viscous dissipation (or \tilde{k} and (say) helicity). A particular example of a two-equations model is MPP's model. Other two-equations models are due to Tucker & Reynolds, Maréchal, Champagne, Harris & Corrsin, Rose, Jones & Launder, Handjalic & Launder, etc...

(G.5) Other methods

- Reynolds stress transport methods use (206)-(207) and an equation for $-\overline{u'v'}$ (Handjalic & Launder, Lumley, Reynolds, etc...)
- Large scale simulation methods introduce a filtering procedure which drops small scale turbulent effects (Kwak, Reynolds & Ferziger, Comte-Bellot & Corrsin, etc...)

1.6 The M.P.P. model of turbulence for isentropic compressible flow

Formulation of the problem for isentropic compressible 2D flow
(The reduced version, with constant helicity) :

$$(210) \quad \frac{\partial \vec{u}}{\partial t} + \nabla \cdot (\rho \vec{u}) = 0$$

$$(211) \quad \frac{\partial \vec{u}}{\partial t} + (\vec{u} \cdot \nabla) \vec{u} + \frac{1}{\rho} \nabla p = \frac{1}{\rho} \nabla \cdot (\rho k R^1 - A_1 \epsilon p \sqrt{R} D(\vec{u}))$$

$$(212) \quad p = K_p^T$$

$$(213) \quad \frac{\partial k}{\partial t} + \vec{u} \cdot \nabla k = \frac{1}{\rho} \nabla \cdot (A_2 \varepsilon^{4/3} \rho \sqrt{k} \nabla R^L) - k \tilde{R}^L \cdot \nabla \vec{u} - \mu_0 k \Psi_q$$

$$(214) \quad \tilde{R}^L = \tilde{R}^L(\tilde{\nabla} \vec{a}), \quad \Psi_q = \Psi_q(\tilde{\nabla} \vec{a})$$

$$(215) \quad \frac{\partial \vec{a}}{\partial t} + (\vec{u} \cdot \nabla) \vec{a} = 0$$

together with appropriate initial and boundary conditions.

ρ, \vec{u}, p and k are mean distributions for the density, velocity field, pressure and turbulent kinetic energy resp.

\tilde{R}^L and Ψ_q are "known" functions of $\tilde{\nabla} \vec{a}$, with \vec{a} giving the Lagrangian coordinates (they are obtained by solving a certain micro-structure problem).

A_1, A_2, K, γ and μ_0 are positive constants while $\varepsilon (> 0)$ is a small parameter (it gives the ratio of large and small scales of length). The fluid is assumed to be viscous, with viscosity very small ($Re = 1/\mu_0 \varepsilon^2$). Finally,

$$\tilde{D}(\vec{u}) \equiv \tilde{\nabla} \vec{u} + \tilde{\nabla} \vec{u}^T - \frac{2}{3} (\nabla \cdot \vec{u}) \text{Id.}$$

Initial conditions hold for ρ, \vec{u}, k and \vec{a} . The boundary conditions are typically as follows:

$$(216) \quad \rho = \rho_\infty, \quad \vec{u} = \vec{u}_\infty, \quad k = k_\infty \quad \text{on } \Gamma_\infty^-$$

$$(217) \quad \vec{u} = 0, \quad k = k_B \quad \text{on } \Gamma_B$$

$$(218.a) \quad \left\{ -\frac{K\gamma}{\gamma-1} \rho^{\gamma-1} \text{Id.} - k \tilde{R}^L + A_1 \varepsilon \sqrt{k} \tilde{D}(\vec{u}) \right\} \cdot \vec{n} = 0 \quad \text{on } \Gamma_\infty^+$$

$$(218.b) \quad \frac{\partial k}{\partial n} = 0 \quad \text{on } \Gamma_\infty^+$$

$$(219) \quad \vec{a} = \vec{x} - t \vec{u}_\infty \quad \text{on } \Gamma_\infty^-$$

An alternative boundary condition on Γ_B is

$$(217') \quad \vec{u} = 0, \quad \frac{\partial \vec{R}}{\partial n} = 0 \quad \text{on } \Gamma_B$$

If one desires to solve this problem accurately, it is necessary to account for the presence of a boundary layer near Γ_B .

This can be achieved by changing (217') into a more complicate (and nonlinear) boundary condition on the normal stress

$$\left(-k \frac{\partial^2 \vec{u}}{\partial n^2} + A_1 \epsilon \sqrt{k} \vec{D}(\vec{u}) \right) \cdot \vec{n}.$$

Adequate forms of this boundary condition will be described below, in Chapters 2 and 3.

To end this Chapter, we give a list of several references that have been used in this preliminary study. We refer to the papers and books quoted in Chapter 0.

- For the general description of the least-square methods for nonlinear pde's, see ref. 4 and the bibliography therein.
- For time discretization schemes, Glowinski & Pironneau's Stokes solvers and the numerical solution of the compressible Navier-Stokes problem, see ref. 3 and the bibliography therein.
- For the description of the Buckley & LeNir's conjugate gradient methods, see ref. 6, 7.
- For the description of turbulent flows, see ref. 15, 16.
- For the description and properties of a turbulent boundary layer, see ref. 8, 14.
- For general results on asymptotic theory, see ref. 11-13.
- For applications of asymptotic theory to fluid mechanics and turbulence, see ref. 13, 26 and 27.
- For turbulence models, see ref. 14, 16-19, and the bibliography in 14, 18.
- For the M.P.P. model, see ref. 1, 2, 20-22.

Notations

- Ω the fluid domain (a regular bounded connected open set in R^2 or R^3)
 $\Gamma = \partial\Omega$
 $\rho = \rho(x, t)$ the fluid density
 $\vec{u} = \vec{u}(x, t)$ " " velocity field
 $e = e(x, t)$ " " total energy
 $\varepsilon = \varepsilon(x, t)$ " " specific internal energy
 $p = p(x, t)$ " " pressure
 $\theta = \theta(x, t)$ " " temperature
 Re " " Reynolds number
 Pr " " Prandtl's number
 $\gamma (= 1.4)$ " " ratio of specific heats
 $\vec{n} = \vec{n}(x)$: the unit outwards normal vector
 M_∞ : the fluid Mach number at infinity
 Δt : time discretization parameter
 $H^1(\Omega) = \{v/v \in L^2(\Omega), \frac{\partial v}{\partial x_i} \in L^2(\Omega), i=1,2\}$
 $H^1(\Gamma_*) = \{v|_{\Gamma_*} / v \in H^1(\Omega)\}$
 $H^1(\Gamma_*)$: the dual space of $H^1(\Gamma_*)$
 $P_1(T)$: the space of polynomial functions on T (a triangle) of degree ≤ 1
 $\vec{a} \otimes \vec{b}$: the second order tensor with components
 $n^+ \quad n u_\tau / v \quad u_\tau \quad \sqrt{\tau_w / \bar{\rho}_e} \quad \tau_w \quad \tau_\ell|_{n=0}$
 $u^+ \quad \tilde{u} / u_\tau$

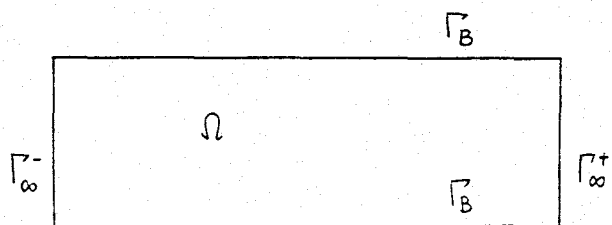
FIGURES

Figure 1:
Channel flow (from left to right)

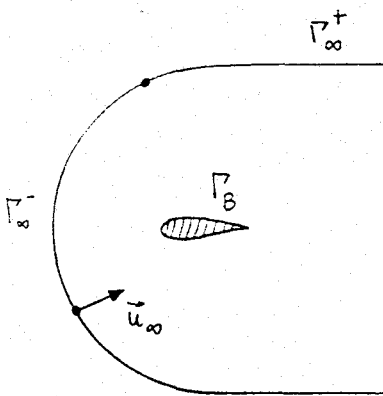


Figure 2:
Flow around and past an obstacle

References

1. D.MCLAUGHLIN-G.PAPANICOLAU-O.PIRONNEAU: Transport of microstructures. SIAM J. Appl. Math. 45,780-797 (1985).
2. T.CHACON-REBOLLO: Etude d'un modèle pour la convection des microstructures. Thèse 3^{ème} Cycle. Univ. Paris VI. Paris (1985).
3. M.O.BRISTEAU-J.PERIAUX: Finite element methods for the calculation of compressible viscous flows using self-adaptive mesh refinement. L.N. Comp. Fluid Dynamics (1986)
4. R.GLOWINSKI: Numerical Methods for Nonlinear Variational Problems. Springer Series in Comp. Phys. Springer-Verlag, New-York (1984).
5. R.GLOWINSKI-O.PIRONNEAU: On a mixed finite element approximation of the Stokes problems (I): Convergence of approximate solution. Num. Math. 33,397-424 (1979).
6. A.BUCKLEY-A.LENIR: QN-like variable storage conjugate gradients. Math. Programm. 27,2,155-175 (1984).
7. C.LEMARECHAL-P.SERVIGNE: Le module M1GC2. Rapport INRIA (1985).
8. H.SCHLICHTING: Teoría de la Capa Límite. Ed. URMO,Bilbao (1972).
9. R.L.PANTON: Incompressible Flows. John-Wiley and Sons, New-York (1984).
10. A.BENSOUSSAN-J.L.LIONS-G.PAPANICOLAU: Asymptotic Analysis for Periodic Structures. Nort-Holland, Amsterdam (1978).
11. W.ECKHAUS: Asymptotic Analysis and Singular Perturbation. Nort-Holland, Amsterdam (1979).
12. J.KEVORKIAN-J.D.COLE: Perturbation Methods in Applied Mathematics Springer-Verlag, New-York (1981).
13. M.VAN DYKE: Perturbation Methods in Fluids Mechanics. Parabolic Press, Palo Alto, California (1975).
14. T.CEBECI-A.M.O.SMITH: Analysis of Turbulence Boundary Layers. Acad. Press, Inc. London (1974).
15. H.TENNEKES-J.L.LUMLEY: A First Cours in Turbulence. The M.I.T. Press, Cambridge (1972).
16. B.E.LAUNDER-D.B.SPALDING: Mathematical Models of Turbulence. Acad. Press, New-York (1972).
17. W.S.REYNOLDS: Physical an analitical foundations, concepts and new directions in turbulence modelling and simulation. Procc. Ecole d'été d'Analyse Numérique, Clamart (1982).
18. J.H.FERZIGER: Simulation of incompressible turbulent flows. Review J. Comp. Phys. 69,1-48 (1987).

19. M.NALLASAMY: Turbulence models and their application to the prediction of internal flow. Review. Comp. Fluid, 230, 218-236 (1987).
20. F.ORTEGON-GALLEG: Rapport INRIA to appear.
21. C.BEGUE: Simulation de la turbulence par méthode d'homogénéisation. Thèse 3^{ème} Cycle. Univ. Paris VI (1983).
22. A.T.PATERA-S.A.ORSZAG: Secondary instability of wall-bounded shear flows. J. Fluid Mech. 128, 347-385 (1983).
23. M.FORTIN: Approximation d'un opérateur de projection et application à un schéma de résolution numérique des équations de Navier-Stokes. Thèse 3^{ème} Cycle. Univ. Paris-Sud (1970).
24. F.THOMASSET: Implementation of Finite Element Methods for Navier-Stokes Equations. Springer-Verlag, New-York (1981).
25. R.GLOWINSKI-A.MARROCCO: Finite element approximation and iterative methods of solution for 2D nonlinear magnetostatic problems. Procc. of COMPUMAG Conf. Oxford, 112-125 (1976).
26. K.YAJNIK: Asymptotic theory of turbulent shear flows. J. Fluid Mech. 42, 2, 411-427 (1970).
27. N.AFZAL: A higher order theory for compressible turbulent boundary layers at moderately Reynolds numbers. J. Fluid Mech. 57, 1, 1-25 (1973).

Capítulo 2

**El modelo M.P.P. de Turbulencia para
flujos compresibles isentrópicos**

3. The M.P.P. model of Turbulence for isentropic compressible flows

As mentioned in the previous Chapters, the M.P.P. model of Turbulence can be extended to isentropic compressible flows under an additional hypothesis of incompressibility for the turbulent fluctuating field.

The first attempt in this direction is due to Chacón [2], who introduced asymptotics for the compressible Euler equations. With the same kind of arguments used in Chapter 2, he derived a model which describes turbulence in the absence of solid walls.

Here, we briefly present the derivation of an asymptotic model of M.P.P. kind for Newtonian slightly viscous and isentropic compressible flow. At a first stage, boundary effects will be ignored. This will lead to a closed model which is further used for numerical simulation. At the end of this Chapter, however, it will be shown how the presence of a boundary layer can be taken into account.

3.1 Description of the model

As in Chapter 2, we assume that the mean flow and the turbulent fluctuation vary spatially in two well separated scales. Denoting by L and l the corresponding length scales and taking $\varepsilon = \frac{l}{L}$, we are interested in the solution of

$$(3.1) \quad \begin{cases} \rho^\varepsilon(u_{,t}^\varepsilon + (u^\varepsilon \cdot \nabla) u^\varepsilon) + \nabla p^\varepsilon = \mu^\varepsilon \varepsilon^2 (\Delta u^\varepsilon + \frac{1}{3} \nabla(\nabla \cdot u^\varepsilon)) \\ \rho_{,t}^\varepsilon + \nabla \cdot (\rho^\varepsilon u^\varepsilon) = 0 \\ p^\varepsilon = K(\rho^\varepsilon)^\gamma, \quad (\gamma > 1) \end{cases}$$

in $\Omega \times [0, T]$, together with initial conditions of the form

$$(3.2) \quad \begin{cases} u^\varepsilon(x, 0) = u_0(x) + \varepsilon^{1/3} w_0(\frac{x}{\varepsilon}, x) \\ \rho^\varepsilon(x, 0) = \rho_0(x) + \varepsilon^{2/3} \sigma_0(\frac{x}{\varepsilon}, x) \end{cases}$$

Here, u_0 and ρ_0 are the mean initial velocity field and density and w_0 and σ_0 are the corresponding initial fluctuations. One assumes that they are all regular functions, that $w_0 = w_0(y, x), \sigma_0 = \sigma_0(y, x)$ are periodic in the variable $y \in Y$ (with again $Y =]-\pi, \pi[$) and also that w_0 and σ_0 have mean zero:

$$\begin{aligned} \langle w_0 \rangle &= \frac{1}{|Y|} \int_Y w_0(y, x) dy = 0, \quad \forall x \in \Omega \\ \langle \sigma_0 \rangle &= \frac{1}{|Y|} \int_Y \sigma_0(y, x) dy = 0, \quad \forall x \in \Omega \end{aligned}$$

The orders of magnitude of the viscosity coefficient in (3.1) and the turbulent fluctuations in (3.2) are motivated by the analogy with Kolmogorov's Analysis. The state equation (3.1) can be used to eliminate p^ε as an unknown of the problem. Indeed, if we set $\mu^\varepsilon = \rho^\varepsilon \nu$ (with $\nu > 0$ being a positive constant), then (3.1) can be re-written as follows:

$$(3.1)' \quad \begin{cases} u_{,t}^\varepsilon + (u^\varepsilon \cdot \nabla) u^\varepsilon + \nabla p_*^\varepsilon = \nu \varepsilon^2 (\Delta u^\varepsilon + \frac{1}{3} \nabla(\nabla \cdot u^\varepsilon)) \\ \rho_{,t}^\varepsilon + \nabla \cdot (\rho^\varepsilon u^\varepsilon) = 0 \\ p_*^\varepsilon = \frac{K\gamma}{\gamma - 1} (\rho^\varepsilon)^{\gamma-1} \end{cases}$$

As for incompressible flows, we introduce asymptotic expansions for u^ε and ρ^ε :

$$(3.3) \quad \begin{aligned} u^\varepsilon(x, t) &\sim u(x, t) + \varepsilon^{1/3} w(y, \tau; x, t) + \varepsilon^{2/3} u^{(1)}(y, \tau; x, t) + \\ &+ \varepsilon u^{(2)}(y, \tau; x, t) + \dots \end{aligned}$$

$$(3.4) \quad \begin{aligned} \rho^\varepsilon(x, t) &\sim \rho(x, t) + \varepsilon^{1/3} \sigma(y, \tau; x, t) + \varepsilon^{2/3} \rho^{(1)}(y, \tau; x, t) + \\ &+ \varepsilon \rho^{(2)}(y, \tau; x, t) + \dots \end{aligned}$$

where

$$y = \frac{a(x, t)}{\varepsilon}, \quad \tau = \frac{t}{\varepsilon^{2/3}}$$

and with the components of $a(x, t)$ being again the Lagrangian coordinates associated to the mean flow:

$$(3.5) \quad a_{,t} + (u \cdot \nabla) a = 0, \quad a(x, 0) = x$$

This leads to a formal asymptotic expansion for p_*^ε which takes the form:

$$(3.6) \quad \begin{aligned} p_*^\varepsilon(x, t) &\sim p_*(x, t) + \varepsilon^{1/3} \Pi_*(y, \tau; x, t) + \varepsilon^{2/3} p_*^{(1)}(y, \tau; x, t) + \\ &+ \varepsilon p_*^{(2)}(y, \tau; x, t) + \dots \end{aligned}$$

Let us take $\Pi_0 = K \rho_0^{\gamma-2} \sigma_0$ and assume that the initial perturbations w_0 and Π_0 are related each other through

$$(3.7) \quad (w_0 \cdot \nabla_y) w_0 + \nabla_y \Pi_0 = 0, \quad \nabla_y w_0 = 0, \quad \text{in } \Omega$$

Then, formal calculus, i.e. identification of the coefficients of the various powers of $\varepsilon^{1/3}$ in (3.1)', leads to:

$$(3.8) \quad \left\{ \begin{aligned} u_{,t} + (u \cdot \nabla) u + \nabla p_* &+ \varepsilon^{2/3} \frac{1}{\rho} \nabla \cdot (\rho \tilde{R}^1) \\ &+ \varepsilon \frac{1}{\rho} (A_{,t}^\sigma + (u \cdot \nabla) A^\sigma + A^\sigma \cdot \nabla u) \\ &+ \varepsilon^{4/3} \frac{1}{\rho} (\nabla \cdot (\rho \tilde{R}^1 + \tilde{R}^\sigma + (\gamma - 1) p_*^{(\gamma-2)/(\gamma-1)} B^\sigma)) \\ &= o(\varepsilon^{4/3}) \end{aligned} \right.$$

$$(3.9) \quad \rho_{,t} + \nabla \cdot (\rho u) + \varepsilon \nabla \cdot A^\sigma = o(\varepsilon)$$

$$(3.10) \quad p_* = \frac{K\gamma}{\gamma-1} \rho^{\gamma-1}$$

where one has used the notation

$$(3.11) \quad \left\{ \begin{array}{l} \tilde{R} = \langle w \otimes w \rangle, \quad A^\sigma = \langle \sigma w \rangle \\ \tilde{R}^1 = \langle w \otimes u^{(2)} + u^{(2)} \otimes w \rangle, \quad \tilde{R}^\sigma = \langle \sigma w \otimes w \rangle \\ B^\sigma = \nabla \langle \sigma^2 \rangle \end{array} \right.$$

The turbulent fluctuations w and σ are given by a solution of

$$(3.12) \quad \left\{ \begin{array}{l} w = \nabla a^{-T} \tilde{w}, \quad \sigma = \frac{\rho^{\gamma-2}}{K\gamma} \Pi \\ \tilde{w}_{,\tau} + (\tilde{w} \cdot \nabla_y) \tilde{w} + \tilde{C} \nabla_y \pi = 0, \quad \nabla_y \cdot \tilde{w} = 0 \quad \text{in } Y \\ (\tilde{w}, \Pi) \quad Y - \text{periodic} \\ \langle \tilde{w} \rangle = 0, \quad \langle \pi \rangle = 0 \\ \frac{1}{2} \langle \tilde{w} \tilde{C}^{-1} \tilde{w} \rangle = q \\ \langle \tilde{w} \tilde{C}^{-1} \tilde{r} \rangle = H \end{array} \right.$$

with $\tilde{r} = \nabla a^T r$, $r = (\nabla a \nabla_y) \times w$, $\tilde{C} = \nabla a^T \nabla a$

Here, $k = \varepsilon^{2/3}q$ and $h = \varepsilon^{2/3}H$ are respectively, the turbulent kinetic energy and helicity at the lowest order. They are given by the solutions of:

$$(3.13) \quad k_{,t} + u \nabla k + \varepsilon^{2/3} \tilde{R} : \nabla u + \varepsilon^{2/3} \nu \psi_q + \varepsilon^{4/3} \frac{1}{\rho} \nabla \cdot (\rho V) = o(\varepsilon^{4/3})$$

$$(3.14) \quad h_{,t} + u \nabla h + \varepsilon^{2/3} \tilde{S} : \nabla u + \varepsilon^{2/3} \nu \psi_h + \varepsilon^{4/3} \nabla \cdot (D + E) = o(\varepsilon^{4/3})$$

with

$$(3.15) \quad \left\{ \begin{array}{ll} \psi_q = \langle (\nabla a \nabla_y) w : (\nabla a \nabla_y) w \rangle & \psi_h = 2 \langle (\nabla a \nabla_y) w : (\nabla a \nabla_y) r \rangle \\ V = \langle \left(\frac{1}{2} |w|^2 + \Pi \right) w \rangle & D = \langle \left(\frac{1}{2} |w|^2 + \Pi \right) r \rangle \\ \tilde{S} = \langle w \otimes r + r \otimes w \rangle & E = \langle w_{,\tau} \cdot \nabla \times w \rangle \end{array} \right.$$

A linearized variant of (3.12) holds for the definition of $u^{(2)}$ (similar arguments can be found in [2]).

3.2 The final form of the model

After some manipulation, it is possible to describe the model as follows

$$(3.16) \quad \begin{cases} u_{,t} + (u \cdot \nabla)u + \frac{1}{\rho} \nabla p + \frac{1}{\rho} \nabla \cdot (\rho k \tilde{R}^1) + \frac{1}{\rho} d_u^\epsilon = 0 \\ \rho_{,t} + \nabla \cdot (\rho u) = 0 \\ p = K p^\gamma \end{cases}$$

In (3.16), \tilde{R}^1 is the reduced Reynolds tensor. It is given by

$$(3.17) \quad \tilde{R}^1 = \langle w' \tilde{\otimes} w' \rangle$$

with w' being, together with π' , a solution of the canonical micro-structure problem:

$$(3.18) \quad \begin{cases} w' = \tilde{\nabla} a^{-T} \tilde{w}', \\ \tilde{w}'_{,\tau} + (\tilde{w}' \cdot \tilde{\nabla}_y) \tilde{w}' + \tilde{C} \tilde{\nabla}_y \Pi' = 0, \quad \tilde{\nabla}_y \cdot \tilde{w}' = 0 \quad \text{in } Y \\ (\tilde{w}', \Pi') \text{ - } Y \text{ - periodic} \\ \langle \tilde{w}' \rangle = 0, \quad \langle \pi' \rangle = 0 \\ \frac{1}{2} \langle \tilde{w}' \tilde{\nabla} a^{-1} \tilde{w}' \rangle = 1 \\ \langle \tilde{w}' \tilde{\nabla} a^{-1} \tilde{r}' \rangle = \frac{h}{k} \end{cases}$$

with $\tilde{r}' = \tilde{\nabla} a^T r'$, $r' = (\tilde{\nabla} a \tilde{\nabla}_y) \times w'$, $\tilde{C} = \tilde{\nabla} a^T \tilde{\nabla} a$

We recall that k and h are respectively the turbulent kinetic energy and the helicity associated to w and $\tilde{\nabla} a$. Of course, a satisfies (3.5); on the other hand, it is formally deduced that k and h solve the transport equations

$$(3.19) \quad k_{,t} + u \nabla k + k [\tilde{R}^1 : \tilde{\nabla} u + \nu \psi_q^1] + \frac{1}{\rho} d_q^\epsilon = 0$$

$$(3.20) \quad h_{,t} + u \nabla h + h [\tilde{S}^1 : \tilde{\nabla} u + \nu \psi_h^1] + \frac{1}{\rho} d_h^\epsilon = 0$$

where \tilde{R}^1 is given by (3.17),

$$(3.21) \quad \tilde{S}^1 = 2 \langle w' \tilde{\otimes} r' \rangle$$

$$(3.22) \quad \psi_q^1 = \langle (\nabla \tilde{a} \nabla_y) w' : (\nabla \tilde{a} \nabla_y) w' \rangle$$

$$(3.23) \quad \psi_h^1 = \langle (\nabla \tilde{a} \nabla_y) w' : (\nabla \tilde{a} \nabla_y) r' \rangle$$

Finally, let us indicate that a coherent analysis suggests the following modelization for the diffusion terms d_u , d_q and d_h (see [2]); here A_1 , A_2 and A_3 are positive constants):

$$(3.24) \quad d_u^\varepsilon = -\nabla \cdot \mathcal{D}_u^\varepsilon, \text{ with } \mathcal{D}_u^\varepsilon = A_1 \rho \varepsilon \sqrt{k} \mathcal{D}(u), \quad \mathcal{D}(u) = \nabla u + \nabla u^T - \frac{2}{3}(\nabla \cdot u) I_d$$

(3.24)

$$(3.25) \quad \begin{cases} d_q^\varepsilon = -\nabla \cdot V_q^\varepsilon, \text{ with } V_q^\varepsilon = A_2 \rho \varepsilon^{4/3} \sqrt{k} \nabla k \\ d_h^\varepsilon = -\nabla \cdot V_h^\varepsilon, \text{ with } V_h^\varepsilon = A_3 \rho \varepsilon^{4/3} \sqrt{h} \nabla h \end{cases}$$

A more compact formulation of the system reads:

$$(3.26) \quad \begin{cases} u_{,t} + (u \cdot \nabla) u + \frac{1}{\rho} \nabla p + \frac{1}{\rho} \nabla \cdot (\rho k R^1) - \frac{1}{\rho} a_1 \varepsilon \nabla \cdot (\rho \sqrt{k} \mathcal{D}(u)) = 0 \\ \rho_{,t} + \nabla \cdot (\rho u) = 0, \quad p = K \rho^\gamma \\ k_{,t} + u \nabla k + k [R^1 : \nabla u + \nu \psi_q] - \frac{1}{\rho} A_2 \varepsilon^{4/3} \nabla \cdot (\rho \sqrt{k} \nabla k) = 0 \\ h_{,t} + u \nabla h + h [S^1 : \nabla u + \nu \psi_h] - \frac{1}{\rho} A_3 \varepsilon^{4/3} \nabla \cdot (\rho \sqrt{h} \nabla h) = 0 \end{cases}$$

Due to the results in Chapter 2, one knows that the closure terms R^1 , S^1 , ψ_q^1 and ψ_h^1 are functions of $C = \nabla \tilde{a}^T \nabla \tilde{a}$, h and k through (3.17), (3.21)-(3.23) and the microstructure problem (3.18). We recall that a satisfies

$$(3.27) \quad a_{,t} + (u \cdot \nabla) a = 0$$

As usual, (3.26)-(3.27) has to be completed with initial and boundary conditions. These take the form

$$(3.28) \quad \begin{bmatrix} u \\ \rho \\ k \\ h \\ a \end{bmatrix}_{t=0} = \begin{bmatrix} u_0(x) \\ \rho_0(x) \\ \frac{\varepsilon^{2/3}}{2} \langle |w_0|^2 \rangle (x) \\ \frac{\varepsilon^{2/3}}{2} \langle w_0 \cdot (\nabla_y \times w_0) \rangle (x) \\ x \end{bmatrix}$$

$$(3.29) \quad \begin{bmatrix} u \\ \rho \\ k \\ h \\ a \end{bmatrix}_{t=0} = \begin{bmatrix} u_{\infty} \\ \rho_{\infty} \\ k_{\infty} \\ h_{\infty} \\ x - tu_{\infty} \end{bmatrix}, \quad \text{at the inflow boundary } \Gamma_{\infty}^-$$

$$(3.30) \quad \left. \begin{array}{l} (-pI\tilde{d} + A_1\rho\varepsilon\sqrt{k}\tilde{D}(u) - \rho k\tilde{R}^1).n = 0 \\ \frac{\partial k}{\partial n} = \frac{\partial h}{\partial n} = 0 \end{array} \right\} \quad \text{at the outflow boundary } \Gamma_{\infty}^+$$

$$(3.31) \quad u = 0, \quad k = k_B, \quad h = h_B \quad \text{on the boundary } \Gamma_B \text{ of a rigid body}$$

Here, $u_{\infty}, \rho_{\infty}, k_{\infty}$ and h_{∞} are prescribed constants. The boundary data k_B and h_B must be carefully chosen (see e.g [1]). It is clear that the Mach number at infinity, M_{∞} , determines the choice of the constant K in (3.26):

$$K = \frac{1}{\gamma M_{\infty}^2}$$

An alternative form of (3.31) relies on the use of the experimental laws of the wall. More precisely, we can imagine we are solving the problem not in the whole domain Ω , but exclusively up to a positive and small distance n_C from the rigid body. If this is sufficiently small, it is accurate to impose a non-homogenous natural condition of the kind

$$(3.32) \quad (A_1\rho\varepsilon\sqrt{k}\tilde{D}(u) - \rho k\tilde{R}^1).n = \rho\varphi(u.s, n_C, \varepsilon).s \quad \text{at distance } n_C$$

where φ is a known function.

Two appropriate choices for φ are (see e.g. [4]):

1. The potential law.

According to experimental results, this seems to be valid for moderate M_{∞} and $\Re = |u_{\infty}|L\nu^{-1}\varepsilon^{-2} \cong 10^5$. It is given implicitly by

$$(3.33) \quad \frac{u.s}{u_{\tau}} = C(q)(\Re n_C u_{\tau})^{1/q}, \quad u_{\tau}^2 = \left[(A_1\rho\varepsilon\sqrt{k}\tilde{D}(u) - k\tilde{R}^1).n \right].s$$

Here, $q \cong 7$ and $C(q)$ has been found experimentally.

2. The logarithmic law.

It is more accurate for higher values of \Re . Using the same notation for u_τ as before, φ is now easily found from the equality

$$(3.34) \quad \frac{u_s}{u_\tau} = \frac{1}{\kappa} \log(\Re n_C u_\tau) + C_*$$

where $\kappa (\cong .40)$ and C_* are also determined by experience.

Clearly, a condition such as (3.32) can be easily incorporated to the variational formulation of the averaged momentum equation as non-linear boundary integral on Γ_B . This provides a first step in the computation of boundary layer effects.

Concerning k and h , it is also adequate to relate them to the friction velocity u_τ . As suggested by experimental results, one can replace, for instance, the Dirichlet condition k in (3.31) by

$$(3.35) \quad k = \gamma_q u_\tau^2 \text{ at distance } n_C$$

where γ_q is a positive constant (again obtained from experimental results). For further details, see e.g. [3].

References

- [1] C.BEGUE: *Simulation de la Turbulence par Méthode d'Homogénéisation*
Thèse 3^{ème} Cycle Paris VI, Décembre 1983.
- [2] T.CHACON: *Etude d'un Modèle pour la Convection des Microstructures.*
Thèse 3^{ème} Cycle Paris VI.
- [3] C.DESCHENES: *Simulation par éléments fins d'un écoulement interne turbulent avec le modèle $k - \epsilon$*
Thèse M. Sc. Univ. Laval, Canada (1986)
- [4] H.SCHLICHTING: *Teoría de la capa límite*
Ediciones Urno (1972)

Capítulo 3

Métodos numéricos para la resolución del
modelo M.P.P. de Turbulencia
bidimensional para un flujo compresible
isentrópico

4. NUMERICAL METHODS

For simplicity, in this Chapter we limit ourselves to the description of the numerical methods for isentropic compressible 2D flows. We recall that our unknowns are the mean density, velocity field and pressure (ρ , \vec{u} and \vec{p}), the turbulent kinetic energy and the Lagrangian coordinates (k and $\vec{\alpha}$). Since the problem is two-dimensional, helicity is ignored. Thus, the closure terms R' and ψ_q are (for the moment being) written as known functions of $\nabla \vec{\alpha}$.

We consider the following formulation of the problem:

$$(1) \quad \frac{\partial \vec{u}}{\partial t} + (\vec{u} \cdot \nabla) \vec{u} + \frac{1}{\rho} \nabla p + \frac{1}{\rho} \nabla \cdot (\rho k R'(\nabla \vec{\alpha})) - \frac{1}{\rho} A_1 \varepsilon \nabla \cdot (\rho \sqrt{k} D(\vec{u})) = 0$$

$$(2) \quad \frac{\partial p}{\partial t} + \nabla \cdot (\rho \vec{u}) = 0$$

$$(3) \quad \frac{\partial k}{\partial t} + \vec{u} \cdot \nabla k + [R'(\nabla \vec{\alpha}) : \nabla \vec{u} + \mu_0 \psi_q(\nabla \vec{\alpha})] k - A_2 \varepsilon^{\frac{1}{3}} \frac{1}{\rho} \nabla \cdot (\rho \sqrt{k} \nabla k) = 0$$

$$(4) \quad \frac{\partial \vec{\alpha}}{\partial t} + (\vec{u} \cdot \nabla) \vec{\alpha} = 0$$

$$(5) \quad \vec{p} = K \rho^\gamma$$

with the following boundary and initial conditions:

$$(6) \quad \begin{cases} \vec{u} = \vec{u}_\infty \\ \rho = \rho_\infty \\ k = k_\infty \\ \vec{\alpha} = \vec{x} - t \vec{u}_\infty \end{cases} \quad \text{on } T_\infty^-$$

$$(7) \quad \begin{cases} \vec{u} = 0 \\ k = k_B \end{cases} \quad \text{on } T_B$$

$$(8) \quad \begin{cases} \left[-\frac{\gamma}{\gamma-1} \frac{1}{\rho} \vec{p} \vec{I} d + k R'(\nabla \vec{\alpha}) - A_1 \varepsilon \sqrt{k} D(\vec{u}) \right] \vec{n} = 0 \\ \frac{\partial k}{\partial n} = 0 \end{cases} \quad \text{on } T_\infty^+$$

$$(9) \quad \begin{cases} \vec{u}(x, 0) = \vec{u}_0(x) \\ p(x, 0) = p_0(x) \\ k(x, 0) = k_0(x) \\ \vec{\alpha}(x, 0) = \vec{x} \end{cases}$$

We introduce the new variable:

$$\sigma = \ln p$$

Then, problem (1)-(9) can be written:

$$(10) \quad \frac{\partial \vec{u}}{\partial t} + (\vec{u} \cdot \nabla) \vec{u} + 8k \tilde{R}^{(k-1)\sigma} \nabla \sigma + \nabla \cdot (k \tilde{R}'(\nabla \vec{\alpha})) + k \tilde{R}'(\nabla \vec{\alpha}) \cdot \nabla \sigma - A_1 \varepsilon \nabla \cdot (\sqrt{k} D(\vec{u})) - A_1 \varepsilon \sqrt{k} D(\vec{u}) \cdot \nabla \sigma = 0$$

$$(11) \quad \frac{\partial \sigma}{\partial t} + \nabla \cdot \vec{u} + \vec{u} \cdot \nabla \sigma = 0$$

$$(12) \quad \frac{\partial k}{\partial t} + \vec{u} \cdot \nabla k + [\tilde{R}'(\nabla \vec{\alpha}) : \nabla \vec{u} + \mu_0 \Psi_g(\nabla \vec{\alpha})] k - A_2 \varepsilon^{4/3} \nabla \cdot (\sqrt{k} \nabla k) - A_2 \varepsilon^{4/3} \sqrt{k} \nabla k \cdot \nabla \sigma = 0$$

$$(13) \quad \frac{\partial \vec{\alpha}}{\partial t} + (\vec{u} \cdot \nabla) \vec{\alpha} = 0$$

$$(14) \quad \begin{cases} \vec{u} = \vec{u}_\infty \\ \sigma = \sigma_\infty = \ln p_\infty \\ k = k_\infty \\ \vec{\alpha} = \vec{x} - t \vec{u}_\infty \end{cases} \quad \text{on } T_\infty^-$$

$$(15) \quad \begin{cases} \vec{u} = 0 \\ k = k_B \end{cases} \quad \text{on } T_B^-$$

$$(16) \quad \begin{cases} \left[-\frac{\chi}{\delta t} K e^{(\chi-1)\delta t} \tilde{I} \tilde{d} + k R^T (\nabla \tilde{a}) - A_1 \epsilon \sqrt{k D} (\tilde{u}) \right] \tilde{n} = 0 \\ \frac{\partial k}{\partial n} = 0 \end{cases} \quad \text{on } \tilde{T}_\infty^+$$

$$(17) \quad \begin{cases} \tilde{u}(x, 0) = \tilde{u}_0(x) \\ \tilde{G}(x, 0) = \tilde{G}_0(x) = \ln f_0(x) \\ k(x, 0) = k_0(x) \\ \tilde{a}(x, 0) = \tilde{x} \end{cases}$$

4.1 Time discretization

Let us define

$$\tilde{U} = (\tilde{G}, \tilde{u}, \tilde{k})$$

(10)-(12) is of the general form

$$(18) \quad \frac{\partial \tilde{U}}{\partial t} + G(\tilde{u}, \tilde{a}) = 0$$

Let Δt be a time step discretization parameter. We have used an implicit two-stepped scheme (Gear) for \tilde{U} in equation (18), and an explicit scheme (Lax-Wendroff) for \tilde{a} in equation (13). For $n \geq 0$, with \tilde{U}^n and \tilde{a}^n approximating $\tilde{U}(\cdot, n \Delta t)$ and $\tilde{a}(\cdot, n \Delta t)$, \tilde{U}^{n+1} and \tilde{a}^{n+1} are obtained from:

$$\frac{3\tilde{U}^{n+1} - 4\tilde{U}^n + \tilde{U}^{n-1}}{2\Delta t} + G(\tilde{U}^{n+1}, \tilde{a}^{n+1}) = 0 \quad \text{for } n \geq 1$$

$$\tilde{a}^{n+1} = \tilde{a}^n - \Delta t \left[(\tilde{u}^{n+1}, \nabla) \tilde{a}^n \right] + \tilde{\gamma}(\Delta t)^2 \left[(\tilde{u}^{n+1}, \nabla) ((\tilde{u}^{n+1}, \nabla) \tilde{a}^n) \right] \quad \text{for } n \geq 0$$

$$\frac{1}{2} \leq \tilde{\gamma} \leq 1$$

\vec{u}^0 and \vec{a}^0 are obtained from the initial data (17). \vec{u}^1 is obtained by using two steps of an implicit backward Euler scheme, with time step $\frac{2\Delta t}{3}$ to keep the same matrices, and then performing standard interpolation.

Hence, at step (n+1) the system to be solved is:

$$(19) \quad \alpha \vec{u} + (\vec{u} \cdot \nabla) \vec{u} + \gamma k \epsilon^{(x-1)} \nabla \sigma + \nabla \cdot (k R'(\nabla \vec{a})) + k R'(\nabla \vec{a}) \cdot \nabla \sigma - A_1 \epsilon \nabla \cdot (\sqrt{k} D(\vec{u})) - A_1 \epsilon \sqrt{k} D(\vec{u}) \cdot \nabla \sigma = \vec{f}_n$$

$$(20) \quad \alpha \sigma + \nabla \cdot \vec{u} + \vec{u} \cdot \nabla \sigma = h_n$$

$$(21) \quad \alpha k + \vec{u} \cdot \nabla k + [R'(\nabla \vec{a}) : \nabla \vec{u} + \mu_0 \Psi_g(\nabla \vec{a})] k - A_2 \epsilon^{4/3} \nabla \cdot (\sqrt{k} \nabla k) - A_2 \epsilon^{4/3} \sqrt{k} \nabla k \cdot \nabla \sigma = g_n$$

$$(22) \quad \vec{a} = \vec{a}^n - \Delta t [(\vec{u} \cdot \nabla) \vec{a}^n] + \tilde{\gamma} (\Delta t)^2 [(\vec{u} \cdot \nabla) ((\vec{u} \cdot \nabla) \vec{a}^n)]$$

with the boundary conditions (14), (15) and (16), where:

$$\alpha = \frac{3}{2\Delta t}$$

$$\vec{f}_n = \frac{4\vec{u}^n - \vec{u}^{n-1}}{2\Delta t}$$

$$h_n = \frac{4\sigma^n - \sigma^{n-1}}{2\Delta t}$$

$$g_n = \frac{4k^n - k^{n-1}}{2\Delta t}$$

Remark: For the initial Euler's scheme, we use the same equations (19), (20), (21) with:

$$\vec{f}_0 = \alpha \vec{u}^0, \quad h_0 = \alpha \sigma^0, \quad g_0 = \alpha k_0$$

$$\vec{f}_{2/3} = \alpha \vec{u}^{2/3}, \quad h_{2/3} = \alpha \sigma^{2/3}, \quad g_{2/3} = \alpha k^{2/3}.$$

Equations (19)–(21) can be rewritten:

$$(23) \quad \alpha \vec{u} - \mu \Delta \vec{u} + \beta \nabla \sigma - \vec{\Phi}(\sigma, \vec{u}, k, \nabla \vec{a}) = \vec{f}_n$$

$$(24) \quad \alpha \sigma + \nabla \cdot \vec{u} + \vec{u} \cdot \nabla \sigma = h_n$$

$$(25) \quad \alpha k - \lambda \Delta k - X(\sigma, \vec{u}, k, \nabla \vec{a}) = g_n$$

where:

$$\mu = A_1 \varepsilon \sqrt{k_{\text{can}}}$$

k_{can} is a characteristic value for the kinetic energy k ,

$$\beta = \gamma K e^{(y-1)\sigma_{\text{can}}}$$

σ_{can} is a characteristic value for the logarithmic density $\sigma = \log \rho$,

$$\lambda = A_2 \varepsilon^{4/3} \sqrt{k_{\text{can}}}$$

$$(26) \quad \vec{\Phi}(\sigma, \vec{u}, k, \nabla \vec{a}) = (\beta - \gamma K e^{(y-1)\sigma}) \nabla \sigma - \nabla \cdot (k \tilde{R}'(\nabla \vec{a})) - k \tilde{R}'(\nabla \vec{a}) \cdot \nabla \sigma - (\vec{u} \cdot \nabla) \vec{u} + A_1 \varepsilon \nabla \cdot [\sqrt{k} \tilde{D}(\vec{u}) - \sqrt{k_{\text{can}}} \nabla \vec{u}] + A_1 \varepsilon \sqrt{k} \tilde{D}(\vec{u}) \cdot \nabla \sigma$$

$$(27) \quad X(\sigma, \vec{u}, k, \nabla \vec{a}) = A_2 \varepsilon^{4/3} \nabla \cdot [(\sqrt{k} - \sqrt{k_{\text{can}}}) \nabla k] + A_2 \varepsilon^{4/3} \sqrt{k} \nabla k \cdot \nabla \sigma - \vec{u} \cdot \nabla k - [\tilde{R}'(\nabla \vec{a}); \nabla \vec{u} + \mu_0 \Psi_q(\nabla \vec{a})] k$$

4.2 Block relaxation

To solve system (23)-(25), (22) we use the following block relaxation algorithms:

Algorithm 1

- a) Take $\vec{u}_c = \vec{u}^n$, $\sigma_c = \sigma^n$
 - b) Find $\vec{\alpha}$, from:
- $$(28) \quad \vec{\alpha} = \vec{\alpha}^n - \Delta t [(\vec{u}_c \cdot \nabla) \vec{\alpha}^n] + \tilde{\gamma} (\Delta t)^2 [(\vec{u}_c \cdot \nabla) ((\vec{u}_c \cdot \nabla) \vec{\alpha}^n)]$$

- c) Take $\vec{\alpha}_c = \vec{\alpha}$
- d) Find k , the solution of

$$(29) \quad \begin{cases} \alpha k - \lambda \Delta k - X(\sigma_c, \vec{u}_c, k, \nabla \vec{\alpha}_c) = g_n \\ k = k_\infty \quad \text{on } T_\infty^- \\ k = k_B \quad \text{on } T_B \\ \frac{\partial k}{\partial n} = 0 \quad \text{on } T_\infty^+ \end{cases}$$

- e) Take $k_c = k$
- f) Find (σ, \vec{u}) , the solution of

$$(30) \quad \begin{cases} \alpha \vec{u} - \mu \Delta \vec{u} + \beta \nabla \sigma - \vec{\Phi}(\sigma, \vec{u}, k_c, \nabla \vec{\alpha}_c) = \vec{f}_n \\ \alpha \sigma + \nabla \cdot \vec{u} + \vec{u} \cdot \nabla \sigma = h_n \\ \vec{u} = \vec{u}_\infty, \sigma = \sigma_\infty \quad \text{on } T_\infty^- \\ \vec{u} = 0 \quad \text{on } T_B \\ [-K_e^{(x-1)} + K_c R'(\nabla \vec{\alpha}_c) - A_1 \varepsilon \sqrt{k_c} D(\vec{u})] \vec{n} = 0 \quad \text{on } T_\infty^+ \end{cases}$$

- g) Test. If it is not satisfied, take $\vec{u}_c = \vec{u}$, $\sigma_c = \sigma$ and go back to step b).

A variant of this algorithm is:

Algorithm 2

Replace step g) by:

g') Test. If it is not satisfied, take $\vec{u}_c = \vec{u}$, $\sigma_c = \sigma$ and turn back to d).

The simplest version:

Algorithm 3

Perform only once steps a)-f).

4.3 Variational formulations

We consider the following functional spaces:

$$S = \{\theta / \theta \in H^1(\Omega), \theta = 0 \text{ on } T_\infty^-\}$$

$$V = \{v / v \in H^1(\Omega), v = 0 \text{ on } T_B \cup T_\infty^-\}$$

$$R = S \times S$$

$$W = V \times V$$

$$V_k = \{k / k \in H^1(\Omega), k = k_\infty \text{ on } T_\infty^-, k = k_B \text{ on } T_B\}$$

$$S_\sigma = \{\sigma / \sigma \in H^1(\Omega), \sigma = \sigma_\infty \text{ on } T_\infty^-\}$$

$$W_u = \{\vec{u} / \vec{u} \in H^1(\Omega)^2, \vec{u} = \vec{u}_\infty \text{ on } T_\infty^-, \vec{u} = 0 \text{ on } T_B\}$$

$$V_\sigma = \{\sigma / \sigma \in H^1(\Omega), \sigma = \sigma_\infty \text{ on } T_\infty^-, \sigma = 0 \text{ on } T_B\}$$

and, for $\lambda \in H^{1/2}(T_B)$,

$$V_\lambda = \{\sigma / \sigma \in H^1(\Omega), \sigma = 0 \text{ on } T_\infty^-, \sigma = \lambda \text{ on } T_B\}$$

I. The equation for the Lagrangian coordinates

An equivalent variational formulation of (28) is:

$$(31) \quad \left\{ \begin{array}{l} \int_{\Omega} \vec{\alpha} \cdot \vec{\varphi} = \int_{\Omega} \vec{\alpha}^n \cdot \vec{\varphi} - \Delta t \int_{\Omega} (\vec{u}_c \cdot \nabla) \vec{\alpha}^n \cdot \vec{\varphi} - \tilde{\gamma} (\Delta t)^2 \int_{\Omega} (\nabla \cdot \vec{u}_c) (\vec{u}_c \cdot \nabla) \vec{\alpha}^n \cdot \vec{\varphi} \\ \quad - \tilde{\gamma} (\Delta t)^2 \int_{\Omega} (\vec{u}_c \cdot \nabla) \vec{\alpha}^n \cdot (\vec{u}_c \cdot \nabla) \vec{\varphi} + \tilde{\gamma} (\Delta t)^2 \int_{\partial \Omega} ((\vec{u}_c \cdot \nabla) \vec{\alpha}^n \cdot \vec{\varphi}) (\vec{u}_c \cdot \vec{n}) \\ \forall \vec{\varphi} \in \mathcal{R}, \vec{\alpha} \in \vec{\alpha}_{\infty} + \mathcal{R}, \vec{\alpha}_n \in H^1(\Omega)^2, \vec{\alpha}_{\infty} = \vec{x} - (n+1) \Delta t \vec{u}_{\infty} \text{ on } T_{\infty}^- \end{array} \right.$$

II. The equation for the turbulent kinetic energy

A least-squares formulation of (29) is:

$$(32) \quad \left\{ \begin{array}{l} \text{Min } \mathcal{L}(\tau) = \frac{\alpha}{2} \int_{\Omega} |k - \tau|^2 + \frac{\lambda}{2} \int_{\Omega} |\nabla(k - \tau)|^2 \\ \tau \in T_k \end{array} \right.$$

with $k = k(\tau)$, being the solution of

$$(33) \quad \left\{ \begin{array}{l} \alpha k - \lambda \Delta k = X(\vec{u}_c, \vec{u}_c, \tau, \nabla \vec{u}_c) + g_n \\ k = k_{\infty} \text{ on } T_{\infty}^- \\ k = k_B \text{ on } T_B \\ -\lambda \frac{\partial k}{\partial n} = (-\lambda + A_2 \varepsilon^{4/3}) \frac{\partial \tau}{\partial n} \text{ on } T_{\infty}^+ \end{array} \right.$$

III. The coupled equations for the logarithmic density and velocity

A least-squares formulation of system (30) is:

$$(34) \quad \left\{ \begin{array}{l} \text{Min } J(\eta, \vec{w}) = \frac{\alpha}{2} \int_{\Omega} |\sigma - \eta|^2 + \frac{A}{2} \left[\alpha \int_{\Omega} |\vec{u} - \vec{w}|^2 + \mu \int_{\Omega} |\nabla(\vec{u} - \vec{w})|^2 \right] \\ (\eta, \vec{w}) \in S_\sigma \times W_\mu \end{array} \right.$$

with $A > 0$ and $\sigma = \sigma(\eta, \vec{w})$, $\vec{u} = \vec{u}(\eta, \vec{w})$, the solution of:

$$(35) \quad \left\{ \begin{array}{l} \alpha \vec{u} - \mu \Delta \vec{u} + \beta \nabla \sigma = \vec{\Phi}(\eta, \vec{w}, k_c, \nabla \vec{a}_c) + \vec{f}_n \\ \alpha \sigma + \nabla \cdot \vec{u} = - \vec{w} \cdot \nabla \eta + h_n \\ \vec{u} = \vec{u}_\infty, \quad \sigma = \sigma_\infty \quad \text{on } T_\infty^- \\ \vec{u} = 0 \quad \text{on } T_B \\ \mu \frac{\partial \vec{u}}{\partial n} - \beta \sigma \vec{n} = \left[-\beta \eta + \frac{\chi}{\gamma-1} K e^{(\chi-1)\eta} \right] \vec{n} \\ \quad + \left[k_c R'(\nabla \vec{a}_c) - A_1 \epsilon (\sqrt{k_c} D(\vec{w}) - \sqrt{k_{can}} \nabla \vec{w}) \right] \vec{n} \quad \text{on } T_\infty^+ \end{array} \right.$$

4.4 Conjugate gradient algorithms

To solve problems (34) and (32), we have used Buckley & Lenir's conjugate gradient algorithm.

In both cases, the main difficulty consists of the computation of gradients, which will be detailed below.

- 1) The linear (state) equation (33) associated to a (control), can be equivalently formulated as the following variational equality:

$$\left\{ \begin{aligned}
 & \alpha \int_{\Omega} [k\psi + \lambda] \nabla k \nabla \psi = \langle X(\zeta_c, \vec{u}_c, \tau, \nabla \vec{\alpha}_c), \psi \rangle + \int_{\Omega} g_n \psi = \\
 & \equiv -A_2 \varepsilon^{4/3} \int_{\Omega} ((\bar{\tau} - \bar{\tau}_{can}) \nabla \tau \cdot \nabla \psi + A_2 \varepsilon^{4/3} \int_{\Omega} \bar{\tau} (\nabla \tau \cdot \nabla \zeta_c) \psi \\
 & - \int_{\Omega} (\vec{u}_c \cdot \nabla \tau) \psi - \int_{\Omega} [\mathcal{R}'(\nabla \vec{\alpha}_c) : \nabla \vec{u}_c + \mu_0 \psi_q (\nabla \vec{\alpha}_c)] \tau \psi \\
 & + \int_{\Omega} g_n \psi
 \end{aligned} \right. \\
 \forall \psi \in \mathcal{V}, \quad k \in \mathcal{V}_k
 \end{math}$$

For the functional ϕ in (32), we have:

$$\left\{ \begin{aligned}
 \langle \phi'(\tau), \psi \rangle &= \int_{\Omega} [\alpha(k - \tau)(k'(\tau) \cdot \psi - \psi) + \lambda \nabla(k - \tau) \cdot \nabla(k'(\tau) \cdot \psi - \psi)] \\
 &= \alpha \int_{\Omega} (\tau - k) \psi + \lambda \int_{\Omega} \nabla(\tau - k) \cdot \nabla \psi \\
 &- \alpha \int_{\Omega} (k'(\tau) \cdot \psi)(\tau - k) - \lambda \int_{\Omega} \nabla(k'(\tau) \cdot \psi) \cdot \nabla(\tau - k)
 \end{aligned} \right. \\
 \forall \tau \in \mathcal{V}_k, \quad \forall \psi \in \mathcal{V}
 \end{math>$$

$\ell = k'(\tau) \cdot \psi$ verifies:

$$\left\{ \begin{aligned}
 & \alpha \int_{\Omega} [\ell \psi + \lambda] \nabla \ell \nabla \psi = \langle \frac{\partial X}{\partial \tau}(\zeta_c, \vec{u}_c, \tau, \nabla \vec{\alpha}_c) \cdot \psi, \psi \rangle \equiv - \int_{\Omega} (\vec{u}_c \cdot \nabla \psi) \psi \\
 & - A_2 \varepsilon^{4/3} \int_{\Omega} \nabla((\bar{\tau} - \bar{\tau}_{can}) \psi) \cdot \nabla \psi + A_2 \varepsilon^{4/3} \int_{\Omega} (\nabla(\bar{\tau} \psi) \cdot \nabla \zeta_c) \psi \\
 & - \int_{\Omega} [\mathcal{R}'(\nabla \vec{\alpha}_c) : \nabla \vec{u}_c + \mu_0 \psi_q (\nabla \vec{\alpha}_c)] \psi \psi
 \end{aligned} \right. \\
 \forall \psi \in \mathcal{V}, \quad \forall \psi \in \mathcal{V}, \quad \forall \tau \in \mathcal{V}_k
 \end{math>$$

Hence:

$$(39) \quad \left\{ \begin{aligned} \langle \mathcal{L}^1(\tau), \psi \rangle &= \alpha \int_{\Omega} (\tau - k) \psi + \lambda \int_{\Omega} \nabla(\tau - k) \cdot \nabla \psi \\ &\quad - \left\langle \frac{\partial X}{\partial \tau}(\kappa_c, \vec{u}_c, \tau, \nabla \vec{u}_c) \cdot \psi, \tau - k \right\rangle \end{aligned} \right.$$

where k is the state associated to τ , i.e. the solution of Poisson's problem (36).

2) For the functional J in (34), we have:

$$(40) \quad \begin{aligned} \left\langle \frac{\partial J}{\partial \eta}(\eta, \vec{w}), \theta \right\rangle &= \alpha \int_{\Omega} (\sigma - \eta) \left(\frac{\partial \sigma}{\partial \eta} \cdot \theta - \theta \right) + A \left[\alpha \int_{\Omega} (\vec{u} - \vec{w}) \left(\frac{\partial \vec{u}}{\partial \eta} \cdot \theta \right) + \mu \int_{\Omega} \nabla(\vec{u} - \vec{w}) \nabla \left(\frac{\partial \vec{u}}{\partial \eta} \cdot \theta \right) \right] \\ &= \alpha \int_{\Omega} (\eta - \sigma) \theta + \alpha \int_{\Omega} (\sigma - \eta) \left(\frac{\partial \sigma}{\partial \eta} \cdot \theta \right) \\ &\quad + A \left[\alpha \int_{\Omega} (\vec{u} - \vec{w}) \left(\frac{\partial \vec{u}}{\partial \eta} \cdot \theta \right) + \mu \int_{\Omega} \nabla(\vec{u} - \vec{w}) \nabla \left(\frac{\partial \vec{u}}{\partial \eta} \cdot \theta \right) \right] \end{aligned}$$

$$(41) \quad \begin{aligned} \left\langle \frac{\partial J}{\partial \vec{w}}(\eta, \vec{w}), \vec{\sigma} \right\rangle &= \alpha \int_{\Omega} (\sigma - \eta) \left(\frac{\partial \sigma}{\partial \vec{w}} \cdot \vec{\sigma} \right) + A \alpha \int_{\Omega} (\vec{u} - \vec{w}) \left(\frac{\partial \vec{u}}{\partial \vec{w}} \cdot \vec{\sigma} - \vec{\sigma} \right) \\ &\quad + A \mu \int_{\Omega} \nabla(\vec{u} - \vec{w}) \nabla \left(\frac{\partial \vec{u}}{\partial \vec{w}} \cdot \vec{\sigma} - \vec{\sigma} \right) \\ &= A \left[\alpha \int_{\Omega} (\vec{w} - \vec{u}) \vec{\sigma} + \mu \int_{\Omega} \nabla(\vec{w} - \vec{u}) \nabla \vec{\sigma} \right] + \alpha \int_{\Omega} (\sigma - \eta) \left(\frac{\partial \sigma}{\partial \vec{w}} \cdot \vec{\sigma} \right) \\ &\quad + A \left[\alpha \int_{\Omega} (\vec{u} - \vec{w}) \left(\frac{\partial \vec{u}}{\partial \vec{w}} \cdot \vec{\sigma} \right) + \mu \int_{\Omega} \nabla(\vec{u} - \vec{w}) \nabla \left(\frac{\partial \vec{u}}{\partial \vec{w}} \cdot \vec{\sigma} \right) \right] \end{aligned}$$

$$\forall (\eta, \vec{w}) \in S_\sigma \times W_u, \quad \forall \theta \in S, \quad \forall \vec{\sigma} \in W$$

From (35), we obtain that $(\frac{\partial \vec{v}}{\partial \eta} \cdot \theta), (\frac{\partial \vec{u}}{\partial \eta} \cdot \theta)$ and $(\frac{\partial \vec{v}}{\partial \vec{w}}, \vec{s}), (\frac{\partial \vec{u}}{\partial \vec{w}}, \vec{s})$ verify:

$$(42) \quad \left\{ \begin{array}{l} \alpha \int_{\Omega} \left(\frac{\partial \vec{u}}{\partial \eta} \cdot \theta \right) \vec{z} + \mu \int_{\Omega} \nabla \left(\frac{\partial \vec{u}}{\partial \eta} \cdot \theta \right) \nabla \vec{z} + \beta \int_{\Omega} \nabla \left(\frac{\partial \vec{v}}{\partial \eta} \cdot \theta \right) \cdot \vec{z} = \left\langle \frac{\partial \vec{v}}{\partial \eta} (\eta, \vec{w}, k_c, \nabla \vec{a}_c) \cdot \theta, \vec{z} \right\rangle \\ \alpha \int_{\Omega} \left(\frac{\partial \vec{v}}{\partial \eta} \cdot \psi \right) \psi + \int_{\Omega} \left(\nabla \cdot \left(\frac{\partial \vec{u}}{\partial \eta} \cdot \theta \right) \right) \psi = - \int_{\Omega} (\vec{w} \cdot \nabla \theta) \psi \\ \forall \theta \in S, \forall \vec{z} \in W, \forall \psi \in S \end{array} \right.$$

$$(43) \quad \left\{ \begin{array}{l} \alpha \int_{\Omega} \left(\frac{\partial \vec{u}}{\partial \vec{w}} \cdot \vec{v} \right) \vec{z} + \mu \int_{\Omega} \nabla \left(\frac{\partial \vec{u}}{\partial \vec{w}} \cdot \vec{v} \right) \nabla \vec{z} + \beta \int_{\Omega} \nabla \left(\frac{\partial \vec{v}}{\partial \vec{w}} \cdot \vec{v} \right) \cdot \vec{z} = \left\langle \frac{\partial \vec{v}}{\partial \vec{w}} (\eta, \vec{w}, k_c, \nabla \vec{a}_c) \cdot \vec{v}, \vec{z} \right\rangle \\ \alpha \int_{\Omega} \left(\frac{\partial \vec{v}}{\partial \vec{w}} \cdot \vec{v} \right) \psi + \int_{\Omega} \left(\nabla \cdot \left(\frac{\partial \vec{u}}{\partial \vec{w}} \cdot \vec{v} \right) \right) \psi = - \int_{\Omega} (\vec{v} \cdot \nabla \eta) \psi \\ \forall \vec{v} \in W, \forall \vec{z} \in W, \forall \psi \in S \end{array} \right.$$

We introduce now the couple $(\vec{\zeta}, \vec{\xi})$ (the adjoint state) as the solution of the following linear (adjoint) system:

$$(44) \quad \left\{ \begin{array}{l} \alpha \int_{\Omega} \vec{\zeta} \cdot \vec{z} + \mu \int_{\Omega} \nabla \vec{\zeta} \cdot \nabla \vec{z} + \int_{\Omega} \vec{\zeta} \cdot (\nabla \cdot \vec{z}) = \alpha \left[\alpha \int_{\Omega} (\vec{u} - \vec{w}) \cdot \vec{z} + \mu \int_{\Omega} \nabla (\vec{u} - \vec{w}) \cdot \nabla \vec{z} \right] \\ \alpha \int_{\Omega} \vec{\zeta} \cdot \psi + \beta \int_{\Omega} \vec{\xi} \cdot \nabla \psi = \alpha \int_{\Omega} (\vec{v} - \vec{u}) \cdot \psi \\ \forall \vec{z} \in W, \forall \psi \in S, (\vec{\zeta}, \vec{\xi}) \in S \times W \end{array} \right.$$

System (44) can be reformulated in the following way:

$$(45) \quad \left\{ \begin{array}{l} \alpha \vec{\xi} - \mu \Delta \vec{\xi} - \nabla \zeta = A \left[\alpha (\vec{u} - \vec{w}) - \mu \Delta (\vec{u} - \vec{w}) \right] \\ \alpha \vec{\xi} - \beta \nabla \cdot \vec{\xi} = \alpha (\sigma - \eta) \\ \vec{\xi} = 0, \zeta = 0 \quad \text{on } T_\infty^- \\ \vec{\xi} = 0 \quad \text{on } T_B \\ -\mu \frac{\partial \vec{\xi}}{\partial n} - \vec{\xi} \vec{n} = -A \mu \frac{\partial (\vec{u} - \vec{w})}{\partial n} \quad \text{on } T_\infty^+ \end{array} \right.$$

Now, taking $\psi = \frac{\partial \sigma}{\partial \eta} \cdot \theta$, $\vec{z} = \frac{\partial \vec{u}}{\partial \eta} \cdot \theta$ in (44) and

$\psi = \zeta$, $\vec{z} = \vec{\xi}$ in (42), we obtain:

$$\begin{aligned} & \alpha \int_{\Omega} ((\sigma - \eta) \left(\frac{\partial \sigma}{\partial \eta} \cdot \theta \right) + A \left[\alpha \int_{\Omega} (\vec{u} - \vec{w}) \left(\frac{\partial \vec{u}}{\partial \eta} \cdot \theta \right) + \mu \int_{\Omega} \nabla (\vec{u} - \vec{w}) \nabla \left(\frac{\partial \vec{u}}{\partial \eta} \cdot \theta \right) \right]) = \\ &= \left\langle \frac{\partial \vec{\Phi}}{\partial \eta} (\eta, \vec{w}, k_c, \nabla \vec{a}_c) \cdot \theta, \vec{\xi} \right\rangle - \int_{\Omega} (\vec{w} \cdot \nabla \theta) \zeta \end{aligned}$$

Also, taking $\psi = \frac{\partial \sigma}{\partial w} \cdot \vec{v}$, $\vec{z} = \frac{\partial \vec{u}}{\partial w} \cdot \vec{v}$ in (44) and

$\psi = \zeta$, $\vec{z} = \vec{\xi}$ in (43) one has:

$$\begin{aligned} & \alpha \int_{\Omega} ((\sigma - \eta) \left(\frac{\partial \sigma}{\partial w} \cdot \vec{v} \right) + A \left[\alpha \int_{\Omega} (\vec{u} - \vec{w}) \left(\frac{\partial \vec{u}}{\partial w} \cdot \vec{v} \right) + \mu \int_{\Omega} \nabla (\vec{u} - \vec{w}) \nabla \left(\frac{\partial \vec{u}}{\partial w} \cdot \vec{v} \right) \right]) = \\ &= \left\langle \frac{\partial \vec{\Phi}}{\partial w} (\eta, \vec{w}, k_c, \nabla \vec{a}_c) \cdot \vec{v}, \vec{\xi} \right\rangle - \int_{\Omega} (\vec{v} \cdot \nabla \eta) \zeta \end{aligned}$$

Finally, we have the following expressions for the partial derivatives of J :

$$\begin{aligned} \left\langle \frac{\partial J}{\partial \eta}(\eta, \vec{w}), \theta \right\rangle &= \alpha \int_{\Omega} (\eta \cdot \vec{v}) \theta - \int_{\Omega} (\vec{w} \cdot \nabla \theta) \vec{\xi} \\ &\quad + \left\langle \frac{\partial \vec{\Phi}}{\partial \eta}(\eta, \vec{w}, k_c, \nabla \vec{\alpha}_c) \cdot \theta, \vec{\xi} \right\rangle \end{aligned}$$

$$\begin{aligned} \left\langle \frac{\partial J}{\partial \vec{w}}(\eta, \vec{w}), \vec{v} \right\rangle &= \mu \left[\int_{\Omega} (\vec{w} - \vec{u}) \vec{v} + \nu \int_{\Omega} \nabla(\vec{w} - \vec{u}) \nabla \vec{v} \right] - \int_{\Omega} (\vec{v} \cdot \nabla \eta) \vec{\xi} \\ &\quad + \left\langle \frac{\partial \vec{\Phi}}{\partial \vec{w}}(\eta, \vec{w}, k_c, \nabla \vec{\alpha}_c) \cdot \vec{v}, \vec{\xi} \right\rangle \end{aligned}$$

with

$$\begin{aligned} &\left\langle \frac{\partial \vec{\Phi}}{\partial \eta}(\eta, \vec{w}, k_c, \nabla \vec{\alpha}_c) \cdot \theta, \vec{\xi} \right\rangle = \\ &= \left\langle \left[(\beta - \gamma K e^{(k-1)\eta}) \nabla \theta - \gamma(k-1) K e^{(k-1)\eta} \theta \nabla \eta - k_c R^1 \cdot \nabla \theta + A_1 \varepsilon \sqrt{k_c} D(\vec{w}) \cdot \nabla \theta \right], \vec{\xi} \right\rangle = \\ &\equiv \int_{\Omega} (\beta - \gamma K e^{(k-1)\eta}) \nabla \theta \cdot \vec{\xi} - \gamma(k-1) K \int_{\Omega} e^{(k-1)\eta} (\nabla \eta \cdot \vec{\xi}) \theta \\ &\quad - \int_{\Omega} k_c (R^1 \cdot \vec{\xi}) \cdot \nabla \theta + A_1 \varepsilon \int_{\Omega} \sqrt{k_c} (D(\vec{w}) \cdot \vec{\xi}) \cdot \nabla \theta \end{aligned}$$

$$\begin{aligned} &\left\langle \frac{\partial \vec{\Phi}}{\partial \vec{w}}(\eta, \vec{w}, k_c, \nabla \vec{\alpha}_c) \cdot \vec{v}, \vec{\xi} \right\rangle = \\ &= \left\langle \left[-(\vec{w} \cdot \nabla) \vec{v} - (\vec{v} \cdot \nabla) \vec{w} + A_1 \varepsilon \nabla \cdot (\sqrt{k_c} D(\vec{v}) - \sqrt{k_c} \nabla \vec{v}) + A_1 \varepsilon \sqrt{k_c} D(\vec{v}) \cdot \nabla \eta \right], \vec{\xi} \right\rangle = \\ &\equiv \int_{\Omega} \left(-(\vec{w} \cdot \nabla) \vec{v} - (\vec{v} \cdot \nabla) \vec{w} \right) \vec{\xi} - A_1 \varepsilon \int_{\Omega} \left(\sqrt{k_c} D(\vec{v}) - \sqrt{k_c} \nabla \vec{v} \right) \cdot \nabla \vec{\xi} + A_1 \varepsilon \int_{\Omega} \sqrt{k_c} (D(\vec{v}) \cdot \nabla \eta) \cdot \vec{\xi} \end{aligned}$$

4.5 The solution of (Quasi-Stokes) problems (35) and (44)

To solve problems (35) and (44) we have used the generalized Glowinski & Pironneau's method described in 1.3 - C) of Chapter 1.

Briefly speaking, this reduces the task to the achievement of the following steps:

- 1) To obtain the state function (\vec{U}, \vec{W}) associated to a control (η, \vec{W}) (problem (35)):

$$\left\{ \begin{array}{l} \alpha^2 \int_{\Omega} \sigma_0 \psi + (\beta + \alpha \mu) \int_{\Omega} \nabla \sigma_0 \cdot \nabla \psi = \alpha \int_{\Omega} (-\vec{W} \cdot \nabla \eta + h_n) \psi - \int_{\Omega} (\nabla \cdot \vec{f}_n) \psi \\ \quad - \int_{\Omega} (\nabla^* \vec{\Phi}(\eta, \vec{W}, k_c, \vec{v}_c) \psi - \mu) \int_{\Omega} (-\Delta^* (\vec{W} \cdot \nabla \eta) + \Delta^* h_n) \psi \end{array} \right. \quad (*)$$

$$\forall \psi \in \mathcal{T}, \quad \sigma_0 \in \mathcal{T}_{\sigma}$$

$$\left\{ \begin{array}{l} \alpha \int_{\Omega} \vec{u}_0 \cdot \vec{\sigma} + \mu \int_{\Omega} \nabla \vec{u}_0 \cdot \nabla \vec{\sigma} = \beta \int_{\Omega} \sigma_0 (\nabla \cdot \vec{\sigma}) + \int_{\Omega} \vec{f}_n \cdot \vec{\sigma} + \langle \vec{\Phi}(\eta, \vec{W}, k_c, \vec{v}_c), \vec{\sigma} \rangle \\ \forall \vec{\sigma} \in \mathcal{W}, \quad \vec{u}_0 \in \mathcal{W}_{\mu} \end{array} \right.$$

$$\left\{ \begin{array}{l} \alpha^2 \int_{\Omega} \psi_0 \psi + (\beta + \alpha \mu) \int_{\Omega} \nabla \psi_0 \cdot \nabla \psi = \int_{\Omega} (\alpha \sigma_0 + \nabla \cdot \vec{u}_0 - h_n + \vec{W} \cdot \nabla \eta) \psi \\ \forall \psi \in \mathcal{T}, \quad \psi_0 \in \mathcal{T} \end{array} \right.$$

(*) Operators with * are understood as approximations in some generalized sense.

$$\left\{ \begin{array}{l} B_{GP} \lambda = - \left(\frac{\partial \psi_0}{\partial n} \Big|_{T_B \cup T_\infty}, \psi_0 \Big|_{T_\infty^+} \right) , \quad \lambda \in H^{1/2}(T_B) \\ \text{where } B_{GP} \text{ is the linear component of operator } A_{GP}, \\ (\text{see Chapter 1}) \end{array} \right.$$

$$\left\{ \begin{array}{l} \alpha^2 \int_{\Omega} \sigma_\lambda \varphi + (\rho_0 + \alpha \mu) \int_{\Omega} \nabla \sigma_\lambda \cdot \nabla \varphi = 0 \\ \forall \varphi \in \mathcal{T}, \quad \sigma_\lambda \in \mathcal{V}_\lambda \end{array} \right.$$

$$\left\{ \begin{array}{l} \alpha \int_{\Omega} \vec{u}_\lambda \cdot \vec{\sigma} + \mu \int_{\Omega} \nabla \vec{u}_\lambda \cdot \nabla \vec{\sigma} = \beta \int_{\Omega} \sigma_\lambda (\nabla \cdot \vec{\sigma}) \\ \forall \vec{\sigma} \in \vec{W}, \quad \vec{u}_\lambda \in \vec{W} \end{array} \right.$$

2) To obtain the adjoint state:

$$\left\{ \begin{array}{l} \alpha^2 \int_{\Omega} \sigma_0 \varphi + (\beta + \alpha \mu) \int_{\Omega} \nabla \sigma_0 \cdot \nabla \varphi = \alpha^2 \int_{\Omega} ((\zeta - \eta) \varphi - \mu \int_{\Omega} \Delta^*(\zeta - \eta) \varphi \\ + A\beta \int_{\Omega} (\alpha \nabla \cdot (\vec{u} - \vec{w}) - \mu \nabla^* \cdot (\Delta(\vec{u} - \vec{w}))) \varphi \end{array} \right.$$

$$\left. \begin{array}{l} \forall \varphi \in \mathcal{T}, \quad \sigma_0 \in \mathcal{V} \end{array} \right.$$

$$\left\{ \begin{array}{l} \alpha \int_{\Omega} \vec{u}_0 \cdot \vec{\sigma} + \mu \int_{\Omega} \nabla \vec{u}_0 \cdot \nabla \vec{\sigma} = - \int_{\Omega} \sigma_0 (\nabla \cdot \vec{\sigma}) + A\alpha \int_{\Omega} ((\vec{u} - \vec{w}) \cdot \vec{\sigma} + A\mu \int_{\Omega} \nabla(\vec{u} - \vec{w}) \cdot \nabla \vec{\sigma} \\ \forall \vec{\sigma} \in \vec{W}, \quad \vec{u}_0 \in \vec{W} \end{array} \right.$$

$$\left\{ \begin{array}{l} \alpha^2 \int_{\Omega} \psi_0 \psi + (\beta + \alpha \mu) \int_{\Omega} \nabla \psi_0 \nabla \psi = \int_{\Omega} (\alpha \zeta_0 - \beta \nabla \cdot \vec{u}_0 - \alpha (\zeta - \eta)) \psi \\ \forall \psi \in \mathcal{V}, \psi_0 \in \mathcal{V} \end{array} \right.$$

$$\left\{ \begin{array}{l} B_{GP} \lambda = - \left(\frac{\partial \psi_0}{\partial n} \Big|_{T_B \cup T_\infty^-}, \psi_0 \Big|_{T_\infty^+} \right) \\ \lambda \in H^{-1/2}(T_B) \end{array} \right.$$

$$\left\{ \begin{array}{l} \alpha^2 \int_{\Omega} \zeta_\lambda \psi + (\beta + \alpha \mu) \int_{\Omega} \nabla \zeta_\lambda \nabla \psi = 0 \\ \forall \psi \in \mathcal{V}, \zeta_\lambda \in \mathcal{V}_\lambda \end{array} \right.$$

$$\left\{ \begin{array}{l} \alpha \int_{\Omega} \vec{u}_\lambda \vec{v} + \mu \int_{\Omega} \nabla \vec{u}_\lambda \nabla \vec{v} = - \int_{\Omega} \zeta_\lambda (\nabla \cdot \vec{v}) \\ \forall \vec{v} \in \mathcal{W}, \vec{u}_\lambda \in \mathcal{W} \end{array} \right.$$

4.6 Space discretization

The space discretization is achieved using finite element techniques.

Let \mathcal{C}_h be a triangulation of Ω , which we assume, for simplicity, to be a polygonal bounded domain of \mathbb{R}^2 .

We introduce the following discrete space

$$H_h^1 = \{ \psi_h \mid \psi_h \in C^0(\bar{\Omega}), \psi_h|_T \in P_1, \forall T \in \mathcal{C}_h \}$$

P_1 is the space of those polynomials of degree ≤ 1 .

The spaces $S, V, S_\sigma, V_k, \dots$ etc. are approximated by the subspaces of H_h^1 defined by the boundary conditions satisfied by the functions belonging to S, V, S_σ, \dots

One obtains immediately the discrete problems by means of a standard approximation of the corresponding spaces and variational formulations above.

We have used mass-lumped numerical approximation for all integrals, except for those stemming from transport terms.

4.7 Preconditionning and working variables

In practice, we change variables τ , (η, \bar{w}) into working variables $\hat{\tau}$, $(\hat{\eta}, \hat{w})$ and then apply Buckley & Lenir's algorithm to the corresponding new least-squares problems.

We detail this change for turbulent kinetic energy τ . The procedure for (η, \bar{w}) is analogous.

Let \tilde{A}_3 be the matrix associated to the solution of the discrete Poisson problem:

$$\begin{cases} \alpha k - \lambda \Delta k = g \\ + \text{Dirichlet conditions on } T_{BUT_\infty} \end{cases}$$

i. e. $\tilde{A}_3 = (\tilde{a}_{ij})_{1 \leq i, j \leq M}$, $M = \dim H_h^1$

$$\tilde{a}_{ij} = \alpha \int_m w_i w_j + \lambda \int_m \nabla w_i \cdot \nabla w_j \quad (*)$$

with $\{w_i\}_{1 \leq i \leq M}$ being the canonical basis of H_h^1 and with the superscript (ml) denoting mass-lumped integration.

Then, the approximation of problem (32) is

$$\begin{cases} \text{Min } \phi_0(\tau) = \frac{1}{2} (\tilde{A}_3(k-\tau), (k-\tau)) + C \\ \tau \in T_{h,k} \end{cases} \quad (**)$$

(we have omitted subscripts h in τ and k ; we have also identified $\tau \in T_{h,k}$ with $\{\tau(i)\}_{i \in \mathcal{S}} \in \mathbb{R}^M$, $\mathcal{S} = \{\text{vertices of } \mathcal{C}_h\}$)

(*) In practice, matrix \tilde{A}_3 is partially modified in order to impose Dirichlet conditions.

(**) C is a constant due to the previous observation concerning \tilde{A}_3 .

Let $\tilde{A}_3 = \tilde{L}_3 \cdot \tilde{L}_3^t$ be Cholesky's factorization for \tilde{A}_3 .
Then

$$\mathcal{L}(\tau) = \frac{1}{2} (\tilde{L}_3^t(k-\tau), \tilde{L}_3^t(k-\tau))$$

We introduce the change of variable

$$\hat{\tau} = \tilde{L}_3^{-t} \tau$$

and the functional

$$\hat{\mathcal{L}}(\hat{\tau}) = \mathcal{L}(L_3^{-t} \hat{\tau}) = \frac{1}{2} |k - \tau|^2$$

We apply Buckley & Lenir's algorithm to the problem

$$\begin{cases} \min \hat{\mathcal{L}}(\hat{\tau}) \\ \hat{\tau} = L_3^{-t} \tau, \tau \in V_{h,k} \end{cases}$$

For the gradient of the working functional, we have:

$$\hat{\mathcal{L}}'(\hat{\tau}) = \tilde{L}_3^{-1} \cdot \nabla \mathcal{L}(L_3^{-t} \hat{\tau}) = \tilde{L}_3^{-1} \cdot \{ \langle \mathcal{L}'(\tau), w_i \rangle \}_{i \in \mathcal{S}}$$

Hence, for each computation of the gradient $\hat{\mathcal{L}}'(\hat{\tau})$ we have to compute:

a) $\tau = \tilde{L}_3^{-t} \hat{\tau}$

b) the state k associated to τ

c) $\nabla \mathcal{L} \equiv \{ \langle \mathcal{L}'(\tau), w_i \rangle \}_{i \in \mathcal{S}}$

d) $\hat{\mathcal{L}}'(\hat{\tau}) = \tilde{L}_3^{-t} \cdot \nabla \mathcal{L}$

Capítulo 4

Simulación numérica de la Turbulencia
mediante técnicas asintóticas
para algunos flujos compresibles:
Flujo sobre una rampa 2D
y flujo en torno a una doble elipse

Chapter 2

Numerical simulation of Turbulence by asymptotic techniques for some compressible flows: Flow over a 2D ramp and flow around a double ellipse.

In this Chapter, our work concerning the numerical simulation of Turbulence for compressible isentropic and fully compressible fluids will be described. We intend to simulate Turbulence by means of asymptotic techniques. On the other hand, the generation of Turbulence near solid walls is modelled, essentially, by the use of "wall laws". We first introduce our model problems. Next, we shall give a brief description of the solution techniques and, finally, we shall present our numerical results for two Test cases.

2.1 The model problems.

2.1.1 The model equations.

Consider 2-D Navier-Stokes equations for compressible isentropic flows with $\mathfrak{R} = O(\varepsilon^{-2})$, $0 < \varepsilon \ll 1$:

$$(2.1) \quad \begin{cases} u_{,t}^\varepsilon + (u^\varepsilon \cdot \nabla) u^\varepsilon + \frac{1}{\rho^\varepsilon} \nabla p^\varepsilon = \frac{\mu_0 \varepsilon^2}{\rho} \nabla \cdot (\rho^\varepsilon D(u^\varepsilon)), \\ \rho_{,t}^\varepsilon + \nabla \cdot (\rho^\varepsilon u^\varepsilon) = 0, \\ p^\varepsilon = K(\rho^\varepsilon)^\gamma \quad (\gamma > 1). \end{cases}$$

in $\Omega \times]0, T[$, together with initial conditions in two well separated scales:

$$(2.2) \quad \begin{cases} u^\varepsilon(x, 0) = u_0(x) + \varepsilon^{1/3} u'_0(\frac{x}{\varepsilon}, x), \\ \rho^\varepsilon(x, 0) = \rho_0(x) + \varepsilon^{2/3} \rho'_0(\frac{x}{\varepsilon}, x). \end{cases}$$

In (2.1)

$$(2.3) \quad D(u) = \nabla u + \nabla u^T - \frac{2}{3} \nabla \cdot u I$$

is the stress tensor and

$$K = \frac{1}{\gamma M_\infty^2}.$$

Also, in (2.2), u_0 and ρ_0 are the mean initial velocity field and density and u'_0 and ρ'_0 are the corresponding initial fluctuations. One assumes that they are all smooth functions, that $u'_0 = u'_0(y, x)$, $\rho'_0 = \rho'_0(y, x)$ are periodic in the variable $y \in Y$ (with $Y =]-\pi, \pi[^3$) and also that u'_0 and ρ'_0 have mean zero:

$$\langle u'_0 \rangle = \frac{1}{|Y|} \int_Y u'_0(y, x) dy = 0 \quad \forall x \in \Omega.$$

$$\langle \rho'_0 \rangle = \frac{1}{|Y|} \int_Y \rho'_0(y, x) dy = 0 \quad \forall x \in \Omega.$$

In the M.P.P. model, this flow is governed (in mean) by a system of partial differential equations for the mean velocity $u(x, t)$, density $\rho(x, t)$, pressure

$p(x, t)$, kinetic turbulent energy $k(x, t)$ and the inverse of the Lagrangian coordinates $a(x, t)$, given by:

$$(2.4) \quad \begin{cases} u_{,t} + (u \cdot \nabla)u + \frac{1}{\rho} \nabla p + \frac{1}{\rho} \nabla \cdot (\rho k R) = \frac{c_u}{\rho} \nabla \cdot (\rho \sqrt{k} D(u)), \\ \rho_{,t} + \nabla \cdot (\rho u) = 0, \quad p = K p^*, \\ k_{,t} + u \nabla k + k(R : \nabla u + \mu^0 \psi) = \frac{c_k}{\rho} \nabla \cdot (\rho \sqrt{k} \nabla k), \\ a_{,t} + (u \cdot \nabla)a = 0, \end{cases}$$

with the initial conditions

$$(2.5) \quad \begin{bmatrix} u \\ \rho \\ k \\ a \end{bmatrix}_{t=0} = \begin{bmatrix} u_0(x) \\ \rho_0(x) \\ \frac{\varepsilon^{2/3}}{2} \langle |u'_0|^2 \rangle(x) \\ x \end{bmatrix}.$$

In (2.4) c_u and c_k are numerical constants; the other closure terms are functions of ∇a . Indeed

$$(2.6) \quad R = \nabla a \tilde{R}(C) \nabla a^T, \quad \psi = \psi(C), \quad \text{with} \quad C = \nabla a^T \nabla a$$

and

$$(2.7) \quad \tilde{R}(C) = \langle \tilde{w} \otimes \tilde{w} \rangle, \quad \psi(C) = \langle |\nabla_y \times (C^{-1} \tilde{w})|^2 \rangle,$$

where \tilde{w} verifies the so-called *canonical microstructure problem*:

$$(2.8) \quad \begin{cases} \tilde{w}_{,r} + (\tilde{w} \cdot \nabla_y) \tilde{w} + \tilde{C} \nabla_y \pi = 0, \quad \nabla_y \cdot \tilde{w} = 0 \quad \text{in } Y, \\ (\tilde{w}, \pi) \quad Y - \text{periodic}, \\ \frac{1}{2} \langle \tilde{w} \tilde{C}^{-1} \tilde{w} \rangle = 1, \quad \langle \tilde{w} \rangle = 0, \quad \tilde{w} \quad \text{odd}, \end{cases}$$

This is a simplified model which does not include turbulent helicity ([10]).

We also consider another model problem for ideal fluid that includes an equation for the temperature. In this model, the state equation is

$$(2.9) \quad p = (\gamma - 1) \rho \theta$$

and the temperature θ is governed by the equation

$$(2.10) \quad \theta_{,t} + u \nabla \theta + (\gamma - 1) \theta \nabla \cdot u = \frac{c_\theta}{\rho} \nabla \cdot (\rho \sqrt{k} \nabla \theta) + u_0 \varepsilon^2 F(\nabla u),$$

where $c_\theta = c_u \gamma / \text{Pr}$, with Pr being the Prandtl number of the fluid. In (2.10), $F(\nabla u)$ is a quadratic function, defined as follows:

$$F(\nabla u) = \frac{4}{3} (u_{1,1}^2 + u_{2,2}^2 + (u_{2,1}^2 + u_{1,2}^2) - u_{1,1} u_{2,2}).$$

The equation for the temperature has been adapted from the usual energy equation for the M.P.P. model. Indeed, (2.10) has been derived by including a turbulent diffusion for θ similar to that appearing in (2.4) for the velocity u . On the other hand, the diffusion terms for θ and for u are assumed to be related as in the original Navier-Stokes equations: $\frac{c_\theta}{c_u} = \frac{\gamma}{\text{Pr}}$. Of course, at this stage, this must be considered a tentative.

Thus the corresponding model PDE's are:

$$(2.11) \quad \begin{cases} u_{,t} + (u \cdot \nabla) u + \frac{1}{\rho} \nabla p + \frac{1}{\rho} \nabla \cdot (\rho k R) = \frac{c_u}{\rho} \nabla \cdot (\rho \sqrt{k} D(u)), \\ \rho_{,t} + \nabla \cdot (\rho u) = 0, \quad p = K p^\gamma, \\ k_{,t} + u \nabla k + k(R : \nabla u + \mu_0 \psi) = \frac{c_k}{\rho} \nabla \cdot (\rho \sqrt{k} \nabla k), \\ \theta_{,t} + u \nabla \theta + (\gamma - 1) \theta \nabla \cdot u = \frac{c_\theta}{\rho} \nabla \cdot (\rho \sqrt{k} \nabla \theta) + \mu_0 \varepsilon^2 F(\nabla u), \\ a_{,t} + (u \cdot \nabla) a = 0. \end{cases}$$

2.1.2 The boundary conditions.

We consider standard boundary conditions on velocity, density and temperature ([3,7]). Also, we assume Dirichlet inflow constant valued boundary conditions for the turbulent kinetic energy. This means that the flow coming inside the computational domain bears a certain level of Turbulence. Moreover, we model the generation of Turbulence on solid walls by introducing "laws of the wall" ([12]).

The outflow boundary conditions are all of Neumann type, in order to avoid reflections on the outflow boundary.

We shall assume that the boundary Γ of our computational domain Ω is divided into two pieces. The first of them is Γ_B , which corresponds to a solid wall; the second one is an artificial piece "at infinity" and is itself composed by the inflow (Γ_∞^-) and outflow (Γ_∞^+) parts. Thus,

$$\Gamma_\infty^- = \{x \in \Gamma / u(x).n(x) < 0\},$$

where $n(x)$ is the outward unitary normal vector to Γ (cf. Fig. A).

1. Inflow:

$$(2.12) \quad \left\{ \begin{array}{l} u|_{\Gamma_\infty^-} = u_\infty = \begin{pmatrix} \cos \alpha \\ \sin \alpha \end{pmatrix}, \\ \rho|_{\Gamma_\infty^-} = 1, \\ k|_{\Gamma_\infty^-} = k_{\text{car}} = \varepsilon^{2/3}, \\ \theta|_{\Gamma_\infty^-} = \frac{1}{\gamma(\gamma-1)M_\infty^2} = \theta_\infty. \end{array} \right.$$

All variables are made dimensionless with the free stream values (uniform flow at infinity).

2. Solid walls:

Since the M.P.P. model does not take into account the existence of turbulent boundary layers, we have introduced specific nonlinear boundary conditions on Γ_B . These are related to certain experimental "laws of the wall".

Let $P \in \Omega$ be a point inside the boundary layer and let n and s be the normal and tangent unit vectors to Γ_B at the projection Q on Γ_B . Let y be the distance from P to Q (see Fig. B). Then, a “law of the wall” can be stated as follows:

$$\frac{u.s}{u^*} \Big|_{\Gamma_B} = g(y^+), \quad y^+ = \left(\frac{u^* y}{\mu_0 \varepsilon^2} \right).$$

Here, u^* is the friction velocity at the point Q . In Turbulence modelling, this velocity is usually given by

$$u^* = \sqrt{\nu(\tau(Q).n).s},$$

where ν is the viscosity of the fluid and τ is the total (laminar plus turbulent) stress tensor. The corresponding definition in our case is then

$$u^* = \sqrt{(c_u \sqrt{k D(u).n}).s}.$$

The specific form of g is given by Reichard's law (this was already described in a former report [7]). In particular, it includes the so-called logarithmic law of the wall, where

$$g(y^+) = \frac{1}{K} \log y^+ + c_{\text{int}},$$

in the fully turbulent sublayer ($y^+ > 50$; see Chapter 1) of the inner part of the boundary layer.

The law allows to obtain u^* in terms of $u.s$ ([11]). This yields

$$(2.13) \quad c_u \sqrt{k D(u).n} = G(u.s).s \quad \text{on } \Gamma_B,$$

i.e. nonlinear boundary conditions of the Neumann kind for u .

The boundary conditions for k are imposed by analogy with the $k - \epsilon$ model:

$$(2.14) \quad k = c_k |u^*|^2 \quad \text{on } \Gamma_B.$$

These are nonlinear boundary conditions of the Dirichlet kind.

Finally, the boundary conditions for θ on Γ_B correspond to the well known free stream behaviour:

$$(2.15) \quad \theta = \theta_B = \theta_\infty + \frac{1}{\gamma M_\infty^2} \quad \text{on } \Gamma_B$$

(linear Dirichlet boundary conditions).

3. Outflow

As announced, one sets Neumann boundary conditions on Γ_∞^+ for all variables:

$$(2.16) \quad \begin{cases} (c_u \sqrt{k} D(u) - kR - (\gamma - 1) \theta \log \rho I).n = 0, \\ \frac{\partial k}{\partial n} = 0, \\ \frac{\partial \theta}{\partial n} = 0. \end{cases}$$

2.1.3 The closure terms.

Due to frame invariance, it is proved that ([6.10])

$$R(\nabla a) = a_0(\mathbf{i})I + a_1(\mathbf{i})\bar{C}, \quad \bar{C} = \nabla a \nabla a^T,$$

$$\psi(\nabla a) = \psi_0(\mathbf{i}),$$

where \mathbf{i} is the only non-trivial invariant of \bar{C} : $\mathbf{i} = \text{tr}(\bar{C})$. Then

$$(2.17) \quad \begin{cases} \nabla \cdot (k\rho R) = \nabla \cdot (k\rho a_1 \nabla a \nabla a^T) + \nabla p', \\ R : \nabla u = a_0 \nabla \cdot u + a_1 \nabla a \nabla a^T : \nabla u. \end{cases}$$

The closure functions a_0 , a_1 and ψ have already been evaluated by the numerical solution of the canonical microstructure problem ([10]).

2.2 The numerical solution.

In this Section, we briefly describe the solution techniques which have been used for our second model (2.11). These techniques rely upon least squares reformulation and are adapted from those used to solve the other model problem (2.4). A detailed description of the latter was presented in a previous report ([7]).

We shall replace the system (2.11) by an equivalent one written in terms of the logarithmic density, $\sigma = \log \rho$, instead of ρ . This is the following:

$$(2.18) \quad \begin{cases} u_{,t} + (u \cdot \nabla)u + (\gamma - 1)(\theta \nabla \sigma + \nabla \theta) + \nabla \cdot (kR) + kR \nabla \sigma \\ \quad = c_u [\nabla \cdot (\sqrt{k} D(u)) + \sqrt{k} D(u) \nabla \sigma], \\ \sigma_{,t} + u \nabla \sigma + \nabla \cdot u = 0, \quad p = K p^*, \\ k_{,t} + u \nabla k + k(R : \nabla u + \mu_0 \psi) = c_k [\nabla \cdot (\sqrt{k} \nabla k) + \sqrt{k} \nabla k \cdot \nabla \sigma], \\ \theta_{,t} + u \nabla \theta + (\gamma - 1) \nabla \cdot u \\ \quad = c_\theta [\nabla \cdot (\sqrt{k} \nabla \theta) + \sqrt{k} \nabla \theta \cdot \nabla \sigma] + \mu_0 \varepsilon^2 F(\nabla u), \\ a_{,t} + (u \cdot \nabla)a = 0. \end{cases}$$

The boundary conditions for σ are obtained from (2.12) (only inflow boundary conditions are imposed).

Let us also remark that the outflow boundary conditions for velocity, defined by (2.16), remain unchanged.

We shall write system (2.18), after time discretization, as a fixed point equation with linear “active” operator for the variables (σ, u, k, θ) .

2.2.1 Semi-discretization in time.

Time derivative is discretized by second order Gear’s scheme:

$$\frac{df}{dt} \Big|_{t=t^{n+1}} \simeq \frac{3f^{n+1} - 4f^n + f^{n-1}}{2\Delta t}.$$

Time stepping consists of 3 blocks:

1. $(a^n, u^n, \sigma^n, k^n, \theta^n) \rightarrow (u^{n+1}, \sigma^{n+1}, \theta^{n+1})$, the solution of

$$(2.19) \quad \begin{cases} \alpha u - \mu \Delta u + (\gamma - 1) \theta_B \nabla \sigma - \phi(\sigma, u, \theta) = f^n, \\ \alpha \sigma + u \nabla \sigma + \nabla \cdot u = g^n, \\ \alpha \theta - \delta \Delta \theta - \chi(\sigma, u, \theta) = h^n, \\ + \text{Boundary conditions,} \end{cases}$$

with

$$\mu = c_u \sqrt{k_{\text{car}}}, \quad \delta = c_\theta \sqrt{k_{\text{car}}} \quad \text{and} \quad \alpha = \frac{3}{2\Delta t}.$$

Here,

$$(2.20) \quad \begin{cases} g^n = \frac{4\sigma^n - \sigma^{n-1}}{2\Delta t}, & f^n = \frac{4u^n - u^{n-1}}{2\Delta t}, \\ h^n = \frac{4\theta^n - \theta^{n-1}}{2\Delta t}, & \end{cases}$$

$$(2.21) \quad \begin{cases} \phi(\sigma, u, \theta) = -(u \cdot \nabla) u \\ + c_u \nabla \cdot (\sqrt{k^n} D(u) - \sqrt{k_{\text{car}}} \nabla u) \\ - (\gamma - 1) \nabla \theta + (\gamma - 1)(\theta_B - \theta) \nabla \sigma \\ + c_u \sqrt{k^n} D(u) \nabla \sigma \\ - \nabla \cdot (k^n R^n) - k^n R^n \nabla \sigma, \end{cases}$$

$$(2.22) \quad \begin{cases} \chi(\sigma, u, \theta) = -u \nabla \theta - (\gamma - 1) \theta \nabla \cdot u \\ + c_\theta \nabla \cdot [(\sqrt{k^n} - \sqrt{k_{\text{car}}}) \nabla \theta] \\ + c_\theta \sqrt{k^n} \nabla \theta \cdot \nabla \sigma - \mu_0 \varepsilon^2 F(\nabla u). \end{cases}$$

2. $(a^n, u^{n+1}) \rightarrow a^{n+1}$: Lax-Wendroff scheme

$$(2.23) \quad \begin{cases} a^{n+1} = a^n - \Delta t (u^{n+1} \cdot \nabla) u^{n+1} \\ + d(\Delta t)^2 u^{n+1} \nabla ((u^{n+1} \cdot \nabla) u^{n+1}), \\ u^{n+1}|_{\Gamma_\infty^-} = x - u_\infty t_{n+1}, \end{cases}$$

with $0 < d < 1$.

3. $(a^{n+1}, u^{n+1}, \sigma^{n+1}, k^n, \theta^{n+1}) \rightarrow k^{n+1}$, the solution of

$$(2.24a) \quad \begin{cases} \alpha k - \xi \Delta k \Lambda(k) = p^n, \\ \xi = c_k \sqrt{k_{\text{car}}}, \quad p^n = \frac{-4k^n + k^{n-1}}{2\Delta t}, \\ \Lambda(k) = -u^{n+1} \nabla k - k(R^{n+1} : \nabla u^{n+1} + \mu_0 \psi^{n+1}) \\ \quad + c_k \sqrt{k} \nabla k \cdot \nabla \sigma^{n+1} + c_k \nabla \cdot [(\sqrt{k} - \sqrt{k_{\text{car}}}) \nabla k]. \end{cases}$$

The inflow and outflow boundary conditions for k^{n+1} are the same already defined in (2.12) and (2.16). The nonlinear Dirichlet boundary condition (2.14) has been linearized:

$$(2.24b) \quad k^{n+1}|_{\Gamma_B} = c_k |u^{n+1}|^2.$$

2.2.2 The solution of the nonlinear problems.

All nonlinear problems are solved through least squares formulation. This leads to optimal control problems solved by algorithms of the conjugate gradient kind.

In particular the problem verified by $(u^{n+1}, \sigma^{n+1}, \theta^{n+1})$ can be formulated as follows:

Consider the spaces S_∞ , W_∞ and V_∞ given by

$$S_\infty = \{\sigma \in H^1(\Omega) / \sigma|_{\Gamma_\infty^-} = \sigma_\infty\},$$

$$W_\infty = \{u \in (H^1(\Omega))^2 / u|_{\Gamma_\infty^-} = u_\infty\},$$

$$V_\infty = \{\theta \in H^1(\Omega) / \theta|_{\Gamma_\infty^-} = \theta_\infty, \theta|_{\Gamma_B} = \theta_B\}.$$

Then, $(u^{n+1}, \sigma^{n+1}, \theta^{n+1})$ is a solution of

$$\text{Minimize } J(\eta, w, \tau) \quad \text{over } S_\infty \times W_\infty \times V_\infty,$$

with J given by

$$(2.25) \quad J(\eta, w, \tau) = \frac{\alpha}{2} \int_{\Omega} |\eta - \sigma|^2 dx$$

$$+\frac{\mu}{2} \int_{\Omega} \alpha|w-u|^2 + \mu|\nabla(w-u)|^2 dx \\ +\frac{\delta}{2} \int_{\Omega} \alpha|\tau-\theta|^2 + \delta|\nabla(\tau-\theta)|^2 dx$$

and $(\sigma, u, \theta) \in S_\infty \times W_\infty \times V_\infty$ being the solution of a linear problem in Ω . More precisely, σ , u and θ are required to satisfy:

$$(2.26) \quad \begin{cases} \alpha u - \mu \Delta u + \beta \nabla \sigma = \phi(\eta, w, \tau) + f^n, \\ \alpha \sigma + \nabla \cdot u = g^n - w \cdot \nabla \eta, \\ \alpha \theta - \delta \Delta \theta = \chi(\eta, w, \tau) + h^n, \end{cases}$$

with the following boundary conditions:

Velocity:

$$(2.27) \quad \begin{cases} [\mu \nabla(w-u) - \beta(\sigma-\eta)I + (\gamma-1)\tau\eta I \\ \quad + k^n R^n - c_u \sqrt{k^n} D(w)].n = 0 \quad \text{on } \Gamma_\infty^+, \end{cases}$$

$$(2.28) \quad [\mu \nabla(w-u) - c_u \sqrt{k^n} D(w)].n = G(w.s).s \quad \text{on } \Gamma_B.$$

Temperature:

$$(2.29) \quad \delta \frac{\partial \theta}{\partial n} = (\delta + c_\theta \sqrt{k^n}) \frac{\partial \tau}{\partial n} \quad \text{on } \Gamma_\infty^+.$$

Of course, due to the fact that (σ, u, θ) is in $S_\infty \times W_\infty \times V_\infty$, one has for (σ, u, θ) the same inflow conditions which hold for (η, w, τ) . For instance,

$$(2.30) \quad \sigma = 0 \quad \text{on } \Gamma_\infty^-.$$

Let us remark that (2.27) and (2.28) are two different Neumann conditions imposed on two different parts of the boundary of Ω . These can be introduced in a rather standard way in the weak formulation of the velocity equation in (2.26). Nevertheless, the special structure of the function $\phi(\eta, w, \tau)$ makes it convenient to give a particular formulation for each of these conditions. The main interest of this particular formulation is to avoid unnecessary computations that arise in the case of the standard formulation.

In order to illustrate how the boundary conditions for u are included in the variational formulation of problem (2.26), let us consider the following model problem:

$$(2.31) \quad \begin{cases} -\Delta u = \nabla f_1 + \nabla f_2 & \text{in } \Omega, \\ \frac{\partial u}{\partial n} + (f_1 + f_2) \cdot n = g_1 & \text{on } \Gamma_1, \\ \frac{\partial u}{\partial n} + f_1 \cdot n = g_2 & \text{on } \Gamma_2. \end{cases}$$

Introducing the linear spaces

$$W_i = \{u \in (H^1(\Omega))^2 / u|_{\Gamma_i} = 0\}, \quad i = 1, 2.$$

problem (2.31) can be formulated as follows:

$$(2.32) \quad \int_{\Omega} \nabla u : \nabla v \, dx = - \int_{\Omega} f_1 \nabla \cdot v \, dx + \begin{cases} - \int_{\Omega} f_2 \nabla \cdot v \, dx + \int_{\Gamma_1} g_1 v \, d\gamma, & \forall v \in W_2, \\ \int_{\Omega} \nabla f_2 \cdot v \, dx + \int_{\Gamma_2} g_2 v \, d\gamma, & \forall v \in W_1. \end{cases}$$

A standard weak formulation (2.31) is the following

$$(2.33) \quad \int_{\Omega} \nabla u : \nabla v \, dx = \int_{\Omega} \nabla(f_1 + f_2) \cdot v \, dx + \int_{\Gamma_1} (g_1 - (f_1 + f_2) \cdot n) \, d\Gamma + \int_{\Gamma_2} (g_2 - f_1 \cdot n) \, d\Gamma, \quad \forall v \in H^1(\Omega)^2.$$

After discretization, the boundary integrals in (2.33) would require a larger amount of computation than those in (2.32), while the amount of computation required by the integrals on Ω would be very close in both cases.

Let us also remark that both formulations (2.32) and (2.33) are equivalent if the boundary of Ω is sufficiently smooth.

Finally, to formulate problem (2.24) (which is satisfied by k^{n+1}) as an optimal control problem, let us introduce the linear manifold

$$E_{\infty} = \{k \in H^1(\Omega) / k|_{\Gamma_{\infty}} = k_{\text{car}}, \quad k|_{\Gamma_B} = k_B\},$$

where $k_B = c_k |u^{*n+1}|^2$. The function k^{n+1} is a solution of

$$\min_{\lambda \in E_\infty} F(\lambda), \quad F(\lambda) = \frac{\alpha}{2} \int_{\Omega} |\lambda - k|^2 + \frac{\xi}{2} \int_{\Omega} |\nabla(\lambda - k)|^2,$$

where k is the solution of the linear Poisson problem

$$(2.34) \quad \begin{cases} k \in E_\infty, \\ \alpha k - \xi \Delta k = \Lambda(\lambda) + p^n, \\ \xi \frac{\partial k}{\partial n} = \xi \frac{\partial \lambda}{\partial n}, \quad \text{on } \Gamma_\infty^+. \end{cases}$$

These least squares formulation are solved via a Buckley-Lenir conjugate gradient algorithm ([4]). This needs the computation of the gradient, which is obtained through the solution of an adjoint problem. The calculation of the gradient was already presented in a former report ([7]). Here, it will only be mentionned that the actual use of quasi-Newton-like conjugate gradient algorithms leads to an improvement of about 50% on computation time face to standard (Fletcher-Reeves) conjugate gradient algorithms.

2.2.3 The solution of linear problems.

Finally, we need to solve the following linear problems:

Poisson problems for the unknowns (u, σ) . These are needed to obtain the temperature θ in (2.26) and the kinetic energy k in (2.34).

Quasi-Stokes problems for the unknowns (u, σ) . They are solved using a variant of Glowinski-Pironneau's method, which reduces essentially to a "cascade" of Poisson problems and a linear system with a relatively small and fixed matrix. The solution of the Quasi-Stokes problems was also described in detail in [7].

2.2.4 Discretization in space.

All variables are discretized using a continuous piecewise linear finite element approximation.

In practice, the computation of integrals involving closure terms does not set any particular problem, as the closure terms are interpolated by piecewise constant approximations.

All details concerning the practical implementation of the method can be found in [7].

2.3 Numerical experiments.

We have tested our codes in two different cases. The first one corresponds to a boundary layer on a ramp of angle $\beta = 15^\circ$. The second one corresponds to the flow around a double ellipse. In both cases, the geometrical data were fixed by [8].

The values of the parameters defining the boundary conditions are the following:

$$\text{Test 1: } \begin{cases} u|_{\Gamma_\infty^-} = \begin{pmatrix} 1 \\ 0 \end{pmatrix}, \\ M_\infty = 5, \quad \Re = 10000, \\ k_{\text{car}} = \varepsilon^{2/3}, \quad \varepsilon = 0.01, \quad \mu_0 = 1, \\ \gamma = 1.4 \end{cases}$$

$$\text{Test 2: } \begin{cases} u|_{\Gamma_\infty^-} = \begin{pmatrix} \cos \alpha \\ \sin \alpha \end{pmatrix}, \quad \alpha = 0^\circ, \quad \alpha = 10^\circ, \quad \alpha = 15^\circ, \\ M_\infty = 2, \quad \Re = 250, \\ k_{\text{car}} = \varepsilon^{2/3}, \quad \varepsilon = 0.02, \quad \mu_0 = 1, \\ \gamma = 1.4 \end{cases}$$

The convergence of the numerical codes has been verified by running Test 1 at low Mach numbers with two different grids. The agreement between the results seems to be satisfactory. We have simulated the flow of Test 1 with both models (2.4) and (2.11) (isentropic and fully compressible fluid, respectively). This allows to compare the results in two different cases. On the other hand, the flow of Test 2 has been simulated only for fully compressible fluid. (model (2.11)).

Let us remark that our models are meaningful only when applied to transient turbulent flows. Indeed, in the stationary case, the closure terms vanish, and problems (2.4) and (2.11) are reduced to a system of conservation laws (see [2]).

2.3.1 Conclusions.

The numerical results seem to indicate that these models, as well as the numerical methods which have been used to solve them, are adequate to give qualitative prediction of compressible flows at moderate Mach number. The performance is limited by the following features:

1. An increasing instability (oscillations of all variables in the normal direction to the ramp, inside the boundary layer) appears as the Mach number increases in Test 1.
2. The shocks in Test 2 are not properly captured.
3. The temperature distribution in test 2 does not seem to be sufficiently accurate.

The first problem seems to be a consequence of the high Mach number. The same discretization, when applied to the laminar Navier-Stokes equations, begins to be unstable for M_∞ near 3.

The second one seems to be a consequence of the large numerical Reynolds numbers, and also of the inadaptation of the mesh. This can be avoided with the use of adaptive grid generation. This work is now in progress.

The third problem seems to be a consequence of the model equation that has been taken in (2.11). Our efforts are now being centered towards the improvement of this.

2.3.2 Captions of the Figures.

Figures 1 to 11 correspond to Test 1; Figures 2 to 6 correspond to an isentropic compressible fluid; Figures 7 to 11 correspond to a fully compressible fluid.

Figure 1: Triangulation. The density of the grid points in the direction normal to the wall increases exponentially in order to reach a reasonable resolution in the boundary layer.

Figure 2: Isolines for density, at $t = 1$. A boundary layer appears near the wall, downstream the corner of the ramp. A large increase of the values of the density is observed, ranging from 0.58 to 2.9.

Figures 3, 4: Density at $t = 2$. A situation similar to the one at time $t = 1$ occurs. Here, some instabilities near the boundary layer downstream the corner are observed. Also, there is a layer of low density near the wall, upstream the corner. Actually, at time $t = 3$, the fluid particles have already traversed the whole domain.

Figure 5: Density at $t = 3$. A zone of high density appears inside the boundary layer downstream just around the corner. This seems to be related to the formation of a zone of recirculation after the corner.

Figure 6: Kinetic turbulent energy, at $t = 3$. The kinetic energy is almost constant in all the computational domain, excepting on a boundary layer near

the ramp, downstream and upstream the corner. A large peak of energy appears downstream the corner. This peak seems to correspond to the physics of the problem, as it is located just after the zone of recirculation, more precisely at the reattachment point.

Figures 7, 8: Density at $t = 2$ and $t = 3$, respectively. A situation similar to that corresponding to isentropic fluid at $t = 2$ occurs (Figures 3-5). Here, the boundary layer downstream the corner is thicker than in the isentropic case. Also, there is a layer of low density beside the wall upstream the corner. The range of values reached by the density is here somewhat smaller than in the isentropic case.

Figures 9, 10: Temperature at $t = 2$ and $t = 3$ respectively. A thin boundary layer along the ramp occurs at $t = 2$, with almost linear variation of temperature θ in the normal direction to the wall. At later times, the thickness of this layer increases and some instabilities in the normal variation of θ appear.

Figure 11: Kinetic turbulent energy at $t = 3$. A situation similar to that of the isentropic case occurs (Figure 6). Here, the zone of high level of energy is located downstream the one in Figure 6.

Figures 12 to 20 correspond to Test 2 (fully compressible fluid). The values of α , the angle of incidence, are:

- $\alpha = 0^\circ$: Figures 13, 14 and 15;
- $\alpha = 10^\circ$: Figures 16, 17 and 18;
- $\alpha = 15^\circ$: Figures 19 and 20.

Figure 12: Triangulation. This triangulation was constructed in order to obtain a high density of triangles at the expected location of boundary layers

and shocks. However, the actual location of boundary layer and shocks in our experiments is somewhat different.

Figures 13, 14: Density at $t = 1$. The maximum value of the isolines describes roughly the position of a shock in front and around the body. Nevertheless, the low numerical Reynolds number of the problem (in particular, in a small region in front of the “nose” of the body) produces a high numerical diffusion, so that there is not a true shock. There is also a strip of high density just upstream the point of junction between the upper and lower ellipses. This corresponds to another physical shock, roughly located at that position.

Figure 15: Velocity field at $t = 1$. The density of arrows describes roughly the positions of the shock. This Figure indicates that a further improvement of the triangulation is needed in order to represent more accurately the shock in larger regions.

Figure 16: Density at $t = 1$. The same comments as in the case $\alpha = 0^\circ$ can be made. Here, the strip around the front shock is somewhat turned counterclockwise, as corresponds to the incidence angle. Also, the small upper shock is only very slightly captured by our numerical solution.

Figure 17: Velocity field at $t = 1$. Same comments as in Figure 15.

Figure 18: Temperature at $t = 1$. A very thick layer of high temperature occurs around the body, followed by a thinner layer of transition to a lower value. This is only a first approach to the solution of the problem and the lack of precision has still to be confirmed by further results.

Figure 19: Density at $t = 1$. Same comments as in Figure 16.

Figure 20: Velocity field at $t = 1$. Same comments as in Figure 15.

References

- [1] N. AZFAL: J. Fluid Mech. (1973), vol. 57, part 1, pp. 1-25.
- [2] C. BEGUE, B. CARDOT, O. PIRONNEAU: *Simulation of Turbulence with Transient Mean.*
Rapport de Recherche I.N.R.I.A., Rocquencourt 1989.
- [3] M.O. BRISTEAU, J. PERIAUX: *Finite Elements Methods for the calculation of compressible viscous flows using self-adaptive mesh refinements.*
Rapport de Recherche I.N.R.I.A., Rocquencourt 1987.
- [4] BUCKLEY, A. LENIR: Math. Programming 27, pp. 155-175, 1983.
- [5] M.C. CALZADA, J.L. CRUZ, M. MARIN: Contribution to the "CEDYA XI - I CONGRESO DE MATEMATICA APLICADA".
Fuengirola (Málaga, Spain), September 1989.
- [6] T. CHACÓN : *Etude d'un Modèle pour la Convection des Microstructures.*
Thèse 3ème Cycle Paris VI.
- [7] T. CHACÓN, J. COUCE, M.R. ECHEVARRÍA, E. FERNÁNDEZ-CARA,
J.D. MARTÍN, F. ORTEGÓN:

(a) *Mathematical modelling of Turbulence: Validation of the Numerical Simulation of Turbulence by asymptotic techniques. Two-dimensional analysis of the heat transfert in the re-circulating zone of the HERMES aircraft.*

Reports 1, 2 and 3 of the HERMES Contract RDANE 23/87, University of Sevilla, 1987, 1988 and 1990.

(b) Contributions to the "CEDYA XI - I CONGRESO DE MATEMATICA APLICADA".

Fuengirola (Málaga, Spain), September 1989.

(c) Contribution to the "I CONGRESO DE LA SOCIEDAD ESPAÑOLA DE METODOS NUMERICOS EN INGENIERIA".

Las Palmas (Gran Canaria, Spain), June 1990.

(d) To appear.

- [8] I.N.R.I.A., G.A.M.N.I.-S.M.A.I.: Numerical tests proposed for the *Workshop on Hypersonic Flows for Reentry Problems*.

Antibes (France), January 1.990.

- [9] D. MACLAUGHLIN, G. PAPANICOLAOU, O. PIRONNEAU: SIAM J. Appl. Math. 45, p. 780-797 (1985).

- [10] F. ORTEGÓN:

(a) *Modélisation des écoulements turbulents à deux échelles par méthode d'Homogénéisation.*

Thèse de Doctorat, Université Paris VI, 1989.

(b) *Propiedades estructurales de los términos de cierre del modelo M.P.P.*, Contribution to the "CEDYA XI - I CONGRESO DE MATEMATICA APLICADA"

Fuengirola (Málaga, Spain), September 1989.

- [11] C.PARÉS *Estudio de ciertos tipos de condiciones de contorno para las ecuaciones de Navier-Stokes incompresibles.*

Tesis Doctoral, Universidad de Málaga (España), 1988.

- [12] H.SCHLICHTING: *Boundary Layer Theory.*

Academic Press, New York 1970.

MODULEF : CARA

RAMPA

25/10/88

RAMPA, NOPO

780 POINTS

780 NOEUDS

1444 ELEMENTS

1444 TRIANGLES

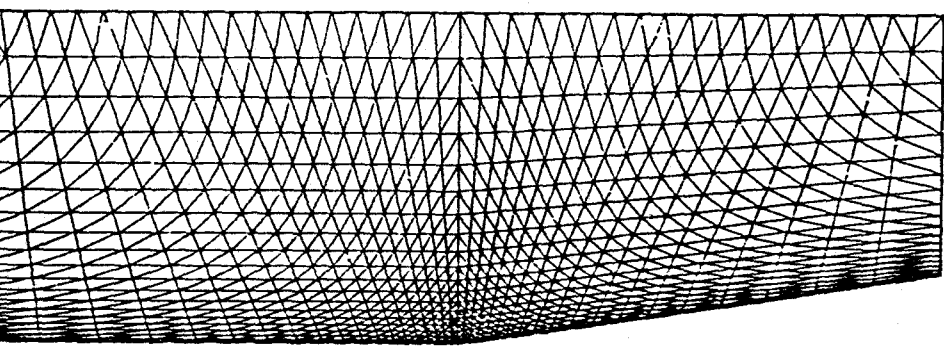
0 TROU(S)

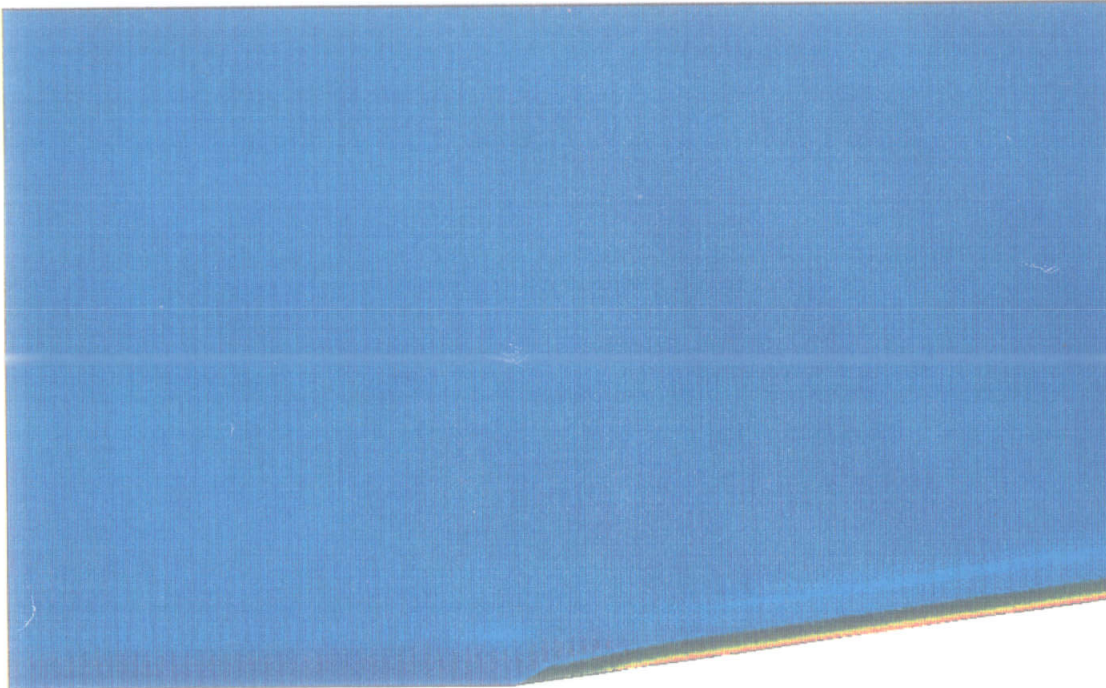
COIN BAS GAUCHE :

-0.15 -1.9

COIN HAUT DROIT :

3.2 2.9





MODULE FE : CARA

08/06/89

RAMPA1.MAI1

RAMPA1.C001

RAMPA1.DENB1

780 POINTS

780 NOEUDS

1444 ELEMENTS

1444 TRIANGLES

COIN BAS GAUCHE :

1.3 -0.26

COIN HAUT DROIT :

1.8 0.34

EXTREMA DU CHAMP B

0.58 2.9

EXTREMA DES ISOVALEURS

0.58 2.9

50 ISOVALEURS

FINIR : 0

CONTINUER : 1

VUE SUIVANTE : 2

VUE PRECEDENTE : 3

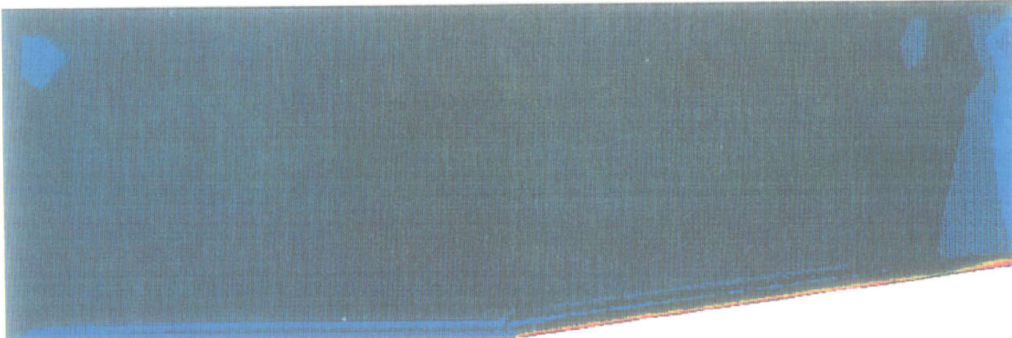
RAFRAICHIR : 4

ZOOM + : 5

ZOOM - : 6

VALEUR : 7

SOFTCOPIE : 8



MODULE :CARA

08/06/89

RAMPA1.MAI1

RAMPA1.C001

RAMPA1.DENB2

780 POINTS

780 NOEUDS

1444 ELEMENTS

1444 TRIANGLES

COIN BAS GAUCHE :

-0.15 -1.3

COIN HAUT DROIT :

3.2 2.3

EXTREMA DU CHAMP B

0.41 2.6

EXTREMA DES ISOVALEURS

0.41 2.6

50 ISOVALEURS

FINIR : 0

CONTINUER : 1

VUE SUIVANTE : 2

VUE PRECEDENTE : 3

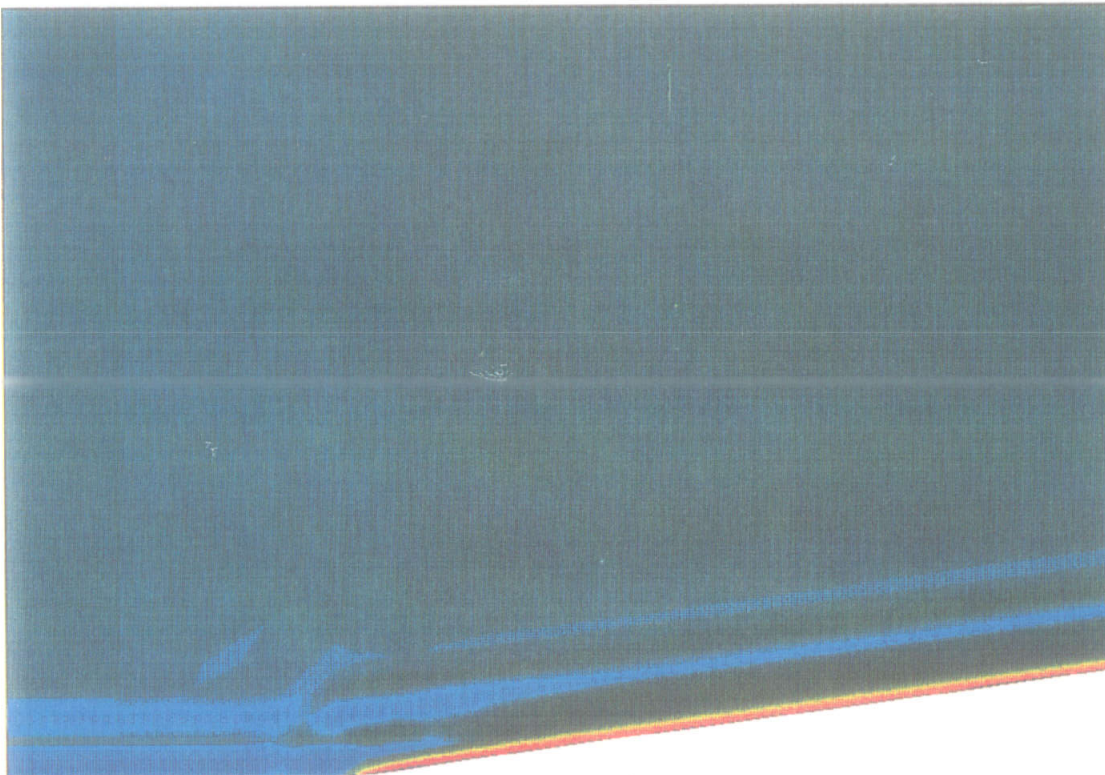
RAFRAICHIR : 4

ZOOM + : 5

ZOOM - : 6

VALEUR : 7

SOFTCOPIE : 8



MODULEFF :CARA

08/06/89

RAMPA1.MAI1

RAMPA1.C001

RAMPA1.DENB2

780 POINTS

780 NOEUDS

1444 ELEMENTS

1444 TRIANGLES

COIN BAS GAUCHE :

1.3 -0.27

COIN HAUT DROIT :

2.0 0.51

EXTREMA DU CHAMP B

0.41 2.6

EXTREMA DES ISOVALEURS

0.41 2.6

50 ISOVALEURS

FINIR : 0

CONTINUER : 1

VUE SUIVANTE : 2

VUE PRECEDENTE : 3

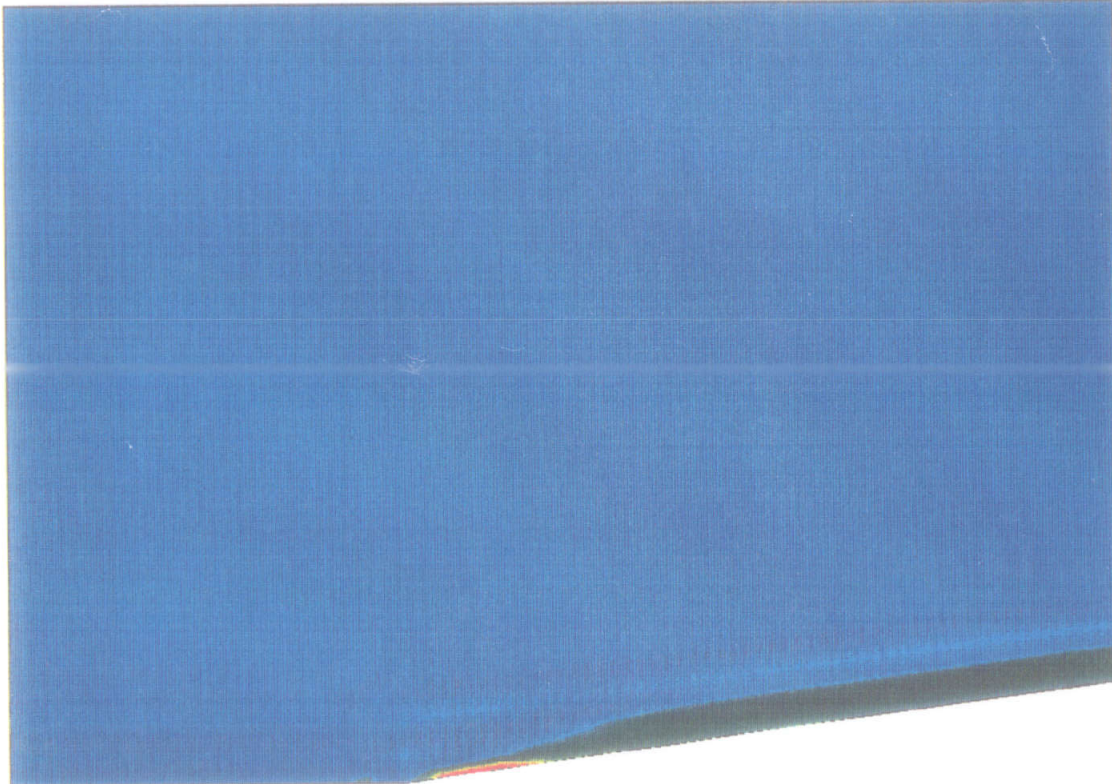
RAFRAICHEUR : 4

ZOOM + : 5

ZOOM - : 6

VALEUR : 7

SOFTCOPIE : 8



MODULE F :CARA

08/06/89

RAMPA1.MAI1

RAMPA1.C001

RAMPA1.DENB3

780	POINTS
780	NOEUDS
1444	ELEMENTS
1444	TRIANGLES

COIN BAS GAUCHE :

1.1 -0.37

COIN HAUT DROIT :

2.1 0.71

EXTREMA DU CHAMP B

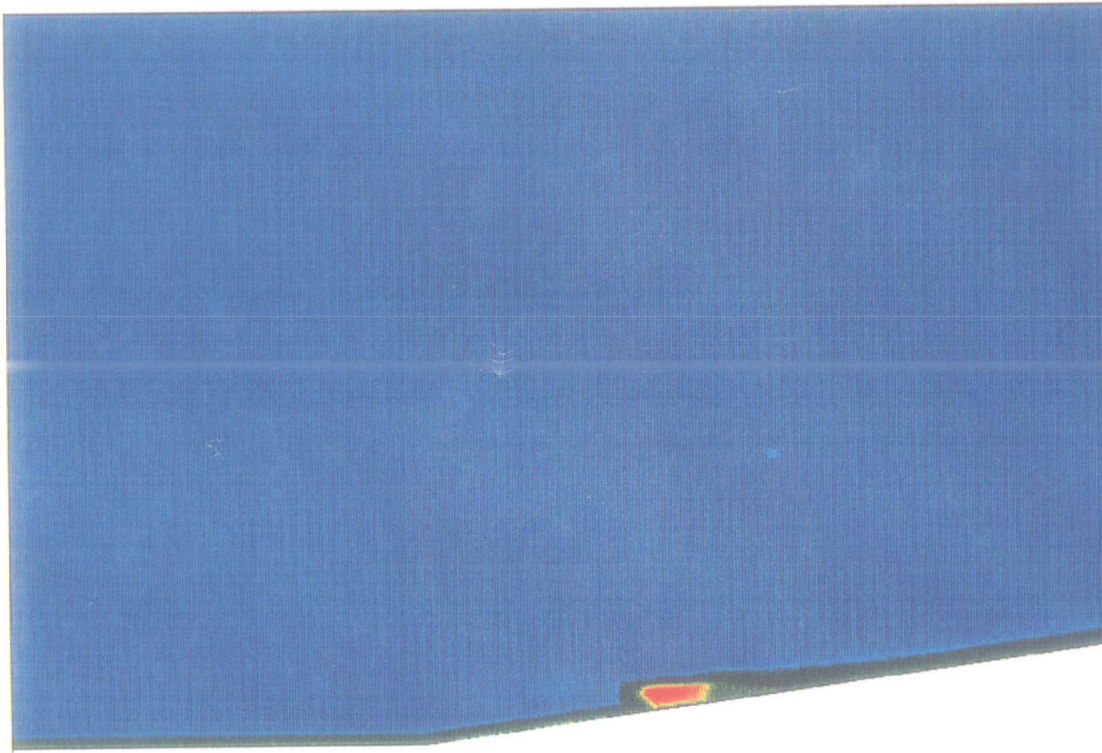
0.51 3.7

EXTREMA DES ISOVALEURS

0.51 3.7

50 ISOVALEURS

FINIR	:	0
CONTINUER	:	1
VUE SUIVANTE	:	2
VUE PRECEDENTE	:	3
RAFRAICHER	:	4
ZOOM +	:	5
ZOOM -	:	6
VALEUR	:	7
SOFTCOPIE	:	8



MODULE :CARA

16/06/89

RAMPA1.MAI1

RAMPA1.C001

RAMPA1.ENEB3

780	POINTS
780	NOEUDS
1444	ELEMENTS
1444	TRIANGLES

COIN BAS GAUCHE :

1.2 -0.30

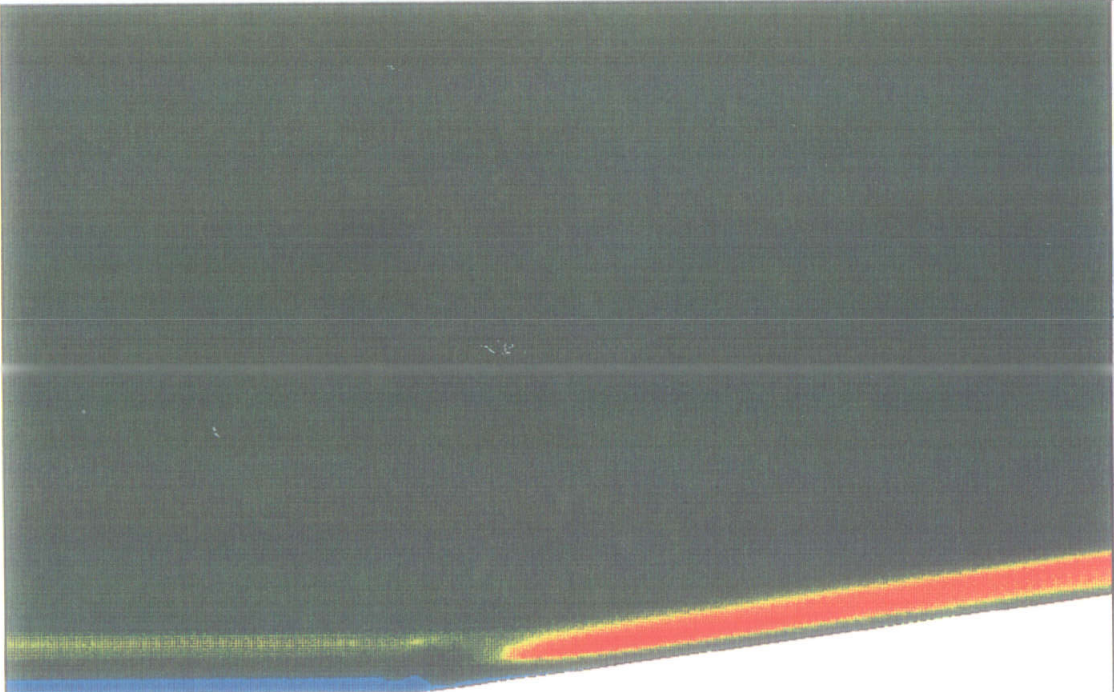
COIN HAUT DROIT :

2.0 0.49

EXTREMA DU CHAMP B
0.00E+00 0.93E-02
EXTREMES ISOVALEURS
-0.50E-03 0.95E-02

50 ISOVALEURS

FINIR	:	0
CONTINUER	:	1
VUE SUIVANTE	:	2
VUE PRECEDENTE	:	3
RAFRAICHER	:	4
ZOOM +	:	5
ZOOM -	:	6
VALEUR	:	7
SOFTCOPIE	:	8



MODULEFF :CARA

12/06/89

RAMPA1.MAI1

RAMPA1.C001

RAMPA1T.DENB2

780	POINTS
780	NOEUDS
1444	ELEMENTS
1444	TRIANGLES

COIN BAS GAUCHE :

1.1 -0.55

COIN HAUT DROIT :

2.3 0.77

EXTREMA DU CHAMP B

0.93E-01 2.0

EXTREMA DES ISOVALEURS

0.93E-01 2.0

50 ISOVALEURS

FINIR	:	0
CONTINUER	:	1
VUE SUIVANTE	:	2
VUE PRECEDENTE	:	3
RAFRAICHER	:	4
ZOOM +	:	5
ZOOM -	:	6
VALEUR	:	7
SOFTCOPIE	:	8

MODULEF :CARA

12/06/89

RAMPA1.MAI1

RAMPA1.C001

RAMPA1T.DENB3

780 POINTS

780 NOEUDS

1444 ELEMENTS

1444 TRIANGLES

COIN BAS GAUCHE :

1.1 -0.46

COIN HAUT DROIT :

-2.1 0.65

EXTREMA DU CHAMP B

0.21 5.4

EXTREMA DES ISOVALEURS

0.21 5.4

50 ISOVALEURS

FINIR : 0

CONTINUER : 1

VUE SUIVANTE : 2

VUE PRECEDENTE : 3

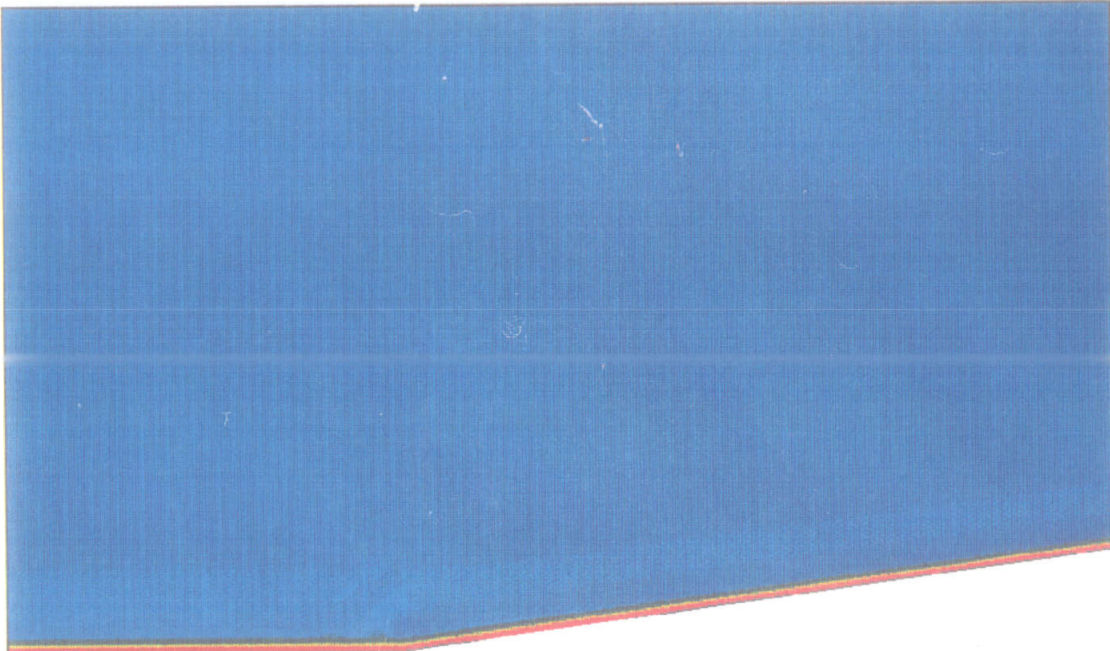
RAFRAICHIR : 4

ZOOM + : 5

ZOOM - : 6

VALEUR : 7

SOFTCOPIE : 8



MODULEFF :CARA

12/06/89

RAMPA1, MAI1

RAMPA1, C001

RAMPA1T, TEMB2

780	POINTS
780	NOEUDS
1444	ELEMENTS
1444	TRIANGLES

COIN BAS GAUCHE :

1.1 -0.49

COIN HAUT DROIT :

2.1 0.59

EXTREMA DU CHAMP B

-0.15E-01 0.43

EXTREMA DES ISOVALEURS

-0.15E-01 0.43

50 ISOVALEURS

FINIR	:	0
CONTINUER	:	1
VUE SUIVANTE	:	2
VUE PRECEDENTE	:	3
RAFRAICHER	:	4
ZOOM +	:	5
ZOOM -	:	6
VALEUR	:	7
SOFTCOPIE	:	8

MODULE : CARA

16/06/89

RAMPA1.MAI1

RAMPA1.C001

RAMPA1T.TEMB3

780 POINTS

780 NOEUDS

1444 ELEMENTS

1444 TRIANGLES

COIN BAS GAUCHE :

1.3 -0.29

COIN HAUT DROIT :

2.0 0.50

EXTREMA DU CHAMP B

-0.13 0.43

EXTREMA DES ISOVALEURS

-0.13 0.43

50 ISOVALEURS

FINIR : 0

CONTINUER : 1

VUE SUIVANTE : 2

VUE PRECEDENTE : 3

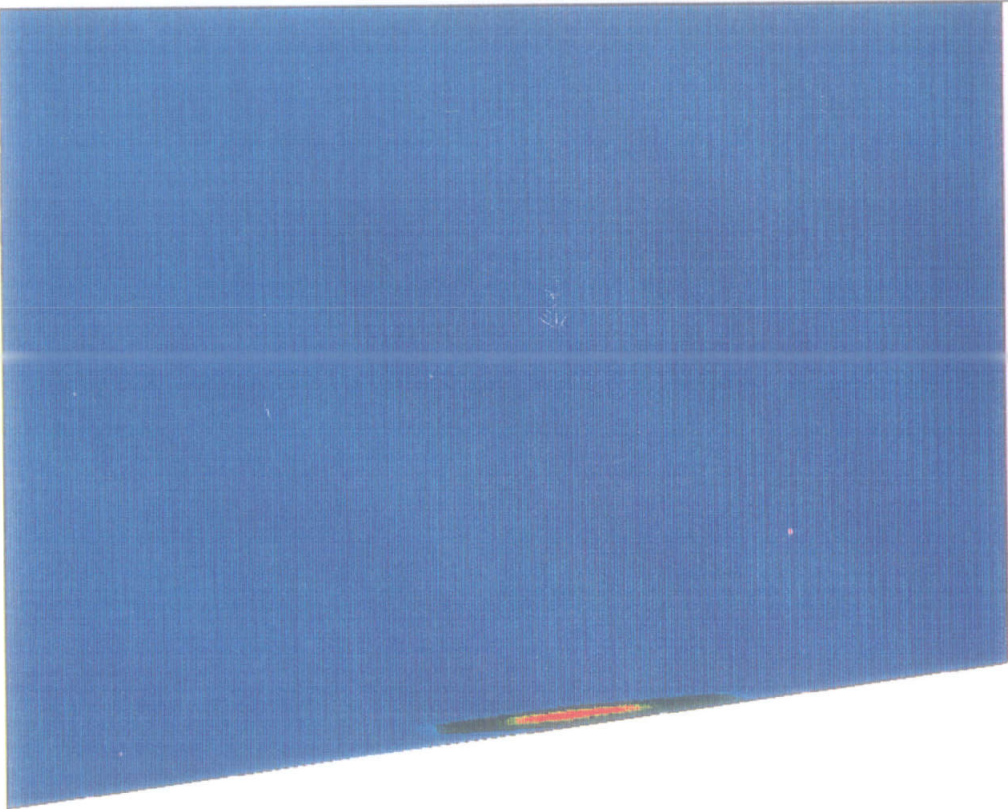
RAFRAICHIR : 4

ZOOM + : 5

ZOOM - : 6

VALEUR : 7

SOFTCOPIE : 8



MODULE : CARA

16/06/89

RAMPA1.MAI1

RAMPA1.C001

RAMPA1T.ENEB3

780 POINTS

780 NOEUDS

1444 ELEMENTS

1444 TRIANGLES

COIN BAS GAUCHE :

2.1 -0.26

COIN HAUT DROIT :

3.1 0.81

EXTREMA DU CHAMP B

0.00E+00 0.67E-01

EXTREMA DES ISOVALEURS

-0.10E-02 0.70E-01

20 ISOVALEURS

FINIR : 0

CONTINUER : 1

VUE SUIVANTE : 2

VUE PRECEDENTE : 3

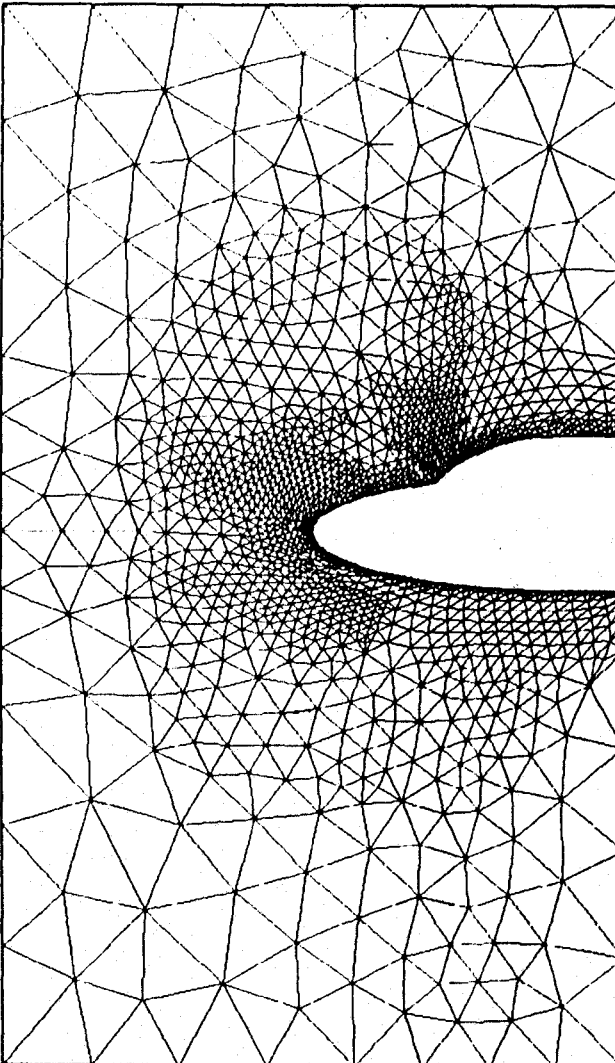
RAFRAICHER : 4

ZOOM + : 5

ZOOM - : 6

VALEUR : 7

SOFTCOPIE : 8



MODULE FF : CARA

08/06/89

CLIPSE2R.MAI1

CLIPSE2R.C001

1414 POINTS
1414 NOEUDS
2677 ELEMENTS
2677 TRIANGLES

COIN BAS GAUCHE :

-0.20 -0.15

COIN HAUT DROIT :

0.77E-01 0.15

FINIR : 0
CONTINUER : 1
VUE SUIVANTE : 2
VUE PRECEDENTE : 3
RAFRACHIR : 4
ZOOM + : 5
ZOOM - : 6
SOFTCOPIE : 8



MODULE F :CARA

08/06/89

ELIPSE2R.MAI1

ELIPSE2R.C001

ELIPSE2RC.DENB1

1414	POINTS
1414	NOEUDS
2677	ELEMENTS
2677	TRIANGLES

COIN BAS GAUCHE :

-0.20 -0.15

COIN HAUT DROIT :

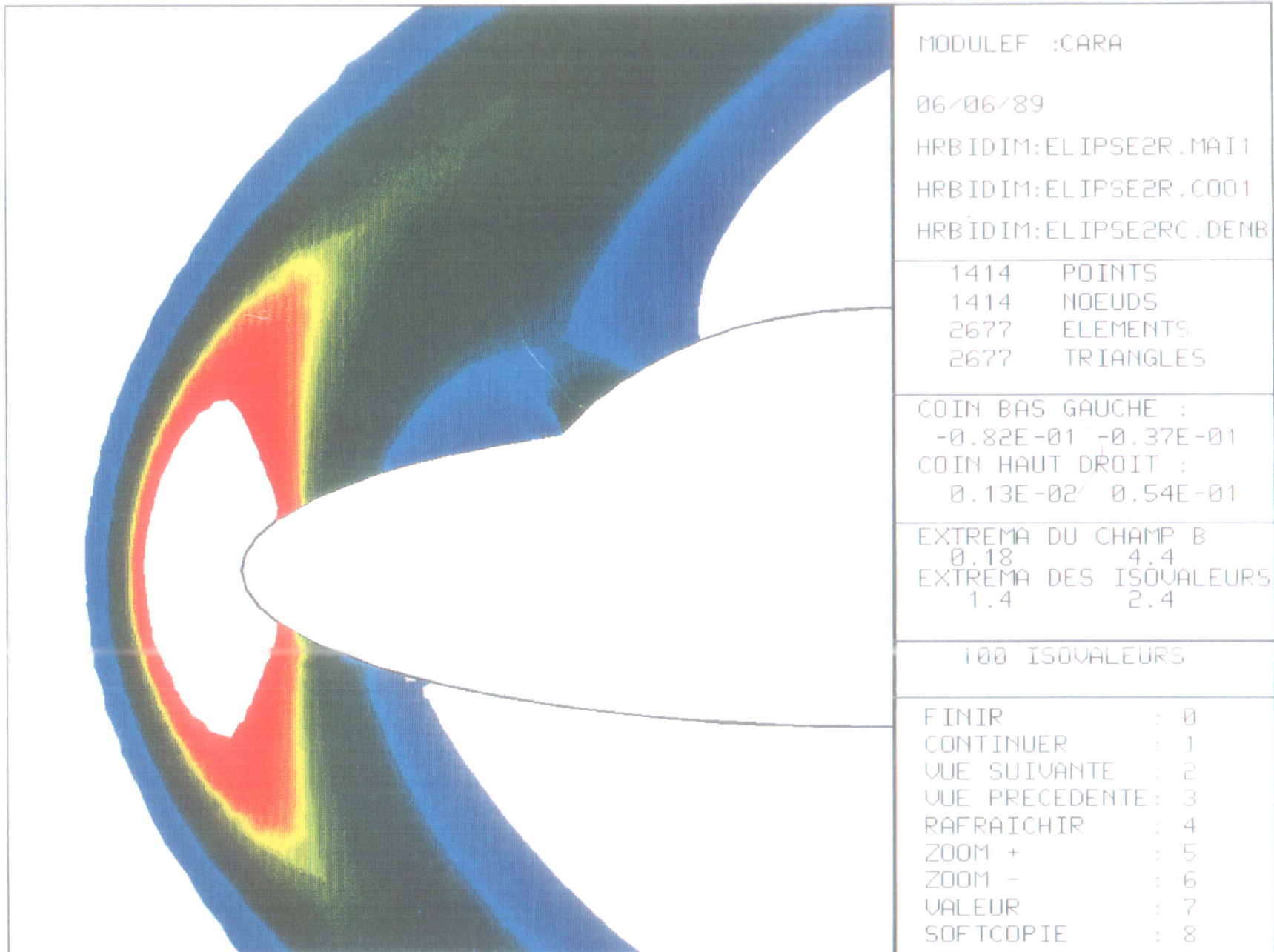
0.77E-01 0.15

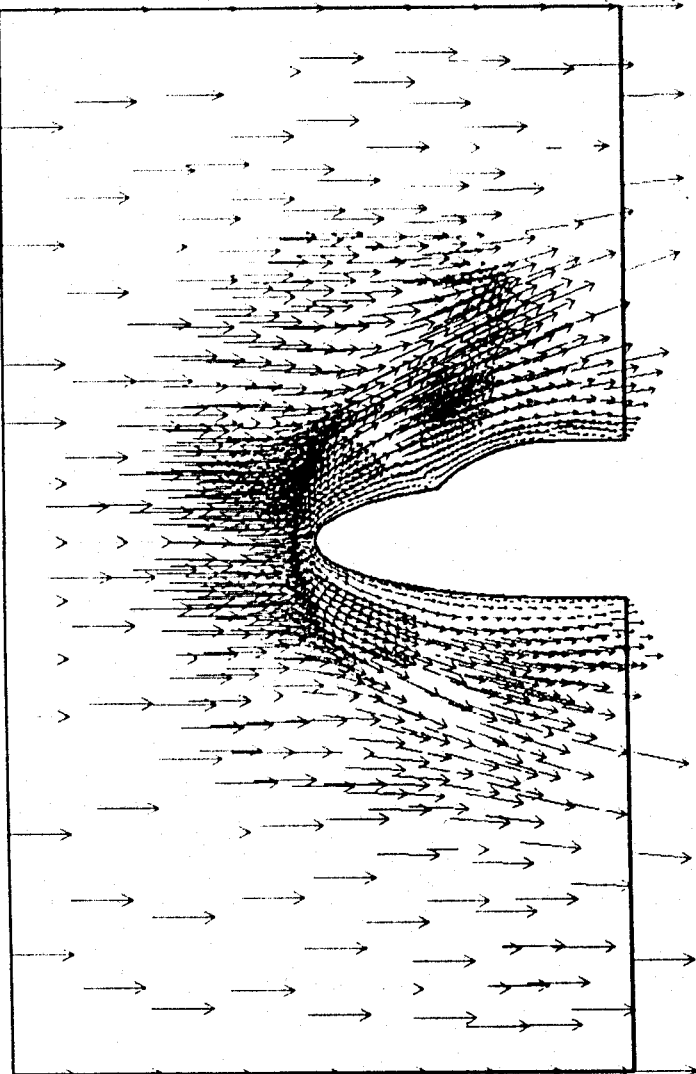
EXTREMA DU CHAMP B
0.18 4.4

EXTREMA DES ISOVALEURS
0.18 4.4

100 ISOVALEURS

FINIR	:	0
CONTINUER	:	1
VUE SUIVANTE	:	2
VUE PRECEDENTE	:	3
RAFRAICHIR	:	4
ZOOM +	:	5
ZOOM -	:	6
VALEUR	:	7
SOFTCOPIE	:	8





MODULEF : CARA

12/06/89

ELIPSE2R. MAI1

ELIPSE2R. COO1

ELIPSE2RC. VELB1

1414 POINTS

1414 NOEUDS

2677 ELEMENTS

2677 TRIANGLES

COIN RAS GAUCHE :

-0.20 -0.15

COIN HAUT DROIT :

0.77E-01 0.15

EXTREMA DU CHAMP B :

0.00E+00 1.0

ECHELLE

1.4 CM. = 1.0

VITESSES

FINIR . 0

CONTINUER . 1

VUE SUIVANTE . 2

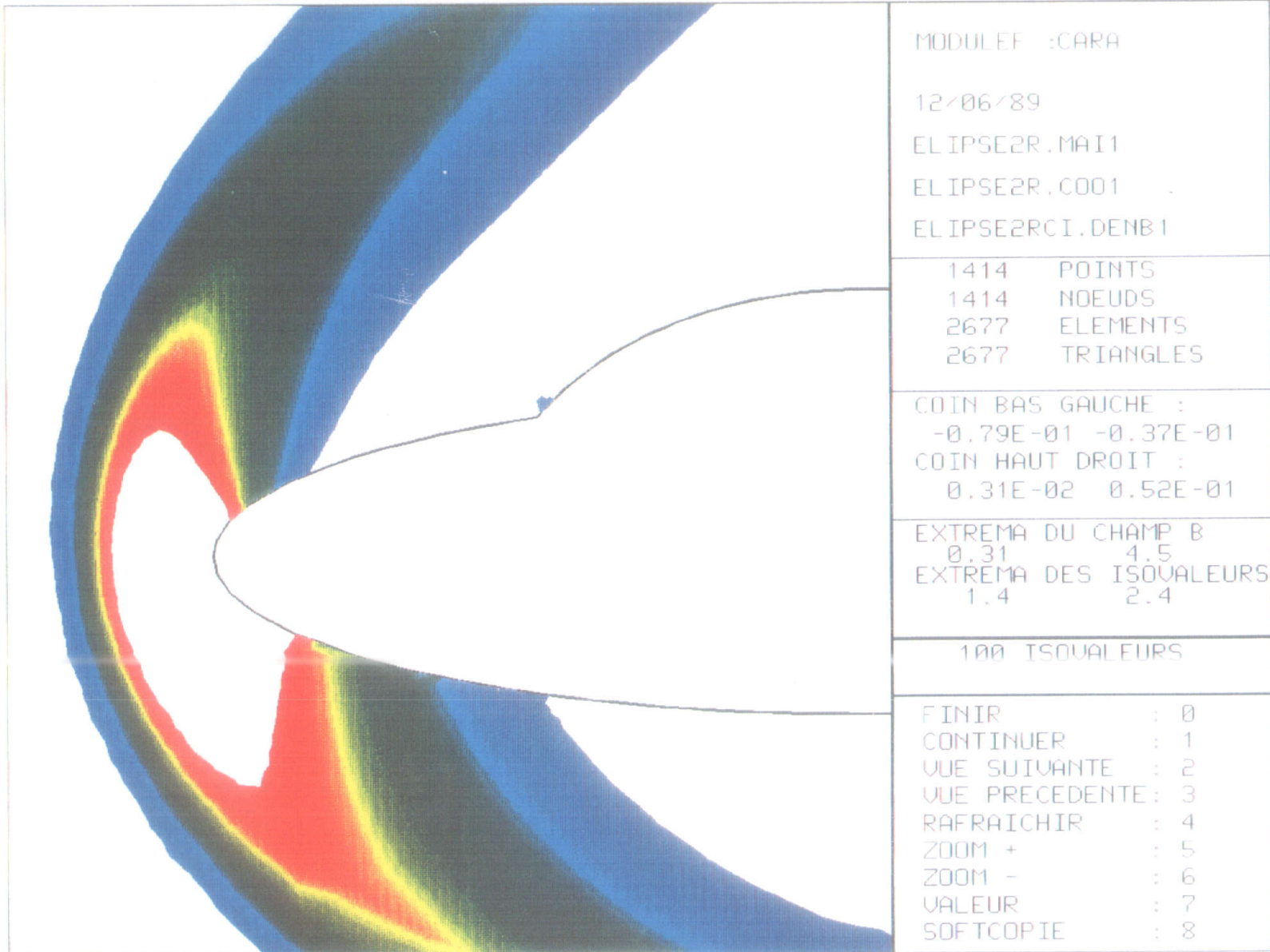
VUE PRECEDENTE . 3

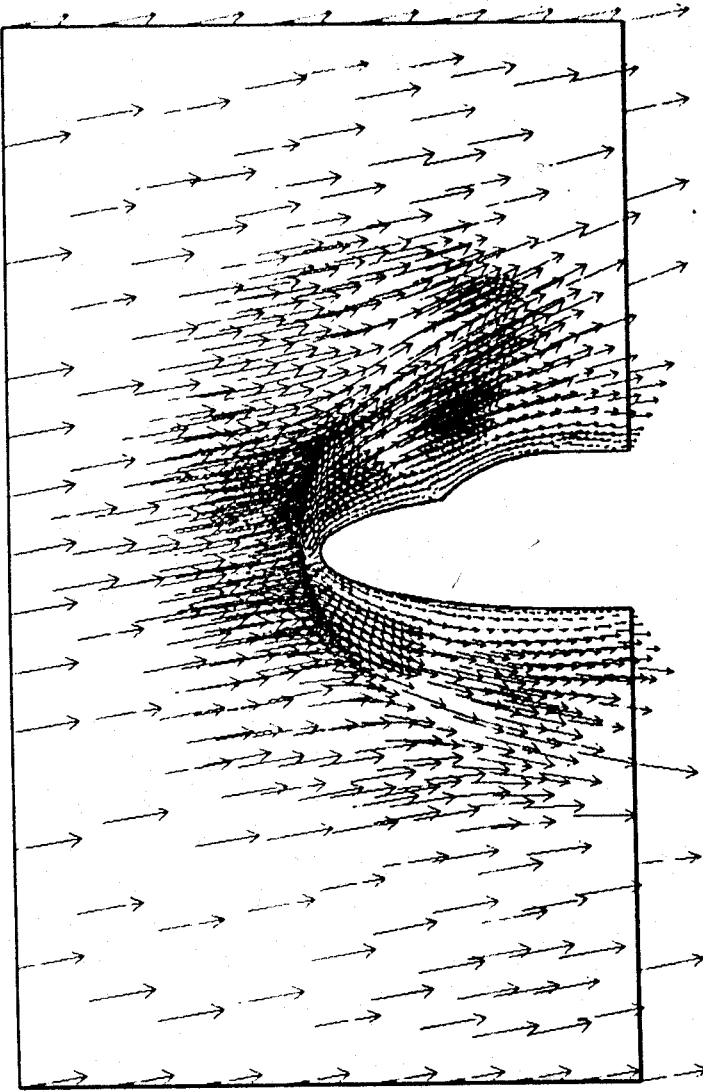
RAFRAICHIR . 4

ZOOM + . 5

ZOOM - . 6

SOFTCOPIE . 8





MODULEF : FARA

12/06/89

ELIPSE2R. MAI1

ELIPSE2R. C001

ELIPSE2RCI. VELB1

1414 POINTS

1414 NOEUDS

2677 ELEMENTS

2677 TRIANGLES

COIN BAS GAUCHE :

-0.20 -0.15

COIN HAUT DROIT :

0.77E-01 0.15

EXTREMA DU CHAMP B :

0.00E+00 1.0

ECHELLE

1.5 CM. = 1.0

VITESSES

FINIR . 0

CONTINUER . 1

VUE SUIVANTE . 2

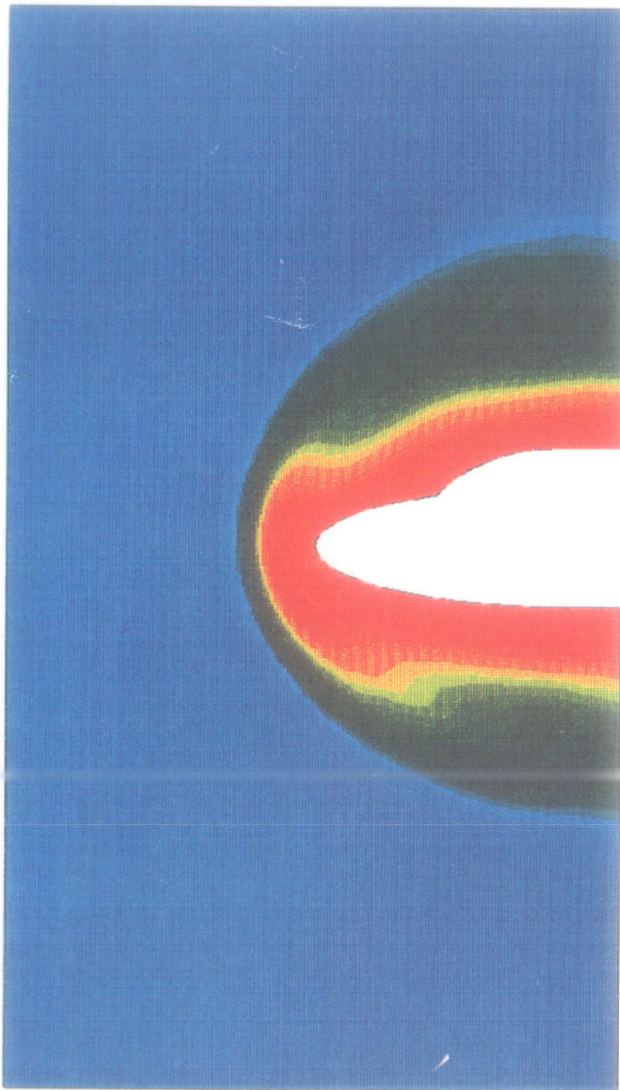
VUE PRECEDENTE . 3

RAFRAICHIR . 4

ZOOM + . 5

ZOOM - . 6

SOFTCOPIE . 8



MODULE FF :CARA

16/06/89

ELIPSE2R.MAI1

ELIPSE2R.C001

ELIPSE2RCI.TEMB1

1414	POINTS
1414	NOEUDS
2677	ELEMENTS
2677	TRIANGLES

COIN BAS GAUCHE :

-0.20 -0.15

COIN HAUT DROIT :

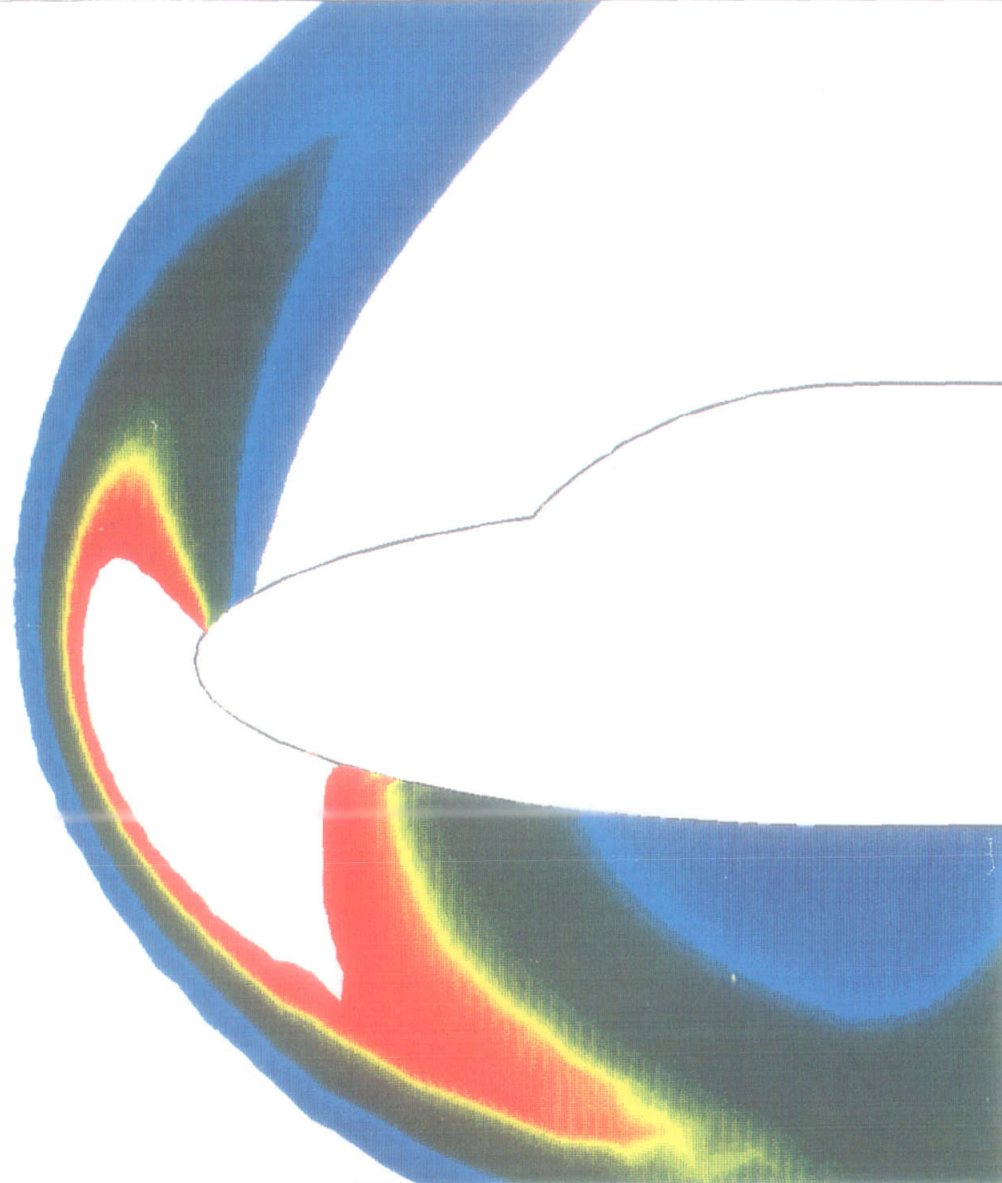
0.77E-01 0.15

EXTREMA DU CHAMP B
0.45 0.83

EXTREMA DES ISOVALEURS
0.45 0.83

30 ISOVALEURS

FINIR	:	0
CONTINUER	:	1
VUE SUIVANTE	:	2
VUE PRECEDENTE	:	3
RAFRAICHIR	:	4
ZOOM +	:	5
ZOOM -	:	6
VALEUR	:	7
SOFTCOPIE	:	8



MODULE FE : CARA

16/06/89

ELIPSE2R.MAI1

ELIPSE2R.C001

ELIPSE2RCII.DENB1

1414 POINTS

1414 NOEUDS

2677 ELEMENTS

2677 TRIANGLES

COIN BAS GAUCHE :

-0.86E-01 -0.47E-01

COIN HAUT DROIT :

0.13E-01 0.60E-01

EXTREMA DU CHAMP B

0.18 4.6

EXTREMA DES ISOVALEURS

1.4 2.4

100 ISOVALEURS

FINIR : 0

CONTINUER : 1

VUE SUIVANTE : 2

VUE PRECEDENTE : 3

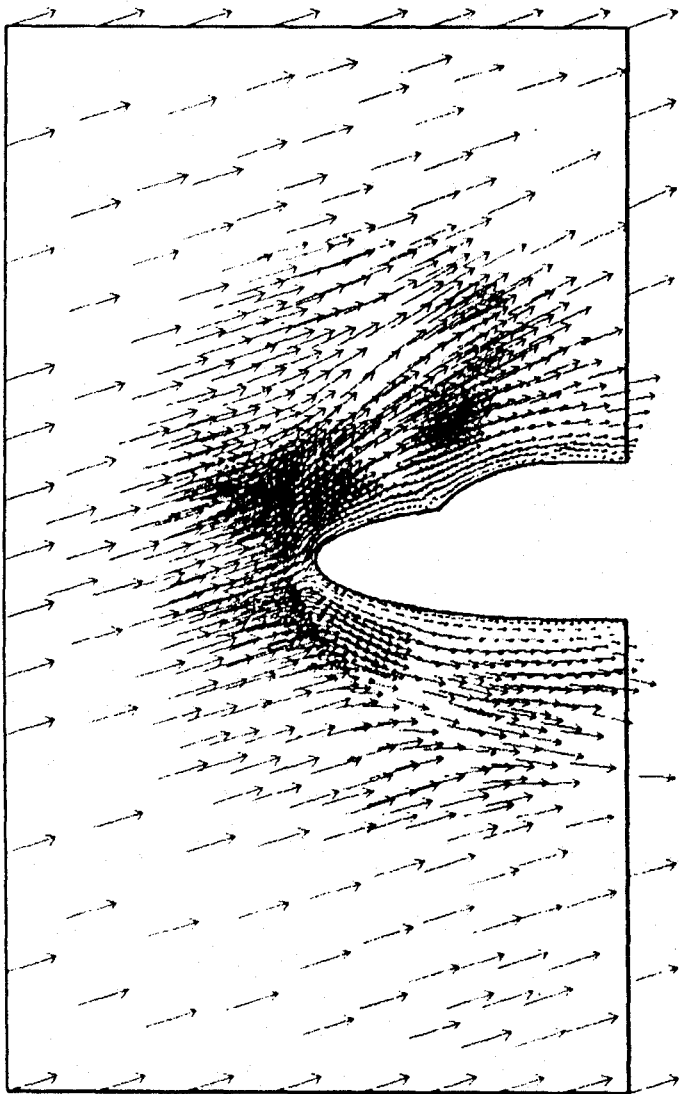
RAFRAICHIR : 4

ZOOM + : 5

ZOOM - : 6

VALEUR : 7

SOFTCOPIE : 8



MODULE FF :CARA

16/06/89

CLIPSE2R.MAI1

CLIPSE2R.C001

CLIPSE2RCII.VELB1

1414 POINTS

1414 NOEUDS

2677 ELEMENTS

2677 TRIANGLES

COIN BAS GAUCHE :

-0.20 -0.15

COIN HAUT DROIT :

0.77E-01 0.15

EXTREMA DU CHAMP B

0.00E+00 1.0

ECHELLE

1.2 CM. = 1.

VITESSES

FINIR : 0

CONTINUER : 1

VUE SUIVANTE : 2

VUE PRECEDENTE : 3

RAFRAICHEUR : 4

ZOOM + : 5

ZOOM - : 6

SOFTCOPIE : 8

PARTE II

A continuación se presentan los capítulos 1, 2 y 3 de la segunda parte, que se corresponden, respectivamente con los trabajos siguientes:

- *The numerical solution of some elliptic problems with nonlinear discontinuities using exact regularization*, Computers & Mathematics with Applications, Vol. 29, No. 12, pp. 57-66.
- *On the computation of steady vortex pairs*, aceptado para publicación en Comp. & Math. with Appl.
- *The numerical solution of some elliptic nonscalar problems with nonlinear discontinuities*, enviado a Comp. & Math. with Appl.

Capítulo 1

Resolución numérica de algunos
problemas elípticos con no linealidades
discontinuas mediante regularización
exacta

The numerical solution of some elliptic problems with nonlinear discontinuities using exact regularization.

Rosa ECHEVARRÍA*

Abstract

We illustrate with numerical experiments the behavior of certain algorithms based on exact regularization. First, we consider an elliptic PDE with a nonlinear discontinuity. Then, we deal with a semilinear elliptic problem which can be used to model the equilibrium of a confined plasma.

Keywords and phrases: Exact regularization, elliptic partial differential equations with nonlinear discontinuities, finite element methods.

1 Introduction

The goal of this paper is to illustrate with numerical experiments the behavior of certain algorithms of a particular kind involving exact regularization when they are used to solve two particular problems: A boundary value problem for a nonlinear elliptic PDE and a semilinear elliptic system which serves to model the equilibrium of a confined plasma.

In both cases, the main difficulty is due to the presence of a discontinuous nonlinearity. This implies that fixed point like algorithms are not feasible, because the iterates are not well defined. In the second case, an additional difficulty is the presence of a constraint.

The algorithms used in this paper have been introduced in [1] (see also [2]). They use:

1. Variational reformulation, so that each problem is expressed as the search of critical points of a functional that is the difference of two convex continuous functions.
2. Exact regularization. This permits to replace the original problems by other equivalent regular problems. Then, critical points are characterized as the solution of new equivalent (dual) problems for which fixed point algorithms are well defined.

Furthermore, for the numerical solution of the examples considered in this paper, we have used

3. Finite element approximation techniques.

For the computations in this paper and also for the presentation of the numerical results, we have used the MODULEF finite element library (see [3]).

In a forthcoming paper, we will apply similar techniques to other related (but different) problems (some of them, possibly, have no variational formulation, others involve a system of PDE's, ...).

*Dpto. Ecuaciones Diferenciales y Análisis Numérico, University of Sevilla, C/ Tarfia s/n, 41012 SEVILLA, SPAIN

2 A first problem: An elliptic PDE with a nonlinear discontinuity

Our problem is the following:

$$(1) \quad \left\{ \begin{array}{l} \text{Find } u \in H^2(\Omega) \text{ such that} \\ -\Delta u(x) \in H(u(x) + \alpha(x)) \text{ a.e. in } \Omega \\ u = 0 \text{ on } \partial\Omega \end{array} \right.$$

Here, Ω is an open bounded set in \mathbb{R}^2 with smooth boundary $\partial\Omega$, the function $\alpha : \Omega \rightarrow \mathbb{R}$ is given and H is the following maximal monotone operator (depending on a parameter $a \in \mathbb{R}$), associated to Heavyside's function:

$$H(s) = \begin{cases} 0 & \text{for } s < 0 \\ [0, a] & \text{for } s = 0 \\ a & \text{for } s > 0 \end{cases}$$

In the general context introduced in [1], a variational formulation can be obtained by taking

$$H = L^2(\Omega), \quad V = H_0^1(\Omega), \quad B : \text{the compact embedding } H_0^1(\Omega) \hookrightarrow L^2(\Omega)$$

$$f : H_0^1(\Omega) \rightarrow \mathbb{R}, \quad f(v) = \frac{1}{2} \int_{\Omega} |\nabla v|^2 dx, \quad \forall v \in H_0^1(\Omega)$$

$$g : L^2(\Omega) \rightarrow \mathbb{R}, \quad g(q) = \int_{\Omega} G(x, q) dx, \quad \forall q \in L^2(\Omega)$$

with $G(x, s) = a(s + \alpha(x))_+$ $\forall (x, s) \in \Omega \times \mathbb{R}$ (so that $\partial_s G(x, s) = H(s + \alpha(x))$). Then, problem (1) can be rewritten as

$$(2) \quad \text{Find } u \in H_0^1(\Omega) \text{ such that } \partial f(u) - B^* \partial g(Bu) \ni 0.$$

Algorithm and Convergence

In this case, Algorithm 1 in [1] reads as follows:

(a) Fix $\lambda > 0$ and choose $p_0 \in L^2(\Omega)$.

(b) Then, for any given $k \geq 0$ and $p_k \in L^2(\Omega)$,

(b.1) Compute $u_{k+1} \in H_0^1(\Omega)$, by solving $\begin{cases} -\Delta u = p_k \text{ in } \Omega \\ u = 0 \text{ on } \partial\Omega \end{cases}$

(b.2) Set $p_{k+1}(x) = H_{\lambda}(u_{k+1}(x) + \alpha(x) + \lambda p_k(x))$ a.e. in Ω .

In (b.2), H_{λ} is the Yosida approximation to the maximal monotone operator H , i.e.

$$H_{\lambda} = \frac{1}{\lambda} (Id - (Id + \lambda H)^{-1})$$

It can be proved (see [1]) that any sequence $\{u_k\}$ generated by this algorithm possesses subsequences which converge weakly in $H_0^1(\Omega)$. The limit of any such subsequence is a solution to problem (2).

Finite Element Discretization

For simplicity, it will be assumed that the domain Ω is a polygon. Let T_h be a triangulation of Ω . We use P_1 -Lagrange (piecewise linear) finite element approximation.

Consider the finite dimensional space

$$V_h = \{v_h; v_h \in C^0(\bar{\Omega}), \quad v_h|_T \in P_1 \quad \forall T \in T_h\}$$

and its subspace

$$V_h^0 = \{v_h; v_h \in V_h, \quad v_h = 0 \text{ on } \partial\Omega\}$$

Of course, V_h and V_h^0 must be viewed as approximations to $H^1(\Omega)$ and $H_0^1(\Omega)$, respectively. Let $\{a_i\}_{i=1}^n$ be the set of nodal points of T_h belonging to Ω . Then it is well known that a function $v_h \in V_h^0$ is uniquely determined by the values $v_h(a_k)$, $k = 1, 2, \dots, n$. It is thus customary to introduce the canonical basis $\{\varphi_1, \dots, \varphi_n\}$ of V_h^0 , where

$$\varphi_i \in V_h^0 \quad \text{and} \quad \varphi_i(a_j) = \delta_{ij} \quad \forall i, j = 1, 2, \dots, n$$

Observe that

$$v_h = \sum_{i=1}^n v_h(a_i) \varphi_i \quad \forall v_h \in V_h^0$$

Accordingly, we introduce the following approximations to the Dirichlet problems arising in step (b.1) (see above):

$$\begin{cases} \text{Find } u_h \in V_h^0 \text{ such that} \\ \int_{\Omega} \nabla u_h \nabla \varphi_i dx = \int_{\Omega} p_{h,k} \varphi_i dx \quad \forall \varphi_i \in V_h^0 \end{cases}$$

In order to solve this problem, we identify any function $v_h \in V_h^0$ with the corresponding vector $\bar{v} \in \mathbb{R}^n$, $\bar{v} = (v_i)_{i=1}^n$, $v_i = v_h(a_i)$. It is readily seen that our task is to solve the n -dimensional linear system $A\bar{u} = b_k$, where A and b_k are given as follows:

$$\begin{aligned} A &= (a_{ij})_{i,j=1}^n, & a_{ij} &= \int_{\Omega} \nabla \varphi_i \nabla \varphi_j dx \\ b_k &= (b_i^k)_{i=1}^n, & b_i^k &= \int_{\Omega} p_{h,k} \varphi_i dx \end{aligned}$$

The matrix A , which is common to all the iterates, is symmetric and definite positive. It is also a sparse matrix and, if an appropriate numerotation of the nodal points is chosen, it has nonvanishing components only near the diagonal line. Consequently, it can be written in the form $A = LL^t$ using Cholesky's method. The triangular matrix L can be computed at the beginning of the iterations.

Essentially, at each step of the algorithm, the computations to carry out are the following:

- Compute the second member b_k (using a numerical integration formula).
- Solve the linear triangular systems $Ly = b_k$ and $L^t u = y$.
- Compute $p_{h,k+1}$, i.e. the vector $p_{k+1} \in \mathbb{R}^n$ given by

$$p_i^{k+1} = H_\lambda(u_i^{k+1} + \alpha(a_i) + \lambda p_i^k), \quad i = 1, 2, \dots, n$$

Numerical experiences

Some numerical tests have been made taking $\Omega = (0, 1) \times (-1, 1)$ and using a regular triangulation with 800 points and 1482 triangles (accordingly, $h \sim 0.05$).

Our data have been $a = 1$,

$$\alpha(x) = \begin{cases} 0.063 & \text{if } x \in \Omega_1 \\ 0 & \text{otherwise} \end{cases}$$

with $\Omega_1 = [0.3, 0.7] \times [-0.5, 0.5]$. The domain and the triangulation are shown in Figures 1 and 2.

The algorithm has been initialized with $p_0(x) \equiv 1$ in all the cases, and the convergence criterium has been $\|p_{k+1} - p_k\| < \varepsilon = 10^{-5}$. The algorithm has been tested for different values of λ . In Figure 3, the relationship between the values of λ and the corresponding needed iterations is displayed.

In Figures 4 and 5, we present several views of the computed solution. This solution implicitly determines a free boundary: the curve $u(x) + \alpha(x) = 0$. Figures 6 to 9 are concerned with $u + \alpha$.

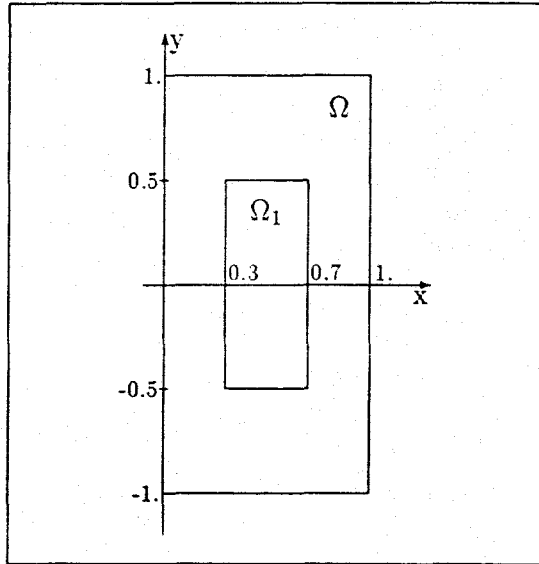


Figure 1. The domain Ω where the problem is solved, with the subdomain Ω_1 arising in the definition of the function α .

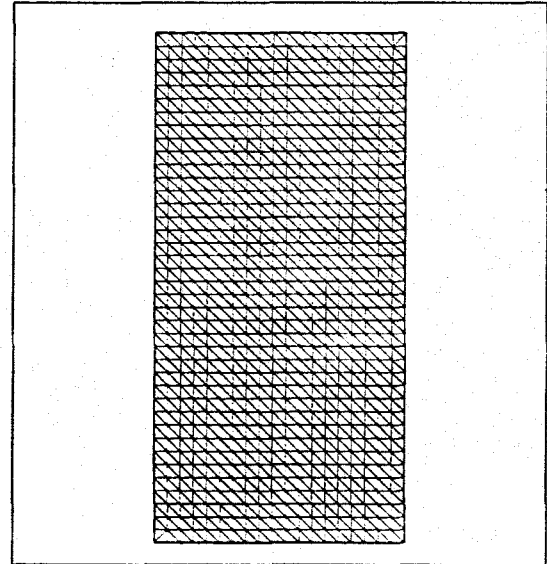


Figure 2. The triangulation of Ω . Number of triangles: 1482. Number of nodes: 800.

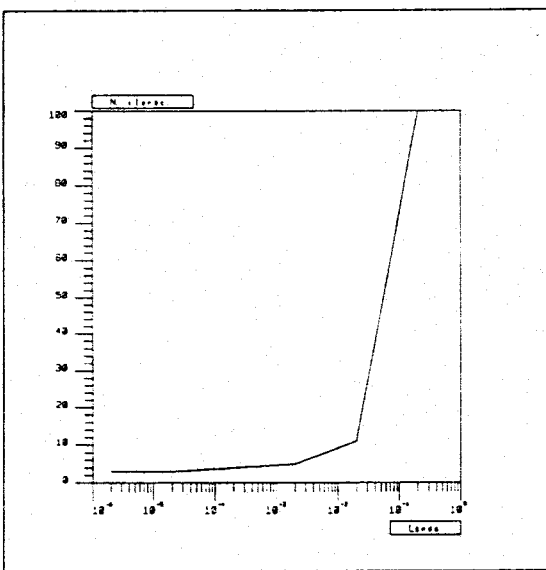


Figure 3. Behavior of the algorithm. Relationship between λ and the number of iterations needed.

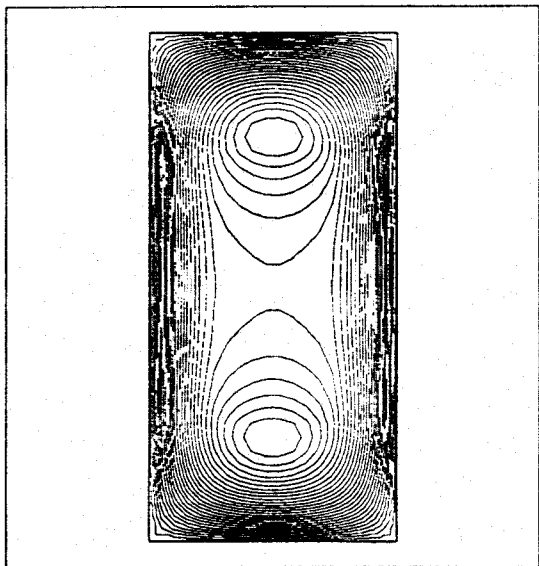


Figure 4. Isolines of the computed solution to problem (1).

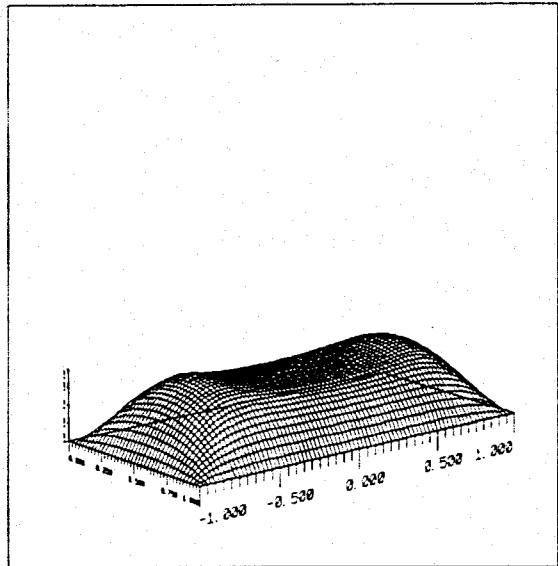


Figure 5. Three-dimensional representation of the computed solution. The values are multiplied by a factor 6.

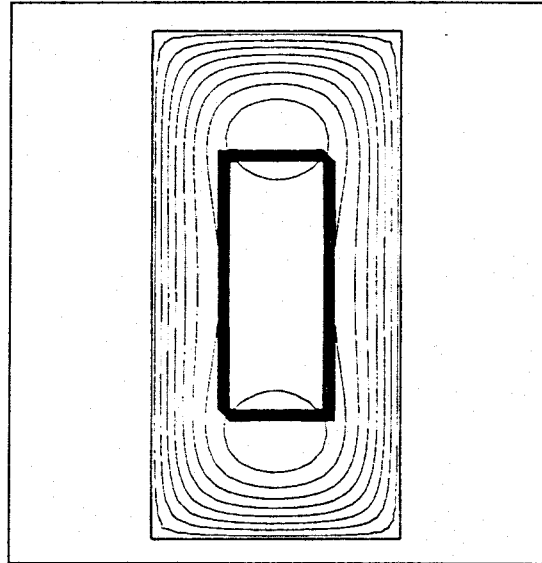


Figure 6. Isolines of the function $u + \alpha$.

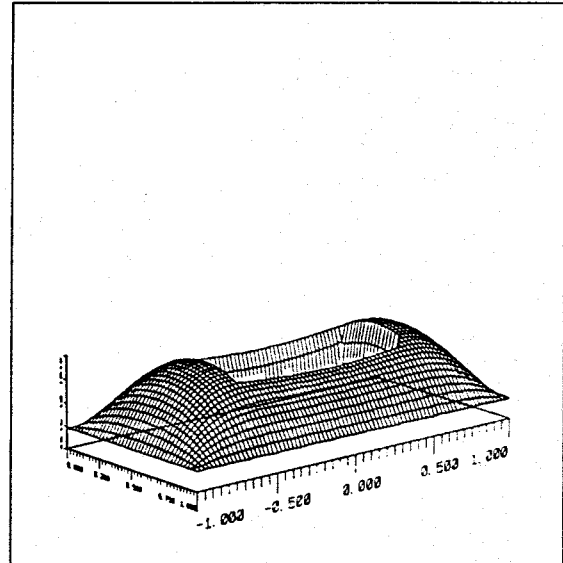


Figure 7. Three-dimensional representation of the function $u + \alpha$, multiplied by a factor 6.

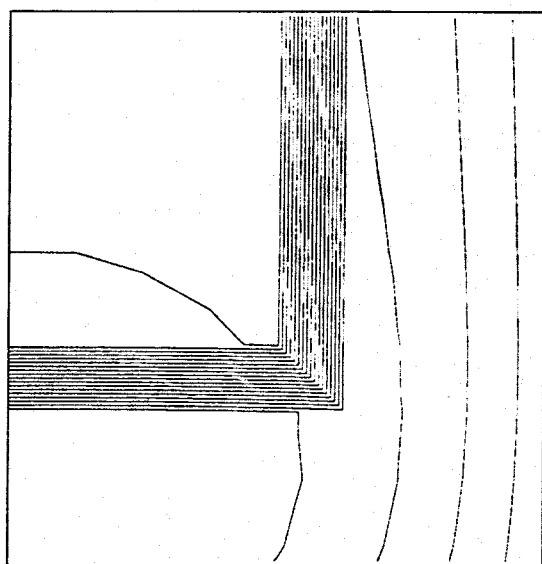


Figure 8. Detail of the isolines represented in Figure 6.

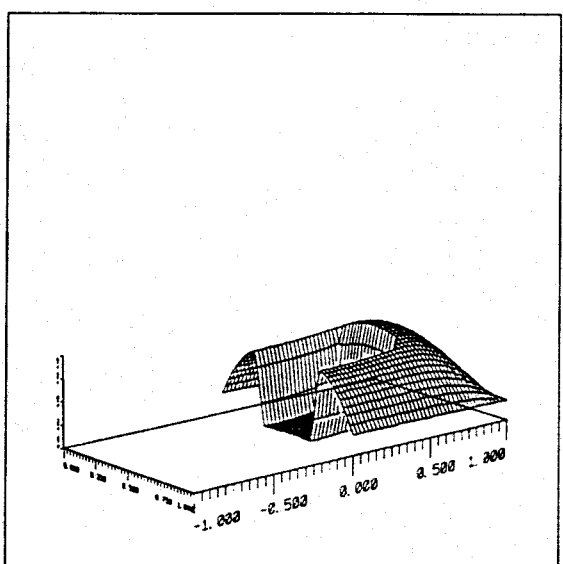


Figure 9. Representation of the function in Figure 7 over a half domain.

3 A second problem: The equilibrium of a plasma in a toroidal cavity

We consider a problem which serves to model the equilibrium of a plasma confined in a Tokamak. We will suppose that the confinement domain is axially symmetric. Consequently, we introduce cylindrical coordinates (r, θ, z) , we assume that the z -axis coincides with the center line of the toroid and we denote by Ω the cross section in the halfplane

$$\Pi = \{(r, \theta, z); (r, \theta, z) \in \mathbb{R}^3, \theta = 0, r > 0\}.$$

In the sequel, we assume that the boundary $\partial\Omega$ is smooth and, also, that $\bar{\Omega} \subset \{(r, z); (r, z) \in \mathbb{R}^2, r > 0\}$.

In this section, our problem is the following:

$$(3) \quad \left\{ \begin{array}{l} \text{Find } u \in H^2(\Omega) \text{ and } \beta \in \mathbb{R} \text{ such that} \\ -\mathcal{L}u \equiv -\frac{\partial}{\partial r}\left(\frac{1}{r}\frac{\partial u}{\partial r}\right) - \frac{\partial}{\partial z}\left(\frac{1}{r}\frac{\partial u}{\partial z}\right) \in rH(u) \quad \text{a.e. in } \Omega, \quad x = (r, z) \\ u = \beta \quad \text{on } \partial\Omega \\ -\int_{\partial\Omega} \frac{1}{r} \frac{\partial u}{\partial n} d\sigma = I \end{array} \right.$$

Here, H is as in Section 2. The parameter I is given and represents the total current crossing the plasma; and u is the flux function for the magnetic field (for more details on the physical meaning of the previous quantities, see [4,5]).

A solution (u, β) to (3) for which $\beta > 0$ defines a free boundary, the boundary of the region occupied by the plasma:

$$\Omega_p = \{x; x \in \Omega, u(x) < 0\}$$

Problem (3) admits a weak formulation:

$$(4) \quad \left\{ \begin{array}{l} \text{Find } u \in H_0^1(\Omega) \oplus \mathbb{R} \text{ such that} \\ \int_{\Omega} \frac{1}{r} \nabla u \nabla v dx = \int_{\Omega} rH(u)v dx, \quad \forall v \in H_0^1(\Omega) \\ \int_{\Omega} rH(u) dx = I \end{array} \right.$$

In order to reformulate (4) as the search of a critical point, following [1], we introduce

$$H = L^2(\Omega), \quad V = H_0^1(\Omega) \oplus \mathbb{R}, \quad B : \text{the compact embedding } V \hookrightarrow H,$$

$$K = \{q; q \in H, \int_{\Omega} q dx \leq I\},$$

$$f : V \longrightarrow \mathbb{R}, \quad f(v) = \frac{1}{2} \int_{\Omega} \frac{1}{r} |\nabla v|^2 dx + \alpha I, \quad \forall v = \tilde{v} + \alpha \in V,$$

$$g : H \longrightarrow \mathbb{R}, \quad g(q) = \int_{\Omega} G(x, q(x)) dx, \quad \forall g \in H$$

where $G(x, s) = ars_+$, (so that $\partial_s G(x, s) = rH(s)$). Now, our purpose is to solve the following (dual) problem:

$$(5) \quad \begin{cases} \text{Min } J^*(q) = g^*(q) - f^*(B^*q) \\ \text{subject to } q \in \partial K \end{cases}$$

The set K is a closed semispace of $L^2(\Omega)$ and $\partial K = \{ q ; q \in H, \int_{\Omega} q dx = I \}$. Therefore, the usual associated normal cone at $q \in \partial K$ is $N_{\partial K}(q) = \mathbb{R}$, for all q .

Algorithm and Convergence

Algorithm 2, proposed in [1] for constrained problems of this kind reads in this case as follows:

(a) Fix $\lambda > 0$ and choose $p_0 \in L^2(\Omega)$

(b) Then, for any given $k \geq 0$ and $p_k \in L^2(\Omega)$,

(b.1) Compute $\tilde{u}_{k+1} \in H_0^1(\Omega)$, by solving $\begin{cases} -\mathcal{L}u = p_k & \text{in } \Omega \\ u = 0 & \text{on } \partial\Omega \end{cases}$

(b.2) Compute $\beta_{k+1} \in \mathbb{R}$ by solving the scalar equation

$$F_k(\beta) \equiv \int_{\Omega} (rH)_\lambda(\tilde{u}_{k+1} + \beta + \lambda p_k) dx = I$$

(b.3) Set $p_{k+1}(x) = (rH)_\lambda(\tilde{u}_{k+1}(x) + \beta_{k+1} + \lambda p_k(x))$ a.e. in Ω .

This algorithm can be compared with the one proposed in [6] by M. Sermange, which involves approximate regularization only. To be well defined, it is necessary that, for each $p_k \in \partial K$ and $\tilde{u}_{k+1} \in H_0^1(\Omega)$, there exists at least one solution $\beta_{k+1} \in \mathbb{R}$ to the corresponding equation in (b.2). This fact is proved in [1]: actually, it is shown there that the sequence $\{\beta_k\}$ is uniformly bounded in a more general case.

In order to establish the convergence of the previous algorithm, we will prove the following result:

Theorem 1 Assume $p_0 \in \partial K$ and $p_0 \geq 0$ a.e. in Ω . Then the sequence $\{(\tilde{u}_k, \beta_k)\}$ possesses subsequences which converge in $H_0^1(\Omega) \times \mathbb{R}$. If (\tilde{u}, β) is the limit of such a subsequence, then $(\tilde{u} + \beta, \beta)$ is a solution to (4).

PROOF: By construction $\{p_k\}$ is uniformly bounded in $L^2(\Omega)$. As a consequence, $\{(p_k, \beta_k)\}$ is bounded in $L^2(\Omega) \times \mathbb{R}$; therefore, it possesses weakly convergent subsequences and, also, $\{\tilde{u}_k\}$ is bounded in $H^2(\Omega)$. Extracting new subsequences if necessary, one has

$$\begin{aligned} p_\mu &\rightarrow p \text{ weakly in } L^2(\Omega), \quad \beta_\mu \rightarrow \beta \\ \tilde{u}_\mu &\rightarrow \tilde{u} \text{ weakly in } H^2(\Omega) \text{ and strongly in } H_0^1(\Omega) \end{aligned}$$

It can be proved that $\lim_{k \rightarrow \infty} \|p_{k+1} - p_k\|_{L^2}^2 = 0$ by using the inequality

$$J^*(p_{k+1}) \leq J^*(p_k) - \frac{\lambda}{2} \|p_{k+1} - p_k\|_{L^2}^2$$

and the fact that J^* is bounded from below. Then, from relations $p_\mu \in \partial K$ and $p_\mu \in rH(B(\tilde{u}_\mu + \beta_\mu) + \lambda(p_{\mu-1} - p_\mu))$, one sees that

$$p \in \partial K \text{ and } p \in rH(B(\tilde{u} + \beta))$$

Finally, if we denote by S the inverse of the operator $-\mathcal{L}$ with homogeneous Dirichlet conditions on $\partial\Omega$, we can write $\tilde{u}_{\mu+1} = SB^*p_\mu \forall \mu$. Hence, $\tilde{u} = SB^*p$, i.e.

$$\begin{cases} -\mathcal{L}\tilde{u} = p & \text{in } \Omega \\ \tilde{u} = 0 & \text{on } \partial\Omega. \end{cases}$$

Consequently, $(\tilde{u} + \beta, \beta)$ solves (4). ■

In a similar way, an iterative algorithm can be introduced and a convergence result can be established for a more general problem

$$\begin{cases} -\mathcal{L}u(x) \in \partial G(x, u(x)) & \text{a.e. in } \Omega, \quad x = (r, z) \\ u = \beta & \text{on } \partial\Omega \\ -\int_{\partial\Omega} \frac{1}{r} \frac{\partial u}{\partial n} d\sigma = I \end{cases}$$

where G must satisfy appropriate assumptions.

Finite Element Discretization

We use the same P_1 -Lagrange finite element approximation introduced in Section 2. Then, each problem

$$\begin{cases} -\mathcal{L}u = p_k & \text{in } \Omega \\ u = 0 & \text{on } \partial\Omega \end{cases}$$

can be written as a linear system $\tilde{A}\tilde{u} = \tilde{b}_k$ where

$$\begin{aligned} \tilde{A} &= (\tilde{a}_{ij})_{i,j=1}^n, & \tilde{a}_{ij} &= \int_{\Omega} \frac{1}{r} \nabla \varphi_i \cdot \nabla \varphi_j dx \\ \tilde{b}_k &= (\tilde{b}_i^k)_{i=1}^n, & \tilde{b}_i^k &= \int_{\Omega} p_{h,k} \varphi_i dx \end{aligned}$$

By means of a Cholesky factorization $\tilde{A} = \tilde{L}\tilde{L}^t$, we see that, at each step, our task in (b.1) is reduced to

- a) The computation of the second member $b_k \in \mathbb{R}^n$.
- b) The numerical solution of two linear triangular systems.

The scalar equation in (b.2) now converts into

$$(6) \quad F_{h,k}(\beta) \equiv \int_{\Omega} p_{h,k}(\beta) dx = I$$

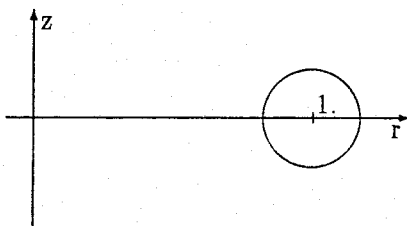
where $p_{h,k}(\beta)$ is determined by

$$p_{h,k}(\beta) \in V_h, \quad (p_{h,k}(\beta))(a_i) = (r_i H)_\lambda(u_i^{k+1} + \beta + \lambda p_i^k), \quad \forall i = 1, 2, \dots, n$$

(here, $a_i = (r_i, z_i)$ is the i -th nodal point). The function $F_{h,k}$ is nondecreasing, so that equation (6) is easily solvable.

Numerical experiences

For the numerical tests, we have chosen as Ω the open ball centered at $(1, 0)$ with radius 0.2. We have taken $a = 5$, and $I = 0.5$.



These choices correspond to the Tokamak of Fontenay-Aux-Roses (cf. [6]). We have used a triangulation of Ω with 894 points and 1726 triangles which can be seen, together with a three-dimensional representation of a part of the toroidal domain, in Figures 11 and 12.

We have used the initialization $p_0(x) \equiv 1$ and the convergence test $\|p_{k+1} - p_k\| < \varepsilon = 10^{-4}$. In Figures 13 and 14, the solution and the free boundary (the region occupied by the plasma) are visualized. Figures 15 to 18 show the free boundaries found for other values of the total current parameter I . The results are in practice identical to those in [6].

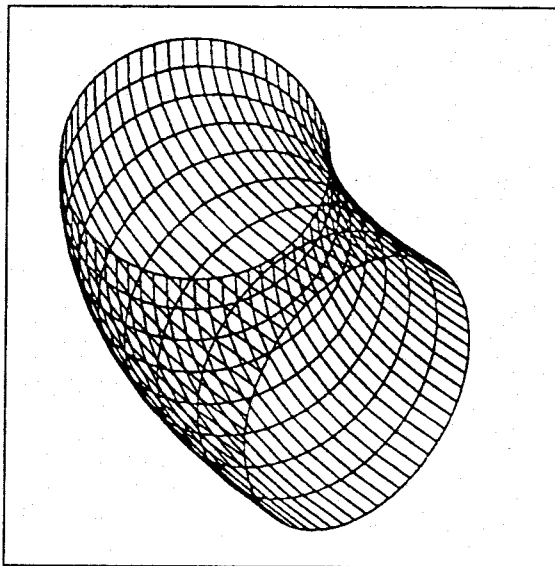


Figure 11. Three-dimensional representation of a portion of the toroid.

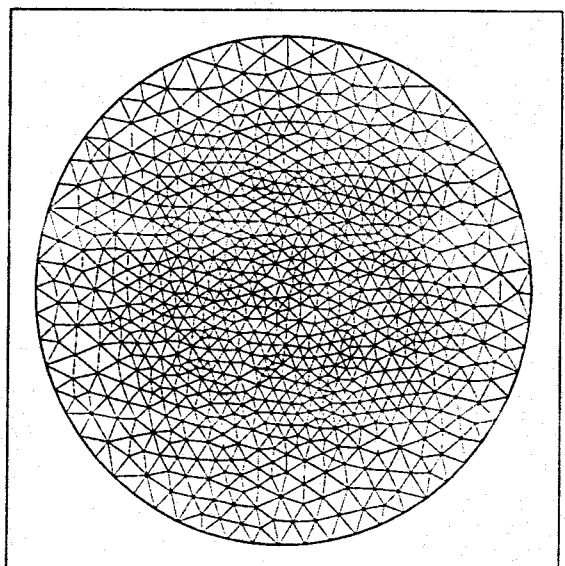


Figure 12. Triangulation of the domain Ω . Number of triangles: 1776. Number of nodes: 890.

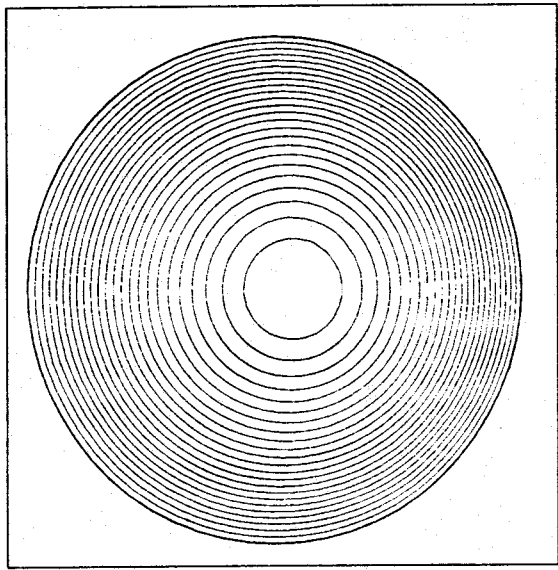


Figure 13. Isolines of the computed solution.

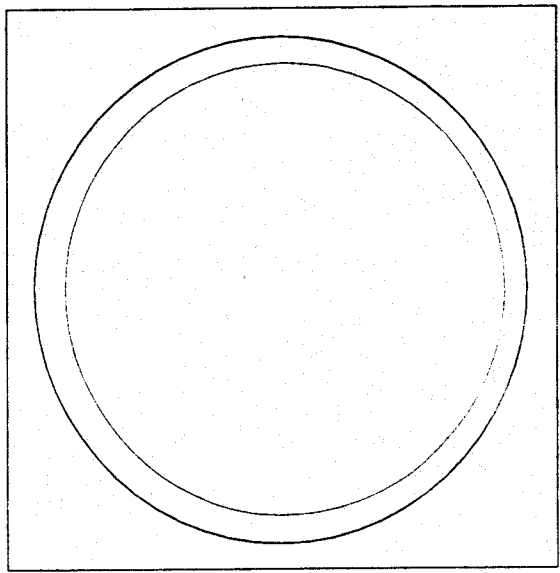


Figure 14. The free boundary defined by the solution. Region occupied by the plasma.

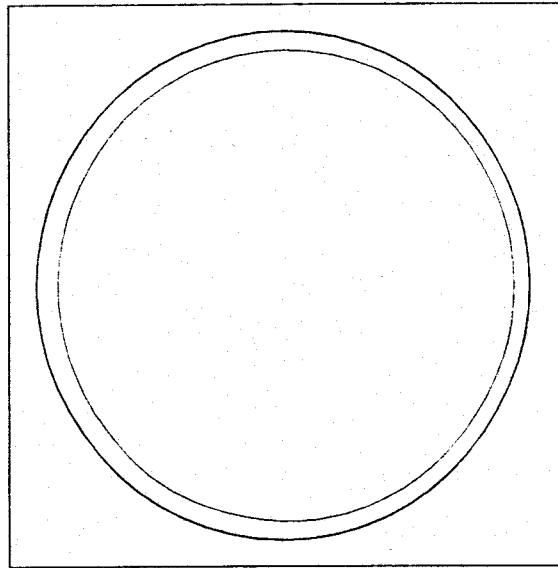


Figure 15. The free boundary for $I = 0.55$.

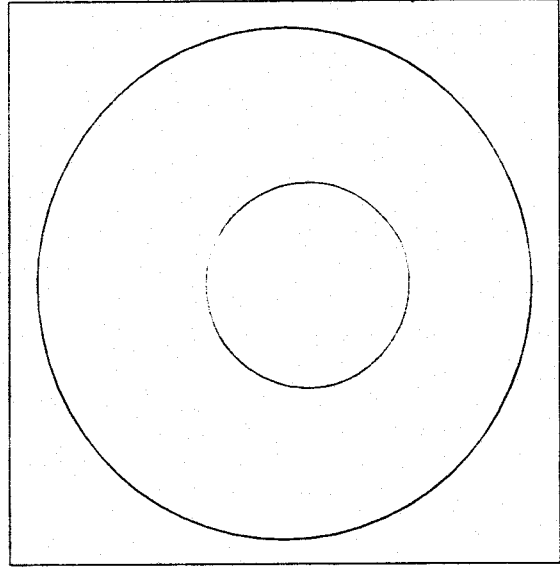


Figure 16. The free boundary for $I = 0.1$.

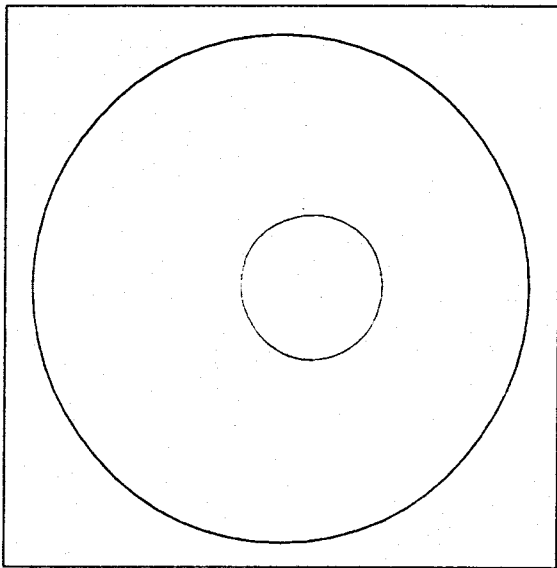


Figure 17. The free boundary for $I = 0.05$.

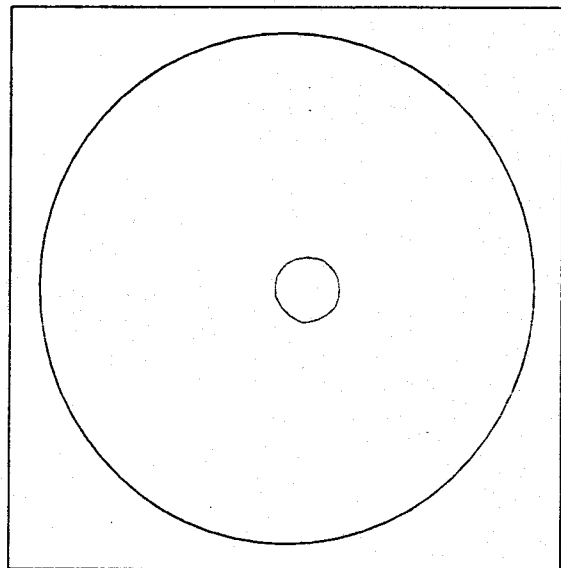


Figure 18. The free boundary for $I = 0.01$.

References

- [1] E. FERNANDEZ-CARA & C. MORENO, *Critical Point Approximation Through Exact Regularization*. Math. of Comp. Vol. 50, No. 181, January 1988, pp 139-153.
- [2] E. FERNANDEZ-CARA & C. MORENO, *Exact regularization and critical point approximation*, in Contributions to Nonlinear Partial Differential Equations, Vol. II. (J.I. Diaz and P.L. Lions Ed.), Longman Scientific & Technical, 1987.
- [3] M. BERNADOU et al, *MODULEF: Une Bibliothèque Modulaire d'Éléments Finis*, INRIA, Rocquencourt, 1985.
- [4] R. TÉMAM, *A nonlinear eigenvalue problem: The shape at equilibrium of a confined plasma*, Arch. Rational Mech. Anal., Vol. 60, 1975, pp. 51-73.
- [5] R. TÉMAM, *Remarks on a free boundary problem arising in plasma physics*, Comm. Partial Differential Equations, Vol. 2, 1977, pp. 41-61.
- [6] M. SERMANGE, *Thèse*, Université Paris XI, 1982.

Capítulo 2

**Resolución numérica de algunos
problemas de la teoría de vórtices
estacionarios**

On the numerical computation of steady vortex pairs.

Rosa ECHEVARRÍA*

Abstract

We present several algorithms for the computation of the solution to some semilinear elliptic problems with discontinuous nonlinearities. These are related to the equilibrium of steady vortex pairs. We illustrate with numerical experiments. First, we consider a problem which possesses an equivalent variational formulation. Then, by analogy, we propose an algorithm in the context of a nonvariational problem.

1 Introduction

In this paper we are concerned with the numerical solution of some problems related to the equilibrium of steady vortex pairs in an ideal fluid. To this purpose, we will use some iterative algorithms which are very close to those in [1] (see also [2]), and rely on exact regularization. Our problems are written as semilinear elliptic systems, for which the main difficulty is the presence of a discontinuous nonlinearity.

For the solution of a first problem considered in this paper (see (2) below), the underlying idea is to introduce a variational reformulation. This reduces the task to the search of the critical points of a functional that is the difference of two convex functions. Then, using exact regularization, the original problems are replaced by other equivalent regular problems for which fixed point iterates are well defined.

In the case of a second problem (see (15)), unfortunately, there is no known variational equivalent formulation. However, we also present an iterative algorithm, where the specific iterates are defined by analogy with the variational case.

For the numerical solution, we use finite element approximation techniques. For the computations, as well as for the visualization of the numerical results, we have used the MODULEF finite element code (see [3]).

The plan is as follows. In Section 2, we recall a general problem modelling the equilibrium of vortex pairs in an ideal fluid. Section 3 deals with the variational case: we present several algorithms, we justify some theoretical aspects and, also, we present numerical results. Finally, in Section 4, we consider the nonvariational case.

*Dpto. Ecuaciones Diferenciales y Análisis Numérico. University of Sevilla, C/ Tarfia s/n, 41012 SEVILLA, SPAIN

2 The general problem

The general problem we consider is the following (see, e.g. [4]):

$$\begin{cases} -\Delta u(x) \in H(u(x) - Wx_1 - Z) & \text{a.e. in } \Omega, \quad x = (x_1, x_2), \\ u \in H_0^1(\Omega), \\ \int_{\partial\Omega} |\nabla u|^2 dx = \eta. \end{cases} \quad (1)$$

Here, Ω is the following bounded open set

$$\Omega = \{x \in \mathbb{R}^2; x = (x_1, x_2), 0 < x_1 < a, -b < x_2 < b\};$$

H is the maximal monotone operator (depending on a parameter $\alpha \in \mathbb{R}$), associated to Heaviside's function:

$$H(s) = \begin{cases} 0 & \text{for } s < 0, \\ [0, \alpha] & \text{for } s = 0, \\ \alpha & \text{for } s > 0; \end{cases}$$

the parameter W represents the constant velocity of the fluid at infinity in the direction Ox_2 , and η is the (prescribed) kinetic energy of the vortex motion. For the meaning of Z , see below.

The equations are required to be satisfied in a subset of the half-plane $\Pi = \{x = (x_1, x_2); x \in \mathbb{R}^2, x_1 > 0\}$ because the fluid motion is supposed to be symmetric about $x_1 = 0$. In the study of steady vortex pairs, parameters a and b are devoted to tend to $+\infty$, in order to recover the original problem in the whole half-plane.

If we denote by ψ the Stokes stream function, then u is $u = \psi + Wx_1 + Z$ and represents the perturbation of ψ due to the vortex motion. The previous system can be viewed as a free boundary problem. The region

$$A = \{x \in \Omega; x = (x_1, x_2), \psi(x) = u(x) - Wx_1 - Z > 0\},$$

which is half the vortex pair, is "a priori" unknown (the amount of fluid flowing between the vortex boundary ∂A and the axis $x_1 = 0$ is given by Z).

Besides the case of a vortex pair, (1) serves to model equilibrium in various related phenomena, arising in other contexts (see, e.g. [5] and the bibliography therein). In particular, the similar situation corresponding to the equilibrium of an axisymmetric vortex ring can be found in [6].

In this paper, we are interested in solving two specific problems based on the general formulation (1). They are the following:

A) *Free vortex velocity, with vanishing flux parameter*

Given $\eta > 0$ and $Z = 0$, find u and $W > 0$ satisfying (1).

B) *Free flux parameter*

Given $\eta > 0$ and $W > 0$, find u and $Z > 0$ satisfying (1).

Apparently, problem B) does not posses an equivalent variational formulation, i.e., we cannot identify the solutions to problem B) with the critical point of a functional (see [7]).

3 The variational case: free vortex velocity, with vanishing flux parameter

As we have pointed out in Section 1, our problem is the following:

$$\begin{cases} \text{Find } u \in H_0^1(\Omega) \text{ and } W \in \mathbb{R} \text{ such that} \\ -\Delta u(x) \in H(u(x) - Wx_1) \quad \text{a.e. in } \Omega, \quad x = (x_1, x_2), \\ \int_{\Omega} |\nabla u|^2 dx = \eta. \end{cases} \quad (2)$$

As noticed in [1], it would be interesting to rewrite (2) as a problem of the kind

$$\begin{cases} \text{Min } J^*(q) = g^*(q) - f^*(B^*q) \\ \text{subject to } q \in \partial K. \end{cases} \quad (3)$$

for adequate f , g , B and K . Here, g^* and f^* are the conjugate of the convex, proper and l.s.c. functions g and f , B^* is the adjoint of the bounded linear operator B , and ∂K is the boundary of the closed convex set K .

Thus, we take¹

$$H = L^2(\Omega), \quad V = H_0^1(\Omega), \quad B : \text{the compact embedding } H_0^1(\Omega) \hookrightarrow L^2(\Omega).$$

$$K = \{q \in L^2(\Omega); \quad \int_{\Omega} (BSB^*q) \cdot q dx \leq \eta\}.$$

$$f : H_0^1(\Omega) \longrightarrow \mathbb{R}, \quad f(v) = \frac{1}{2} \int_{\Omega} |\nabla v|^2 dx \quad \forall v \in H_0^1(\Omega).$$

$$g : L^2(\Omega) \longrightarrow \mathbb{R}, \quad g(q) = \int_{\Omega} G(x, q) dx \quad \forall q \in L^2(\Omega),$$

where S stands for the inverse of $-\Delta$ with homogeneous Dirichlet conditions and $G(x, s) = \alpha(s - x_1)_+$ $\forall (x, s) \in \Omega \times \mathbb{R}$ (so that $\partial_s G(x, s) = H(s - x_1)$). The set K is a closed convex subset of $L^2(\Omega)$ whose boundary is given as follows:

$$\partial K = \{q \in L^2(\Omega); \quad \int_{\Omega} (BSB^*q) \cdot q dx = \eta\}.$$

Hence, for each $q \in \partial K$, the corresponding normal cone is the set

$$N_{\partial K}(q) = \{\rho BSB^*q : \rho \in \mathbb{R}\}.$$

In this context, we know that if $p \in L^2(\Omega)$ is a solution to (3), there exists a constant $\Lambda \in \mathbb{R}$ such that

$$\Lambda BSB^*p \in \partial g^*(p) - \partial(f^* \circ B^*)(p) = \partial g^*(p) - B\partial f^*(B^*p) \quad (4)$$

(Λ is a Lagrange multiplier associated to p). Let us set $u = SB^*p$ (so that $-\Delta u = B^*p$) and $\beta = \Lambda + 1$. Then, (4) can be written in the form

$$p \in H(\beta Bu - x_1). \quad (5)$$

¹In [1], Section 6, one can find another choice of the functionals and spaces that leads to the same iterates.

If $\beta > 0$, taking $W = \frac{1}{\beta}$, one finds that

$$p \in H(Bu - Wx_1). \quad (6)$$

Finally, since $p \in \partial K$, one also has:

$$\int_{\Omega} (BSB^*q) \cdot q \, dx = \int_{\Omega} Bu \cdot p \, dx = \int_{\Omega} u \cdot B^*p \, dx = \int_{\Omega} |\nabla u|^2 \, dx = \eta$$

and, consequently, (u, W) is a solution of (2).

In the sequel, we make the assumption that

$$\eta < \int_{\Omega} |\nabla u_{\alpha}|^2 \, dx \equiv F_{\alpha},$$

where u_{α} is the unique solution to

$$\begin{cases} -\Delta u = \alpha & \text{in } \Omega \\ u = 0 & \text{on } \partial\Omega. \end{cases}$$

Obviously, this is a necessary condition for the existence of a solution to (2).

The algorithms

In [1], the following algorithm is proposed to solve constrained problems of the kind (3):

- (a) Fix $\lambda > 0$ and choose $p_0 \in H$.
- (b) Then, for any given $k \geq 0$ and $p_k \in H$, compute u_{k+1} and p_{k+1} by solving

$$\begin{cases} u_{k+1} \in \partial f^*(B^*p_k) + B^{-1}N_{\partial K}(p_k), \\ p_{k+1} = g'_{\lambda}(Bu_{k+1} + \lambda p_k), \quad p_{k+1} \in \partial K. \end{cases} \quad (7)$$

Here, g'_{λ} is the Yosida approximation to the maximal monotone operator ∂g , i.e.

$$g'_{\lambda} = \frac{1}{\lambda}(Id - (Id + \lambda \partial g)^{-1})$$

Let us briefly explain the meaning of (7) : The component of u_{k+1} in $B^{-1}N_{\partial K}(p_k)$ must be chosen so that p_{k+1} verifies $p_{k+1} \in \partial K$.

In the context of (2), this algorithm reads as follows:

ALGORITHM 1

- (a) Fix $\lambda > 0$ and choose $p_0 \in L^2(\Omega)$.

Compute $u_0 \in H_0^1(\Omega)$ by solving

$$\begin{cases} -\Delta u = p_0 & \text{in } \Omega, \\ u = 0 & \text{on } \partial\Omega. \end{cases}$$

(b) Then, for any given $k \geq 0$, $p_k \in L^2(\Omega)$, and $u_k \in H_0^1(\Omega)$,

(b.1) Compute $\beta_{k+1} \in \mathbb{R}$ by solving the equation

$$F_k(\beta) \equiv \int_{\Omega} |\nabla v_k(\beta)|^2 dx = \eta, \quad (8)$$

where $v_k(\beta)$ is (by definition) the solution to

$$\begin{cases} -\Delta v = H_\lambda(\beta u_k - x_1 + \lambda p_k) & \text{in } \Omega, \\ v = 0 & \text{on } \partial\Omega. \end{cases} \quad (9)$$

(b.2) Then, set

$$\begin{aligned} p_{k+1} &= H_\lambda(\beta_{k+1} u_k - x_1 + \lambda p_k), \\ u_{k+1} &= v_k(\beta_{k+1}). \end{aligned}$$

A variant of Algorithm 1 is given by the following iterates:

ALGORITHM 2

(a) Fix $\bar{\lambda} > 0$ and choose $\bar{p}_0 \in L^2(\Omega)$.

Compute $\bar{u}_0 \in H_0^1(\Omega)$ by solving

$$\begin{cases} -\Delta \bar{u} = \bar{p}_0 & \text{in } \Omega, \\ \bar{u} = 0 & \text{on } \partial\Omega. \end{cases}$$

(b) Then, for any given $k \geq 0$, $\bar{p}_k \in L^2(\Omega)$, and $\bar{u}_k \in H_0^1(\Omega)$,

(b.1) Compute $W_{k+1} \in \mathbb{R}$ by solving the equation

$$\bar{F}_k(W) \equiv \int_{\Omega} |\nabla \bar{v}_k(W)|^2 dx = \eta, \quad (10)$$

where $\bar{v}_k(W)$ is the solution to

$$\begin{cases} -\Delta \bar{v} = H_{\bar{\lambda}}(\bar{u}_k - W x_1 + \bar{\lambda} \bar{p}_k) & \text{in } \Omega, \\ \bar{v} = 0 & \text{on } \partial\Omega. \end{cases} \quad (11)$$

(b.2) Then, set

$$\begin{aligned} \bar{p}_{k+1} &= H_{\bar{\lambda}}(\bar{u}_k - W_{k+1} x_1 + \bar{\lambda} \bar{p}_k), \\ \bar{u}_{k+1} &= \bar{v}_k(W_{k+1}). \end{aligned}$$

Let us prove that the iterates of Algorithm 2 are well defined, i.e. that for each k there exists at least one solution $W_{k+1} \in \mathbb{R}$ to equation (10). The function \bar{F}_k is continuous, nonincreasing and bounded; indeed

$$0 \leq \bar{F}_k(W) \leq F_\alpha \equiv \int_{\Omega} |\nabla u_\alpha|^2 dx$$

For $\epsilon > 0$, we denote by Ω_ϵ the set

$$\Omega_\epsilon = \{x = (x_1, x_2); x \in \Omega, \epsilon \leq x_1\}$$

We have

$$\bar{F}_k(W) = \int_{\Omega} H_{\bar{\lambda}}(\bar{u}_k + \bar{\lambda}\bar{p}_k - Wx_1)\bar{v}_k(W) dx \leq C(\Omega) \int_{\Omega} |H_{\bar{\lambda}}(\bar{u}_k + \bar{\lambda}\bar{p}_k - Wx_1)|^2 dx,$$

where $C(\Omega)$ is a constant depending only on Ω . For any given $\rho > 0$, let $\epsilon > 0$ be such that

$$\text{meas}(\Omega - \Omega_\epsilon) < \frac{\rho}{C(\Omega)\alpha^2}$$

Then, if $W \geq W^*(\epsilon) = \frac{1}{\epsilon}(\max_{x \in \Omega} u_\alpha(x) + \bar{\lambda}\alpha)$ one has

$$H_{\bar{\lambda}}(\bar{u}_k + \bar{\lambda}\bar{p}_k - Wx_1) = 0 \quad \text{in } \Omega_\epsilon$$

and, consequently,

$$\bar{F}_k(W) \leq C(\Omega) \int_{\Omega - \Omega_\epsilon} |H_{\bar{\lambda}}(u_\alpha + \bar{\lambda}\alpha - Wx_1)|^2 dx \leq C(\Omega)\alpha^2 \text{meas}(\Omega - \Omega_\epsilon) < \rho.$$

i.e. $\lim_{W \rightarrow +\infty} \bar{F}_k(W) = 0$.

On the other hand, for $W \leq W_*(\epsilon) = \frac{-\lambda\alpha}{\epsilon}$, one has:

$$H_{\bar{\lambda}}(\bar{u}_k + \bar{\lambda}\bar{p}_k - Wx_1) = \alpha \quad \text{in } \Omega_\epsilon$$

Let us denote by $z_{\alpha,\epsilon}$ the solution to

$$\begin{cases} -\Delta z = \chi_{\alpha,\epsilon} & \text{in } \Omega, \\ z = 0 & \text{on } \partial\Omega, \end{cases}$$

where $\chi_{\alpha,\epsilon}$ is α times the characteristic function of Ω_ϵ . Then, for all $W \leq W_*(\epsilon)$, one has $\bar{v}_k(W) \geq z_{\alpha,\epsilon}$ in Ω and

$$\bar{F}_k(W) \geq \int_{\Omega_\epsilon} \alpha z_{\alpha,\epsilon} dx = F_\alpha - \left(\int_{\Omega} \alpha u_\alpha dx - \int_{\Omega_\epsilon} \alpha z_{\alpha,\epsilon} dx \right).$$

Now, for given $\rho > 0$ we can choose $\epsilon > 0$ so that $\int_{\Omega} \alpha u_\alpha dx - \int_{\Omega_\epsilon} \alpha z_{\alpha,\epsilon} dx < \rho$. Therefore,

$$\lim_{W \rightarrow -\infty} \bar{F}_k(W) = F_\alpha$$

It is now clear that, if $0 < \eta < F_\alpha$, there exists at least one solution $W_{k+1} \in \mathbb{R}$ to the equation (10) (this argument also shows that $\{W_{k+1}\}$ is uniformly bounded).

Let us mention that, concerning Algorithm 1, it can be proved that for each k there exists λ such that (8) possesses a solution.

Finite Element Approximation

The main difficulty in the algorithms above is the computation of the solutions to equations (8) and (10). Indeed, this requires the numerical solution of possibly many Dirichlet problems of the kinds (9) or (11). This can be made easily using finite element techniques. We shall use a P_1 -Lagrange (piecewise linear) finite element approximation. Let T_h be a triangulation of $\bar{\Omega}$ and let $\{a_i\}_{i=1}^n$ be the set of the corresponding nodal points. For the sake of simplicity in the exposition, we shall suppose that they have been numbered in such a way that the first n_0 points belong to Ω (this is not essential for the following).

Consider the finite dimensional space

$$V_h = \{v_h; v_h \in C^0(\bar{\Omega}), v_h|_T \in P_1 \quad \forall T \in T_h\}$$

and its subspace

$$V_h^0 = \{v_h; v_h \in V_h, v_h = 0 \text{ on } \partial\Omega\}$$

Of course, V_h and V_h^0 must be viewed as approximations to $H^1(\Omega)$ and $H_0^1(\Omega)$, respectively. Then, it is well known that a function $v_h \in V_h$ (resp. $w_h \in V_h^0$) is uniquely determined by the values $v_h(a_k)$ for $k = 1, 2, \dots, n$. (resp. the values $w_h(a_k)$ for $k = 1, 2, \dots, n_0$). It is thus customary to introduce the canonical basis $\{\varphi_1, \dots, \varphi_n\}$ of V_h , where

$$\varphi_i \in V_h \quad \text{and} \quad \varphi_i(a_j) = \delta_{ij} \quad \forall i, j = 1, 2, \dots, n.$$

Accordingly, the canonical basis of V_h^0 is $\{\varphi_1, \dots, \varphi_{n_0}\}$. Observe that

$$v_h = \sum_{i=1}^n v_h(a_i) \varphi_i \quad \forall v_h \in V_h \quad \text{and} \quad w_h = \sum_{i=1}^{n_0} w_h(a_i) \varphi_i \quad \forall w_h \in V_h^0.$$

For practical purposes, we shall identify any function $v_h \in V_h$ (resp. $w_h \in V_h^0$) with the corresponding vector $\bar{v} \in \mathbb{R}^n$, $\bar{v} = (v_i)_{i=1}^n$, $v_i = v_h(a_i)$ (resp. $\bar{w} \in \mathbb{R}^{n_0}$, $\bar{w} = (w_i)_{i=1}^{n_0}$, $w_i = w_h(a_i)$).

Let us now explain how a numerical approximation to the solution to the scalar equations (8) and (10) can be found. To fix ideas, we will only speak of equation (10). Let us denote by $\bar{P}_k(W)$ the second member in the Dirichlet problem (11), i.e. $\bar{P}_k(W) = H_{\bar{\lambda}}(\bar{u}_k - Wx_1 + \bar{\lambda}\bar{p}_k)$. The scalar equation (10) now converts into

$$\bar{F}_{h,k}(W) \equiv \int_{\Omega} \bar{P}_{h,k}(W) \bar{v}_{h,k}(W) dx = \eta, \quad (12)$$

where $\bar{v}_{h,k}(W)$ verifies:

$$\begin{cases} \bar{v}_{h,k}(W) \in V_h^0 \\ \int_{\Omega} \nabla \bar{v}_{h,k}(W) \nabla \varphi_i dx = \int_{\Omega} \bar{P}_{h,k}(W) \varphi_i dx \quad \forall i = 1, \dots, n_0 \end{cases} \quad (13)$$

and $\bar{P}_{h,k}(W)$ is

$$\bar{P}_{h,k}(W) \in V_h, \quad \bar{P}_{h,k}(W)(a_i) = H_{\bar{\lambda}}(\bar{u}_i^k - Wx_{i,1} + \bar{\lambda}\bar{p}_i^k), \quad \forall i = 1, 2, \dots, n \quad (14)$$

(here, $(x_{i,1}, x_{i,2})$ stand for the coordinates of the i -th nodal point).

The function $\bar{F}_{h,k}(W)$ is nonincreasing, so that equation (12) is easily solvable by an iterative method. Of course, this needs, at each step, the computation of the solution to (13) for a given value of W . It is readily seen that this is just to solve the n_0 -dimensional linear system $A\bar{v}_k(W) = b_k(W)$, where A and $b_k(W)$ are given as follows:

$$\begin{aligned} A &= (a_{ij})_{i,j=1}^{n_0}, & a_{ij} &= \int_{\Omega} \nabla \varphi_i \nabla \varphi_j dx \\ b_k(W) &= (b_i^k(W))_{i=1}^{n_0}, & b_i^k(W) &= \int_{\Omega} \bar{P}_{h,k}(W) \varphi_i dx \end{aligned}$$

The matrix A , which is common to all the iterates, is symmetric and definite positive. It is also a sparse matrix and, if an appropriate renumeration of the nodal points is performed, all nonvanishing components will be near the diagonal line. Consequently, it will be easy to solve all the previous linear systems via Cholesky's method. Of course, the triangular matrix L which provides the factorization $A = LL^t$ must be computed at the beginning of the program.

In short, at each iteration of the algorithm for solving the scalar equation (12), for a given value of W , the computations to carry out are:

- Compute $\bar{P}_{h,k}(W)$ given by (14).
- Compute the second member $b_k(W)$.
- Solve the linear triangular systems $Ly = b_k(W)$ and $L^t\bar{v}_k(W) = y$.
- Compute the value of $\bar{F}_{h,k}(W)$, i.e. the integral $\int_{\Omega} \bar{P}_{h,k}(W) \bar{v}_{h,k}(W) dx$

Numerical experiences with Algorithm 2

For the numerical tests we have taken $\Omega = (0, 10) \times (-10, 10)$ and $\eta = 3$. We have used a mesh with 1375 points and 2608 triangles, which are smaller in the region occupied by the vortex (see Figure 1). We have made several computations which correspond to different values of the parameter α .

We have initialized the iterates with the constant function $p_0(x) \equiv 1$ in all cases. The convergence criterium has been

$$\|p_{k+1} - p_k\| < \varepsilon = 10^{-5}.$$

We present in Figures 2-5 different views of the stream function, $\psi = u - Wx_1$ in the case $\alpha = 1$, obtained with $\lambda = 10^{-6}$. Figures 6-11 show the results in the cases $\alpha = 1.5$, $\alpha = 2$ and $\alpha = 4$, obtained with $\lambda = 10^{-7}$.

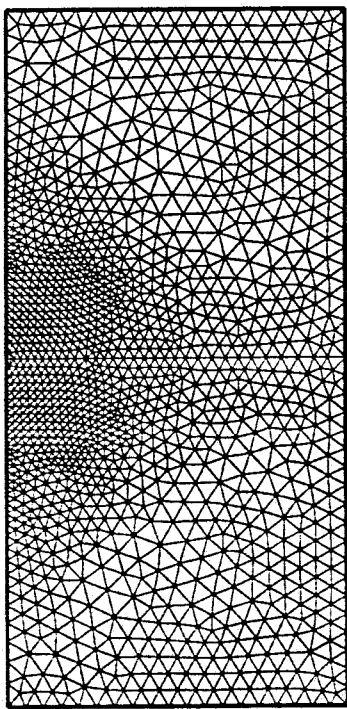


Figure 1. Triangulation of the domain Ω . Number of triangles: 2608. Number of nodal points: 1375.

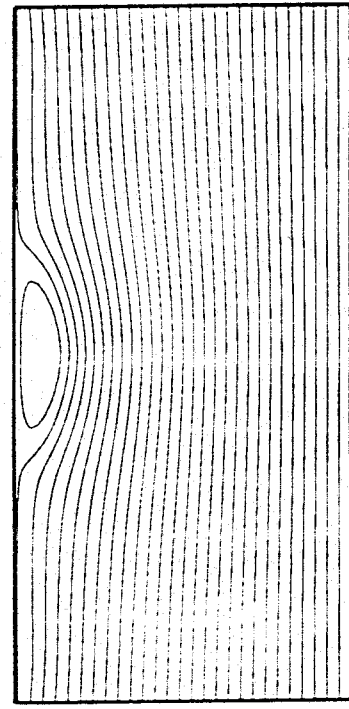


Figure 2. Isolines of the stream function $\psi = u - Wx_1$, for the data $\alpha = 1, \eta = 3$.

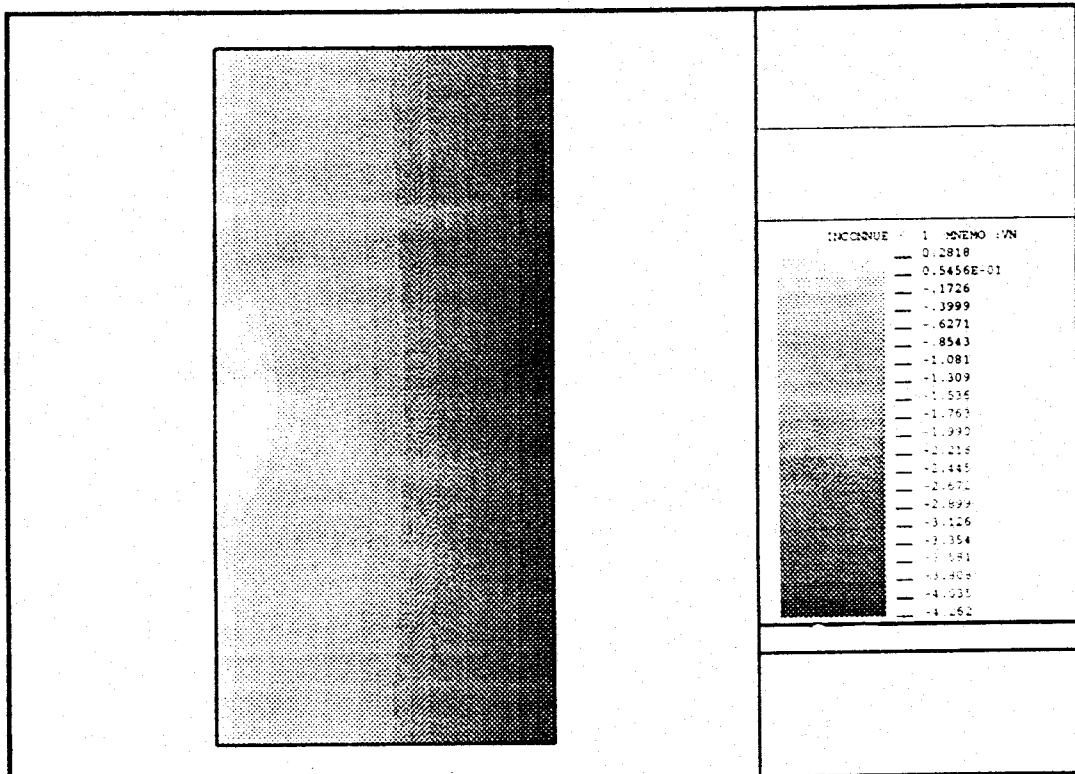


Figure 3. Representation of the values of the computed function $\psi = u - Wx_1$, for the data $\alpha = 1, \eta = 3$.

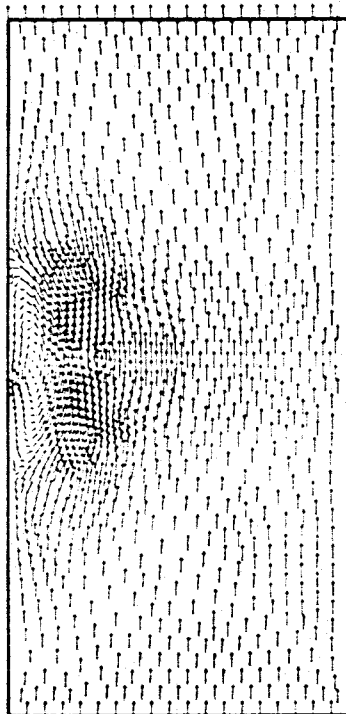


Figure 4. Representation of the velocity field $\vec{v} = \left(\frac{\partial \psi}{\partial x_2}, -\frac{\partial \psi}{\partial x_1} \right)$.

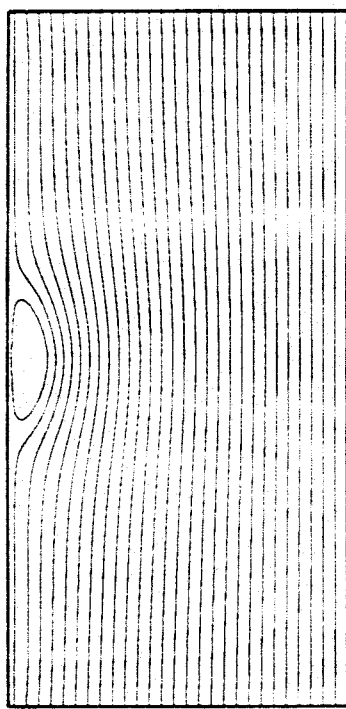


Figure 6. Stream lines for the data $\alpha = 1.5$, $\eta = 3$. Computed value of $W = 0.5303524$.

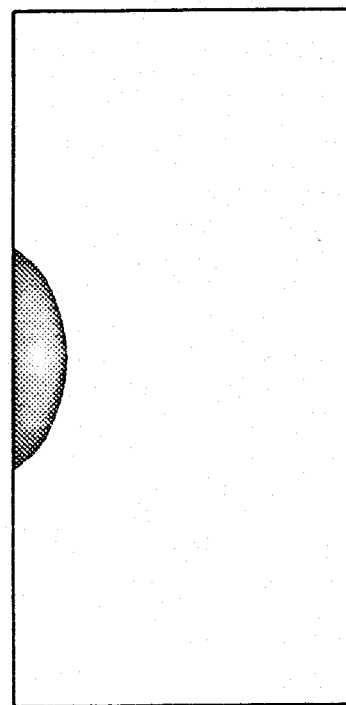


Figure 5. Region occupied by the vortex, i.e. $A = \{x \in \Omega; \psi(x) > 0\}$, for the data $\alpha = 1$, $\eta = 3$.

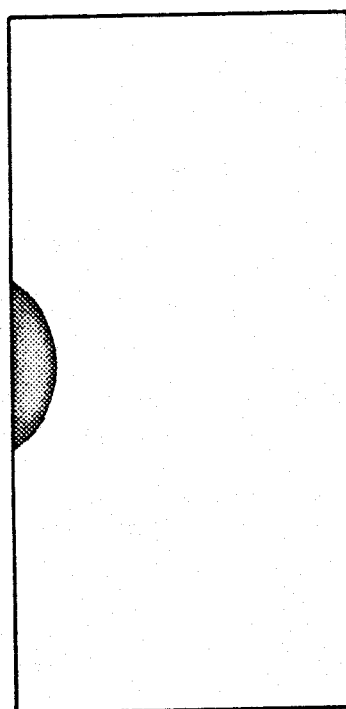


Figure 7. Vorticity region for the same case.

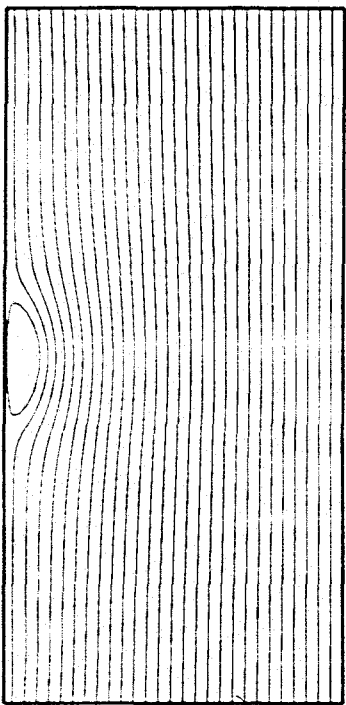


Figure 8. Stream lines for the data
 $\alpha = 2, \eta = 3$. Computed value of
 $W = 0.5868746$.

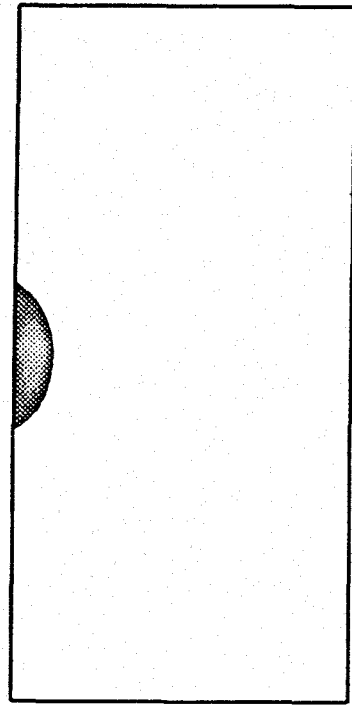


Figure 9. Vorticity region for the
same case.

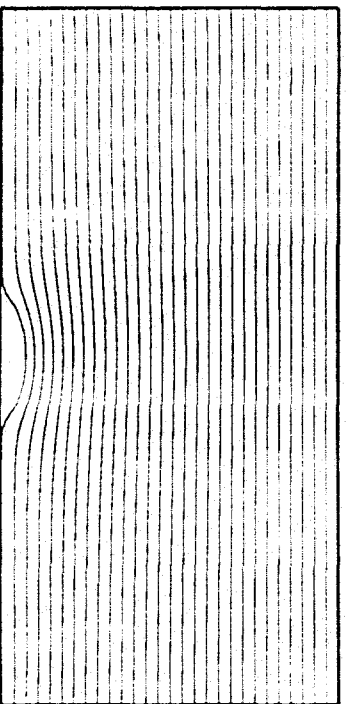


Figure 10. Stream lines for the data
 $\alpha = 4, \eta = 3$. Computed value of
 $W = 0.8348695$.

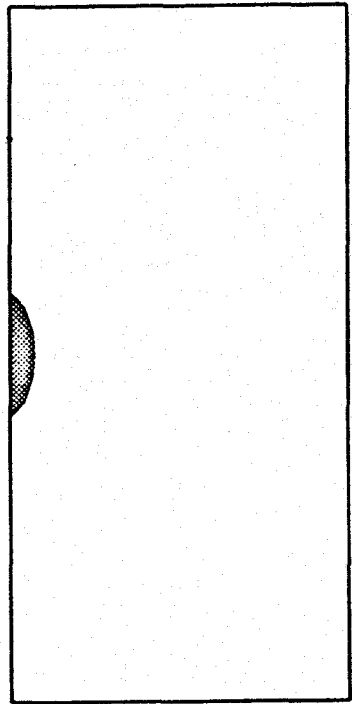


Figure 11. Vorticity region for the
same case.

Comparison of the algorithms

In accordance with our tests, the behaviour of Algorithm 2 is much more stable. It converges always if the value of λ is small enough ($\lambda \leq 0.001$). Furthermore, the number of iterates needed for convergence in the case of Algorithm 1 is too sensible to the initial value W . Furthermore, Algorithm 1 also needs for convergence to be more accurate in the solution of scalar equations. This is not surprising, because the right hand sides in the Dirichlet problems in Algorithm 1 are much more nonlinear than those in Algorithm 2. In the cases where both algorithms converge, the results are similar.

λ	Algorithm 1		Algorithm 2	
	N. Iter.	W_0	N. Iter.	W_0
10^{-3}	—	—	—	—
10^{-4}	—	—	13	0.43225139
10^{-5}	9	0.42134008	9	0.42134380
10^{-6}	—	—	9	0.42623562
10^{-7}	—	—	9	0.42623562

Table 1: Dependence of the Algorithms on the value of λ , for an initialization $W_0 = 0.3$.

W_0	Algorithm 1		Algorithm 2	
	N. Iter.	W	N. Iter.	W
0.1	9	0.42134279	9	0.42138773
0.2	9	0.42134270	9	0.42139536
0.25	—	—	9	0.42136800
0.3	—	—	9	0.42623562
0.32	9	0.42134058	9	0.42134523
0.4	9	0.42134362	8	0.42134398
0.5	—	—	8	0.42135161
0.57	9	0.42134041	9	0.42134762
0.6	—	—	15	0.41447192
0.62	9	0.42134339	9	0.42627427
0.7	9	0.42134804	9	0.42134368

Table 2: Dependence of Algorithms on the initialization of W_0 for $\lambda = 10^{-7}$.

4 The nonvariational case: free flux parameter

In this section, the problem under consideration is the following:

$$\begin{cases} \text{Find } u \in H_0^1(\Omega) \text{ and } Z \in \mathbb{R} \text{ such that} \\ -\Delta u(x) \in H(u(x) - Wx_1 - Z) \quad \text{a.e. in } \Omega, \quad x = (x_1, x_2), \\ \int_{\Omega} |\nabla u|^2 dx = \eta \end{cases} \quad (15)$$

As we have already said in Section 2, we cannot find a variational formulation for (15). Nevertheless, based on the iterates proposed and tested for problem (1) in Section 3, we propose here the following, analogous to Algorithm 2, for problem (15):

ALGORITHM 3

- (a) Fix $\lambda > 0$ and choose $p_0 \in L^2(\Omega)$.

Compute $u_0 \in H_0^1(\Omega)$ by solving

$$\begin{cases} -\Delta u = p_0 & \text{in } \Omega, \\ u = 0 & \text{on } \partial\Omega. \end{cases}$$

- (b) Then, for any given $k \geq 0$, $p_k \in L^2(\Omega)$, and $u_k \in H_0^1(\Omega)$,

- (b.1) Compute $Z_{k+1} \in \mathbb{R}$ by solving the equation

$$G_k(Z) \equiv \int_{\Omega} |\nabla \hat{v}_k(Z)|^2 dx = \eta, \quad (16)$$

where $\hat{v}_k(Z)$ is the solution of

$$\begin{cases} -\Delta \hat{v} = H_{\lambda}(u_k - Wx_1 - Z + \lambda p_k) & \text{in } \Omega, \\ \hat{v} = 0 & \text{on } \partial\Omega. \end{cases} \quad (17)$$

- (b.2) Then, set

$$\begin{aligned} p_{k+1} &= H_{\lambda}(u_k - Wx_1 - Z_{k+1} + \lambda p_k) \\ u_{k+1} &= \hat{v}_k(Z_{k+1}) \end{aligned}$$

To prove that this algorithm is well defined, we will show that, for fixed W and with u_k and p_k being given by the algorithm, there exists at least one solution to equation (16). The function $G_k(Z)$ in (16) can be also be written in the form

$$G_k(Z) \equiv \int_{\Omega} H_{\lambda}(u_k - Wx_1 - Z + \lambda p_k) \hat{v}_k(Z) dx.$$

Then, it is clear that $G_k(Z)$ is continuous, nonincreasing and bounded, because

$$0 \leq G_k(Z) \leq F_{\alpha}, \quad \forall k \geq 0, \quad \forall Z \in \mathbb{R}.$$

We have the inequalities

$$-Wa \leq u_k - Wx_1 + \lambda p_k \leq \max_{x \in \Omega} u_\alpha + \lambda \alpha.$$

Consequently, there exist $Z^* = \max_{x \in \Omega} u_\alpha + \lambda \alpha$ and $Z_* = -Wa - \lambda \alpha$ such that, for $Z \geq Z^*$, $G_k(Z) = 0$, and for $Z \leq Z_*$, $G_k(Z) = F_\alpha$.

Therefore, as $0 < \eta < F_\alpha$, equation (16) has always solution. Indeed, the sequence $\{Z_k\}$ is uniformly bounded.

(???)

4.1 Numerical experiences

For the numerical experiences, we have used the same triangulation that in Section 3 (see Figure 1). We visualize here the results for the data $\alpha = 1$, $\eta = 3$, $W = 0.32$. In Figure 12, the relationship between the value of λ used and the number of iterations needed is shown. Figures 13-15 are concerned with the stream function $\psi = u - Wx_1 - Z$, and in Figure 16 is represented the velocity field $\vec{v} = (\frac{\partial \psi}{\partial x_2}, -\frac{\partial \psi}{\partial x_1})$. Finally, in Figure 17 we show the graph of the computed function $Z = Z(W)$.

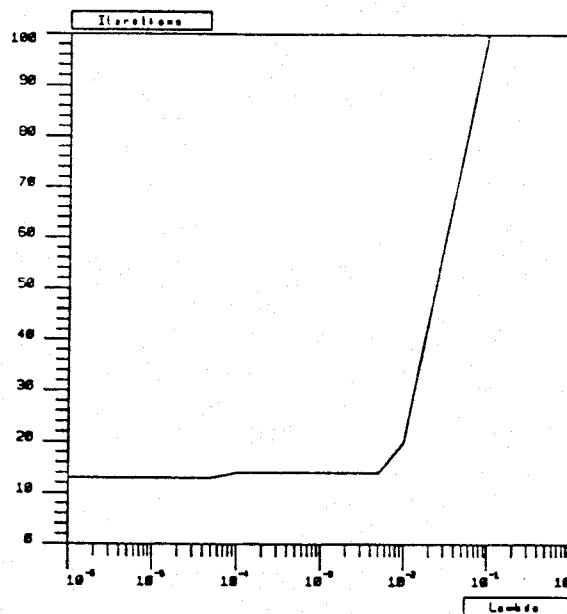


Figure 12. Dependence of the number of iterations on the value of λ .

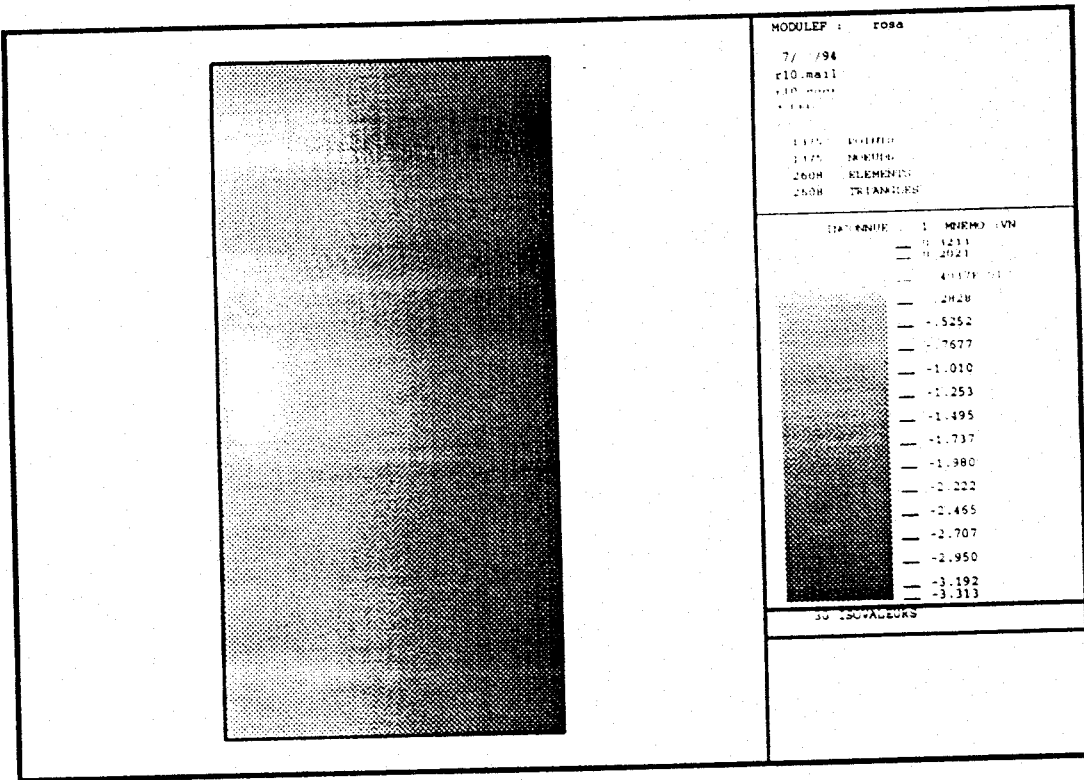


Figure 13. Representation of the values of the function $\psi = u - Wx_1 - Z$, for the data $\alpha = 1$, $\eta = 3$, $W = 0.32$. Computed value of $Z = 0.11324509$.

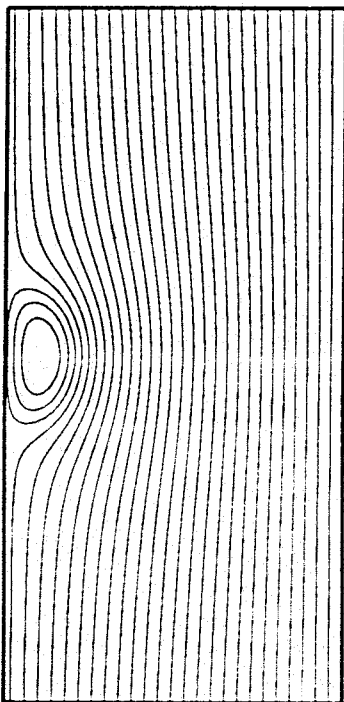


Figure 14. Streamlines for the same data.

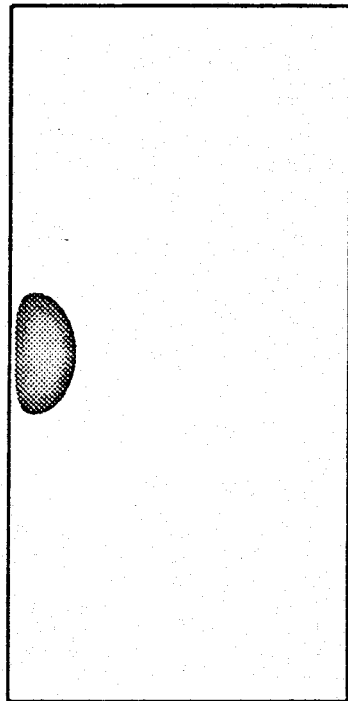


Figure 15. Vorticity region for the same case, i.e. $A = \{x \in \Omega; \psi = u - Wx_1 - Z > 0\}$.

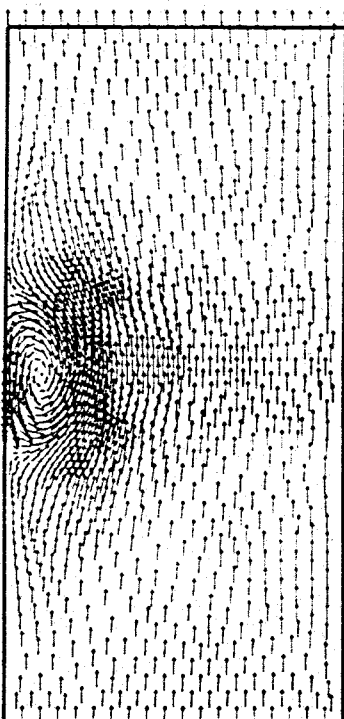


Figure 16. Representation of the velocity field, $\vec{v} = (\frac{\partial \psi}{\partial x_2}, -\frac{\partial \psi}{\partial x_1})$.

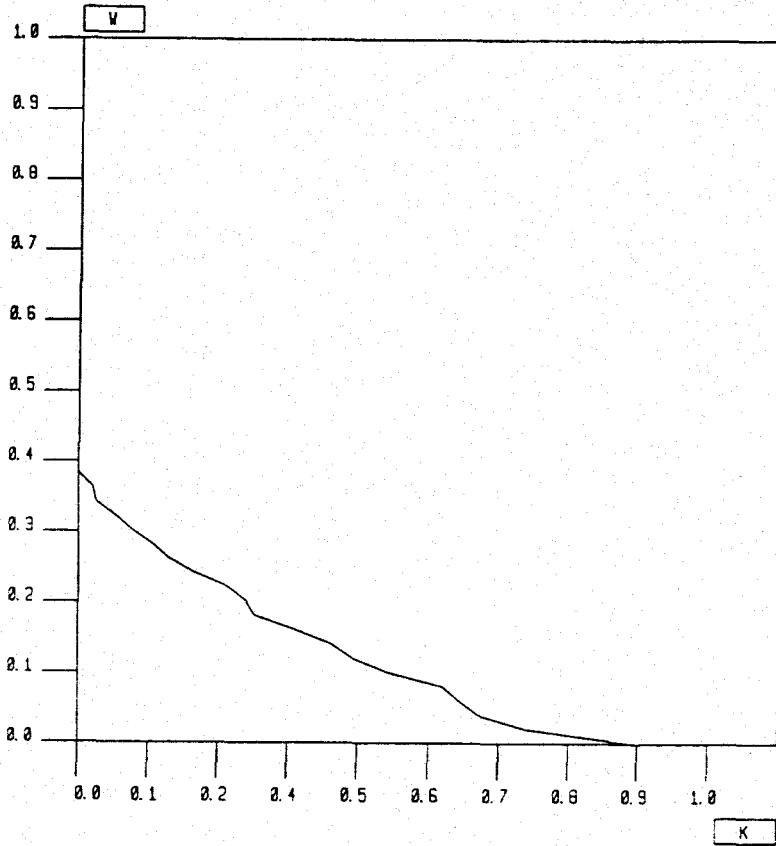


Figure 17. Graph of the computed function $Z = Z(W)$.

References

- [1] E. FERNÁNDEZ-CARA & C. MORENO, *Critical Point Approximation Through Exact Regularization*, Math. of Comp. Vol. 50, No. 181, January 1988, pp 139-153.
- [2] E. FERNÁNDEZ-CARA & C. MORENO, *Exact regularization and critical point approximation*, in Contributions to Nonlinear Partial Differential Equations, Vol. II. (J.I. Díaz and P.L. Lions Ed.), Longman Scientific & Technical, 1987.
- [3] M. BERNADOU et al, *MODULEF: Une Bibliothèque Modulaire d'Éléments Finis*, INRIA, Rocquencourt, 1985.
- [4] J. NORBURY, *Steady planar vortex pairs in an ideal fluid*, Comm. Pure Appl. Math., Vol. 28, 1975, pp. 679-700.
- [5] H. BERESTYCKI, E. FERNÁNDEZ-CARA & R. GLOWINSKI, *A Numerical study of some questions in vortex rings theory*. RAIRO Anal. Numér., Vol. 18, 1984, pp. 7-85.
- [6] L.E. FRAENKEL & M.S. BERGER, *On the global theory of vortex rings in an ideal fluid*, Acta Math., Vol. 132, 1974, pp. 13-51.
- [7] H. BERESTYCKI, *Some free boundary problems in plasma physics and fluid mechanics*, in Applications of Nonlinear Analysis to the Physical Sciences, H. Amann, N. Bazley & K. Kirchgassner Ed., Pitman, London, 1981.

Capítulo 3

Resolución numérica de algunos
problemas no escalares con no
linealidades discontinuas

The numerical solution of some elliptic nonscalar problems with nonlinear discontinuities

Rosa ECHEVARRÍA*

Abstract

This paper is devoted to the numerical solution of some semilinear elliptic systems with nonlinear discontinuities. The motivation is the modelling of single, irreversible, nonisothermal stationary reactions of zero order. The numerical solution is achieved through an iterative procedure. This uses exact regularization. We justify the convergence of the algorithm and, also, we present some numerical results.

1 Introduction

The aim of this work is to test numerically an algorithm which has been proposed in [5] to solve semilinear elliptic systems of partial differential equations. As a model problem we have chosen a system of two equations with nonlinear discontinuities. This arises in the mathematical modelling of chemical reactions and in combustion theory, with two different sets of boundary conditions. We also justify the convergence of the algorithm from a theoretical viewpoint.

In a previous work (see [7]), we were concerned with another algorithm, proposed in [8], to solve scalar elliptic semilinear problems with discontinuities. The present algorithm relies on the same ideas, but in a more complicate framework. Indeed, the arguments in [8] cannot be transferred to the nonscalar case as well.

The plan is as follows. In Section 2, we present the model problem. In Section 3, we recall the formulation of a general problem and the algorithm from [5]. Then, we explain how this can be applied in our context: in particular, we present and justify some convergence results. Finally, Section 4 deals with the numerical approximation. In order to illustrate the behaviour of the algorithm, we present some numerical results.

MODULEF finite element code (see [2]) has been used for part of the computations and also for the visualization of the numerical results.

*Dpto. Ecuaciones Diferenciales y Análisis Numérico. University of Sevilla. C/ Tarfia s/n, 41012 SEVILLA, SPAIN

2 Formulation of the problems

We will be concerned with the numerical solution of the semilinear elliptic system

$$\begin{cases} -\Delta u(x) \in -\mu^2 H(u(x)+1) \exp\left(\frac{\gamma v(x)}{v(x)+1}\right) \\ -\Delta v(x) \in \nu \mu^2 H(u(x)+1) \exp\left(\frac{\gamma v(x)}{v(x)+1}\right) \end{cases} \quad \text{a.e. in } \Omega, \quad (1)$$

together with appropriate boundary conditions that we indicate below. Here, $\Omega \subset \mathbb{R}^N$ is a bounded open set and H is the maximal monotone operator associated to Heavyside's function:

$$H(s) = \begin{cases} 0 & \text{for } s < 0, \\ [0, 1] & \text{for } s = 0, \\ 1 & \text{for } s > 0; \end{cases}$$

Such a system serves to describe a single, irreversible, nonisothermal stationary reaction of zero order (see [1]). The unknowns u and v are nonnegative and represent, respectively, the concentration and the temperature of the reactant, μ^2 is the Thiele modulus, ν is the Prater temperature and γ is the Arrhenius number.

We will consider two different sets of boundary conditions. The first set consists of homogeneous Dirichlet boundary conditions:

$$u = v = 0 \quad \text{on } \Omega. \quad (2)$$

These can be viewed as a limit for those usually considered in practice (see e.g. [1], [6], [9]). In the second case, we impose the (not necessarily realistic) boundary conditions:

$$\begin{cases} u = 0 \quad \text{on } \Gamma_1 \cup \Gamma_3, & \frac{\partial u}{\partial n} = 0 \quad \text{on } \Gamma_2, \\ v = 0 \quad \text{on } \Gamma_1, & \frac{\partial v}{\partial n} = 0 \quad \text{on } \Gamma_2 \cup \Gamma_3, \end{cases} \quad (3)$$

where Γ_1 , Γ_2 and Γ_3 are disjoint parts of $\partial\Omega$ such that $\Gamma_1 \cup \Gamma_2 \cup \Gamma_3 = \Omega$.

Existence results for problem (1),(2) can be found in [6]. In what concerns problem (1),(3) let us indicate that existence follows from the results in section 3.3 under certain assumptions on the parameters γ , ν and μ^2 . For other cases, we also refer to [6].

3 Algorithms and convergence

3.1 A general problem

Following [5], we consider the more general problem

$$\begin{cases} -\Delta u \in -\alpha(u)f(v) & \text{in } \Omega, \\ -\Delta v \in \beta(u)g(v) & \text{in } \Omega, \\ (\text{Boundary Conditions}) & \text{on } \partial\Omega, \end{cases} \quad (4)$$

where f and g are C^1 functions and α and β are maximal monotone set-valued functions. It will be seen below that this system can also be written in the following form for appropriate data:

$$\left\{ \begin{array}{l} \text{Find } \begin{pmatrix} u \\ v \end{pmatrix} \in V_1 \times V_2 \text{ such that} \\ \partial F \begin{pmatrix} u \\ v \end{pmatrix} - (K_v^* \circ \partial G) \left(\sigma \begin{pmatrix} u \\ v \end{pmatrix} \right) \ni 0, \end{array} \right. \quad (5)$$

In (5), V_1, V_2, X_1, X_2 are real Hilbert spaces and $V_i \hookrightarrow X_i$, with dense and compact embeddings for $i = 1, 2$. We make the usual identifications

$$V_i \hookrightarrow X_i \equiv X'_i \hookrightarrow V'_i,$$

for $i = 1, 2$. $F : V_1 \times V_2 \rightarrow \mathbb{R}$ is a convex C^1 function, $G : X_1 \times X_2 \rightarrow \mathbb{R}$ is a proper, lower semicontinuous and convex function, σ is a linear operator, $\sigma \in \mathcal{L}(V_1 \times V_2; X_1 \times X_2)$ and $\{K_w; w \in V_2\}$ is a family of linear operators $K_w \in \mathcal{L}(V_1 \times V_2; X_1 \times X_2)$.

Notice that (5) also reads

$$\left\{ \begin{array}{l} \text{Find } \begin{pmatrix} u \\ v \end{pmatrix} \in V_1 \times V_2 \text{ and } \begin{pmatrix} p \\ q \end{pmatrix} \in X_1 \times X_2 \text{ such that} \\ K_v^* \begin{pmatrix} p \\ q \end{pmatrix} \in \partial F \begin{pmatrix} u \\ v \end{pmatrix}, \\ \begin{pmatrix} p \\ q \end{pmatrix} \in \partial G \left(\sigma \begin{pmatrix} u \\ v \end{pmatrix} \right). \end{array} \right. \quad (6)$$

The algorithm proposed in [5] is the following:

Algorithm (AG)

(a) Fix $\lambda > 0$ and choose $\begin{pmatrix} p_0 \\ q_0 \end{pmatrix} \in X_1 \times X_2$ and $v_0 \in V_2$.

(b) Then, for any given $k \geq 0$, $\begin{pmatrix} p_k \\ q_k \end{pmatrix} \in X_1 \times X_2$ and $v_k \in V_2$, compute $\begin{pmatrix} u_{k+1} \\ v_{k+1} \end{pmatrix} \in V_1 \times V_2$, the solution to

$$\partial F \begin{pmatrix} u_{k+1} \\ v_{k+1} \end{pmatrix} = K_{v_k}^* \begin{pmatrix} p_k \\ q_k \end{pmatrix}$$

and set

$$\begin{pmatrix} p_{k+1} \\ q_{k+1} \end{pmatrix} = G'_\lambda \left(\sigma \begin{pmatrix} u_{k+1} \\ v_{k+1} \end{pmatrix} + \lambda \begin{pmatrix} p_k \\ q_k \end{pmatrix} \right).$$

Here, G'_λ is the Yosida approximation of the maximal monotone operator ∂G . We recall that G'_λ is single-valued and Lipschitz continuous and is given as follows:

$$G'_\lambda = \frac{1}{\lambda} (Id - (Id + \lambda \partial G)^{-1})$$

The main result in [5] is the following theorem, where the convergence of **(AG)** is established under certain hypotheses.

Theorem 1 Assume the following is satisfied:

- HYP.1 $R(\partial G)$ is bounded in $X_1 \times X_2$,
- HYP.2 $D(\partial F^*) \subset R(K_v^*)$, $\forall v \in V_2$ and $\partial F^* \circ K_v^*$ is single-valued for all $v \in V_2$,
- HYP.3 For every bounded set $B \subset X_1 \times X_2$

$$\bigcup_{v \in V_2} (\partial F^* \circ K_v^*)(B)$$

is bounded in $V_1 \times V_2$.

- HYP.4 σ is compact and the mapping

$$(v, p, q) \mapsto K_v^* \begin{pmatrix} p \\ q \end{pmatrix}$$

is completely continuous,

- HYP.5 For every bounded set $W \subset V_2$ there exists $\nu = \nu(W)$, with $0 < \nu < 1$, such that

$$\left\| P_2 \partial F^* \left(K_v^* \begin{pmatrix} p \\ q \end{pmatrix} \right) - P_2 \partial F^* \left(K_w^* \begin{pmatrix} p \\ q \end{pmatrix} \right) \right\|_{V_2} \leq \nu \|v - w\|_{V_2}$$

for all $v, w \in W$ and for any $\begin{pmatrix} p \\ q \end{pmatrix} \in R(\partial G)$.

Let $\begin{pmatrix} p_0 \\ q_0 \end{pmatrix} \in X_1 \times X_2$ and $v_0 \in V_2$ be given. If the sequence generated by **(AG)** satisfies

$$\begin{pmatrix} p_{k+1} \\ q_{k+1} \end{pmatrix} - \begin{pmatrix} p_k \\ q_k \end{pmatrix} \text{ converges to } 0 \text{ in } X_1 \times X_2. \quad (7)$$

then, it possesses weakly convergent subsequences and the limit of any such subsequence is a solution to (6). ■

We will briefly recall the main ideas in the proof of this theorem. First, using HYP.3, one proves there exist subsequences that converge weakly. More precisely, one can find subsequences, indexed with ρ , such that

$$\begin{pmatrix} p_\rho \\ q_\rho \end{pmatrix} - \begin{pmatrix} \bar{p} \\ \bar{q} \end{pmatrix} \quad \text{and} \quad \begin{pmatrix} u_{\rho+1} \\ v_{\rho+1} \end{pmatrix} - \begin{pmatrix} \bar{u} \\ \bar{v} \end{pmatrix}$$

resp. in $X_1 \times X_2$ and $V_1 \times V_2$ and $\begin{pmatrix} u_\rho \\ v_\rho \end{pmatrix}$ also converges weakly to, say, $\begin{pmatrix} \bar{z} \\ \bar{w} \end{pmatrix}$. From HYP.4 and (7), one has

$$K_{v_\rho}^* \begin{pmatrix} p_\rho \\ q_\rho \end{pmatrix} \longrightarrow K_{\bar{w}}^* \begin{pmatrix} \bar{p} \\ \bar{q} \end{pmatrix} \quad \text{strongly in } V'_1 \times V'_2$$

and

$$\sigma \begin{pmatrix} u_{\rho+1} \\ v_{\rho+1} \end{pmatrix} + \lambda \left[\begin{pmatrix} p_{\rho+1} \\ q_{\rho+1} \end{pmatrix} - \begin{pmatrix} p_\rho \\ q_\rho \end{pmatrix} \right] \longrightarrow \sigma \begin{pmatrix} \bar{u} \\ \bar{v} \end{pmatrix} \quad \text{strongly in } X_1 \times X_2.$$

Consequently,

$$\begin{pmatrix} \bar{u} \\ \bar{v} \end{pmatrix} \in \partial F^* \left(K_{\bar{w}}^* \begin{pmatrix} \bar{p} \\ \bar{q} \end{pmatrix} \right) \quad \text{and} \quad \begin{pmatrix} \bar{p} \\ \bar{q} \end{pmatrix} \in \partial G \left(\sigma \begin{pmatrix} \bar{u} \\ \bar{v} \end{pmatrix} \right).$$

Finally, writting the index ρ in the form $\rho = k(n)$, $n = 1, 2, \dots$ and using HYP.5, one sees that

$$\|v_{k(n)+1} - v_{k(n)}\| \leq B_{n-1} + \nu \|v_{k(n-1)+1} - v_{k(n-1)}\| \quad \forall n \geq 1,$$

$0 \leq \nu < 1$ and with $B_n \rightarrow 0$. Then, Lemma 2 below implies that

$$\|v_{k(n)+1} - v_{k(n)}\| = \|v_{\rho+1} - v_\rho\| \longrightarrow 0$$

i.e. $\bar{w} = \bar{v}$, which ends the proof. ■

Lemma 2 Assume $\{a_n\}$ and $\{B_n\}$ are bounded sequences of nonnegative numbers with $B_n \rightarrow 0$ satisfying

$$a_n \leq B_{n-1} + \nu a_{n-1} \quad \forall n \geq 1,$$

where $0 \leq \nu < 1$. Then $a_n \rightarrow 0$. ■

A detailed analysis reveals that, in the proof of theorem 1, HYP.3-HYP.5 can in fact be replaced by the following weaker assumptions, which must hold for every $\begin{pmatrix} p_0 \\ q_0 \end{pmatrix} \in X_1 \times X_2$ and every $v_0 \in V_2$:

HYP.3' $(\partial F^* \circ K_{v_k}^*) \begin{pmatrix} p_k \\ q_k \end{pmatrix}$ is uniformly bounded in $V_1 \times V_2$,

HYP.4' σ is compact; furthermore, if (v_ρ, p_ρ, q_ρ) converges weakly in $V_2 \times X_1 \times X_2$, then

$$K_{v_\rho}^* \begin{pmatrix} p_\rho \\ q_\rho \end{pmatrix} \text{ converges strongly in } V'_1 \times V'_2$$

HYP.5' There exists a number ν with $0 \leq \nu < 1$, such that

$$\left\| P_2 \partial F^* \left(K_{v_{k+1}}^* \begin{pmatrix} p_k \\ q_k \end{pmatrix} \right) - P_2 \partial F^* \left(K_{v_k}^* \begin{pmatrix} p_k \\ q_k \end{pmatrix} \right) \right\|_{V_2} \leq \nu \|v_{k+1} - v_k\|_{V_2} \quad \forall k \geq 0.$$

3.2 A first application: Dirichlet boundary conditions

We consider here problem (1),(2) that obviously agrees with (4) for:

$$f(v) = \mu^2 \exp\left(\frac{\gamma v}{v+1}\right), \quad g(v) = \nu \mu^2 \exp\left(\frac{\gamma v}{v+1}\right), \\ \alpha(u) = \beta(u) = H(u+1).$$

In order to rewrite (1),(2) in the context of (5), we set

$$V_1 = V_2 = H_0^1(\Omega), \quad X_1 = X_2 = L^2(\Omega), \\ F\begin{pmatrix} u \\ v \end{pmatrix} = \frac{1}{2} \int_{\Omega} |\nabla u|^2 dx + \frac{1}{2} \int_{\Omega} |\nabla v|^2 dx \quad \forall u, v \in H_0^1(\Omega).$$

$$G\begin{pmatrix} p \\ q \end{pmatrix} = \int_{\Omega} G_0\begin{pmatrix} p(x) \\ q(x) \end{pmatrix} dx, \quad \text{where } G_0\begin{pmatrix} r \\ s \end{pmatrix} = (r+1)_+ + (s+1)_+, \\ \sigma\begin{pmatrix} u \\ v \end{pmatrix} = \begin{pmatrix} u \\ u \end{pmatrix} \quad \text{and} \quad K_w\begin{pmatrix} u \\ v \end{pmatrix} = \begin{pmatrix} -f(w)u \\ g(w)v \end{pmatrix}.$$

Then **(AG)** becomes

Algorithm (A1)

(a) Fix $\lambda > 0$. Choose $\begin{pmatrix} p_0 \\ q_0 \end{pmatrix} \in L^2(\Omega) \times L^2(\Omega)$ and $v_0 \in H_0^1(\Omega)$.

(b) For any given $k \geq 0$, $\begin{pmatrix} p_k \\ q_k \end{pmatrix} \in L^2(\Omega) \times L^2(\Omega)$, and $v_k \in H_0^1(\Omega)$, compute $u_{k+1} \in H_0^1(\Omega)$, the solution to

$$\begin{cases} -\Delta u = -\mu^2 p_k \exp\left(\frac{\gamma v_k}{v_k+1}\right) & \text{in } \Omega, \\ u = 0 & \text{on } \partial\Omega \end{cases}$$

and $v_{k+1} \in H_0^1(\Omega)$, the solution to

$$\begin{cases} -\Delta v = \nu \mu^2 q_k \exp\left(\frac{\gamma v_k}{v_k+1}\right) & \text{in } \Omega, \\ v = 0 & \text{on } \partial\Omega. \end{cases}$$

Then set

$$p_{k+1} = H_{\lambda}(u_{k+1} + 1 + \lambda p_k), \\ q_{k+1} = H_{\lambda}(v_{k+1} + 1 + \lambda q_k).$$

The following theorem establishes the convergence of **(AG)** when it is applied to the solution of (4) with homogeneous Dirichlet boundary conditions:

Theorem 3 Assume α, β, f and g are bounded, with

$$\begin{cases} |\alpha(r)| \leq M(\alpha), & |\beta(r)| \leq M(\beta) \quad \forall r \in \mathbb{R}, \\ |f(s)| \leq M(f), & |g(s)| \leq M(g) \quad \forall s \in \mathbb{R}. \end{cases} \quad (8)$$

Let $p_0 \in L^2(\Omega)$, $q_0 \in L^2(\Omega)$ and $v_0 \in H_0^1(\Omega)$ be given and assume that

$$M(\beta) \sup_{t \in \mathbb{R}} |g'(t)| < \lambda_1, \quad (9)$$

with $\lambda_1 = \lambda_1(\Omega)$ being the first eigenvalue for the Laplace operator in Ω with Dirichlet boundary conditions on $\partial\Omega$. Then the sequence generated by (A1) possesses weakly convergent subsequences whose limits solve (4),(2). ■

We are now going to recall the main ideas in the proof of theorem 3. For a detailed proof, see [5]

What we need to prove is that all assumptions in theorem 1 are satisfied. HYP.1 to HYP.4 are easily verified. On the other hand, it is easy to see that HYP.5 means in this case the following:

$$\|\phi(v, q) - \phi(w, q)\|_{H_0^1} \leq \|v - w\|_{H_0^1}$$

for any $v, w \in H_0^1(\Omega)$ and for all $q \in L^2(\Omega)$. Here, $\phi(v, q)$ stands for the unique solution to

$$\begin{cases} -\Delta \tilde{v} = g(v)q & \text{in } \Omega, \\ \tilde{v} = 0 & \text{on } \partial\Omega. \end{cases}$$

But one can prove that

$$\|\phi(v, q) - \phi(w, q)\|_{H_0^1} \leq \lambda_1^{-\frac{1}{2}} \|(g(v) - g(w))q\|_{L^2} \leq \lambda_1^{-1} M(\beta) \sup_{t \in \mathbb{R}} |g'(t)| \cdot \|v - w\|_{H_0^1}$$

and, thus, (9) implies HYP.5.

Finally, it remains to check (7). For simplicity, let us just check that $p_{k+1} - p_k$ converges to 0 in X_1 . This can be done by using the following two lemmas:

Lemma 4 Let the sequences $\{\tilde{p}_k\}$ and $\{a_k\}$ be given, with $\tilde{p}_k \in C^0(\bar{\Omega})$ and $a_k \in L^\infty(\Omega)$ for all k . Assume a_k is uniformly bounded in $L^\infty(\Omega)$. Then a subsequence $\{\tilde{p}_{k(n)}\}$ and a function $a \in L^\infty(\Omega)$ exist such that

$$\int_{\Omega} (\tilde{p}_{k(n)+1} - \tilde{p}_{k(n)}) \cdot a_{k(n)} dx \leq \int_{\Omega} (\tilde{p}_{k(n)+1} - \tilde{p}_{k(n)}) \cdot a dx \quad \forall n \geq 1. \quad \blacksquare$$

Lemma 5 Under the assumptions of theorem 2, there exist functions z_2, z_3, \dots which are uniformly bounded in $L^\infty(\Omega)$ and satisfy

$$\lambda \|p_{k+1} - p_k\|_{L^2} \leq \int_{\Omega} (u_{k+1} - z_{k+1})(p_{k+1} - p_k) dx. \quad \blacksquare$$

Lemma 4 is proved in [5]. Lemma 5 stems easily from the fact that α is a maximal monotone operator. Using these two lemmas, one can write

$$\lambda \|p_{k+1} - p_k\|_{L^2}^2 \leq \int_{\Omega} (u_{k+1} - z_{k+1})(\tilde{p}_{k+1} - \tilde{p}_k) dx + \frac{M}{2^k} \quad \forall k,$$

where the sequence $\{z_k\}$ is uniformly bounded in $L^\infty(\Omega)$, M is a constant (the same for all k), and $\tilde{p}_m \in C^0(\overline{\Omega})$ is such that

$$\|p_k - \tilde{p}_k\|_{L^2} \leq \frac{1}{2^k} \quad \forall k \geq 0.$$

As a consequence, from lemma 4 we know there exists a subsequence, indexed with $k(n)$, satisfying

$$\lambda \|p_{k(n)+1} - p_{k(n)}\|_{L^2}^2 \leq \int_{\Omega} a \cdot (\tilde{p}_{k(n)+1} - \tilde{p}_{k(n)}) dx + \frac{M}{2^{k(n)}}.$$

Hence,

$$\lambda_1 \sum_{n=1}^{\infty} \|p_{k(n)+1} - p_{k(n)}\|_{L^2}^2 < +\infty$$

and, in particular, $\|p_{k(n)+1} - p_{k(n)}\|_{L^2}$ converges to 0. The same argument, repeated for an arbitrary subsequence of $\{p_k\}$ (and $\{q_k\}$) leads to (7).

It is clear that problem (4),(2) is not exactly in the conditions of theorem 3 but, as observed in the end of paragraph 3.1, HYP.3'-HYP.5' can be used. Choosing the initial function v_0 in $H_0^1(\Omega)$, with $v_0 \geq 0$, all the v_k generated by the algorithm are nonnegative. Since both f and g are bounded in \mathbb{R}^+ , we can easily check that HYP.3' and HYP.4' are satisfied. Furthermore, HYP.5' is satisfied if we change (9) by

$$M(\beta) \sup_{t \geq 0} |g'(t)| < \lambda_1. \quad (10)$$

Thus, convergence for (A1) is ensured whenever parameters γ , ν , and μ^2 are such that (10) holds, i.e. whenever

$$\begin{cases} \nu\mu^2\gamma < \lambda_1 & \text{if } \gamma < 2, \\ 4\nu\mu^2\gamma^{-1} \exp(\gamma - 2) < \lambda_1 & \text{if } \gamma \geq 2. \end{cases} \quad (11)$$

3.3 A second application: mixed Dirichlet-Neumann boundary conditions

In this section, we consider problem (1),(3). In order to rewrite this system in the form (5), at present we set

$$\begin{aligned} V_1 &= \{u \in H^1(\Omega); u = 0 \text{ on } \Gamma_1 \cup \Gamma_3\}, \\ V_2 &= \{v \in H^1(\Omega); v = 0 \text{ on } \Gamma_1\}, \\ X_1 &= X_2 = L^2(\Omega) \end{aligned}$$

$$F \begin{pmatrix} u \\ v \end{pmatrix} = \frac{1}{2} \int_{\Omega} |\nabla u|^2 dx + \frac{1}{2} \int_{\Omega} |\nabla v|^2 dx, \quad \forall u, v \in V_1 \times V_2,$$

$$G \begin{pmatrix} p \\ q \end{pmatrix} = \int_{\Omega} G_0 \begin{pmatrix} p(x) \\ q(x) \end{pmatrix} dx, \quad \text{where } G_0 \begin{pmatrix} r \\ s \end{pmatrix} = (r+1)_+ + (s+1)_+,$$

$$\sigma \begin{pmatrix} u \\ v \end{pmatrix} = \begin{pmatrix} u \\ u \end{pmatrix} \quad \text{and} \quad K_w \begin{pmatrix} u \\ v \end{pmatrix} = \begin{pmatrix} -f(w)u \\ g(w)v \end{pmatrix}.$$

It will be assumed that $\partial\Omega$ is regular enough. The corresponding problem (6) reads as follows:

$$\left\{ \begin{array}{l} \text{Find } \begin{pmatrix} u \\ v \end{pmatrix} \in W_1 \times W_2 \text{ and } \begin{pmatrix} p \\ q \end{pmatrix} \in X_1 \times X_2 \text{ such that} \\ \begin{pmatrix} p \\ q \end{pmatrix} \in \begin{pmatrix} \alpha(u) \\ \beta(u) \end{pmatrix}, \quad \begin{cases} -\Delta u = pf(v) & \text{in } \Omega, \\ \frac{\partial u}{\partial n} = 0 & \text{on } \Gamma_2 \end{cases} \quad \text{and} \\ \begin{cases} -\Delta v = qg(v) & \text{in } \Omega, \\ \frac{\partial v}{\partial n} = 0 & \text{on } \Gamma_2 \cup \Gamma_3. \end{cases} \end{array} \right.$$

In this context, the particularization of **(AG)** is as follows:

Algorithm (A2)

- (a) Fix $\lambda > 0$. Choose $\begin{pmatrix} p_0 \\ q_0 \end{pmatrix} \in L^2(\Omega) \times L^2(\Omega)$ and $v_0 \in V_2$.
 - (b) For any given $k \geq 0$, $\begin{pmatrix} p_k \\ q_k \end{pmatrix} \in L^2(\Omega) \times L^2(\Omega)$ and $v_k \in V_2$, compute $u_{k+1} \in V_1$, the solution to
- $$\begin{cases} -\Delta u = -\mu^2 p_k \exp\left(\frac{\gamma v_k}{v_k + 1}\right) & \text{in } \Omega, \\ u = 0 & \text{on } \Gamma_1 \cup \Gamma_3, \quad \frac{\partial u}{\partial n} = 0 & \text{on } \Gamma_2 \end{cases}$$

and $v_{k+1} \in V_2$, the solution to

$$\begin{cases} -\Delta v = \nu \mu^2 q_k \exp\left(\frac{\gamma v_k}{v_k + 1}\right) & \text{in } \Omega, \\ v = 0 & \text{on } \Gamma_1, \quad \frac{\partial v}{\partial n} = 0 & \text{on } \Gamma_2 \cup \Gamma_3. \end{cases}$$

Then set

$$\begin{aligned} p_{k+1} &= H_{\lambda}(u_{k+1} + 1 + \lambda p_k), \\ q_{k+1} &= H_{\lambda}(v_{k+1} + 1 + \lambda q_k). \end{aligned}$$

■

That this algorithm converges under certain conditions is implied by the following result:

Theorem 6 Assume α, β, f and g are as in theorem 3. Let $p_0 \in L^2(\Omega)$, $q_0 \in L^2(\Omega)$ and $v_0 \in V_2$ be given and assume also that

$$M(\beta) \sup_{t \in \mathbb{R}} |g'(t)| < \tilde{\lambda}_1,$$

with $\tilde{\lambda}_1 = \tilde{\lambda}_1(\Omega)$ being the first eigenvalue for Laplace's operator in Ω with homogeneous Dirichlet conditions on Γ_1 and homogeneous Neumann conditions on $\Gamma_2 \cup \Gamma_3$. Then, the sequence generated by (A2) possesses weakly convergent subsequences whose limits solve (4), (3).

Proof. As in the case of theorem 3, the hypotheses of theorem 1 will be checked. First, we notice that HYP.1, HYP.3 and HYP.4 are satisfied. Secondly, HYP.2 is a consequence of the well known existence and uniqueness result for the problem

$$\begin{cases} -\Delta u = \bar{p} & \text{in } \Omega, \\ u = 0 & \text{on } \Gamma, \quad \frac{\partial u}{\partial n} = 0 \quad \text{on } \partial\Omega \setminus \Gamma \end{cases}$$

(with $\text{meas}(\Gamma) > 0$), where $\bar{p} \in L^2(\Omega)$.

For each v and w in V_2 , let us denote by $\psi(v, q)$ the unique solution to the problem

$$\begin{cases} -\Delta \psi = g(v)q & \text{in } \Omega \\ \psi = 0 & \text{on } \Gamma_1, \quad \frac{\partial \psi}{\partial n} = 0 \quad \text{on } \Gamma_2 \cup \Gamma_3. \end{cases}$$

Then, it is clear that

$$\|\psi(v, q) - \psi(w, q)\|_{W_2} \leq \tilde{\lambda}_1^{-\frac{1}{2}} \|(g(v) - g(w))q\|_{L^2} \leq \tilde{\lambda}_1^{-\frac{1}{2}} M(\beta) \sup_{t \in \mathbb{R}} |g'(t)| \cdot \|v - w\|_{L^2}$$

for all $v, w \in V_2$ and for all $q \in L^2(\Omega)$. If v and w satisfy homogeneous Neumann conditions on $\Gamma_2 \cup \Gamma_3$, we also have

$$\|v - w\|_{L^2} \leq \tilde{\lambda}_1^{-\frac{1}{2}} \|v - w\|_{W_2}.$$

Consequently, HYP.5' is satisfied provided our assumptions hold. Finally, to check (7) it suffices to argue as in the proof of theorem 3. ■

It is easy to see that the weaker assumption HYP.5' is satisfied by simply imposing

$$M(\beta) \sup_{t \geq 0} |g'(t)| < \tilde{\lambda}_1.$$

Consequently, convergence for (A2) is ensured (in the sense of theorem 6) whenever one has the following for the constants in (1):

$$\begin{cases} \nu\mu^2\gamma < \tilde{\lambda}_1 & \text{if } \gamma < 2 \\ 4\nu\mu^2\gamma^{-1} \exp(\gamma - 2) < \tilde{\lambda}_1 & \text{if } \gamma \geq 2. \end{cases} \quad (12)$$

4 Numerical approximations and results

In this section, we explain how problems (4),(2) and (4),(3) can be solved numerically using respectively algorithms **(A1)** and **(A2)**. In the case of algorithm **(A1)**, we will have to solve at each step two Dirichlet problems with homogeneous boundary conditions and, then, we will have to perform two projections on \mathbb{R} at each nodal point. For algorithm **(A2)**, it will be seen we must solve mixed Dirichlet-Neumann problems with different boundary conditions and, then, project again exactly in the same way.

In both cases, the boundary problems to solve are of the following kind

$$\begin{cases} -\Delta w = F & \text{in } \Omega, \\ w = 0 & \text{on } \Gamma, \quad \frac{\partial w}{\partial n} = 0 & \text{on } \partial\Omega \setminus \Gamma, \end{cases} \quad (13)$$

with $\Gamma = \partial\Omega$, i.e. $\partial\Omega \setminus \Gamma = \emptyset$ for **(A1)**. Let us recall the usual variational weak formulation of the previous problem:

$$\begin{cases} \text{Find } w \in W^0 \text{ such that} \\ \int_{\Omega} \nabla w \cdot \nabla \phi \, dx = \int_{\Omega} F \phi \, dx \quad \forall \phi \in W^0. \end{cases} \quad (14)$$

where $W^0 = \{w \in H^1(\Omega); w = 0 \text{ on } \Gamma\}$.

For the numerical approximation, a P_1 -Lagrange (piecewise linear) finite element approximation can be used. This can be done as follows. For simplicity, assume that the domain Ω is a polygon. Let T_h be a triangulation of Ω and let us denote by $\{a_i\}_{i=1}^n$ the set of the corresponding nodal points. Consider the finite-dimensional space

$$W_h = \{w_h; w_h \in C^0(\bar{\Omega}), \quad w_h|_T \in P_1 \quad \forall T \in T_h\}$$

and its subspace

$$W_h^0 = \{w_h; w_h \in W_h, \quad w_h = 0 \text{ on } \Gamma\}.$$

These spaces are finite-dimensional approximations of, respectively, $H^1(\Omega)$ and W^0 . Let us introduce the usual canonical basis $\{\varphi_1, \dots, \varphi_n\}$ of W_h . The functions φ_i are given as follows

$$\varphi_i \in V_h \quad \text{and} \quad \varphi_i(a_j) = \delta_{ij} \quad \forall i, j = 1, 2, \dots, n.$$

Hence, one can write

$$w_h = \sum_{i=1}^n w_h(a_i) \varphi_i \quad \forall w_h \in W_h.$$

Problem (14) is now approximated by the following:

$$\begin{cases} \text{Find } w_h \in W_h^0 \text{ such that} \\ \int_{\Omega} \nabla w_h \cdot \nabla \phi \, dx = \int_{\Omega} F \phi \, dx \quad \forall \phi \in W_h^0. \end{cases} \quad (15)$$

Thus, it is readily seen that our task reduces to solve a n_0 -dimensional linear system $A\bar{w} = b$, where n_0 is the number of nodal points belonging to $\bar{\Omega} \setminus \Gamma$. The coefficients of the matrix A and the second member b are given by

$$\begin{aligned} A &= (a_{ij})_{i,j=1}^{n_0}, & a_{ij} &= \int_{\Omega} \nabla \varphi_i \nabla \varphi_j dx, \\ b &= (b_i)_{i=1}^{n_0}, & b_i &= \int_{\Omega} F \varphi_i dx. \end{aligned}$$

Consequently, A is symmetric, definite positive, sparse and independent on the function F . If an appropriate numbering of the nodal points is chosen, A has nonvanishing components only near the diagonal line. It is appropriate, thus, to solve the system $A\bar{w} = b$ using Cholesky's factorization method. For more details on the finite element approximation, see e.g. [4].

4.1 Numerical results for problem (1),(2)

For the numerical computations, we have taken as Ω the square $(0, 10) \times (0, 10)$. We have used a triangulation with 2500 points and 4802 triangles (see Figure 1). Accordingly, $h \sim 0.2$.

We have tested different values for the parameters γ , ν and μ^2 . We obtained convergence for (A1) in all cases satisfying (11) (in this case, $\lambda_1 \sim 0.197392$). In general, for small values of μ^2 , we obtained convergence for the whole sequence, whereas for larger μ^2 we found convergent subsequences only.

For problems of this kind, the set where the reactant vanishes, i.e. $u = 0$ (called the *dead core*), plays an important role in applications. See e.g. [6] and the bibliography therein for some theoretical results on the existence of such a *dead core*.

In Figures 2–5 we have displayed the computed functions $u + 1$ and $v + 1$ for the values of the parameters: $\gamma = 1$, $\nu = 0.6$, $\mu^2 = 0.12$ and $\mu^2 = 0.2$. For $\mu^2 = 0.2$ a *dead core* is found.

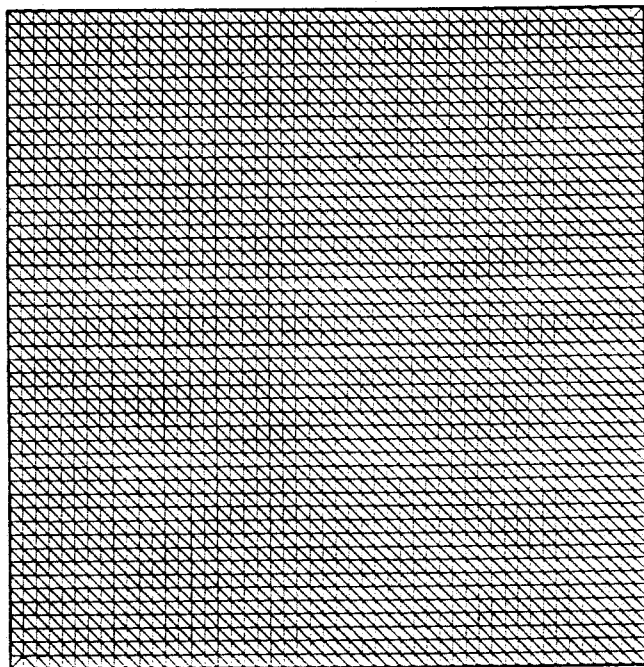


Figure 1. Triangulation of the domain $\Omega = (0, 10) \times (0, 10)$.
Number of triangles: 4802. Number of nodal points: 2500.

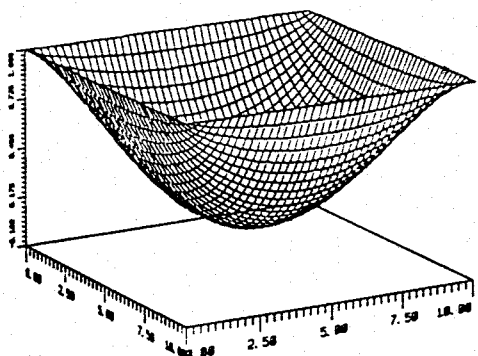


Figure 2. Three-dimensional representation of the computed function $u + 1$.
Values for the parameters: $\gamma = 1$,
 $\nu = 0.6$, $\mu^2 = 0.12$. Minimum value
of u : 0.1132

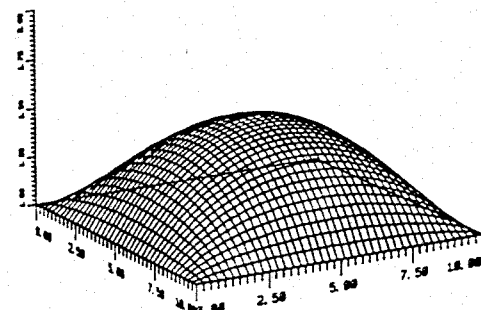


Figure 3. Three-dimensional representation of the computed function $v + 1$.
Values for the parameters: $\gamma = 1$,
 $\nu = 0.6$, $\mu^2 = 0.12$. Maximum value
of v : 1.532

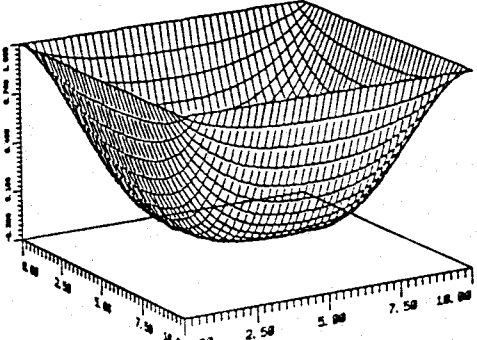


Figure 4. Three-dimensional representation of the computed function $u + 1$. Values for the parameters: $\gamma = 1.$, $\nu = 0.6$, $\mu^2 = 0.2$. Minimum value of u : 0.0153

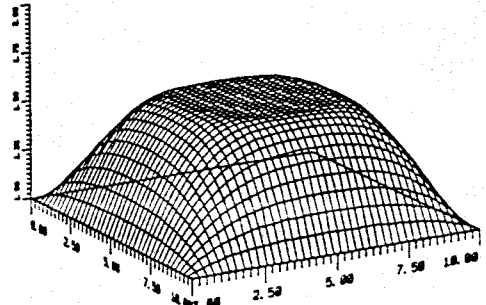


Figure 5. Three-dimensional representation of the computed function $v + 1$. Values for the parameters: $\gamma = 1.$, $\nu = 0.6$, $\mu^2 = 0.2$. Maximum value of v : 1.591

4.2 Numerical results for problem (1),(3)

In this case, we have taken the same domain Ω , with boundaries Γ_1 , Γ_2 and Γ_3 as in Figure 6. We have used the same triangulation (see Figure 1). We found convergence of (A2) in all cases satisfying (12) (here, $\tilde{\lambda}_1 \sim 0.12337$).

Figures 7–14 show the computed functions $u + 1$ and $v + 1$ for the following values of the parameters: $\gamma = 1.$, $\nu = 0.6$, $\mu^2 = 0.01$ and $\mu^2 = 0.15$.

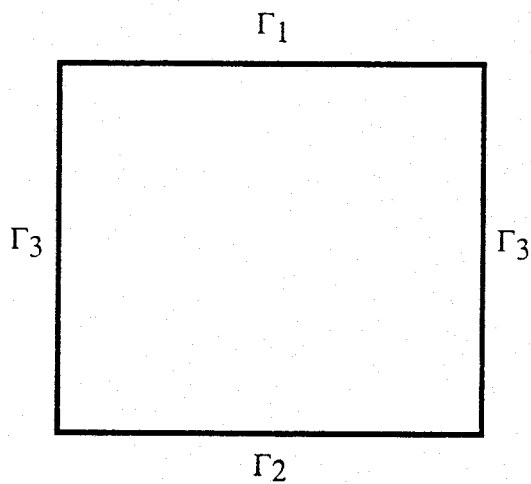


Figure 6. The domain $\Omega = (0, 10) \times (0, 10)$ and the boundaries Γ_1 , Γ_2 and Γ_3 .

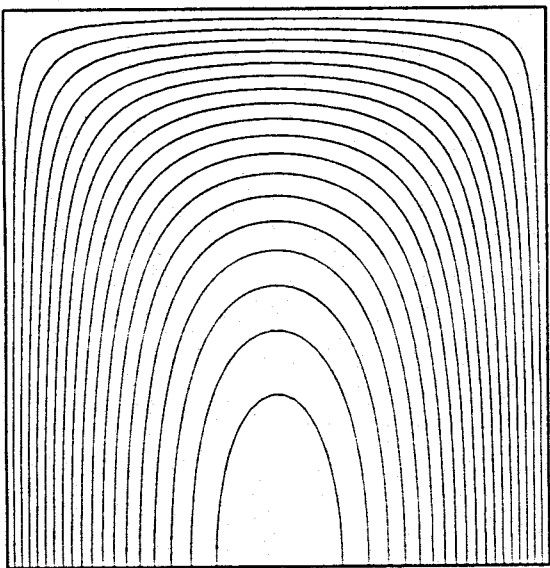


Figure 7. Isolines of the computed function $u + 1$. Values for the parameters: $\gamma = 1.$, $\nu = 0.6$, $\mu^2 = 0.01$. Minimum value of u : 0.8522

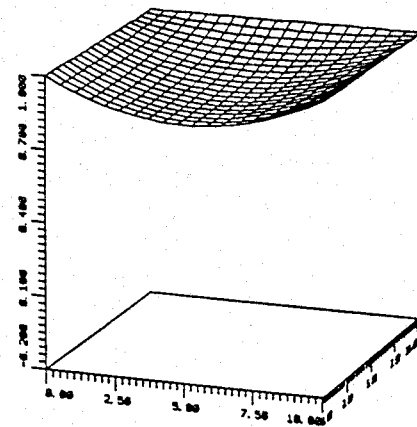


Figure 8. Three-dimensional representation of the computed function $u + 1$. Values for the parameters: $\gamma = 1.$, $\nu = 0.6$, $\mu^2 = 0.2$.

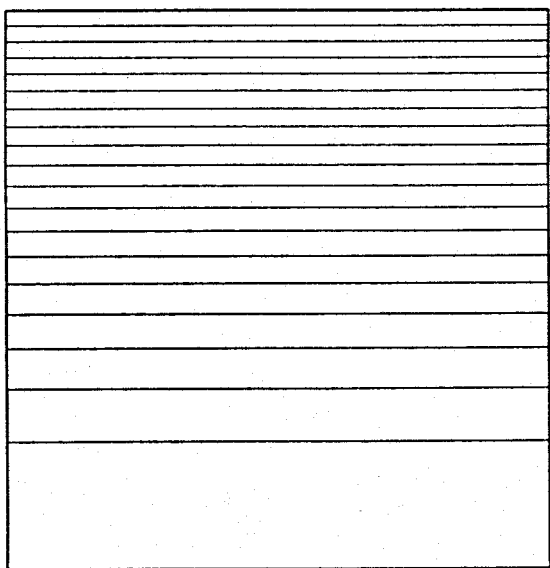


Figure 9. Isolines of the computed function $v + 1$. Values for the parameters: $\gamma = 1.$, $\nu = 0.6$, $\mu^2 = 0.01$. Maximum value of v : 1.388

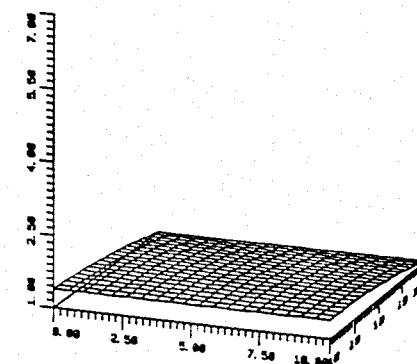


Figure 10. Three-dimensional representation of the computed function $v + 1$. Values for the parameters: $\gamma = 1.$, $\nu = 0.6$, $\mu^2 = 0.01$.

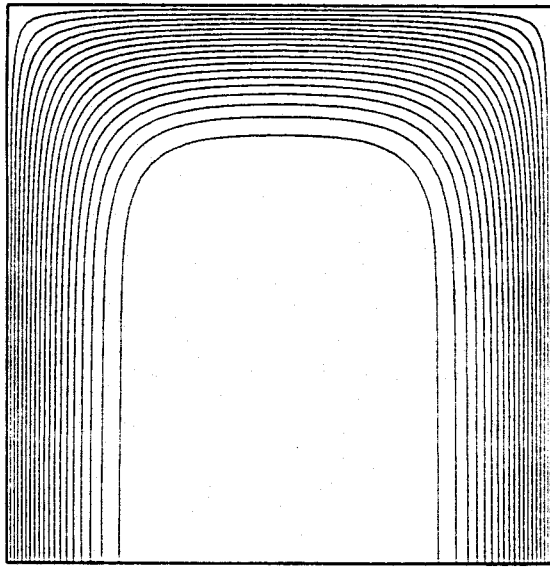


Figure 11. Isolines of the computed function $u + 1$. Values for the parameters: $\gamma = 1.$, $\nu = 0.6$, $\mu^2 = 0.15$. Minimum value of u : -0.021

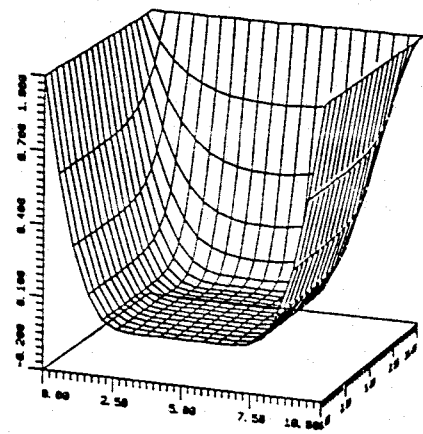


Figure 12. Three-dimensional representation of the computed function $u + 1$. Values for the parameters: $\gamma = 1.$, $\nu = 0.6$, $\mu^2 = 0.15$.

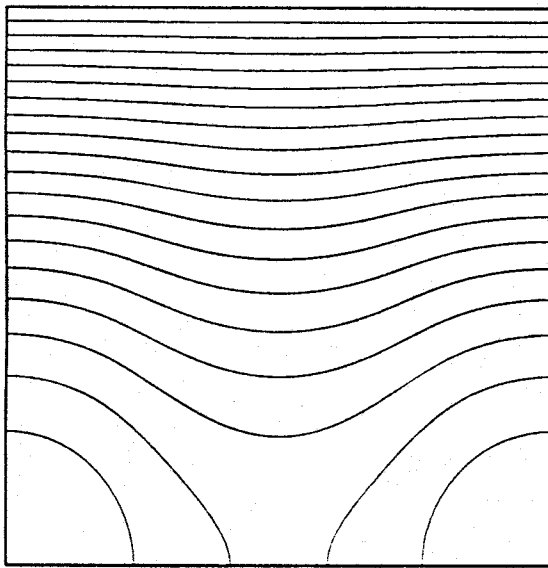


Figure 13. Isolines of the computed function $v + 1$. Values for the parameters: $\gamma = 1.$, $\nu = 0.6$, $\mu^2 = 0.15$. Maximum value of v : 6.608

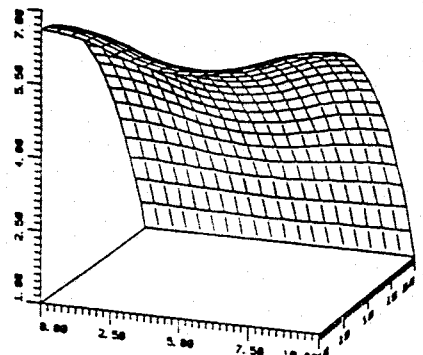


Figure 14. Three-dimensional representation of the computed function $v + 1$. Values for the parameters: $\gamma = 1.$, $\nu = 0.6$, $\mu^2 = 0.15$.

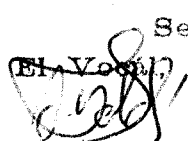
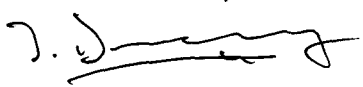
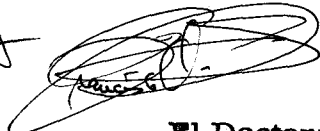
References

- [1] R. ARIS, *The Mathematical Theory of Diffusion and Reaction in Permeable Catalysts*, Clarendon Press, Oxford, 1975.
- [2] M. BERNADOU et al., *MODULEF: Une Bibliothèque Modulaire d'Eléments Finis*, INRIA, Rocquencourt, 1985.
- [3] H. BREZIS, *Analyse Fonctionnelle. Théorie et applications*, Masson, Paris, 1983.
- [4] P.G. CIARLET, *The Finite Element Method for Elliptic Problems*, North-Holland, Amsterdam, 1978.
- [5] M. DELGADO & E. FERNANDEZ-CARA, *An Iterative Method for the Solution of Some Semilinear Elliptic Systems with Discontinuities*, Appl. Math. Optim., No. 31, 1995, pp. 101-116.
- [6] J.I. DIAZ & J. HERNANDEZ, *On the existence of a free boundary for a class of reaction-diffusion systems*, SIAM J. Math. Anal., Vol. 15, No. 4, July 1984, pp. 670-685.
- [7] R. ECHEVARRIA, *The numerical solution of some elliptic problems with nonlinear discontinuities using exact regularization*, Comp. & Math. with Appl. Vol. 29, No. 12, pp. 57-66.
- [8] E. FERNANDEZ-CARA & C. MORENO, *Critical Point Approximation Through Exact Regularization*, Math. of Comp. Vol. 50, No. 181, January 1988, pp. 139-153.
- [9] C.V. PAO, *Nonlinear Parabolic and Elliptic Equations*, Plenum Press, New York, 1992.

UNIVERSIDAD DE SEVILLA

Reunido el Tribunal integrado por los señores siguientes
en el día de la fecha, para juzgar la Tesis Doctoral de
D.^a Rosa Echeverría Líbaro
titulada Algunas aplicaciones del método de elementos
finitos a problemas en derivadas parciales no lineales
acordó otorgarle la calificación de APTO cum LAUDIS
POR UNANIMIDAD.

Sevilla, 22 de Septiembre 1995

El Vocal, El Vocal, El Vocal,




El Presidente

El Secretario,

El Doctorado,

